Award Number: W81XWH-09-1-0359

TITLE: Role of Stat3 and ErbB2 in Breast Cancer

PRINCIPAL INVESTIGATOR: Mulu Geletu, Ph.D.

CONTRACTING ORGANIZATION: Queen's University
Kingston, Ontario, Canada K7L 3N6

REPORT DATE: December 2013

TYPE OF REPORT: Annual Summary

PREPARED FOR: U.S. Army Medical Research and Materiel Command
Fort Detrick, Maryland 21702-5012

REPORT DOCUMENTATION PAGE

Form Approved
OMB No. 0704-0188

1. REPORT DATE	2. REPORT TYPE	3. DATES COVERED
December 2013	Annual Summary	15 September 2009 – 14 September 2013

4. TITLE AND SUBTITLE

Role of Stat3 and ErbB2 in Breast Cancer

5a. CONTRACT NUMBER

5b. GRANT NUMBER
W81XWH-09-1-0359

5c. PROGRAM ELEMENT NUMBER

6. AUTHOR(S)

Mulu Geletu, Ph.D.

E-Mail: mulu.geletu@utoronto.ca

5d. PROJECT NUMBER

5e. TASK NUMBER

5f. WORK UNIT NUMBER

7. PERFORMING ORGANIZATION NAME(S) AND ADDRESS(ES)

Queen's University
Kingston, Ontario, Canada K7L 3N6

8. PERFORMING ORGANIZATION REPORT NUMBER

9. SPONSORING / MONITORING AGENCY NAME(S) AND ADDRESS(ES)
U.S. Army Medical Research and Materiel Command
Fort Detrick, Maryland 21702-5012

10. SPONSOR/MONITOR'S ACRONYM(S)

11. SPONSOR/MONITOR'S REPORT NUMBER(S)

12. DISTRIBUTION / AVAILABILITY STATEMENT
Approved for Public Release; Distribution Unlimited

13. SUPPLEMENTARY NOTES

14. ABSTRACT

Stat3 (Signal Transducer and Activator of Transcription-3) is activated by a number of receptor and nonreceptor tyrosine kinases. We recently demonstrated that engagement of E-cadherin, a calcium-dependent, cell to cell adhesion molecule which is often required for cells to remain tightly associated within the epithelium, also activates Stat3. We now examined the effect of two other classical cadherins, cadherin-11 and N-cadherin, whose expression often correlates with the epithelial to mesenchymal transition occurring in metastasis of carcinoma cells, upon Stat3 phosphorylation and activity. Our results indicate that engagement of these two cadherins also, can trigger a dramatic surge in Stat3 activity. This activation occurs through upregulation of members of the IL6 family of cytokines, and it is necessary for cell survival, proliferation and migration. Interestingly, our results also demonstrate for the first time that, in sharp contrast to Stat3, the activity of Erk (Extracellular Signal Regulated kinase) was unaffected by cadherin-11 engagement. Further examination indicated that, although IL6 was able to activate Erk in sparsely growing cells, IL6 could not induce an increase in Erk activity levels in densely growing cultures. Most importantly, cadherin-11 knock-down did allow Erk activation by IL6 at high densities, indicating that it is indeed cadherin engagement that prevents Erk activation by IL6. The fact that the three classical cadherins tested so far, E-cadherin, N-cadherin and cadherin11, which are present in essentially all tissues, actually activate Stat3 regardless of their role in metastasis, argues for Stat3 as a central survival, rather than invasion factor.

15. SUBJECT TERMS
Stat3, ErBb2, Breast cancer

16. SECURITY CLASSIFICATION OF:			17. LIMITATION OF ABSTRACT	18. NUMBER OF PAGES	19a. NAME OF RESPONSIBLE PERSON
a. REPORT	b. ABSTRACT	c. THIS PAGE			USAMRMC
U	U	U	UU	103	19b. TELEPHONE NUMBER *(include area code)*

Table of Contents

Introduction

Cells in normal tissues or tumors have extensive opportunities for adhesion to their neighbors in a three-dimensional organization, and it recently became apparent that in the study of fundamental cellular processes it is important to take into account the effect of surrounding cells.
The signal transducer and activator of transcription-3 (Stat3) is activated by receptor tyrosine kinases, cytokine receptors and non-receptor tyrosine kinases. Following ligand stimulation, Stat3 is activated through phosphorylation at tyr-705 and migrates to the nucleus where it activates the transcription of genes involved in cell growth and survival[1,2]. Persistent activation of Stat3 has been demonstrated in breast and other cancers, while a constitutively active form of Stat3, Stat3C, is able to transform cultured cells[3] , further pointing to an etiologic role for Stat3 in these tumors. My project deals with the mechanism of Stat3 activation and its role in these tumors, hence the consequences of its inhibition.

We recently discovered a ***novel pathway of activation of Stat3***, a protein involved in cell division, triggered by engagement of ***E-cadherin***, an extensively studied, cell to cell adhesion molecule. Stat3 activation was due to a striking upregulation of the Rac/Cdc42 GTPases[4*] and was followed by a potent downregulation of the p53 tumor suppressor and apoptosis inhibition. Most importantly, this Stat3 activation was resistant to inhibition of a number of tyrosine kinases, including the Src family, IGF1-R, Abl, Fer and EGFR, often activated in breast and other cancers[5*]. We propose the existence of a ***novel pathway of Stat3 activation*** that is triggered by cadherin engagement, which can be especially important in tumor cells.

Another molecule with a profound significance in breast cancer and Stat3 signalling is caveolin-1. Caveolae are cholesterol-rich, 50-100nm flask-shaped invaginations of the plasma membrane, with caveolins (cav1-3), the marker proteins of caveolae, embedded in their lipid bilayer[6-8]**.** The human cav1 gene is found in a tumor suppressor locus on chromosome 7q31.1, which is commonly deleted in a variety of cancers. This led to the hypothesis that this region may encode a tumor suppressor gene[9-11]**.** Cav1 recruits many receptor and non-receptor tyrosine kinases and through binding to its scaffolding-domain, cav1 sequesters the kinases in an inactive form, thereby preventing their involvement in signaling pathways[8]**.** The examination of the effect of this inhibition upon Stat3 activity is very important in Stat3 signalling as well as breast cancer Biology.

These novel aspects of Stat3 biology, namely Stat3 activation triggered by specific cadherin engagement, or Stat3 inhibtion by cav1, could be promising prognostic markers, as well as predictive targets for the treatment of tumors which may be ***resistant*** to inhibition of many ***tyrosine kinase oncogenes*** known to be ***hyperactive in breast cancer***, such as the ErbB2 drug ***Herceptin***.

Body

Specific Aim 1. Examination of the upstream activators of Stat3 in confluent cells

Cell to cell adhesion triggers cytokine gene expression in mouse Balb/c3T3 fibroblasts

In order to examine the possibility that the cell density-mediated, Stat3 activation might occur through secretion of soluble factors, a quantitative RT-PCR array for mRNA of 86 cytokines was performed, by comparing sparsely growing cells to cells grown as dense cultures. The results revealed an increase in mRNA levels of a number of cytokines, including the IL6 family, known to act through the common gp130 subunit, shared by a number of Stat3 activating cytokines, such as IL6, LIF, Ct1 and IL27 (32-fold for IL6 mRNA, Table 1)[24]. To examine whether these cytokines are indeed required for the Stat3 activation observed in confluent cultures, the levels of gp130, the common subunit of the family were reduced through expression of shRNA with a retroviral vector. As shown in Fig. 1 (A and B), gp130 knockdown caused a dramatic reduction in Stat3-ptyr705 levels (Fig. 5B, lanes 1-3 *vs* 4-6), indicating that gp130 activation is at least partly responsible for the Stat3-ptyr705 increase.

Engagement of "mesenchymal" cadherins increases Stat3 activity

The mouse fibroblast line Balb/c3T3 was previously shown to express cadherin-11[14]. In fact, as shown in Fig. 2A, these cells possess significant amounts of cadherin-11 mRNA (upper panel) and protein (lower panel), while E-cadherin mRNA is undetectable. To investigate the effect of cadherin-11 engagement upon Stat3 activity, the impact of cell density was initially examined. Balb/c3T3 cells were plated and when ~50%

confluent, and over several days thereafter, detergent cell extracts were probed by Western blotting for the tyrosine-705 phosphorylated form of Stat3 (Stat3-ptyr705) . As a loading control, the same extracts were probed with an antibody against the abundant heat shock protein, Hsp90[18]. As shown before for a number of normal cell lines[15], Stat3-ptyr705 levels were almost undetectable in sparsely growing, Balb/c3T3 cells (Fig. 2B, lane 1). However, density caused a dramatic increase, and Stat3-ptyr705 plateaued at 2-3 days after confluence (lanes 5-6), to levels approximately half the levels present in cells transformed by the potent Stat3 activator, v-Src (lane 9), and decreased slightly thereafter. Probing for total Stat3 revealed a modest increase with cell density (approximately 2.5 fold, Fig. 2B), possibly due to the fact that the Stat3 promotor itself is one of the Stat3 targets[19]. This activation was specific to Stat3, since the levels of Erk1/2 (and Akt 473), a signal transducer often coordinately activated with Stat3 by a number of growth factors and oncogenes, remained unaffected by cell density (Fig 2B). The above results indicate that cell density causes a specific increase in Stat3-ptyr705 levels in mouse Balb/c3T3 fibroblasts.To examine whether cadherin-11 was indeed responsible for the density-mediated increase in Stat3-ptyr705 levels, cadherin-11 was knocked down through stable sh-RNA expression with a retroviral vector. As shown in Fig. 3A, infection with this vector essentially eliminated cadherin-11 as shown by Western blotting (Fig. 3A, panel a) and immunocytochemistry (panel b). Interestingly, cadherin-11 knockdown resulted in a dramatic reduction in Stat3-ptyr705 levels (panel c), indicating that this cadherin is indeed required for the Stat3, tyr705 phosphorylation observed at high densities. Most importantly, these data also indicate that, at this point, Balb/c3T3 fibroblasts do not express significant amounts of other Stat3 activators (such as other cadherins) that might operate at high cell densities.

The type I classical cadherin, N-cadherin, has also been documented to correlate with metastasis of tumor cells[13], therefore we examined its effect upon Stat3 activity and survival. To this effect, we made use of the null, embryonal stem (ES) cells where E-cadherin was genetically ablated[17]. These cells have very low background levels of Stat3, which might be due to the Leukemia inhibitory factor (LIF) necessary for their growth[17]. Indeed, N-cadherin expression in null cells[33] caused an increase in Stat3-ptyr705, indicating that N-cadherin can also activate the Stat3 pathway in this cellular setting (Fig. 4A, B).

To further confirm the ability of N-cadherin to activate the Stat3 pathway, we transfected a construct of N-cadherin-GFP in HEK-293 cells which express low levels of N-cadherin (Fig. 4C, lane 3). As shown in Fig. 4C (lanes 1 and 2 *vs* lane 3), N-cadherin expression caused a dramatic increase in Stat3-ptyr705 levels, further confirming that N-cadherin also activates Stat3 following transient expression. Taken together, the above data indicate that cadherin-11 and N-cadherin, which, contrary to E-cadherin correlate with metastasis of epithelial cells, also activate the Stat3 pathway.

Cadherin11 engagement is sufficient for direct Stat3 activation

We next investigated whether the Stat3 activation observed at high densities is a direct consequence of the engagement of cadherin-11, or whether cadherin interactions are simply required to bring adjacent cell surfaces into proximity, to initiate signals which are not immediate effects of cadherin ligation. To definitively answer this question, we made use of a recombinant cadherin-11 fragment, encompassing the two distal, extracellular domains of cadherin-11 (11/EC12) to functionalize petri dishes by covalent immobilization. This fragment has been shown to retain biological activity when attached onto solid surfaces[12]. Plastic, 3cm petri dishes were coated with increasing amounts of purified 11/EC12 fragment, from 0 to 1,000μg/ml, and 30,000 Balb/c3T3 cells were plated on these surfaces. Detergent cell extracts were prepared 48 hours later, when cells were 30% confluent, and probed for Stat3-ptyr705 as above. No difference in cell morphology was noted when the cells were plated on these coated surfaces, compared to plastic. As shown in Fig. 5, there was a dramatic and graded increase in Stat3-ptyr705 levels, in proportion to the amounts of 11/EC12 used to decorate these surfaces (lanes 2-5), while there was no increase in Stat3-ptyr705 when Balb/c3T3 cells were plated on petri dishes coated with the corresponding fragment derived from E-cadherin (E/EC12), as a negative control (Fig. 5, lane 1). As a further control, normal mouse breast epithelial HC11 cells which are naturally devoid of cadherin-11 (Fig. 2A), were plated on surfaces coated with 11/EC12 or on the corresponding, E-cadherin fragment E/EC12. As expected, there was no increase in Stat3-ptyr705 when HC11 cells were grown on surfaces coated with 11/EC12 (Fig. 5, lanes 7 and 8), while there was an increase upon growth of HC11 cells on surfaces coated with the homologous E/EC12 fragment (lane 9), which argues for a specificity of cadherin interactions. The increase in Stat3-ptyr705 required at least 20 hrs and was most pronounced when cells were at a confluence of

35% or less, while at higher densities the Stat3 activation caused by direct cell-cell contact obscured the Stat3 activation brought about by cadherin ligation to the 11/EC12 fragment coating the plate. Similar results were obtained with the 10T½, mouse fibroblasts, which also express cadherin 11 (not shown). The increase was specific to Stat3, since no increase in Erk1/2 was ever noted under these conditions (Fig. 5, middle panel). The dramatic and specific increase in Stat3-ptyr705 upon direct cadherin-11 engagement in mouse fibroblasts, which was proportional to the density of 11/EC12 present on the culture surface, indicates that cadherin-11 engagement is sufficient to activate Stat3.

Cadherin-11 engagement increases the activity as well as protein levels of the Rac1/Cdc42 GTPases

Early data demonstrated that cell to cell adhesion activates the Rac1, Rho family GTPase (reviewed in[21]). Therefore, to examine the potential role of Rac1 in the cadherin-11 dependent, Stat3 activation in our system, Rac1 activity was examined in Balb/c3T3 cells grown to different densities. This was performed by assessing the binding between Rac1-GTP and its effector p21-activated kinase (PAK) in cell extracts using pull-down assays as before[17]. As shown in Fig. 6A, confluent Balb/c3T3 cultures had substantially higher Rac1-GTP levels than their counterparts growing at a density of 40% (lane 1 vs 4). Similar results were obtained with mouse 10T½ fibroblasts which also express cadherin-11 (not shown). The above results demonstrate that cell density causes a dramatic increase in the activity of Rac1, in both types of mouse fibroblasts.

It was previously demonstrated that Rac1 can be subjected to proteasome-mediated degradation [21]. Therefore, to explore the potential effect of cadherin-11 engagement upon the levels of ***total*** Rac1 protein, detergent extracts from cells grown to different densities were blotted and probed for Rac1. As shown in Fig. 6A, there was a sharp increase in ***total*** Rac1 protein levels with cell density, which could explain the increase in active Rac1-GTP at high densities. Similar results were obtained with 10T½ mouse fibroblasts (not shown). These results indicate that, in addition to Rac1 ***activity***, cell-cell adhesion also causes a dramatic increase in ***total*** Rac1 protein levels.

To investigate whether the increase in Rac1 protein levels with cell density is due to direct cadherin-11 engagement, Balb/c3T3 cells were plated in 11/EC12-coated dishes as above and Rac1 protein levels examined. As shown in Fig. 6B, plating on 11/EC12-coated surfaces, besides leading to an increase in Stat3-ptyr705, also caused a dramatic increase in Rac1 protein levels. We next examined the effect of cadherin-11 knockdown upon Rac1. Balb-shCad11 cells were plated to different densities and Rac1 levels examined and compared to the parental Balb/c3T3 cells by Western blotting analysis. As shown in Fig. 6C, Balb-shCad11 cells had substantially lower Rac1 levels than the parental Balb/c3T3, indicating that cadherin-11 is required for the cell density-mediated, increase in Rac1 levels. Cdc42 activity and protein levels mirrored Rac1 and displayed a parallel increase with cell (data not shown). The above data taken together further demonstrate that direct cadherin-11 engagement induces the cell-cell adhesion-mediated increase in the levels and activity of these two, Rho family GTPases in Balb/c3T3 and 10T½ fibroblasts.

Rac1 and Cdc42 are required for the Cadherin-11 mediated, Stat3 activity increase

To examine whether the increase in Rac1 levels we observed in confluent Balb/c3T3 cells is actually ***required*** for the Stat3 activity increase, Rac1 levels were reduced through infection with a retroviral vector carrying a Rac1-specific, shRNA insert. Following infection and selection for puromycin resistance, Stat3-ptyr705 levels were examined at different densities as above. As shown in Fig. 6D, there was a substantial reduction in Stat3-ptyr705 levels upon expression of shRac1 at all densities examined. Similar results were obtained upon Cdc42 downregulation (Fig. 6E). The residual Stat3-ptyr705 following shRac1 expression (Fig. 6D) is most probably due to Stat3 phosphorylation mediated by Cdc42, and vice versa. The above data taken together indicate that the Rac1 and Cdc42, Rho family GTPases, which are dramatically activated through cell to cell adhesion, are essential components of the pathway whereby cadherin-11 engagement triggers the Stat3 phosphorylation and activity increase observed at high confluence.

Cell density inhibits the proteasomal degradation of Rac1 in mouse Balb/c3T3 fibroblasts

We next examined the mechanism whereby Rac1 protein levels increase with cell density. As shown in Fig. 7A, there was no increase in Rac1 mRNA levels with cell density, measured by RT-PCR, which points to a

post-transcriptional mechanism. To examine whether this increase in Rac1 protein levels was, in fact, due to inhibition of proteasome-mediated degradation, we at first made use of the MG132 proteasome inhibitor[22]. As shown in Fig. 7B, MG132 treatment of sparsely growing Balb/c3T3 cells caused a substantial increase in Rac1 protein levels as well as Stat3-ptyr705. At the same time, Erk1/2 levels remained unchanged, indicating that, under conditions of low cell to cell adhesion, the proteasome may be involved in Rac1 degradation specifically.

To further demonstrate the importance of ubiquitination, we took advantage of the ts20 cell line, derived from Balb/c3T3 fibroblasts. Due to a mutation in the gene for the ubiquitin activating enzyme E1, which makes it susceptible to accelerated destruction, this line is defective in protein ubiquitination at high temperatures (39^{o}C), while ubiquitination is normal at 34^{o}C [23]. To examine the effect of E1 inactivation upon Rac1 and Stat3-ptyr705 levels, ts20 cells were grown to different densities at 34^{o} or 39^{o}C, along with the parental Balb/c3T3, and Rac1 and Stat3-ptyr705 levels examined. The results (Fig. 7C) revealed that in ts20 cells grown to low densities ($0.5x10^5$ cells/3 cm petri) under permissive conditions (34^{o}C, lane 1) or in the parental Balb/c3T3 at either temperature (lanes 7 and 9), levels of Rac1 and Stat3-ptyr705 were low. In contrast, ts20 cells grown to the same low densities at 39^{o}C had substantially higher Rac1 and Stat3-ptyr705 levels (lanes 1 *vs* 4), pointing to the possibility of a ubiquitination-inhibition effect. The inhibition of ubiquitination was continuously required (see supplementary data Fig. S4). The above data taken together demonstrate that inhibition of the ubiquitin ligase E1 can cause a dramatic increase in both Rac1 and Stat3-ptyr705 levels.

To further examine whether Rac1 itself might actually be a substrate of the proteasome in sparsely growing cells, we examined whether Rac1 is modified by ubiquitin tagging in Balb/c3T3 fibroblasts. To this effect, we searched for the presence of Rac1 in the pool of ubiquitinated proteins, by probing anti-ubiquitin immunoprecipitates for Rac1 by Western blotting. In fact, a somewhat diffuse band of ubiquitin-tagged Rac1, consistent with short chain polyubiquitination [21] was detected in immunoprecipitates from cells grown to 30% confluence (Fig. 7D, lane 3). This protein complex was not present at 100% confluence (lane 4), consistent with inhibition of ubiquitination at high cell densities. When the anti-ubiquitin antibody was replaced with normal rabbit serum (lanes 5 and 6), or buffer alone (not shown), no Rac1 was found in the immunoprecipitates. The above data indicate that Rac1 itself is, in fact, a substrate of the proteasome in sparsely growing cells.

Cadherin-11 engagement does not allow Erk1/2 activation by IL6

Besides Stat3, IL6 stimulation was shown to activate the Erk1/2 (Erk) kinase by triggering its phosphorylation at a TEY sequence[25]. However, our present data demonstrate that levels of doubly-phosphorylated, p-Erk1/2 remained unaffected by cell density (Fig. 2B), or direct cadherin engagement (Fig. 5), although Stat3-ptyr705 levels were dramatically increased. To solve this apparent paradox, we examined the ability of IL6 itself, whose synthesis is induced upon cadherin engagement and is the trigger of Stat3 upregulation, to activate Erk as a function of cell density. Balb/c3T3 cells were grown to 50% or 2 days postconfluence, serum-starved and, following IL6 stimulation, cell extracts were probed for p-Erk or Stat3-ptyr705. As shown in Fig. 8A, at a confluence of 50%, IL6 addition caused a dramatic increase in both Stat3-ptyr705 (upper panel) and p-Erk (lower panel) as expected, based on the published literature[25]. As previously documented, cell density *per se* caused an increase in Stat3-ptyr705 levels (Fig. 8B, upper panel lanes 1-3 *vs* 4-6), and IL6 caused a further activation at both densities (lanes 1 vs 3 and 4 vs 6). Interestingly however, in densely growing cultures IL6 was unable to bring about an increase in p-Erk levels (Fig. 8A, lower panel, lanes 4 and 5), hinting at the possibility of a profound effect of confluence on the response of Balb/c3T3 cells to IL6 addition. To investigate whether this might be due to cadherin function *per se*, the same experiment was conducted with the Balb-shCad11 cells, which are deficient in cadherin-11. As shown in Fig. 8B, in sharp contrast to the parental Balb/c3T3 cells, IL6 could stimulate Erk in densely growing, cadherin-11 deficient, Balb-shCad11 cells (Fig. 8B, lower panel, lanes 3 *vs* 4), clearly indicating that it is indeed cadherin-11 engagement that prevents Erk activation by IL6.

Cadherin-11 plays a positive role in cell division, survival and migration of Balb/c3T3 fibroblasts

Previous results have shown that Stat3 signalling contributes to the induction of anti-apoptotic genes, such as *Bcl-xL* and *mcl-1* [26,27], while it downregulates the p53 promotor [28], thus protecting tumor cells from

apoptosis. To examine the functional consequences of the cadherin-11 mediated, Stat3 activation, we examined the effect of cadherin-11 knockdown in Balb/c3T3 cells. Apoptosis was examined in Balb-shCad11 cells and the parental Balb/c3T3 by terminal deoxynucleotidyl transferase dUTP nick end labeling (TUNEL) staining as before[35]. As shown in Fig. 9A, cadherin-11 deficient, Balb/c3T3 cells succumbed to apoptosis when confluent (panel b), while no apoptosis was noted in the parental Balb/c3T3, even at high densities (panel d), indicating that cadherin-11 plays a positive role in cell survival signalling.

We next evaluated the effect of cadherin-11 downregulation upon the rate of cell growth. As shown in Fig. 9B, cadherin-11 knockdown cells had a doubling time of 35 hrs, while the doubling time of the parental Balb/c3T3 was 24 hrs, indicating that cadherin-11 plays an important, positive role in cell proliferation.

Extensive evidence has indicated that Rac1 is required for cell motility, through the formation of lamellipodia at the leading edge of cells in a wound healing assay[29]. Since cadherin-11 leads to Rac1 activation, we examined the effect of cadherin-11 knockdown upon cell migration. Balb-shCad11 cells were plated in plastic petri dishes. Two days post-confluence, a scratch-wound was introduced to the monolayer using a plastic pipette tip, and the cells allowed to migrate into the gap. As shown in Fig. 9C, 16 hrs later the parental Balb/c3T3 cells had moved to close the wound (b), while in Balb-shCad11 cells a substantial amount of space was still remaining (d). Although the parental Balb/c3T3 cells grow faster than Balb-shCad11, the difference in growth rate cannot account for the increase in rate of migration and gap closure, within 16 hrs. Downregulation of Stat3 through shRNA knockdown[30], or treatment with the CPA7 inhibitor[31] caused a similar decrease in cell migration of Balb/c3T3 cells (not shown), as previously reported in other systems[34,32]. Taken together, the above findings indicate that cadherin-11 is an essential factor necessary for survival, proliferation and migration of Balb/c3T3 cells.

Specific Aim 2: Examination of the role of Stat3 in confluent cultures: Effect of Stat3 upon p53

Cell density causes a dramatic increase in cav1 levels

In our attempt to decipher the interrelationship between Stat3 and p53, we discovered another potential player: Caveolin 1 (cav1), a 22 KDa membrane protein is the major protein responsible for the organization and maintenance of caveolae microdomains[6,8]**.** Cav1 recruits many receptor and non-receptor tyrosine kinases and through binding to its scaffolding-domain, cav1 sequesters the kinases in an inactive form, thereby preventing their involvement in signaling pathways[8]. Early results demonstrated that cell density can increase cav1 levels[38], but the levels of cav1 at confluences beyond 100% had not been examined. To examine the effect of extensive cell to cell adhesion upon cav1 levels, NIH3T3 cells were grown to 70% confluence and over several days thereafter cell extracts were probed for cav1 by western blotting. Our results show that cav1 levels were almost undetectable in sparsely growing cells (Fig. 10A, lanes 1-2) while density caused a dramatic increase (Fig. 10A, lanes 3-5). These results demonstrate that cell density must be taken into account in experiments measuring cav1 levels in a given cell line.

cav1 up-regulation decreases Stat3 activity and induces apoptosis

Previous data demonstrate that p53 up-regulates caveolin-1 gene expression[40], while, in a positive feedback loop, caveolin-1 expression increases the activity of p53[41]. Since Stat3 downregulates p53 by direct promotor binding[39], we explored the potential involvement of Stat3 in p53 upregulation by cav1. wtCav1, fused to red fluorescence protein (wt-cav1-mRFP), were expressed in NIH3T3 or MCF7 cells. The results demonstrated a potent reduction in Stat3-ptyr705 levels upon cav1 overexpression in both cell lines, indicating that cav1 down-regulates Stat3 activity (Fig. 11A , lanes 1-4 vs, 5-8 left panel and lanes 1&4 vs lanes 2-3 right panel). Since Stat3 is known to inhibit p53 transcription through promotor binding[25], these data also point to the possibility that cav1 may, in fact, activate p53 through Stat3 inhibition.

To examine whether cav1 overexpression can also cause apoptosis, NIH3T3 cells transfected with the wt-cav1GFP (Fig. 11B,left panel) and MCF7 cells transfected with the wt-cav1-mRFP(Fig. 11B, right panel) Our results revealed extensive apoptotic death in MCF7 and NIH3T3 cells upon wt-cav1 expression by morphology.

Therefore, our findings point to cav1 as a potent inhibitor of Stat3 activity, and hint at the possibility that Stat3 downregulation by cav1 may be behind the apoptosis observed upon cav1 transfection. In addition, since the Stat3 downregulation by cav1 could upregulate p53, this would also explain the p53 upregulation by cav1 overexpression. Taken together, the above data reveal the presence of a potent, negative regulatory loop between cav1, p53 and Stat3 that leads to apoptosis.

Stat3 overexpression can protect from cav1-mediated apoptosis

Several studies have shown that Stat3 is responsible for transcribing anti-apoptotic genes such as Bcl-Xl and Mcl-1 that promote cell survival[28,42,43]. Since Stat3 promotes cell survival, we examined whether Stat3 could rescue cells from cav1-mediated apoptosis. Therefore, we co-transfected NIH3T3 mouse fibroblasts with EGFP-cav1 and a plasmid expressing the constitutively active form of Stat3, Stat3C (a gift of Dr. Bromberg), and the morphology of the cells was observed over 2 weeks. The results showed that Stat3C co-expression could overcome apoptosis triggered by cav1 (Fig. 12A).

Downregulation of Stat3 upregulates cav1 levels

Although examination of the cav1 promotor did not reveal any *bona fide* Stat3 consensus binding site, a Stat3 binding site is present in cav1 intron 2. Such a functional, Stat3 binding site is present in the fourth intron of the Wnt5a gene[44]. In addition, 2 sp1 transcription factor binding sites exist in the human cav1 gene, where Stat3 may bind in conjunction with sp1, in a manner previously described for the NHE3[45] and VEGF[46] promotors. In fact, our results demonstrated for the first time that, in a feedback loop, Stat3 inhibition following infection with an Adenovirus vector expressing a Stat3-specific, shRNA, resulted in a dramatic increase in cav1 levels (Fig. 12B), indicating that Stat3 also downregulates cav1 expression. Since p53 upregulates cav1[40], and Stat3 blocks the p53 promotor[29], it is possible that Stat3 may block cav1 simply by downregulating p53, rather than downregulating the cav1 promotor directly. Whether the increase in cav1 through Stat3 inhibition is a transcriptional effect will be examined by measuring cav1 mRNA level following Stat3 downregulation. Whether these are, in fact Stat3 binding sites in vivo will be examined by chromatin immunoprecipitation assays.

Cadherin 11 or Rac1 downregulation increases cav1 levels

Cadherin-11 plays a very important role in regulating cellular motility. In fact, previous studies indicated that cadherin-11 is aberrantly expressed in cancer cells with an invasive phenotype and increased risk for metastasis [47, 48]. My recent results (Geletu et al, 2013 BBA-MCR), in agreement with a recent report (Li et al., 2011) also demonstrate that cadherin-11 promotes Rac1 activation and cell migration in metastatic breast cancer cells. On the other hand, cav1 is also part of a signalling pathway that leads to the ubiquitylation and degradation of Rac1[49]. Therefore, we examined the effect of cadherin-11 and Rac1 upon cav1 level. Cadherin-11, or Rac1 were downregulated using shRNA expressing, retroviral constructs. As shown in Fig. 13 (A & B), cadherin-11 or Rac1 knockdown caused an increase in cav1 levels, at all densities examined. These results taken together demonstrate the presence of a potent, negative regulatory loop between cav1 on the one hand, and cadherin-11 and Rac on the other.

Specific Aim 3. Examination of the incidence of Stat3 activation, in conjunction with Rac1 and p53 levels in primary tumors, and correlation with the type of tumor, resistance to Herceptin, disease stage and outcome.

This part of the project is ongoing as a planned collaboration with Dr. Bruce Elliott's lab. A number of different antibodies were tested, using cell pellets and Test TMA. We finished testing all the antibody that we plan to use for our project. Some of the data were recently published (Cass *et al*, ***Cancers***, in press, September, 2012) and will now be expanded to a larger array that will include Rac, cadherin-11, cav1 and survivin.

Key Research Accomplishments

- **Cell to cell adhesion triggers cytokine gene expression in mouse Balb/c3T3 fibroblasts**
- **Engagement of "mesenchymal" cadherins increases Stat3 activity**
- **Cadherin11 engagement is sufficient for direct Stat3 activation**
- **Cadherin-11 engagement increases the activity as well as protein levels of the Rac1/Cdc42 GTPases**
- **Rac1 and Cdc42 are required for the Cadherin-11 mediated, Stat3 activity increase**
- **Cell density inhibits the proteasomal degradation of Rac1 in mouse Balb/c3T3 fibroblasts**
- **Cadherin-11 engagement does not allow Erk1/2 activation by IL6**
- **Cadherin-11 plays a positive role in cell division, survival and migration of Balb/c3T3 fibroblasts**
- **Cell density causes a dramatic increase in cav1 levels**
- **cav1 up-regulation decreases Stat3 activity and induces apoptosis through the scaffolding domain**
- **Stat3 overexpression can protect from cav1-mediated apoptosis**
- **Downregulation of Stat3 upregulates cav1 levels**
- **Cadherin 11 or Rac1 downregulation increases cav1 levels**

Reportable Outcomes

Papers published or in press

1. **Geletu, M.,** Guy, S., Greer, S., Arulanandam, R. and Raptis, L. (2013) Src and Stat3 effects upon gap junctional, intercellular communication in lung cancer lines. **Accepted *Anticancer Research* .**

2. **Geletu, M ,** Arulanandam, R., Chevalier, S., Saez, B., Larue, L., Feracci, H. and Raptis, L. (2013). Classical cadherins control survival through the gp130/Stat3 axis. **Biochim Biophys Acta. 2013 Aug;1833(8):1947-59 *Molecular Cell Research*,**

3. **Geletu M,** Greer S, Arulanandam R, Tomai E and Raptis, L. (2012) Stat3 is a positive regulator of gap junctional intercellular communication in cultured, human lung carcinoma cells. ***BMC Cancer*** 18:605-12

4. **Geletu, M.** Trotman-Grant, A and Raptis, L. (2012). Mind the gap; regulation of gap junctional, intercellular communication by Src oncogene and its effectors. ***Anticancer Research*** 32:4245-50

5. Raptis L, Arulanandam R, Geletu M, Turkson J. (2011). The R(h)oads to Stat3: Stat3 activation by the Rho GTPases. **Exp Cell Res**. 317(13):1787-95

6.Geletu, M. and Raptis, L. (2011). Viral oncogenes and the retinoblastoma family. In: *Retinoblastoma*, Govindasamy Kumaramanickavel Editor. *InTech,* Croatia. In press (Open access, Book chapter). Retrieved from http://www.intechweb.org/subject/....

7. Arulanandam, R., Geletu, M., Feracci, H. and Raptis, L. (2010). Rac^{V12} requires gp130 for Stat3 activation, cell proliferation and migration. ***Experimental Cell Research* 316**, 875-886).

8. Greer S, Honeywell R, Geletu M, Arulanandam R and Raptis L. (2010). Cell density effects on the levels of housekeeping gene products. ***Journal of Immunological Methods* 355**, 76-79.

9. Arulanandam, R, Geletu M and Raptis L. (2010) The Simian Virus 40 Large Tumor antigen requires Src for full neoplastic transformation. ***Anticancer Research***, 30:47-54.

10. Geletu, M., Chaize, C., Arulanandam, R., Vultur, A., Kowolik, C., Anagnostopoulou, A., Jove, R. and Raptis, L. (2009). Stat3 activity is required for gap junctional permeability in normal epithelial cells and fibroblasts. ***DNA and Cell Biology***, 28:319-27.

A Figure from this paper was placed on the cover.

11. Raptis, L, Arulanandam, R., Vultur, A., Geletu, M., Chevalier, S. and Feracci, H. (2009) Beyond structure, to survival: activation of Stat3 by cadherin engagement. ***Biochemistry and Cell Biology* 87**, 835-843

Manuscripts submitted

1. **Geletu, M,** Guy, S, Firth, K, and Raptis L. A functional assay for gap junctional examination; electroporation of adherent cells on Indium-Tin oxide. Submitted to *JoVE*.

2. **Geletu, M,** Greer, S, Guy , S and Raptis, L. Phosphatidylinositol-3 kinase activation increases gap junctional intercellular communication in rat liver epithelial cells. In preparation for submission to the *Journal of Virology.*

Abstracts with poster presentations

1. **Geletu, M., Arulanandam, R., Greer, S., Trotman-Grant, A., Tomai, E. and Raptis, L.** Stat3 is a positive regulator of gap junctional intercellular communication in cultured, human lung carcinoma cells. April 6-10, 2013 Washington, DC , USA.

2. Stephanie Guy, **Mulu Geletu**, Rozanne Arulanandam and Leda Raptis. Cadherin-11 function is required for full neoplastic transformation of mouse fibroblasts by v-Src. April 6-10, 2013 Washington, DC , USA

3. **Mulu Geletu Leda Raptis, , Rozanne Arulanandam**. Cadherin-11 function is required for full neoplastic transformation by v-Src. 103th annual meeting of the American association for Cancer research, March 31-April 4, 2012, Chicago, Illinois

4. **Mulu Geletu, Reva Mohan, Rozanne Arulanandam, Adina Vultur, and Leda Raptis.** 2012 Reciprocal regulation of caveolin-1 and Stat3 in normal fibroblasts and breast carcinoma lines. 103th annual meeting of the American association for Cancer research, March 31-April 4, 2012, Chicago, Illinois

5. **Mulu Geletu, Rozanne Arulanandam, Carmeline D'Abreo, Leda Raptis**. 2011 Cadherin-11 function is required for full neoplastic transformation by v-Src. The inaugural Canadian Cancer Research Conference, November 27-30, 2011 in Toronto, Ontario.

6. **Mulu Geletu, Samantha Greer, and Leda Raptis.** 2011 Activated phosphatidylinositol-3 kinase: An oncogene that increases gap junctional communication. The inaugural Canadian Cancer Research Conference, November 27-30, 2011 in Toronto, Ontario.

7. **Mulu Geletu, Reva Mohan, Rozanne Arulanandam, Bharat Joshi, Ivan Nabi, Leda Raptis.** 2011.Reciprocal regulation of Stat3 and caveolin-1 in normal fibroblasts and breast carcinoma lines. 102th annual meeting of the American association for Cancer research, April 2-6, 2011, Orlando, Florida, USA

8. **Greer, S., Geletu, M. and Raptis, L**,. 2011. Differential effects of polyoma virus middle tumor antigen mutants upon gap junctional, intercellular communication. 102th annual meeting of the American association for Cancer research, April 2-6, 2011, Orlando, Florida, USA.

9. **Mulu Geletu, Reva Mohan, Rozanne Arulanandam, Bharat Joshi, Ivan Nabi, Leda Raptis.** 2011.Reciprocal regulation of Stat3 and caveolin-1 in normal fibroblasts and breast carcinoma lines. The Fourteenth Annual Scientific Meeting for Health Science Research Trainees May 31, 2011 Faculty of Health Sciences, Queen's University.

10. **Mulu Geletu, Reva Mohan, Rozanne Arulanandam, Bharat Joshi, Ivan Nabi, Leda Raptis.** 2011.Reciprocal regulation of Stat3 and caveolin-1 in normal fibroblasts and breast carcinoma lines. Department of Defense (DOD) Breast Cancer Research Program (BCRP) sixth Era of Hope Conference, August 2-5, 2011, Orlando, Florida, USA

11. **Geletu, M. Greer, S. and Raptis, L**. 2011 Activated phosphatidylinositol-3 kinase; an oncogene that increases gap junctional communication. International Gap Junction Conference, August 6-11, Ghent, Belgium

12. **D'Abreo C, Arulanandam R, Geletu M and Raptis L.** 2010. Activated Src increases total Rac levels and requires Rac and IL6 for full neoplastic transformation. 101th annual meeting of the American association for Cancer research, Washington, DC.

13. **Arulanandam, R., Geletu, M., Vultur, A., Cao, J., Larue, L., Feracci, H. and Raptis, L.** 2010. Cadherin-cadherin engagement promotes cell survival via Rac/Cdc42 and Stat3. 101th annual meeting of the American association for Cancer research, Washington, DC.

14. **Mulu Geletu, Reva Mohan, Rozanne Arulanandam, Adina Vultur, and Leda Raptis.** 2010. Reciprocal regulation of Stat3 and the caveolae protein, cav-1. 101th annual meeting of the American association for Cancer research, Washington, DC.

15. **J. Cass, R. Arulanandam, M. Geletu, B. Starova, E. Carefoot, S. SenGupta, B.E. Elliott, and, L. Raptis.** A novel cadherin-dependent Rac/Stat3 pathway in invasive breast cancer. (2010). 101th annual meeting of the American association for Cancer research, Washington, DC.

16. **Rozanne Arulanandam, Mulu Geletu, Adina Vultur, and Leda Raptis.** 2009. The Simian Virus 40 Large Tumor antigen requires Src for full neoplastic transformation. 100th annual meeting of the American association for Cancer research, Denver, Colorado.

Conclusion

The three cadherins described so far, E-cadherin[17] , N-cadherin and cadherin-11, classical, type I and type II cadherins, in various combinations are present in essentially all tissues.
The fact that all activate the same Stat3 pathway, points to a central importance of this pathway in cellular survival and may explain the presence of at least one cadherin in all cells of the organism during embryonic development and homeostasis. For tumor tissues, the demonstration that N-cadherin and cadherin-11 may actually activate Stat3, despite the fact that, contrary to E-cadherin, they promote migration and metastasis[35] , may point to Stat3 as a central survival, rather than metastasis, factor. Most importantly, inhibition of these cadherins would induce apoptosis (through Stat3 inhibition) in metastatic cells specifically, while normal cells expressing E-cadherin would be spared.

.

Table I
qRT-PCR array for cytokines secreted by densely-growing cells

Gene Name	Gene Symbol	Fold Up- or Down-Regulation
Bone morphogenetic protein 1	Bmp1	4.53
Bone morphogenetic protein 10	Bmp10	2.23
Bone morphogenetic protein 2	Bmp2	2.23
Bone morphogenetic protein 3	Bmp3	2.23
Bone morphogenetic protein 4	Bmp4	2.95
Bone morphogenetic protein 5	Bmp5	3.23
Bone morphogenetic protein 6	Bmp6	3.46
Bone morphogenetic protein 7	Bmp7	2.23
Bone morphogenetic protein 8b	Bmp8b	2.23
Colony stimulating factor 1 (macrophage)	Csf1	1.43
Colony stimulating factor 2 (granulocyte-macrophage)	Csf2	9.32
Cardiotrophin 1	Ctf1	-1.11
Cardiotrophin 2	Ctf2	1.22
Fas ligand (TNF superfamily, member 6)	Fasl	2.23
Fibrosin	Fbrs	1.56
Fibroblast growth factor 10	Fgf10	2.23
FMS-like tyrosine kinase 3 ligand	Flt3l	6.15
Growth differentiation factor 1	Gdf1	-1.85
Growth differentiation factor 10	Gdf10	2.23
Growth differentiation factor 11	Gdf11	2.43
Growth differentiation factor 15	Gdf15	-1.24
Growth differentiation factor 2	Gdf2	2.23
Growth differentiation factor 3	Gdf3	2.23
Growth differentiation factor 5	Gdf5	-2.11
Myostatin	Mstn	2.23
Growth differentiation factor 9	Gdf9	3.12
Interferon alpha 2	Ifna2	2.23
Interferon alpha 4	Ifna4	2.23
Interferon beta 1, fibroblast	Ifnb1	2.25
Interferon gamma	Ifng	2.23
Interleukin 10	Il10	2.83
Interleukin 11	Il11	3.71
Interleukin 12B	Il12b	2.23
Interleukin 13	Il13	2.23
Interleukin 15	Il15	6.59
Interleukin 16	Il16	6.87
Interleukin 17B	Il17b	3.1
Interleukin 17C	Il17c	2.23
Interleukin 25	Il25	2.23
Interleukin 17F	Il17f	1.11
Interleukin 18	Il18	6.41
Interleukin 19	Il19	1.57
Interleukin 1 alpha	Il1a	2.23
Interleukin 1 beta	Il1b	2.23
Interleukin 1 family, member 10	Il1f10	2.23
Interleukin 1 family, member 5 (delta)	Il1f5	2.58
Interleukin 1 family, member 6	Il1f6	40.5
Interleukin 1 family, member 8	Il1f8	2.23

Interleukin 1 family, member 9	Il1f9	2.48
Interleukin 1 receptor antagonist	Il1rn	44.02
Interleukin 2	Il2	2.23
Interleukin 20	Il20	2.23
Interleukin 21	Il21	2.23
Interleukin 24	Il24	1.73
Interleukin 27	Il27	2.38
Interleukin 3	Il3	2.23
Interleukin 4	Il4	2.68
Interleukin 7	Il7	2.23
Interleukin 9	Il9	2.23
Inhibin alpha	Inha	6.54
Inhibin beta-A	Inhba	1.69
Left right determination factor 1	Lefty1	4.2
Leukemia inhibitory factor	Lif	2.73
Lymphotoxin A	Lta	2.23
Lymphotoxin B	Ltb	2.23
Macrophage migration inhibitory factor	Mif	4.29
Secretoglobin, family 3A, member 1	Scgb3a1	1.88
Small inducible cytokine subfamily E, member 1	Scye1	1.03
Tumor necrosis factor	Tnf	2.23
Tumor necrosis factor receptor superfamily, member 11b (osteoprotegerin)	Tnfrsf11b	1.3
Tumor necrosis factor (ligand) superfamily, member 10	Tnfsf10	11.79
Tumor necrosis factor (ligand) superfamily, member 11	Tnfsf11	2.23
Tumor necrosis factor (ligand) superfamily, member 12	Tnfsf12	2.57
Tumor necrosis factor (ligand) superfamily, member 13	Tnfsf13	7.36
Tumor necrosis factor (ligand) superfamily, member 13b	Tnfsf13b	2.23
Tumor necrosis factor (ligand) superfamily, member 14	Tnfsf14	6.87
Tumor necrosis factor (ligand) superfamily, member 15	Tnfsf15	2.23
Tumor necrosis factor (ligand) superfamily, member 18	Tnfsf18	2.23
Tumor necrosis factor (ligand) superfamily, member 4	Tnfsf4	2.23
CD40 ligand	Cd40lg	2.23
CD70 antigen	Cd70	3.14
Tumor necrosis factor (ligand) superfamily, member 8	Tnfsf8	2.23
Tumor necrosis factor (ligand) superfamily, member 9	Tnfsf9	1.91
Taxilin alpha	Txlna	-1.13
Glucuronidase, beta	Gusb	-2.03
Hypoxanthine guanine phosphoribosyl transferase 1	Hprt1	1.1
Heat shock protein 90 alpha (cytosolic), class B member 1	Hsp90ab1	-1.32
Glyceraldehyde-3-phosphate dehydrogenase	Gapdh	3.48
Actin, beta	Actb	-1.43
Interleukin 6	Il6	32.67

Figure 1

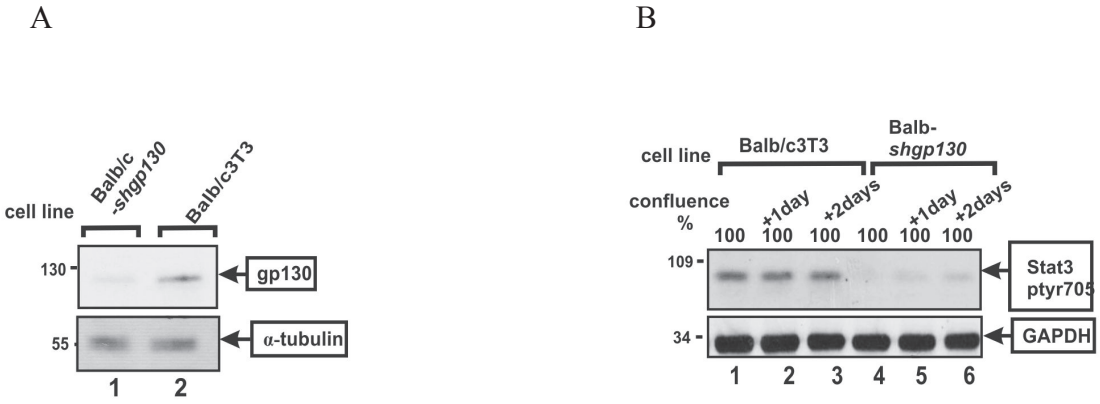

Figure 1: Gp130 knockdown causes a dramatic reduction in Stat3-ptyr705
A: Extracts from Balb/c3T3 cells before (lane 2) or after (lane 1) gp130 knockdown were probed for gp130 or Hsp90 as a loading control.

B: Extracts from Balb/c3T3 cells before (lanes 1-3) or after (lanes 4-6) gp130 knockdown were probed for Stat3-ptyr705 or Hsp90 as a loading control.

Figure 2

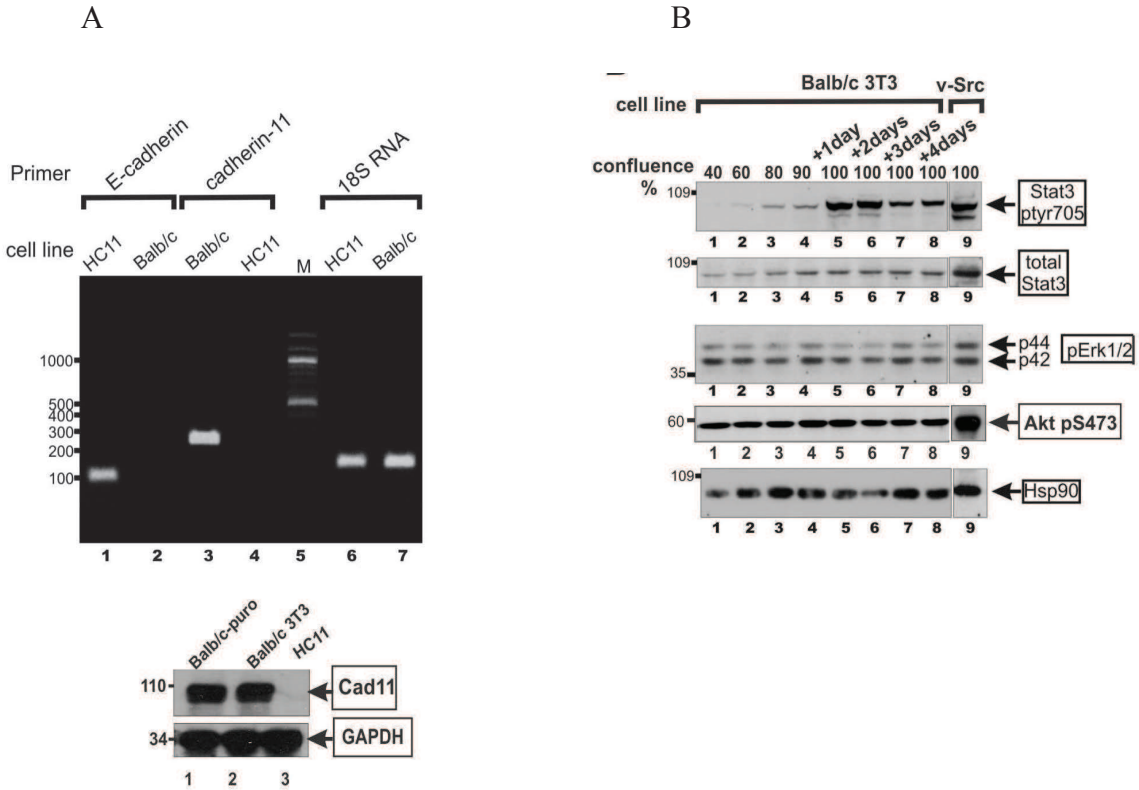

Figure 2: Cell density triggers Stat3 phosphorylation in Balb/c3T3 cells.

A: Balb/c3T3 cells express cadherin-11 but not E-cadherin
Upper panel: RNA extracts from Balb/c3T3, mouse fibroblasts or the HC11, mouse breast epithelial line were probed by RT-PCR for E-cadherin (lanes 1 and 2) or cadherin-11 (lanes 3 and 4), using 18S RNA as an internal control (lanes 6 and 7) (see Materials and Methods). Numbers at the left refer to the oligonucleotide marker lane (M).
Lower panel: Detergent extracts from Balb/c3T3 (lane 2), control Balb/c3T3 cells infected with a pBabe-puro vector and selected for puromycin resistance (lane 1) or mouse breast epithelial HC11 cells were probed for cadherin-11, with GAPDH as a loading control.

B: Cell density upregulates Stat3-ptyr705 levels in Balb/c3T3 cells.
Lysates from Balb/c3T3 fibroblasts grown to increasing densities were resolved by gel electrophoresis and probed for Stat3-ptyr705, total Stat3, phospho-Erk1/2, Akt-pser473 or Hsp90 as a loading control, as indicated (see Materials and Methods). Numbers at the left refer to Molecular Weight markers. vSrc: vSrc- transformed, Balb/c3T3 fibroblasts.

Figure 3

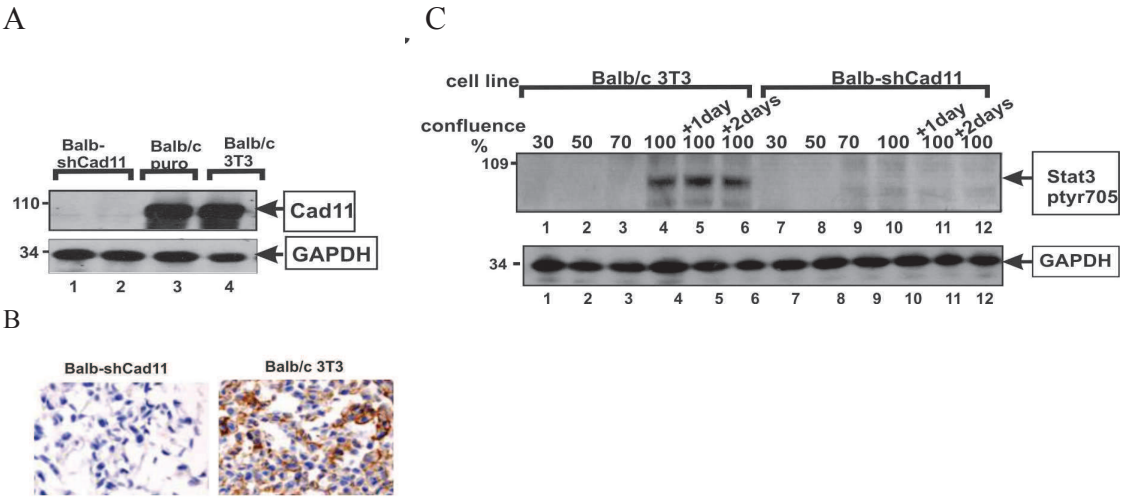

Figure 3: Cadherin-11 knockdown causes a dramatic reduction in Stat3-ptyr705 in Balb/c3T3 cells

a. Extracts from 2 independent clones of sh-Cad11 expressing, Balb/c3T3 clones (lanes 1 and 2), Balb/c3T3 cells infected with an empty vector and selected for puromycin resistance (lane 3) or the parental Balb/c3T3 cells (lane 4), all grown to high densities, were probed for cadherin-11 or GAPDH as a loading control. Note the dramatic reduction in cadherin-11 levels in sh-Cad11-expressing clones, compared to Balb/c3T3.

b. Pellets of Balb/c3T3 (right panel) or Balb-shCad11 (left panel) cells were sectioned and stained for cadherin-11 (see Materials and Methods). Note the absence of staining in Balb-shCad11 cells.

c. Detergent extracts from control Balb/c3T3 (lanes 1-6) or shCad11- expressing, Balb-shCad11 cells (lanes 7-12) were probed for Stat3-ptyr705 or GAPDH as a loading control. Note the dramatic reduction in Stat3-ptyr705 levels in shCad11-expressing clones.

Figure 4

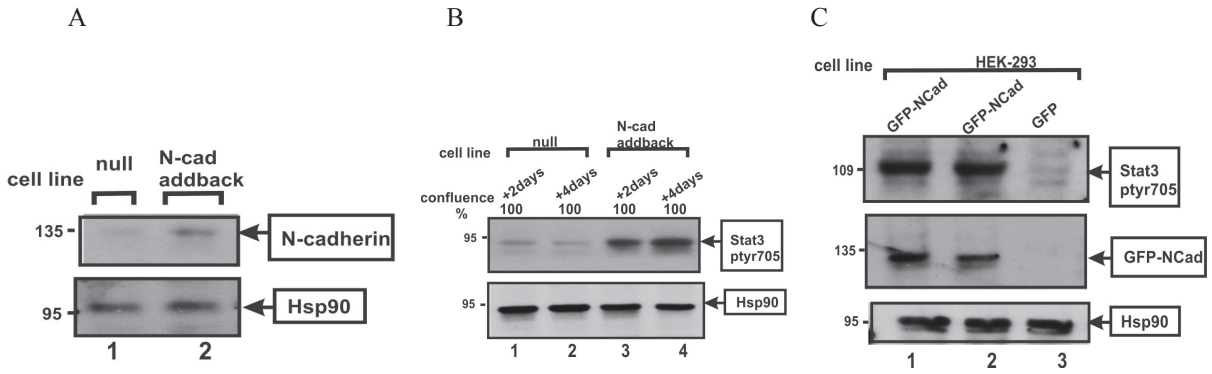

Figure 4: N-cadherin expression increases Stat3-ptyr705 levels
A: ES cells where E-cadherin was genetically ablated (null cells, lane 1) or null cells where N-cadherin was re-expressed (lane 2) were probed for N-cadherin or Hsp90 as a loading control.
B: Null cells (lanes 1,2) or N-cadherin addback cells (lanes 3,4) were probed for Stat3-ptyr705 or Hsp90 as a loading control.
C: HEK-293 cells were transfected with a GFP-Ncadherin plasmid using 5μg (lane 1) or 10μg (lane 2) per 6 cm plate or GFP alone (lane 3), and cell extracts probed 70 hrs later for Stat3-ptyr705, N-cadherin, or Hsp90 as a loading control.

Figure 5

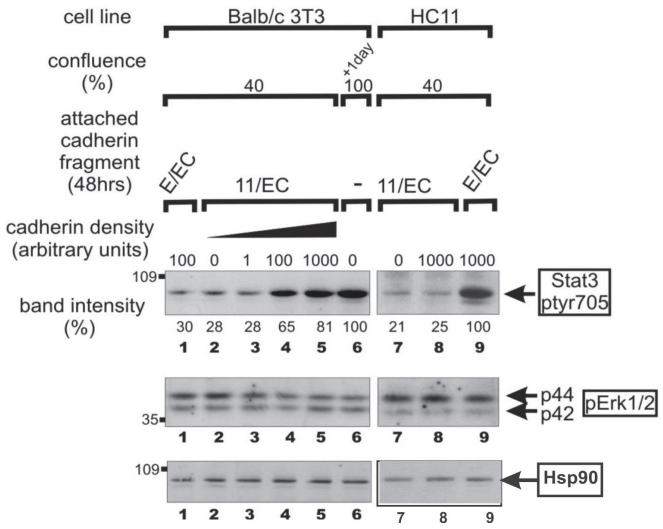

Figure 5: Cadherin-11 engagement is sufficient to activate Stat3 in Balb/c3T3 fibroblasts

Balb/c3T3 cells were grown in plastic 3cm dishes, coated with increasing amounts of the cadherin-11 fragment, 11/EC12 (lanes 2-5). 48 hours later, cell lysates were probed for Stat3-ptyr705, phospho-Erk1/2 or Hsp90 as a loading standard, as indicated. As controls, Balb/c3T3 cells, which are devoid of E-cadherin (Fig. 1A), were grown on a surface coated with the corresponding E-cadherin fragment (E/EC12, lane 1) and HC11 cells which are devoid of cadherin-11 were grown on surfaces coated by 11/EC12 (lane 8), or E/EC12 as a positive control (lane 9). Numbers under the lanes refer to band intensities obtained by densitometric scanning, with Balb/c3T3 cells grown to one day after confluence (lane 6), or HC11 cells grown on surfaces coated with 1,000 μg/ml E/EC12 fragment (lane 9) taken as 100% for lanes 1-6 and 7-9, respectively

Figure 6

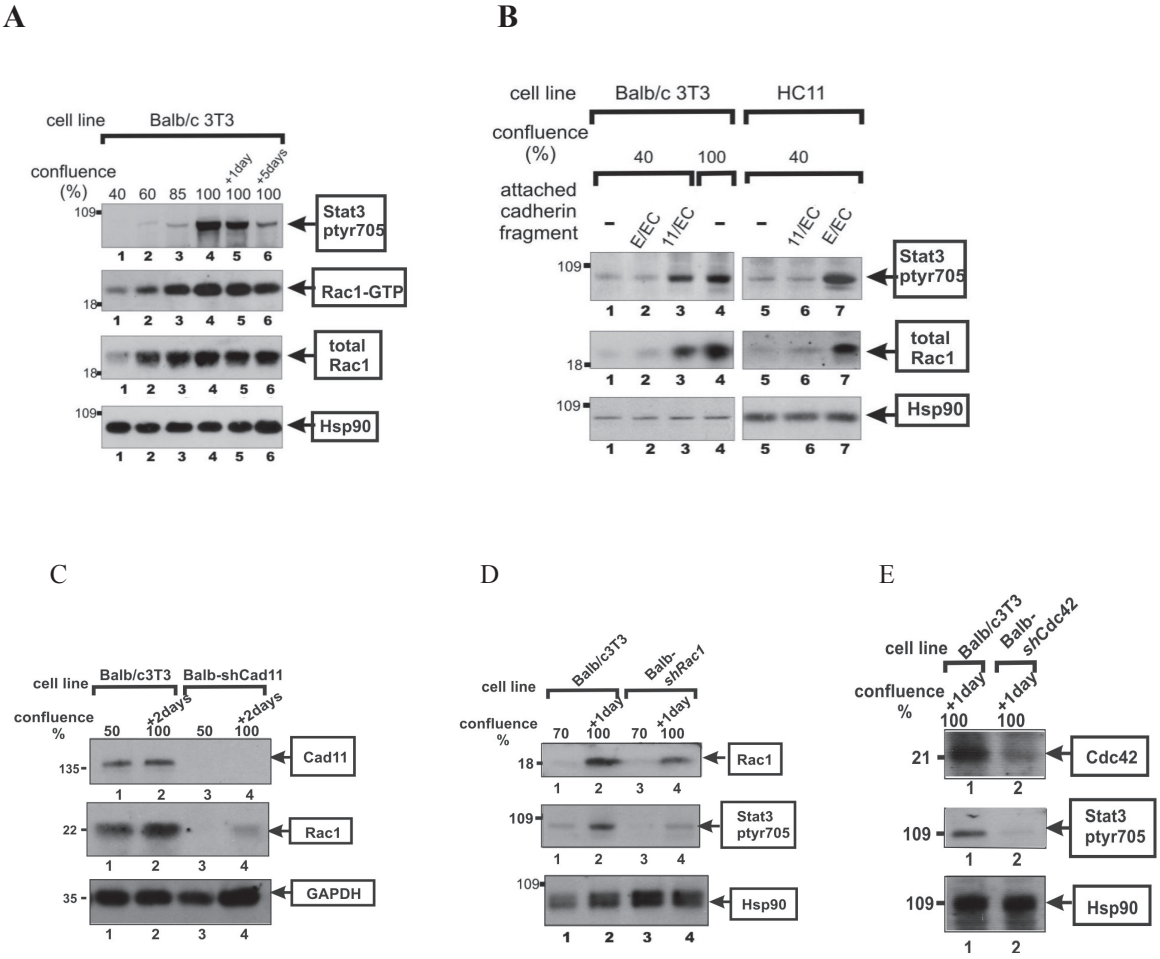

Figure 6

A. Cell density increases the activity as well as protein levels of Rac1 in Balb/c3T3 cells.

Balb/c3T3 cells were grown to different densities, up to 5 days post-confluence, as indicated. Detergent cell lysates were probed for Stat3-ptyr705, active Rac1-GTP, total Rac1 or Hsp90 as a loading control, as indicated. Numbers at the left refer to molecular weight markers.

B. Cadherin-11 engagement is sufficient to increase Rac1 protein levels.

Balb/c3T3 cells were grown in plastic petris coated with 1,000 µg/ml of the 11/EC12 fragment or the E-cadherin-derived, E/EC12 fragment. 48 hours later, detergent cell extracts were probed for Stat3-ptyr705, Rac1 or Hsp90 as a loading control, as indicated. Numbers at the left refer to molecular weight markers.

C. Cadherin-11 knockdown causes a dramatic decrease in Rac1 levels. Balb-shCad11 cells were grown to different densities and cell extracts probed for cadherin-11, Rac1 or Hsp90 as a loading control.

D. Rac1 is required for cadherin-11 mediated, Stat3 activation

Rac1 was downregulated in Balb/c3T3 cells through infection with a retroviral vector (see Materials and Methods). Individual clones were grown to different densities and extracts probed for Rac1, Stat3-ptyr705 or Hsp90 as a loading control, as indicated.

E. Cdc42 is required for cadherin-11 mediated, Stat3 activation

Cdc42 was downregulated in Balb/c3T3 cells through infection with a retroviral vector (see Materials and Methods). Individual clones were grown to different densities and extracts probed for Cdc42, Stat3-ptyr705 or Hsp90 as a loading control, as indicated.

Figure 7

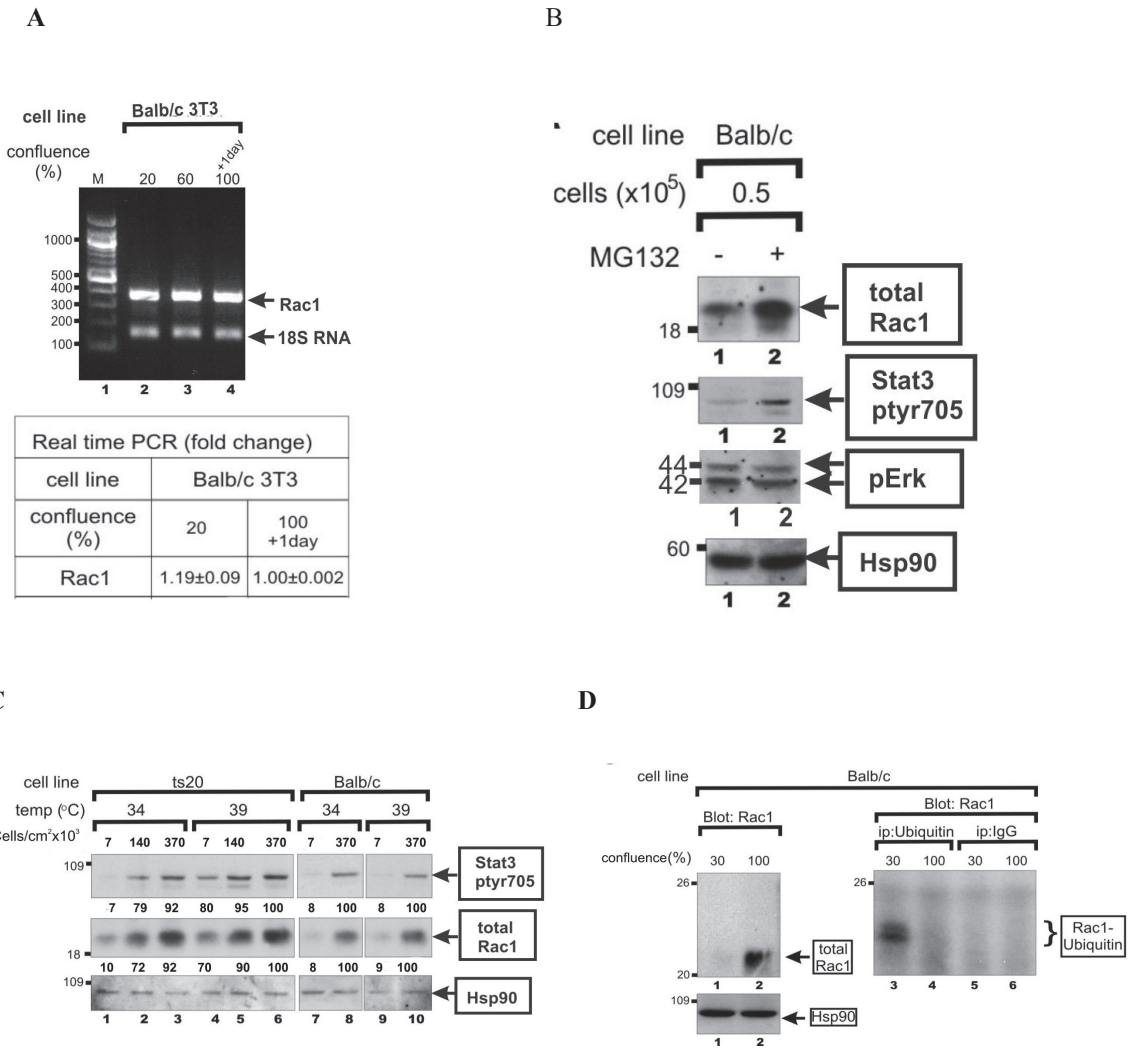

Figure 7

A. Rac1 mRNA levels are not affected by cell density.

Top panel: Balb/c3T3 cells were grown to different densities as indicated and Rac1 mRNA levels examined by RT-PCR, using 18S RNA as a control.

Bottom panel: Real-time RT-PCR was performed as described in Materials and Methods. The relative expression levels of each sample were determined using the 18S and 28S RNA expression levels, as an internal control.

B-D: Cell density inhibits the proteasomal degradation of Rac1 in Balb/c 3T3 cells

B: The proteasome inhibitor, MG132 increases total Rac1 and Stat3-ptyr705 levels.

Sparsely growing Balb/c 3T3 cells were treated with 10μM of the proteasome inhibitor, MG132 (lane 2), or not (lane 1) for 8 hrs. Detergent cell extracts were probed for total Rac1, Stat3-ptyr705, pErk or Hsp90 as a loading standard, as indicated.

C. Inhibition of the E1 ubiquitin activating enzyme increases Rac1 protein levels

ts20 (lanes 1-6) or Balb/c 3T3 (lanes 7-10) cells were grown to different densities, at 34°C (lanes 1-3 and 7-8) or 39°C (lanes 4-6 and 9-10), as indicated. Detergent cell extracts were probed for Stat3-ptyr705, Rac1 or Hsp90 as a loading control. Numbers above the lanes refer to cell numbers/cm^2 in thousands. Numbers under the lanes refer to relative band intensities, with the value of lane 6 taken as 100%.

Note the high levels of Stat3-ptyr705 at a low confluence, at 39°C (lane 4 *vs* lane 1).

D: Rac1 is ubiquitinated *in vivo*, at low cell densities.

Left panel: Extracts from Balb/c3T3 cells grown to 30% or 100% confluence were blotted against Rac1 (arrow).

Right panel: Balb/c3T3 cells were grown to 30% or 100% confluence and anti-ubiquitin immunoprecipitates of detergent cell extracts blotted against Rac1 (lanes 3-4). As a control, extracts from cells grown to 30% confluence were immunoprecipitated with normal rabbit IgG (lanes 5-6). Bracket points to the ubiquitinated Rac1.

Figure 8

A

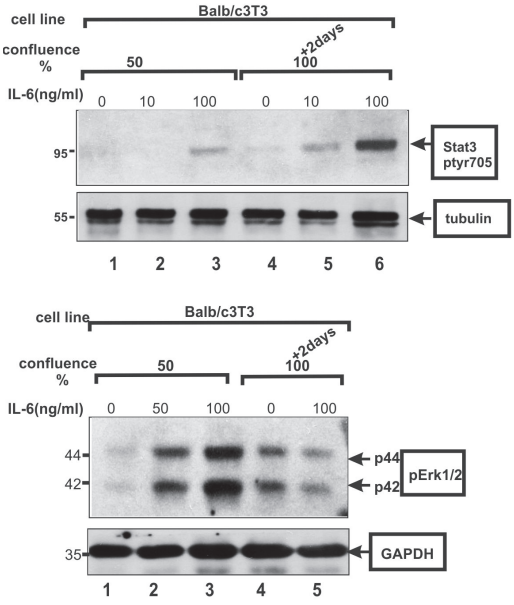

B

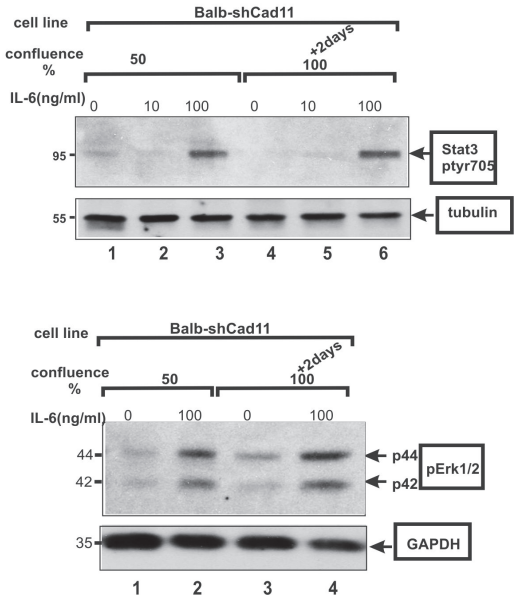

Figure 8
A: IL6 activates Stat3, but not Erk, at high densities in Balb/c3T3 cells. IL6 was added at 0, 10, 50 or 100 ng/mL for 15 min to Balb/c3T3 cells grown to 50% (lanes 1-3), or 2 days postconfluence as indicated and cell extracts probed for Stat3-ptyr705 (upper panel) or Hsp90 as a loading control. Note the absence of Erk activation at high densities (lower panel, lanes 4 and 5).

B: IL6 activates Stat3 and Erk in the absence of cadherin-11. Same as above, cadherin11-deficient, Balb-shCad11 cells. Note the Erk activation at high densities (lower panel, lanes 3 and 4).

Figure 9

A

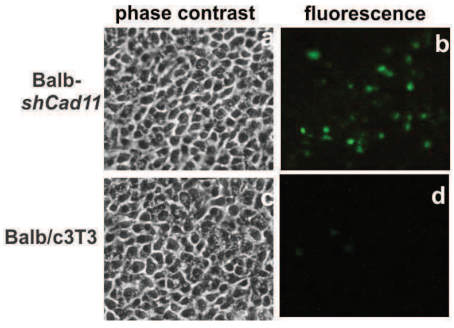

B

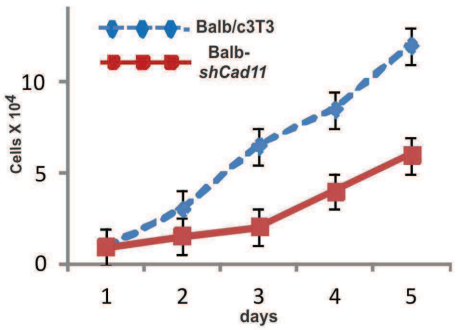

C D

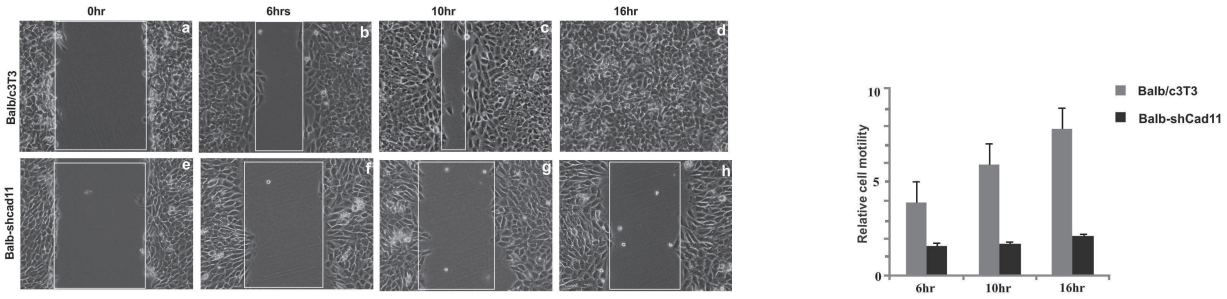

Figure 9

Cadherin-11 engagement promotes survival, proliferation and migration

A: Balb/c3T3 or Balb-shCad11 cells were grown to densities of two days post-confluence and TUNEL-stained for apoptosis assessment (b,d) (see Materials and Methods). a,c: Same fields as in b,d, photographed under phase contrast illumination.

B: Cell proliferation: Balb/c3T3 or Balb-shCad11 cells were grown in Petri dishes in 10% serum and cell numbers obtained over several days, as indicated. Values represent averages of 3 independent experiments.

C-D: Cell migration.

C: Balb/c3T3 (panels a-d) or Balb-shCad11 (panels e-h) cells were cultured to confluence in 10% fetal calf serum, then the monolayer was wounded. Spontaneous wound closure at each of eight marked wound sites for each line, in two independent experiments was monitored by phase contrast microscopy. Representative fields, photographed at 0 (panels a,e), 6 (panels b,f), 10 (panels c,g) or 16 hrs (panels d,h) are shown. Magnification: 140x.

D: Histogram showing relative cell motility for each clone, calculated as area of wound closure at 6, 10 and 16 hrs, compared to t=0. Values represent mean +/- SD of 4 sites per line, in each of two independent experiments.

Figure 10

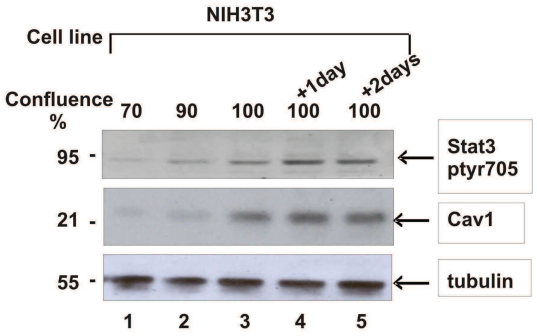

Figure 10. Stat3 activity and cav1 levels increase with cell density.

Lysates from NIH3T3 mouse fibroblasts grown to different densities were probed for Stat3-ptyr705, cav1 or tubulin as a loading control. Note that both Stat3-ptyr705 and cav1 levels increase with cell density, peaking at post-confluence.

Figure 11

A

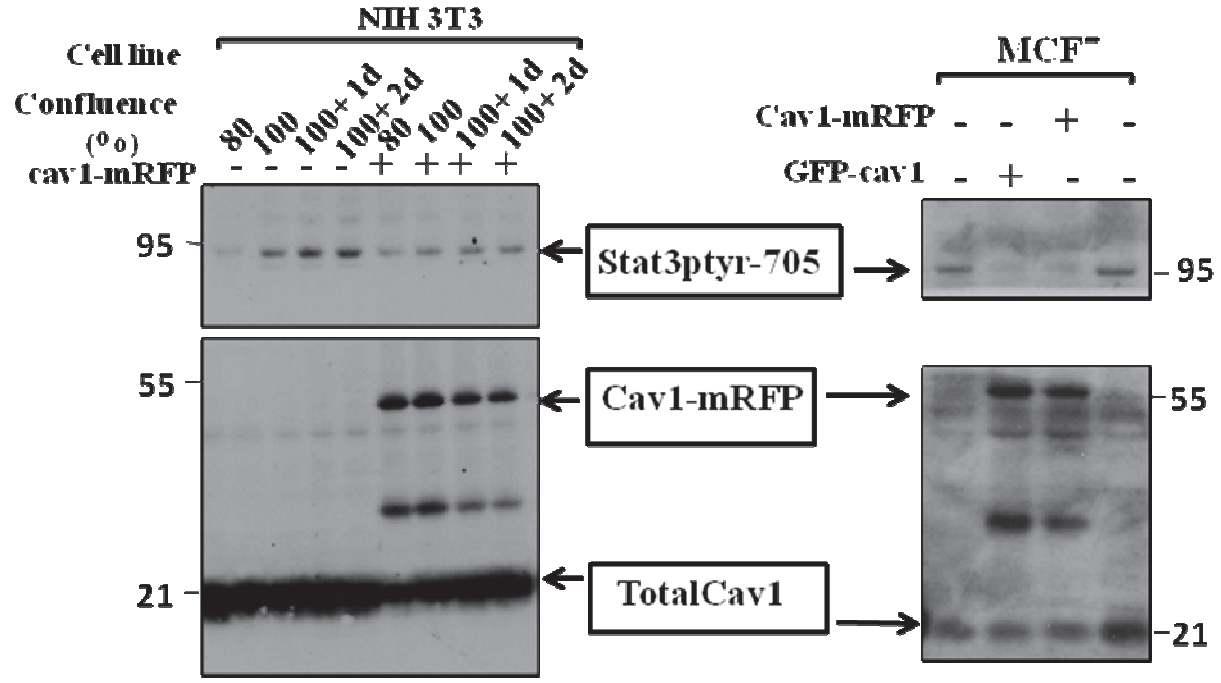

Figure 11. Cav1 upregulation decreases Stat3 activity
A: NIH3T3 and MCF7 cells were transfected with the cav1-mRFP & GFP-cav1 plasmid. Lysates were prepared at different densities and resolved by SDS-PAGE. Western blots were probed for the phosphorylated 705 form of Stat3 and total cav1. Note the cav1-mRFP band (at 55kDa), which indicates cav1-mRFP expression, which corresponds to a decrease in Stat3-ptyr705. Bottom band represents endogenously expressed cav1

B

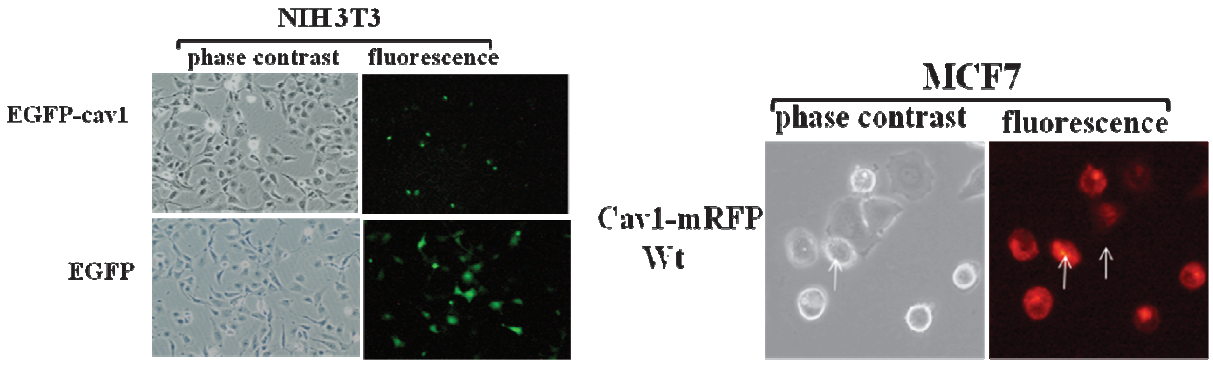

Figure 11. cav1 overexpression induces apoptosis
B: MCF-7 and NIH DL+10 cells were transfected with the cav1mRFP wt. cells were selected with G418 and stable clones were photographed under phase contrast or fluorescence illuminationNote the changes in morphology, indicating apoptosis. Magnification:240x.

Figure 12

A

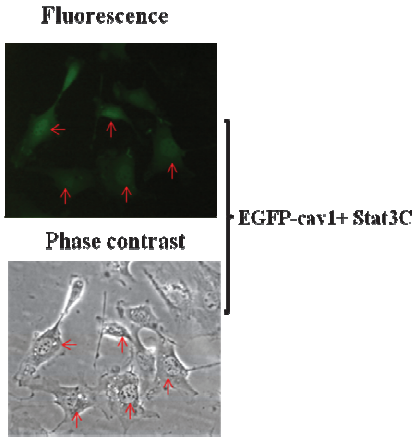

B

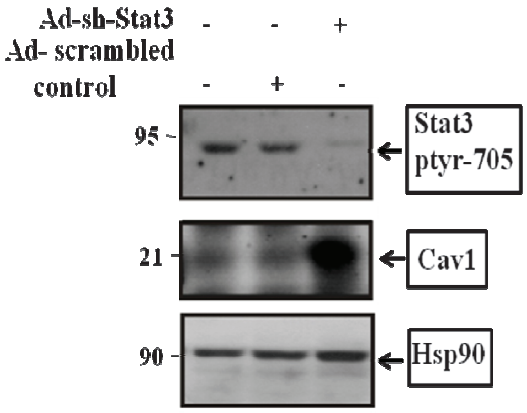

Figure 12. Stat3C co-expression rescues cells from cav1-induced apoptosis.
A: NIH DL+10 fibroblasts were co-transfected with the EGFP-cav1 and Stat3C plasmids. 96 hours later cells were photographed under phase contrast or fluorescence illumination. Note the normal morphology, indicating absence of apoptosis. Magnification: 240x .

Figure 12. Downregulation of Stat3 upregulates cav1 levels.
B: HeLa cells were infected with adenoviral constructs coding for a Stat3 siRNA (Adenovirus Stat3i) or a control vector coding for a scrambled version of the Stat3 siRNA gene (Adenovirus Stat3sc). Cell lysates were prepared approximately 36 hours after infection and the Western blots were probed for phospho-Stat3, total cav1 and tubulun as loading control. The Stat3i adenovirus vector effectively downregulated Stat3-ptyr705. This decrease in pStat3 corresponds to a significant increase in cav1 expression.

Figure 13

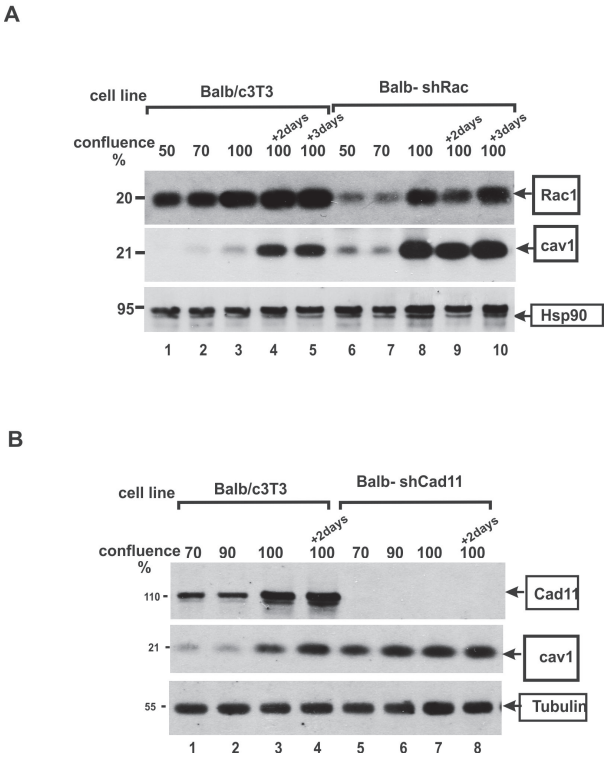

Figure 13: Cadherin 11 and Rac1 downregulation increases cav1 level

A: Rac1 knockdown causes a dramatic increases cav1 levels. Extracts from control Balb/c3T3 cells (lanes 1-5) or sh-Cad11-expressing, cells (lanes 6-10) were probed for rac1, cav1or HSP90 as a loading control. Note the dramatic increase cav1 levels in sh-Rac1 expressing cells.

B: Cadherin-11 knockdown causes a dramatic increases cav1 levels. Balb/c3T3 (lanes 1-4) and Balb-shCad11 cells (lanes 5-8) were grown to different densities and cell extracts probed for cadherin-11, cav1 or tubulin as a loading control. Note the dramatic increase in cav1 levels in sh-Cad11-expressing cells.

References

1. Yu,H., Pardoll,D., & Jove,R. STATs in cancer inflammation and immunity: a leading role for STAT3. *Nat. Rev. Cancer* **9**, 798-809 (2009).
2. Frank,D.A. STAT3 as a central mediator of neoplastic cellular transformation. *Cancer Lett.* **251**, 199-210 (2007).
3. McLemore,M.L. *et al.* STAT-3 activation is required for normal G-CSF-dependent proliferation and granulocytic differentiation. *Immunity.* **14**, 193-204 (2001).
4. Arulanandam,R. *et al.* Cadherin-cadherin engagement promotes survival via Rac/Cdc42 and Stat3. *Molecular Cancer Research* **17**, 1310-1327 (2009).

(*4*)**23**, 2600-2616 (2004).

6. Cohen,A.W., Hnasko,R., Schubert,W., & Lisanti,M.P. Role of caveolae and caveolins in health and disease. *Physiol Rev.* **84**, 1341-1379 (2004).

7. Goetz,J.G., Lajoie,P., Wiseman,S.M., & Nabi,I.R. Caveolin-1 in tumor progression: the good, the bad and the ugly. *Cancer Metastasis Rev.* **27**, 715-735 (2008).

8. Patel,H.H., Murray,F., & Insel,P.A. Caveolae as organizers of pharmacologically relevant signal transduction molecules. *Annu. Rev. Pharmacol. Toxicol.* **48**, 359-391 (2008).

9. Kerr,J. *et al.* Allelic loss on chromosome 7q in ovarian adenocarcinomas: two critical regions and a rearrangement of the PLANH1 locus. *Oncogene* **13**, 1815-1818 (1996).

10. Matsuura,K. *et al.* Loss of heterozygosity of chromosome 9p21 and 7q31 is correlated with high incidence of recurrent tumor in head and neck squamous cell carcinoma. *Anticancer Res.* **18**, 453-458 (1998).

11. Zenklusen,J.C., Oshimura,M., Barrett,J.C., & Conti,C.J. Inhibition of tumorigenicity of a murine squamous cell carcinoma (SCC) cell line by a putative tumor suppressor gene on human chromosome 7. *Oncogene* **9**, 2817-2825 (1994).

12. A. Pierres, H. Feracci, V. Delmas, A.M. Benoliel, J.P. Thiery, P. Bongrand, Experimental study of the interaction range and association rate of surface-attached cadherin 11, Proc. Natl. Acad. Sci. U. S. A 95 (1998) pp. 9256-9261.

13. R.B. Hazan, R. Qiao, R. Keren, I. Badano, K. Suyama, Cadherin switch in tumor progression, Ann. N. Y. Acad. Sci. 1014 (2004) pp. 155-163.

14. M. Orlandini and S. Oliviero, In fibroblasts Vegf-D expression is induced by cell-cell contact mediated by cadherin-11, J. Biol. Chem. 276 (2001) pp. 6576-6581.

15. A. Vultur, J. Cao, R. Arulanandam, J. Turkson, R. Jove, P. Greer, A. Craig, B.E. Elliott, L. Raptis, Cell to cell adhesion modulates Stat3 activity in normal and breast carcinoma cells, Oncogene 23 (2004) pp. 2600-2616.

16. A. Vultur, R. Arulanandam, J. Turkson, G. Niu, R. Jove, L. Raptis, Stat3 is required for full neoplastic transformation by the Simian Virus 40 Large Tumor antigen, Molecular Biology of the Cell 16 (2005) pp. 3832-3846.

17. R. Arulanandam, A. Vultur, J. Cao, E. Carefoot, P. Truesdell, B. Elliott, L. Larue, H. Feracci, L. Raptis, Cadherin-cadherin engagement promotes survival via Rac/Cdc42 and Stat3, Molecular Cancer Research 17 (2009) pp. 1310-1327.

18. H. Mak, A. Naba, S. Varma, C. Schick, A. Day, S.K. SenGupta, M. Arpin, B.E. Elliott, Ezrin phosphorylation on tyrosine 477 regulates invasion and metastasis of breast cancer cells, BMC Cancer 12 (2012) p.82.

19.S. Greer, R. Honeywell, M. Geletu, R. Arulanandam, L. Raptis, housekeeping gene products; levels may change with confluence of cultured cells, Journal of Immunological Methods 355 (2010) pp. 76-79.

20.T. Gritsko, A. Williams, J. Turkson, S. Kaneko, T. Bowman, M. Huang, S. Nam, I. Eweis, N. Diaz, D. Sullivan, S. Yoder, S. Enkemann, S. Eschrich, J.H. Lee, C.A. Beam, J. Cheng, S. Minton, C.A. Muro-Cacho, R. Jove, Persistent activation of stat3 signaling induces survivin gene expression and confers resistance to apoptosis in human breast cancer cells, Clin. Cancer Res. 12 (2006) pp. 11-19.

21. L. Raptis, R. Arulanandam, M. Geletu, J. Turkson, The R(h)oads to Stat3: Stat3 activation by the Rho GTPases, Exp. Cell Res. 317 (2011) pp. 1787-1795.

22. E.A. Lynch, J. Stall, G. Schmidt, P. Chavrier, C. D'Souza-Schorey, Proteasome-mediated degradation of Rac1-GTP during epithelial cell scattering, Mol. Biol. Cell 17 (2006) pp. 2236-2242.

23. Q. Zhu, G. Wani, J. Yao, S. Patnaik, Q.E. Wang, M.A. El Mahdy, M. Praetorius-Ibba, A.A. Wani, The ubiquitin-proteasome system regulates p53-mediated transcription at p21waf1 promoter, Oncogene 26 (2007) pp. 4199-4208.

24. Y. Zhang, J. Turkson, C. Carter-Su, T. Smithgall, A. Levitzki, A. Kraker, J.J. Krolewski, P. Medveczky, R. Jove, Activation of Stat3 in v-Src transformed fibroblasts requires cooperation of Jak1 kinase activity, J. Biol. Chem. 275 (2000) p.24935-24944.

25. P. Fischer and D. Hilfiker-Kleiner, Survival pathways in hypertrophy and heart failure: the gp130-STAT axis, Basic Res. Cardiol. 102 (2007) pp. 393-411.

26. P. Fischer and D. Hilfiker-Kleiner, Role of gp130-mediated signalling pathways in the heart and its impact on potential therapeutic aspects, Br. J. Pharmacol. 153 Suppl 1 (2008) p.S414-S427.

27. J.R. Grandis, S.D. Drenning, Q. Zeng, S.C. Watkins, M.F. Melhem, S. Endo, D.E. Johnson, L. Huang, Y. He, J.D. Kim, Constitutive activation of Stat3 signaling abrogates apoptosis in squamous cell carcinogenesis in vivo, Proc. Nat. Acad. Sci. USA 97 (2000) pp. 4227-4232.

28. P.K. Epling-Burnette, J.H. Liu, R. Catlett-Falcone, J. Turkson, M. Oshiro, R. Kothapalli, Y. Li, J.M. Wang, H.F. Yang-Yen, J. Karras, R. Jove, T.P. Loughran, Jr., Inhibition of STAT3 signaling leads to apoptosis of leukemic large granular lymphocytes and decreased Mcl-1 expression, J. Clin. Invest. 107 (2001) pp. 351-362.

29. G. Niu, K.L. Wright, Y. Ma, G.M. Wright, M. Huang, R. Irby, J. Briggs, J. Karras, W.D. Cress, D. Pardoll, R. Jove, J. Chen, H. Yu, Role of Stat3 in regulating p53 expression and function, Mol. Cell Biol. 25 (2005) pp. 7432-7440.

30. C.D. Nobes and A. Hall, Rho GTPases control polarity, protrusion, and adhesion during cell movement, J. Cell Biol. 144 (1999) pp. 1235-1244.

31. M. Geletu, C. Chaize, R. Arulanandam, A. Vultur, C. Kowolik, A. Anagnostopoulou, R. Jove, L. Raptis, Stat3 activity is required for gap junctional permeability in normal epithelial cells and fibroblasts, DNA & Cell Biol. 28 (2009) pp. 319-327.

32. S.L. Littlefield, M.C. Baird, A. Anagnostopoulou, L. Raptis, Synthesis, characterization and Stat3 inhibitory properties of the prototypical platinum(IV) anticancer drug, [PtCl3(NO2)(NH3)2] (CPA-7), Inorg. Chem. 47 (2008) pp. 2798-2804.

33. L. Larue, C. Antos, S. Butz, O. Huber, V. Delmas, M. Dominis, R. Kemler, A role for cadherins in tissue formation, Development 122 (1996) pp. 3185-3194.

34. Arulanandam, R. (2010). RacV12 requires gp130 for Stat3 activation, cell proliferation and migration.

35. M. J. Pishvaian *et al.*, Cadherin-11 is expressed in invasive breast cancer cell lines. *Cancer research* **59**, 947 (Feb 15, 1999).

36. K. Tomita, Cadherin switching in human prostate cancer progression. (2000).

37. N. M, Focal-adhesion targeting links caveolin-1 to a Rac1-degradation pathway. (2010).

38. Galbiati,F. *et al.* Targeted downregulation of caveolin-1 is sufficient to drive cell transformation and hyperactivate the p42/44 MAP kinase cascade. *EMBO J.* **17**, 6633-6648 (1998).

39. Niu,G. *et al.* Role of Stat3 in regulating p53 expression and function. *Mol. Cell Biol.* **25**, 7432-7440 (2005).

40. Razani,B. *et al.* Caveolin-1 expression is down-regulated in cells transformed by the human papilloma virus in a p53-dependent manner. Replacement of caveolin-1 expression suppresses HPV-mediated cell transformation. *Biochemistry* **39**, 13916-13924 (2000).

41. Galbiati,F. *et al.* Caveolin-1 expression negatively regulates cell cycle progression by inducing G(0)/G(1) arrest via a p53/p21(WAF1/Cip1)-dependent mechanism. *Mol. Biol. Cell* **12**, 2229-2244 (2001).

42. Altieri,D.C. Survivin, cancer networks and pathway-directed drug discovery. *Nat. Rev. Cancer* **8**, 61-70 (2008).

43. Catlett-Falcone,R. *et al.* Constitutive activation of Stat3 signaling confers resistance to apoptosis in human U266 myeloma cells. *Immunity* **10**, 105-115 (1999).

44. Katoh,M. & Katoh,M. STAT3-induced WNT5A signaling loop in embryonic stem cells, adult normal tissues, chronic persistent inflammation, rheumatoid arthritis and cancer (Review). *Int. J. Mol. Med.* **19**, 273-278 (2007).

45. Su,H.W., Wang,S.W., Ghishan,F.K., Kiela,P.R., & Tang,M.J. Cell confluency-induced Stat3 activation regulates NHE3 expression by recruiting Sp1 and Sp3 to the proximal NHE3 promoter region during epithelial dome formation. *Am. J. Physiol Cell Physiol* **296**, C13-C24 (2009).

46. Loeffler,S., Fayard,B., Weis,J., & Weissenberger,J. Interleukin-6 induces transcriptional activation of vascular endothelial growth factor (VEGF) in astrocytes in vivo and regulates VEGF promoter activity in glioblastoma cells via direct interaction between STAT3 and Sp1. *Int. J. Cancer* **115**, 202-213 (2005).

47 M. J. Pishvaian *et al.*, Cadherin-11 is expressed in invasive breast cancer cell lines. *Cancer research* **59**, 947 (Feb 15, 1999).

48 K. Tomita, Cadherin switching in human prostate cancer progression. (2000).

49 N. M, Focal-adhesion targeting links caveolin-1 to a Rac1-degradation pathway. (2010).

Appendices: Attached

Biochimica et Biophysica Acta 1833 (2013) 1947–1959

Contents lists available at SciVerse ScienceDirect

Biochimica et Biophysica Acta

journal homepage: www.elsevier.com/locate/bbamcr

Classical cadherins control survival through the gp130/Stat3 axis

M. Geletu [a], R. Arulanandam [a,1], S. Chevalier [b], B. Saez [c], L. Larue [d], H. Feracci [b], L. Raptis [a,*]

[a] Departments of Microbiology and Immunology, Department of Pathology, and Cancer Center, Queen's University, Kingston, Ontario, Canada K7L 3N6
[b] Université Bordeaux 1, Centre de Recherche Paul Pascal, CNRS UPR 8641, 33600 Pessac, France
[c] Instituto Aragonés de Ciencias de la Salud, Avda. Gomez Laguna 25, 50009, Zaragoza, Spain, and Instituto de Nanociencia de Aragón, Universidad de Zaragoza, Mariano Esquillor, s/n, 50018, Zaragoza, Spain
[d] Institut Curie, INSERM U1021, CNRS UMR3347, 91405, Orsay, France

ARTICLE INFO

Article history:
Received 5 January 2013
Received in revised form 14 March 2013
Accepted 18 March 2013
Available online 27 March 2013

Keywords:
Cadherin
Epithelial cell
Rho GTPase
Signal transduction
Stat3

ABSTRACT

Stat3 (Signal Transducer and Activator of Transcription-3) is activated by a number of receptor and nonreceptor tyrosine kinases. We recently demonstrated that engagement of E-cadherin, a calcium-dependent, cell to cell adhesion molecule which is often required for cells to remain tightly associated within the epithelium, also activates Stat3. We now examined the effect of two other classical cadherins, cadherin-11 and N-cadherin, whose expression often correlates with the epithelial to mesenchymal transition occurring in metastasis of carcinoma cells, upon Stat3 phosphorylation and activity. Our results indicate that engagement of these two cadherins also, can trigger a dramatic surge in Stat3 activity. This activation occurs through upregulation of members of the IL6 family of cytokines, and it is necessary for cell survival, proliferation and migration. Interestingly, our results also demonstrate for the first time that, in sharp contrast to Stat3, the activity of Erk (Extracellular Signal Regulated kinase) was unaffected by cadherin-11 engagement. Further examination indicated that, although IL6 was able to activate Erk in sparsely growing cells, IL6 could not induce an increase in Erk activity levels in densely growing cultures. Most importantly, cadherin-11 knock-down did allow Erk activation by IL6 at high densities, indicating that it is indeed cadherin engagement that prevents Erk activation by IL6. The fact that the three classical cadherins tested so far, E-cadherin, N-cadherin and cadherin11, which are present in essentially all tissues, actually activate Stat3 regardless of their role in metastasis, argues for Stat3 as a central survival, rather than invasion factor.

1. Introduction

Cadherins are a superfamily of transmembrane glycoproteins that are involved in the formation of cell to cell junctions in a variety of tissues [1,2]. Cadherins control the organization, specificity and dynamics of cell–cell adhesion, which is crucial for the development, maintenance and homeostasis of tissue architecture and function [3,4]. Classical cadherins consist of an extracellular domain, a single-pass transmembrane domain and a highly conserved intracellular domain, which interacts with the cytoskeleton via cytoplasmic proteins, such as catenins. The ectodomain consists of five modules (EC1 to EC5) of ~100 amino acids each with internal sequence homology [5,6]. Upon calcium binding, the EC domains change conformation, favoring the formation of cadherin-mediated, adhesive structures between adjacent cells [7,8]. The extracellular segments expressed on the surface of opposing cells interact in a homophilic manner to create highly regulated patterns of attachment, stabilized by cytoskeletal elements inside the cells [9]. Classical cadherins are subdivided into type I (E, N, P and R) and type II (VE, 6–12, 15, 18, 19) based on the structure of their extracellular domains [10]. While both types induce cell to cell adhesion and interact with catenins, cells expressing cadherins 7–11 aggregate less efficiently than cells expressing E- or N-cadherin [11]. These differences could be due to differences in the intrinsic structure of the extracellular EC1 domain that confers adhesive specificity [12–14].

The best characterized classical type I cadherin is the epithelial (E)-cadherin, which is involved in the formation and maintenance of epithelial structures and is abundant in cultured cells of epithelial origin [4,15]. Early results showed that continued plasma membrane expression of E-cadherin is required for cells to remain tightly associated within the epithelium, so that *loss* of E-cadherin function, including mislocalization to the cytoplasm from the membrane, is associated with metastasis of invasive breast cancer [16–18]. Other cadherins however, such as N-cadherin and cadherin-11, recently defined as "mesenchymal" [19], have been positively implicated in cancer as putative proto-oncogenic proteins and are often upregulated in tumor tissues. Indeed, *N-cadherin*

* Corresponding author at: Department of Microbiology and Immunology, Queen's University, Botterell Hall, Rm. 713, Kingston, Ontario, Canada K7L3N6. Tel.: +1 613 533 2462.
E-mail address: raptisl@queensu.ca (L. Raptis).
[1] Present address: Department of Pathology and Molecular Medicine, Centre for Innovative Cancer Therapeutics, Ottawa Hospital Research Institute, 501 Smyth Road, Ottawa, Ontario, Canada K1H 8L6.

0167-4889/$ – see front matter © 2013 Elsevier B.V. All rights reserved.
http://dx.doi.org/10.1016/j.bbamcr.2013.03.014

overexpression and engagement has been reported to be associated with a highly *invasive* phenotype and motility in mammary cell lines [20–22]. In addition, normal squamous epithelial cell lines acquired migratory properties upon transfection with N-cadherin [23]. Interestingly, in certain tumour lines, such as MCF7 breast cancer cells which express E-cadherin and are not motile, transfected N-cadherin conferred a migratory phenotype, despite the presence of the endogenous E-cadherin [21,24].

Cadherin-11 (classical type II) was originally identified in mouse osteoblasts [25], but it was later found to be constitutively expressed in a variety of normal tissues of mesodermal origin, such as areas of the kidney and brain [26], as well as in cultured fibroblasts [27]. Cadherin-11 was also shown to be elevated in a number of cancers where it correlates with a poor prognosis, and is linked to breast cancer metastasis [28,29]. Although it is not expressed in normal human prostate epithelial cells, it is present in prostate cancer, with its expression increasing from primary to metastatic disease to the bone, a tissue where cadherin-11 is abundantly expressed, further suggesting that cadherin-11 could be associated with metastasis [30,31]. It follows that examination of the mechanism of action of the different types of cadherins is of paramount importance in the study of cell to cell adhesion as well as metastasis.

The Signal Transducers and Activators of Transcription (STATs, Stat1 to Stat6) are key mediators of cytokine responses in the mammalian cell. Stat3 is activated by receptor tyrosine kinases, such as the epidermal growth factor receptor (EGFR) or platelet-derived growth factor receptor (PDGFR), as well as the non-receptor tyrosine kinase Src. In quiescent cells Stat3 is found in the cytoplasm. Following receptor stimulation, Stat3 is phosphorylated at the critical tyr-705 by the activated receptor or the associated Jak or Src kinases. This activates Stat3 by stabilizing the association of two monomers through reciprocal Src homology 2 (SH2)-pTyr interactions. The Stat3 dimer then migrates to the nucleus where it activates the transcription of specific genes involved in cell division and survival [32]. Stat3 activity is required for transformation by a number of oncogenes and is found to be hyperactive in a number of cancers [33]. The fact that a constitutively active form of Stat3 alone is sufficient to induce neoplastic transformation points to an etiological role for Stat3 in neoplasia.

We and others recently demonstrated that cell–cell adhesion causes a dramatic increase in the activity of Stat3 in breast carcinoma as well as normal epithelial cells and fibroblasts ([34,35] reviewed in [36]). We further demonstrated that, *in vitro* and *in vivo*, E-cadherin engagement in mouse breast epithelial cells directly induces a dramatic increase in Rac and Stat3 activity, and this constitutes a potent survival signal [37]. This prompted us to examine the effect of the "mesenchymal" cadherins, N-cadherin and cadherin-11, which belong to the type I and type II classical cadherins, respectively, and whose expression often correlates with metastasis, upon Stat3 phosphorylation and activity. Our results indicate that engagement of these cadherins can also trigger a dramatic surge in Stat3 activity. This activation occurs through upregulation of members of the IL6 family of cytokines, which is necessary for cell survival, proliferation and migration. The fact that the "mesenchymal" cadherin-11 and N-cadherin actually activate Stat3, although, contrary to the epithelial E-cadherin, they generally promote metastasis, may point to Stat3 as a central survival, rather than metastasis factor.

Taken together, these data suggest that interference with cadherin-11 or N-cadherin function could induce apoptosis through Stat3 inhibition in metastatic tumor cells specifically, a fact which could have important therapeutic implications.

2. Materials and methods

2.1. Cell lines, culture techniques and gene expression

Normal mouse Balb/c3T3 and Balb/c3T3 transformed by v-Src and mouse 10T½ fibroblasts were grown in Dulbecco's modification of Eagle's medium (DMEM), supplemented with 10% fetal calf serum, as previously described [34].

The plasmid constructs coding for the first two extracellular domains of E-cadherin (E/EC12) or cadherin-11 (11/EC12), fused with a C-terminal hexahistidine tag were previously described [12,13]. Cadherin fragment expression was induced by the addition of IPTG for 2 h. The fragments were purified and attached as before [37]. Cell pellets were resuspended in lysis buffer: 4 M urea, 50 mM Na_2HPO_4 pH 7.8, 20 mM Imidazole and 20 mM β-mercaptoethanol if needed. Purification was carried out by Ni-affinity chromatography as previously described [12,13]. Purified preparations of each cadherin fragment yielded only one band upon analysis by 15% SDS-PAGE and Coomassie blue staining. Purified fragments were attached to plastic petris as follows: Petris were treated with poly-DL-lysine (Sigma # P4158, 0.1 mg/ml in H_2O, for 1 h at room temperature), followed by Calcium-free phosphate buffered saline (PBS) washing and glutaraldehyde treatment (Sigma G-5882, 2.5% in PBS, for 1 h at room temperature). The cadherin fragments were subsequently added at a concentration of 0.5–1000 μg/ml for 2 h, followed by glycine treatment (0.2 M in PBS, overnight). The petris were washed with PBS and incubated with DMEM for 1 h, prior to the addition of cells in complete medium containing serum. Growth of cells on the E/EC12 or 11/EC12 fragments did not cause any detectable change in morphology.

Cell confluence was estimated visually and quantitated by imaging analysis of live cells under phase contrast using a Leitz Diaplan microscope and the MCID-elite software (Imaging Research, St. Catharine's Ont.). In addition, the amount of total protein extracted was also used as a surrogate measure of total cell density. To reduce the variability that might be caused by nutrient depletion in post-confluent cultures, the medium was changed every 24 h.

Rac1 and Cdc42 knockdown were performed using shRNA's expressed through retroviral vectors as described [37].

Fixed cells were assayed for apoptosis using a TUNEL assay (Roche) as previously described [34].

Anti-ubiquitin immunoprecipitations were conducted using the FK2 antibody (Biomol) and GammaBind Plus Sepharose beads (GE Healthcare Life Sciences).

For NFκB inhibition, cells were treated with 20 μm IKK-inhibitorIII (BMS-345541) or 20 μg/ml CAPE (EMD Biosciences). For Jak inhibition, cells were treated with the Jak inhibitor I (EMD Biosciences), for 8 h at 20 μM. For inhibition of the proteasome, cells were treated with MG132 for 8 h at 10 μM. Cell viability was ensured by trypan blue exclusion and by replating the cells in medium lacking the inhibitor.

2.2. Wound healing assay

Cells were plated in 3 cm tissue culture petri dishes in DMEM/10% fetal calf serum, for next day confluence. A wound was made on the confluent monolayer with a plastic pipette tip and cell migration was monitored over a 24-hr period using an Olympus IX70 inverted microscope. Phase contrast images of the same marked fields were captured at various times. The area of wound closure, relative to $t = 0$ h was measured in two independent experiments, four wound sites per cell line, using ImageJ software. Relative cell motility was calculated as the difference between the wound area at $t = 0$ h and the indicated time point. Mean values ± SD per group were calculated, and statistical significance among groups assessed using one-way analysis of variance [38].

2.3. Western blotting

Cell extracts were prepared as described [34]. Following a careful protein determination (BCA-1 Protein assay kit, Sigma), 30 μg of clarified cell extract were loaded. Blots were probed with antibodies against phosphorylated Stat3 tyr-705 and total Stat3 protein (Cell Signalling), Rac1 or Cdc42 (BD Transduction Labs), the dually phosphorylated form of Erk1/2 (Biosource), or Hsp90 (Stressgen) or α-tubulin as loading

standards, followed by alkaline phosphatase-conjugated goat secondary antibodies (Biosource) or horseradish peroxidase-conjugated goat secondary antibodies (Jackson Labs and Pierce). The bands were visualized using enhanced chemiluminescence (ECL), according to the manufacturer's instructions (PerkinElmer Life Sciences, Cat.# NEL602) or using SuperSignal West Femto Maximum Sensitivity Substrate (Pierce, Rockford, Ill.). Quantitation was achieved by fluorimager analysis using the FluorChem program (AlphaInnotech Corp). Luciferase assays for Stat3 transcriptional activity were performed as previously described [34,35].

2.4. Immunohistochemistry

Cell pellets were embedded in paraffin and sectioned. Sections were subsequently deparaffinized and hydrated in a gradient alcohol series from 100% to 70%, then placed under running water for 5 min. Heat-mediated antigen retrieval was performed by heating the slides to 92 °C in low pH buffer for 20 min (Target Retrieval Solution, low pH, Dako), then washed in wash buffer (Dako). Cadherin-11 was detected using rabbit anti-cadherin-11 purified IgG and the Dako EnVision FLEX + Rabbit (linker) kit followed by EnVision + System-HRP labelled polymer (Peroxidase labelled polymer conjugated to goat anti-rabbit IgG, Dako). The color reaction was developed by DAB + chromogen in substrate buffer (Dako), resulting in a brown reaction product. Sections were counterstained with Mayer's hematoxylin, dehydrated in a gradient series of alcohol, cleared in xylene and mounted.

2.5. Rac1 activation assays

They were performed with the Rac1/Cdc42 activation assay kit (Cytoskeleton, #BK035), using beads coated with glutathione-S-transferase (GST) fused to the binding domain of the p21 activated kinase 1 (PAK-PBD) in pulldown assays. Adding twice the amount of PBD-coated beads did not increase the signal, indicating that the amount of binding partner used in the detection was not limiting.

2.6. RT-PCR assays

RT-PCR was performed using Superscript III First-Strand Synthesis kit (Invitrogen) in an Eppendorf Personal Mastercycler. All quantitative RT-PCR reactions were performed with 1x SYBR Green Master Mix (BioRad) using the Corbett Rotor-Gene 6000. Serial ten-fold dilutions of 18S RNA were used as a reference for the standard curve calculation. The primer pairs for Rac1 amplification were: forward primer 5′GGAC ACAGCTGGACAAGAAGA and the reverse primer 5′GGACAGAGAACCG CTCGGATA to generate a 368 bp fragment. For Cdc42 the primer pairs were: forward primer 5′CGACCGCTAAGTTATCCACAG and the reverse primer 5′GCAGCTAGGATAGCCTCATCA to generate a 325 bp fragment. 18S RNA (153 bp) was used as a control.

For quantitative RT-PCR, the delta ct (Δct) value was calculated from the given ct value by the formula: $\Delta ct = (ct_{sample} - ct_{control})$. The fold change was calculated as the value of $1.94^{-\Delta ct}$, 1.94 being the average PCR efficiency. For the qRT-PCR cytokine array, we used the PAMM-021A kit (SA Biosciences) with an RT-PCR for IL6 run in parallel, according to the manufacturer's protocol.

3. Results

3.1. Engagement of "mesenchymal" cadherins increases Stat3 activity

The mouse fibroblast line Balb/c3T3 was previously shown to express cadherin-11 [27]. In fact, as shown in Fig. 1A, these cells possess significant amounts of cadherin-11 mRNA (upper panel) and protein (lower panel), while E-cadherin mRNA is undetectable.

To investigate the effect of cadherin-11 engagement upon Stat3 activity, the impact of cell density was initially examined. Balb/c3T3 cells were plated in plastic petri dishes, and when ~50% confluent, and over several days thereafter, detergent cell extracts were probed by Western blotting for the tyrosine-705 phosphorylated form of Stat3 (Stat3-ptyr705) ([34] (see Materials and methods)). As a loading control, the same extracts were probed with an antibody against the abundant heat shock protein, Hsp90 [39]. As shown before for a number of normal cell lines [34], Stat3-ptyr705 levels were almost undetectable in sparsely growing, Balb/c3T3 cells (Fig. 1B, lane 1). However, density caused a dramatic increase, and Stat3-ptyr705 plateaued at 2–3 days after confluence (lanes 5–6), to levels approximately half the levels present in cells transformed by the potent Stat3 activator, v-Src (lane 9), and decreased slightly thereafter. Probing for total Stat3 revealed a modest increase with cell density (approximately 2.5 fold, Fig. 1B), possibly due to the fact that the Stat3 promotor itself is one of the Stat3 targets [40]. This activation was specific to Stat3, since the levels of Erk1/2 (and Akt 473), a signal transducer often coordinately activated with Stat3 by a number of growth factors and oncogenes, remained unaffected by cell density (Fig. 1B). The above results indicate that cell density causes a specific increase in Stat3-ptyr705 levels in mouse Balb/c3T3 fibroblasts.

We next examined the effect of density upon Stat3 transcriptional activity using Balb/c3T3 cells expressing a Luciferase gene construct under control of a Stat3-specific promotor (p*Luc*TKS3 plasmid, see Materials and methods). As shown in Fig. 1C, there was a dramatic increase in Stat3-dependent transcriptional activity. At the same time, Stat3-independent transcription from the *c-fos*, SRE promotor element was not affected by cell density, suggesting that density induces Stat3 activity specifically. In addition, cell density increased the levels of the Stat3 transcriptional target, survivin (Fig. 1C, lower panel [41]), in keeping with data from other lines (reviewed in [36]). The above data taken together indicate that density increases Stat3, tyr705 phosphorylation and activity in Balb/c3T3 mouse fibroblasts.

To examine whether cadherin-11 was indeed responsible for the density-mediated increase in Stat3-ptyr705 levels, cadherin-11 was knocked down through stable sh-RNA expression with a retroviral vector (see Materials and methods). As shown in Fig. 1D, infection with this vector essentially eliminated cadherin-11 as shown by Western blotting (Fig. 1D, panel a) and immunocytochemistry (panel b). Interestingly, cadherin-11 knockdown resulted in a dramatic reduction in Stat3-ptyr705 levels (panel c), indicating that this cadherin is indeed required for the Stat3, tyr705 phosphorylation observed at high densities. Most importantly, these data also indicate that, at this point, Balb/c3T3 fibroblasts do not express significant amounts of other Stat3 activators (such as other cadherins) that might operate at high cell densities.

The type I classical cadherin, N-cadherin, has also been documented to correlate with metastasis of tumor cells [20], therefore we examined its effect upon Stat3 activity and survival. To this effect, we made use of the null, embryonal stem (ES) cells where E-cadherin was genetically ablated [37]. These cells have very low background levels of Stat3, which might be due to the Leukemia inhibitory factor (LIF) necessary for their growth [37]. Indeed, N-cadherin expression in null cells [4] caused an increase in Stat3-ptyr705, indicating that N-cadherin can also activate the Stat3 pathway in this cellular setting (Fig. S1, B, supplementary data).

To further confirm the ability of N-cadherin to activate the Stat3 pathway, we transfected a construct of N-cadherin-GFP in HEK-293 cells which express low levels of N-cadherin (Fig. S1 C, lane 3). As shown in Fig. S1, C (lanes 1 and 2 *vs* lane 3), N-cadherin expression caused a dramatic increase in Stat3-ptyr705 levels, further confirming that N-cadherin also activates Stat3 following transient expression. Taken together, the above data indicate that cadherin-11 and N-cadherin, which, contrary to E-cadherin correlate with metastasis of epithelial cells, also activate the Stat3 pathway.

3.2. Cadherin11 engagement is sufficient for direct Stat3 activation

We next investigated whether the Stat3 activation observed at high densities is a direct consequence of the engagement of cadherin-11, or

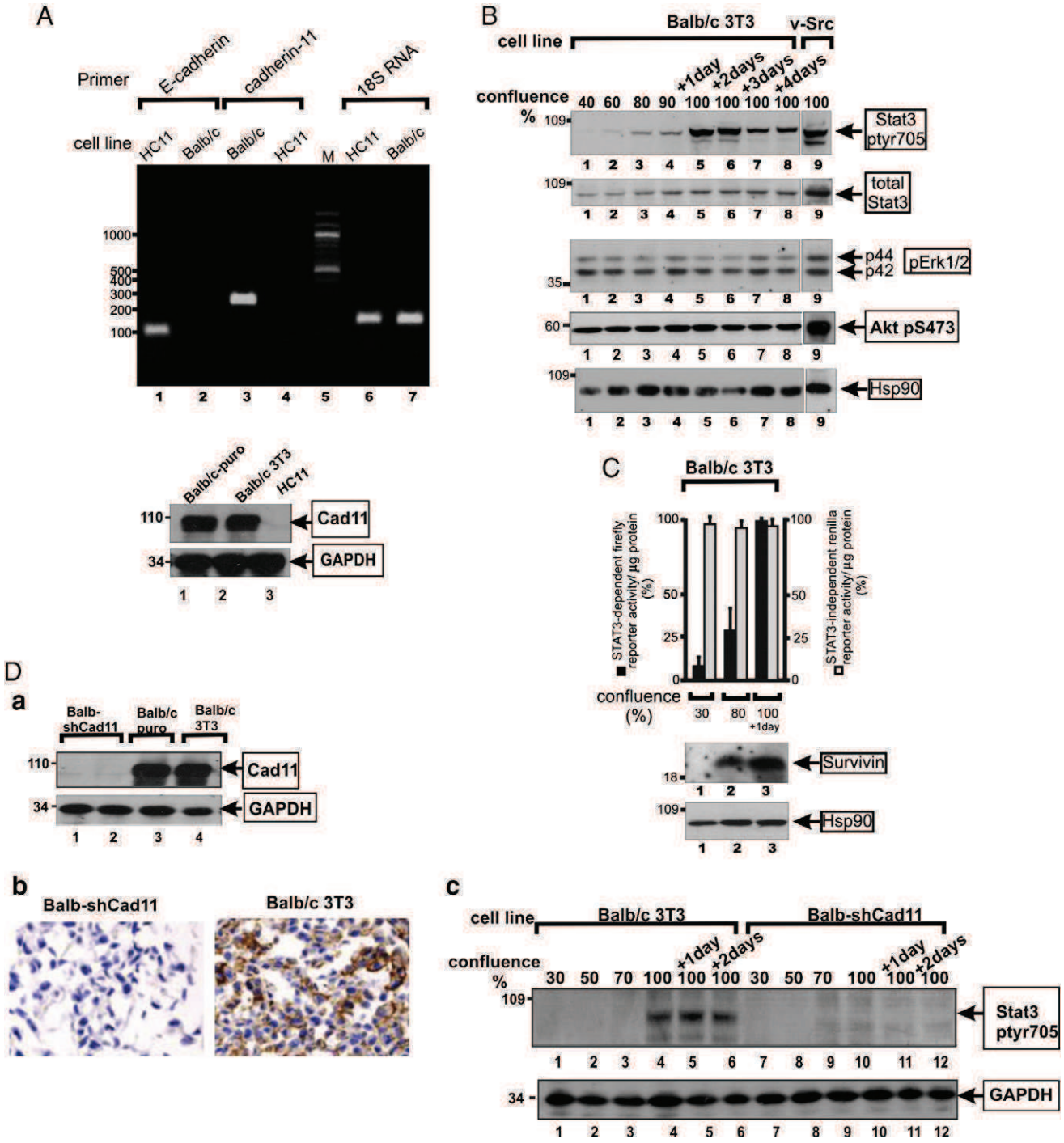

Fig. 1. Cell density triggers Stat3 phosphorylation in Balb/c3T3 cells. A: Balb/c3T3 cells express cadherin-11 but not E-cadherin. Upper panel: RNA extracts from Balb/c3T3, mouse fibroblasts or the HC11, mouse breast epithelial line were probed by RT-PCR for E-cadherin (lanes 1 and 2) or cadherin-11 (lanes 3 and 4), using 18S RNA as an internal control (lanes 6 and 7) (see Materials and methods). Numbers at the left refer to the oligonucleotide marker lane (M). Lower panel: Detergent extracts from Balb/c3T3 (lane 2), control Balb/c3T3 cells infected with a pBabe-puro vector and selected for puromycin resistance (lane 1) or mouse breast epithelial HC11 cells were probed for cadherin-11, with GAPDH as a loading control. B: Cell density upregulates Stat3-ptyr705 levels in Balb/c3T3 cells. Lysates from Balb/c3T3 fibroblasts grown to increasing densities were resolved by gel electrophoresis and probed for Stat3-ptyr705, total Stat3, phospho-Erk1/2, Akt-pser473 or Hsp90 as a loading control, as indicated (see Materials and methods). Numbers at the left refer to molecular weight markers. vSrc: vSrc-transformed, Balb/c3T3 fibroblasts. C: Cell density upregulates Stat3 transcriptional activity in Balb/c3T3 cells. Upper panel: Balb/c3T3 cells were transfected with the Stat3-dependent p*Luc*TKS3 reporter driving a firefly luciferase gene under control of the C-reactive gene promoter element, and the Stat3-independent pRLSRE reporter driving a *Renilla* luciferase gene under control of the c-fos SRE promotor, respectively. Cells were grown to the indicated densities with daily media changes and firefly (■) or *Renilla* (□) luciferase activities determined in cytosolic extracts (see Materials and methods). Values shown represent luciferase units expressed as a percentage of the highest value obtained, means ± SEM of at least 3 experiments, each performed in triplicate. Lower panel: Detergent cell extracts of Balb/c3T3 cells were probed for the Stat3 target, survivin, or Hsp90 as a loading standard, as indicated. Numbers at the left refer to Molecular Weight markers. D: Cadherin-11 knockdown causes a dramatic reduction in Stat3-ptyr705 in Balb/c3T3 cells. a. Extracts from 2 independent clones of sh-Cad11 expressing, Balb/c3T3 clones (lanes 1 and 2), Balb/c3T3 cells infected with an empty vector and selected for puromycin resistance (lane 3) or the parental Balb/c3T3 cells (lane 4), all grown to high densities, were probed for cadherin-11 or GAPDH as a loading control. Note the dramatic reduction in cadherin-11 levels in sh-Cad11-expressing clones, compared to Balb/c3T3. b. Pellets of Balb/c3T3 (right panel) or Balb-shCad11 (left panel) cells were sectioned and stained for cadherin-11 (see Materials and methods). Note the absence of staining in Balb-shCad11 cells. c. Detergent extracts from control Balb/c3T3 (lanes 1–6) or shCad11-expressing, Balb-shCad11 cells (lanes 7–12) were probed for Stat3-ptyr705 or GAPDH as a loading control. Note the dramatic reduction in Stat3-ptyr705 levels in shCad11-expressing clones.

whether cadherin interactions are simply required to bring adjacent cell surfaces into proximity, to initiate signals which are not immediate effects of cadherin ligation. To definitively answer this question, we made use of a recombinant cadherin-11 fragment, encompassing the two distal, extracellular domains of cadherin-11 (11/EC12) to functionalize petri dishes by covalent immobilization. This fragment has been shown to retain biological activity when attached onto solid surfaces [12]. Plastic, 3 cm petri dishes were coated with increasing amounts of purified 11/EC12 fragment, from 0 to 1000 μg/ml, and 30,000 Balb/c3T3 cells were plated on these surfaces (see Materials and methods). Detergent cell extracts were prepared 48 h later, when cells were 30% confluent, and probed for Stat3-ptyr705 as above. No difference in cell morphology was noted when the cells were plated on these coated surfaces, compared to plastic (not shown). As shown in Fig. 2, there was a dramatic and graded increase in Stat3-ptyr705 levels, in proportion to the amounts of 11/EC12 used to decorate these surfaces (lanes 2–5), while there was no increase in Stat3-ptyr705 when Balb/c3T3 cells were plated on petri dishes coated with the corresponding fragment derived from E-cadherin (E/EC12), as a negative control (Fig. 2, lane 1). As a further control, normal mouse breast epithelial HC11 cells which are naturally devoid of cadherin-11 (Fig. 1A), were plated on surfaces coated with 11/EC12 or on the corresponding, E-cadherin fragment E/EC12. As expected, there was no increase in Stat3-ptyr705 when HC11 cells were grown on surfaces coated with 11/EC12 (Fig. 2, lanes 7 and 8), while there was an increase upon growth of HC11 cells on surfaces coated with the homologous E/EC12 fragment (lane 9), which argues for a specificity of cadherin interactions. The increase in Stat3-ptyr705 required at least 20 h and was most pronounced when cells were at a confluence of 35% or less, while at higher densities the Stat3 activation caused by direct cell–cell contact obscured the Stat3 activation brought about by cadherin ligation to the 11/EC12 fragment coating the plate. Similar results were obtained with the 10T½, mouse fibroblasts, which also express cadherin 11 (not shown). The increase

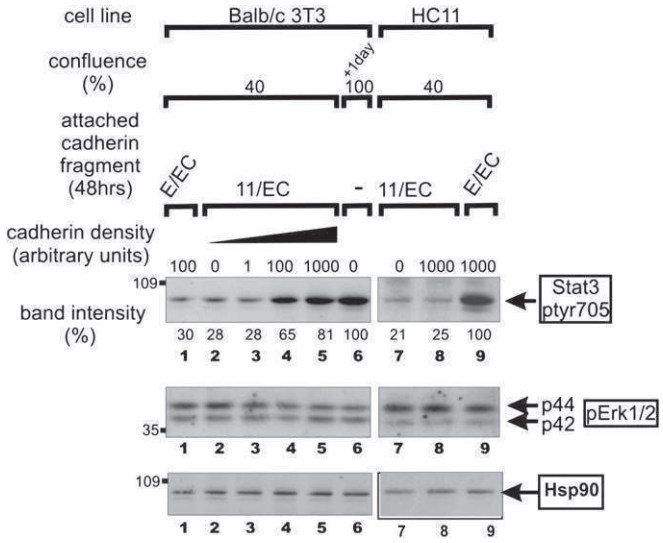

Fig. 2. Cadherin-11 engagement is sufficient to activate Stat3 in Balb/c3T3 fibroblasts. Balb/c3T3 cells were grown in plastic 3 cm dishes, coated with increasing amounts of the cadherin-11 fragment, 11/EC12 (lanes 2–5). 48 h later, cell lysates were probed for Stat3-ptyr705, phospho-Erk1/2 or Hsp90 as a loading standard, as indicated. As controls, Balb/c3T3 cells, which are devoid of E-cadherin (Fig. 1A), were grown on a surface coated with the corresponding E-cadherin fragment (E/EC12, lane 1) and HC11 cells which are devoid of cadherin-11 were grown on surfaces coated by 11/EC12 (lane 8), or E/EC12 as a positive control (lane 9). Numbers under the lanes refer to band intensities obtained by densitometric scanning, with Balb/c3T3 cells grown to one day after confluence (lane 6), or HC11 cells grown on surfaces coated with 1000 μg/ml E/EC12 fragment (lane 9) taken as 100% for lanes 1–6 and 7–9, respectively (see Materials and methods).

was specific to Stat3, since no increase in Erk1/2 was ever noted under these conditions (Fig. 2, middle panel). The dramatic and specific increase in Stat3-ptyr705 upon direct cadherin-11 engagement in mouse fibroblasts, which was proportional to the density of 11/EC12 present on the culture surface, indicates that cadherin-11 engagement is sufficient to activate Stat3.

3.3. Cadherin-11 engagement increases the activity as well as protein levels of the Rac1/Cdc42 GTPases

Early data demonstrated that cell to cell adhesion activates the Rac1, Rho family GTPase (reviewed in [42]). Therefore, to examine the potential role of Rac1 in the cadherin-11 dependent, Stat3 activation in our system, Rac1 activity was examined in Balb/c3T3 cells grown to different densities. This was performed by assessing the binding between Rac1-GTP and its effector p21-activated kinase (PAK) in cell extracts using pull-down assays as before [37] (see Materials and methods). As shown in Fig. 3A, confluent Balb/c3T3 cultures had substantially higher Rac1-GTP levels than their counterparts growing at a density of 40% (lane 1 *vs* 4). Similar results were obtained with mouse 10T½ fibroblasts which also express cadherin-11 (not shown). The above results demonstrate that cell density causes a dramatic increase in the activity of Rac1, in both types of mouse fibroblasts.

It was previously demonstrated that Rac1 can be subjected to proteasome-mediated degradation [43]. Therefore, to explore the potential effect of cadherin-11 engagement upon the levels of *total* Rac1 protein, detergent extracts from cells grown to different densities were blotted and probed for Rac1. As shown in Fig. 3A, there was a sharp increase in *total* Rac1 protein levels with cell density, which could explain the increase in active Rac1-GTP at high densities. Similar results were obtained with 10T½ mouse fibroblasts (not shown). These results indicate that, in addition to Rac1 *activity*, cell–cell adhesion also causes a dramatic increase in *total* Rac1 protein levels.

To investigate whether the increase in Rac1 protein levels with cell density is due to direct cadherin-11 engagement, Balb/c3T3 cells were plated in 11/EC12-coated dishes as above and Rac1 protein levels examined. As shown in Fig. 3B, plating on 11/EC12-coated surfaces, besides leading to an increase in Stat3-ptyr705, also caused a dramatic increase in Rac1 protein levels.

We next examined the effect of cadherin-11 knockdown upon Rac1. Balb-shCad11 cells were plated to different densities and Rac1 levels examined and compared to the parental Balb/c3T3 cells by Western blotting analysis. As shown in Fig. 3C, Balb-shCad11 cells had substantially lower Rac1 levels than the parental Balb/c3T3, indicating that cadherin-11 is required for the cell density-mediated, increase in Rac1 levels.

Cdc42 activity and protein levels mirrored Rac1 and displayed a parallel increase with cell density (Fig. S2). The above data taken together further demonstrate that direct cadherin-11 engagement induces the cell–cell adhesion-mediated increase in the levels and activity of these two, Rho family GTPases in Balb/c3T3 and 10T½ fibroblasts.

3.4. Rac1 and Cdc42 are required for the Cadherin-11 mediated, Stat3 activity increase

To examine whether the increase in Rac1 levels we observed in confluent Balb/c3T3 cells is actually *required* for the Stat3 activity increase, Rac1 levels were reduced through infection with a retroviral vector carrying a Rac1-specific, shRNA insert (see Materials and methods). Following infection and selection for puromycin resistance, Stat3-ptyr705 levels were examined at different densities as above. As shown in Fig. 3D, there was a substantial reduction in Stat3-ptyr705 levels upon expression of shRac1 at all densities examined. Similar results were obtained upon Cdc42 downregulation (Fig. 3E). The residual Stat3-ptyr705 following shRac1 expression (Fig. 3D) is most probably due to

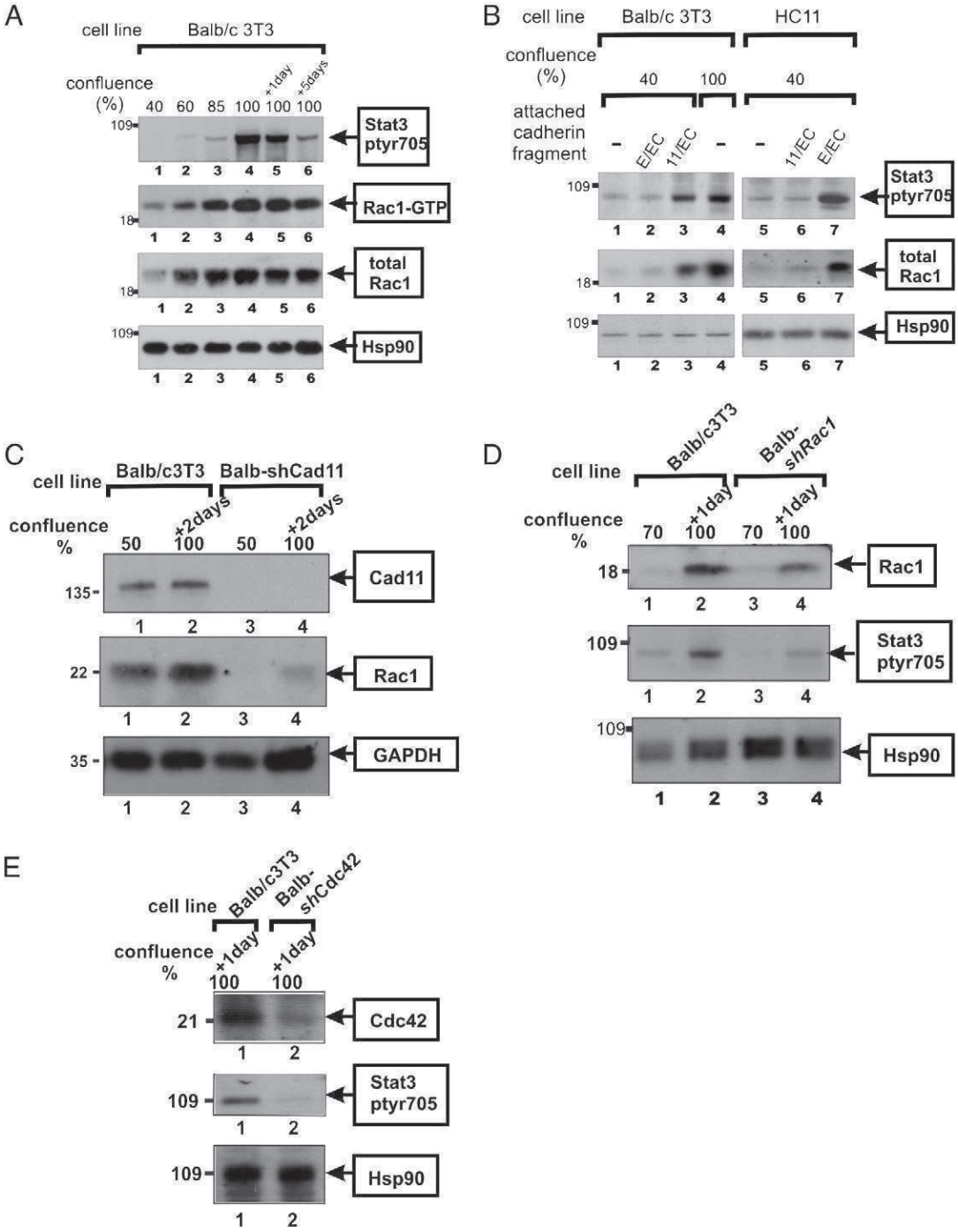

Fig. 3. Cell density increases the activity as well as protein levels of Rac1 in Balb/c3T3 cells. Balb/c3T3 cells were grown to different densities, up to 5 days post-confluence, as indicated. Detergent cell lysates were probed for Stat3-ptyr705, active Rac1-GTP, total Rac1 or Hsp90 as a loading control, as indicated. Numbers at the left refer to molecular weight markers. B. Cadherin-11 engagement is sufficient to increase Rac1 protein levels. Balb/c3T3 cells were grown in plastic petris coated with 1000 μg/ml of the 11/EC12 fragment or the E-cadherin-derived, E/EC12 fragment. 48 h later, detergent cell extracts were probed for Stat3-ptyr705, Rac1 or Hsp90 as a loading control, as indicated. Numbers at the left refer to molecular weight markers. C. Cadherin-11 knockdown causes a dramatic decrease in Rac1 levels. Balb-shCad11 cells were grown to different densities and cell extracts probed for cadherin-11, Rac1 or Hsp90 as a loading control. D. Rac1 is required for cadherin-11 mediated, Stat3 activation. Rac1 was downregulated in Balb/c3T3 cells through infection with a retroviral vector (see Materials and methods). Individual clones were grown to different densities and extracts probed for Rac1, Stat3-ptyr705 or Hsp90 as a loading control, as indicated. E. Cdc42 is required for cadherin-11 mediated, Stat3 activation. Cdc42 was downregulated in Balb/c3T3 cells through infection with a retroviral vector (see Materials and methods). Individual clones were grown to different densities and extracts probed for Cdc42, Stat3-ptyr705 or Hsp90 as a loading control, as indicated.

Stat3 phosphorylation mediated by Cdc42, and vice versa. The above data taken together indicate that the Rac1 and Cdc42, Rho family GTPases, which are dramatically activated through cell to cell adhesion, are essential components of the pathway whereby cadherin-11 engagement triggers the Stat3 phosphorylation and activity increase observed at high confluence.

3.5. Cell density inhibits the proteasomal degradation of Rac1 in mouse Balb/c3T3 fibroblasts

We next examined the mechanism whereby Rac1 protein levels increase with cell density. As shown in Fig. 4A, there was no increase in Rac1 mRNA levels with cell density, measured by RT-PCR, which

points to a post-transcriptional mechanism. To examine whether this increase in Rac1 protein levels was, in fact, due to inhibition of proteasome-mediated degradation, we at first made use of the MG132 proteasome inhibitor [44]. As shown in Fig. 4B, MG132 treatment of sparsely growing Balb/c3T3 cells caused a substantial increase in Rac1 protein levels as well as Stat3-ptyr705. At the same time, Erk1/2 levels

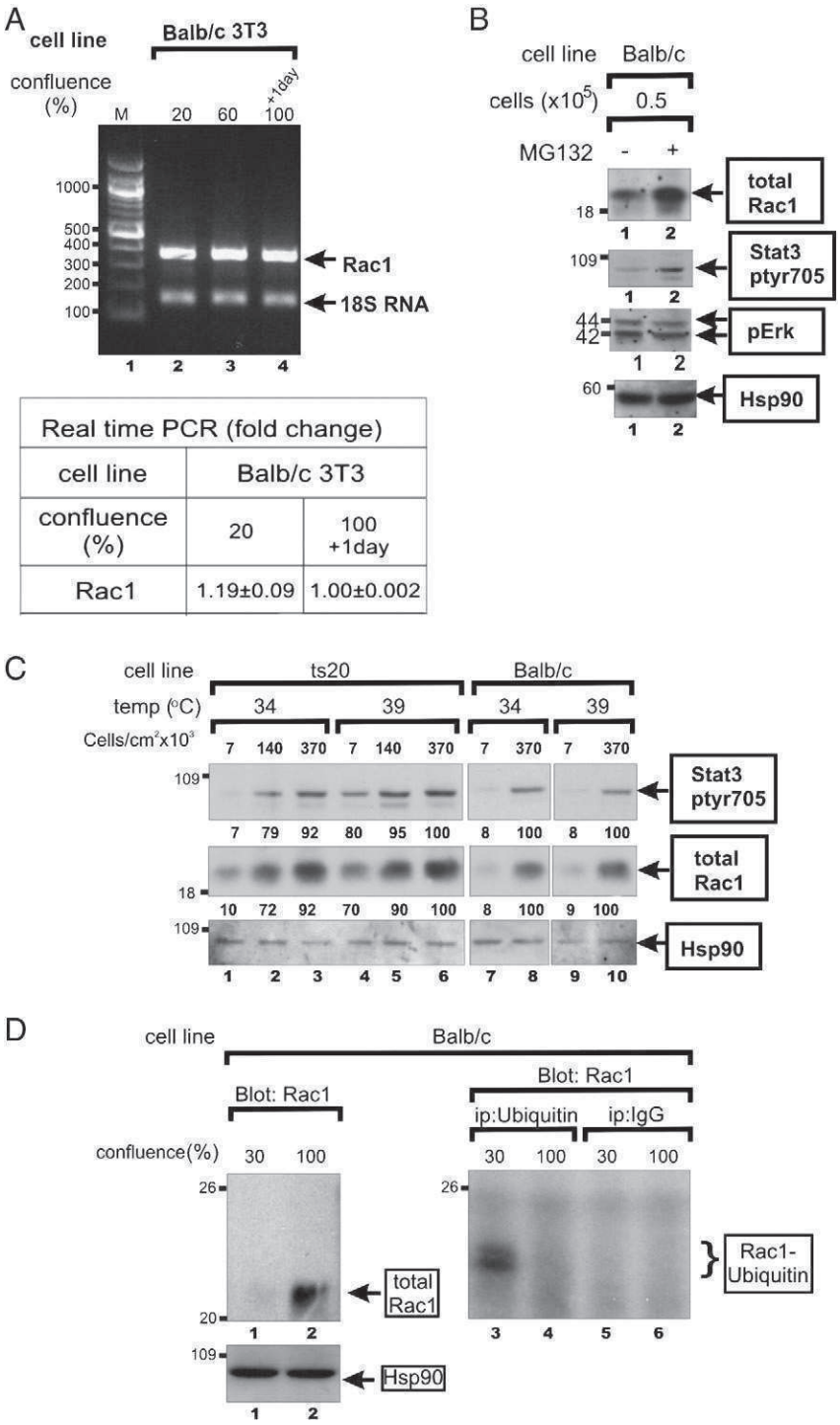

Real time PCR (fold change)		
cell line	Balb/c 3T3	
confluence (%)	20	100 +1day
Rac1	1.19±0.09	1.00±0.002

Fig. 4. A. Rac1 mRNA levels are not affected by cell density. Top panel: Balb/c3T3 cells were grown to different densities as indicated and Rac1 mRNA levels examined by RT-PCR, using 18S RNA as a control (see Materials and methods). Bottom panel: Real-time RT-PCR was performed as described in Materials and methods. The relative expression levels of each sample were determined using the 18S and 28S RNA expression levels, as an internal control. B–D: Cell density inhibits the proteasomal degradation of Rac1 in Balb/c 3T3 cells. B: The proteasome inhibitor, MG132 increases total Rac1 and Stat3-ptyr705 levels. Sparsely growing Balb/c 3T3 cells were treated with 10 μM of the proteasome inhibitor, MG132 (lane 2), or not (lane 1) for 8 h. Detergent cell extracts were probed for total Rac1, Stat3-ptyr705, pErk or Hsp90 as a loading standard, as indicated. C. Inhibition of the E1 ubiquitin activating enzyme increases Rac1 protein levels. ts20 (lanes 1–6) or Balb/c 3T3 (lanes 7–10) cells were grown to different densities, at 34 °C (lanes 1–3 and 7–8) or 39 °C (lanes 4–6 and 9–10), as indicated. Detergent cell extracts were probed for Stat3-ptyr705, Rac1 or Hsp90 as a loading control. Numbers above the lanes refer to cell numbers/cm^2 in thousands. Numbers under the lanes refer to relative band intensities, with the value of lane 6 taken as 100%. Note the high levels of Stat3-ptyr705 at a low confluence, at 39 °C (lane 4 *vs* lane 1). D: Rac1 is ubiquitinated *in vivo*, at low cell densities. Left panel: Extracts from Balb/c3T3 cells grown to 30% or 100% confluence were blotted against Rac1 (arrow). Right panel: Balb/c3T3 cells were grown to 30% or 100% confluence and anti-ubiquitin immunoprecipitates of detergent cell extracts blotted against Rac1 (lanes 3–4). As a control, extracts from cells grown to 30% confluence were immunoprecipitated with normal rabbit IgG (lanes 5–6). Bracket points to the ubiquitinated Rac1.

remained unchanged, indicating that, under conditions of low cell to cell adhesion, the proteasome may be involved in Rac1 degradation specifically.

To further demonstrate the importance of ubiquitination, we took advantage of the ts20 cell line, derived from Balb/c3T3 fibroblasts. Due to a mutation in the gene for the ubiquitin activating enzyme E1, which makes it susceptible to accelerated destruction, this line is defective in protein ubiquitination at high temperatures (39 °C), while ubiquitination is normal at 34 °C [45]. To examine the effect of E1 inactivation upon Rac1 and Stat3-ptyr705 levels, ts20 cells were grown to different densities at 34° or 39 °C, along with the parental Balb/c3T3, and Rac1 and Stat3-ptyr705 levels examined. The results (Fig. 4C) revealed that in ts20 cells grown to low densities (0.5×10^5 cells/3 cm petri) under permissive conditions (34 °C, lane 1) or in the parental Balb/c3T3 at either temperature (lanes 7 and 9), levels of Rac1 and Stat3-ptyr705 were low. In contrast, ts20 cells grown to the same low densities at 39 °C had substantially higher Rac1 and Stat3-ptyr705 levels (lanes 1 *vs* 4), pointing to the possibility of a ubiquitination-inhibition effect. The inhibition of ubiquitination was continuously required (see supplementary data Fig. S4). The above data taken together demonstrate that inhibition of the ubiquitin ligase E1 can cause a dramatic increase in both Rac1 and Stat3-ptyr705 levels.

To further examine whether Rac1 itself might actually be a substrate of the proteasome in sparsely growing cells, we examined whether Rac1 is modified by ubiquitin tagging in Balb/c3T3 fibroblasts. To this effect, we searched for the presence of Rac1 in the pool of ubiquitinated proteins, by probing anti-ubiquitin immunoprecipitates for Rac1 by Western blotting. In fact, a somewhat diffuse band of ubiquitin-tagged Rac1, consistent with short chain polyubiquitination [43] was detected in immunoprecipitates from cells grown to 30% confluence (Fig. 4D, lane 3). This protein complex was not present at 100% confluence (lane 4), consistent with inhibition of ubiquitination at high cell densities. When the anti-ubiquitin antibody was replaced with normal rabbit serum (lanes 5 and 6), or buffer alone (not shown), no Rac1 was found in the immunoprecipitates. The above data indicate that Rac1 itself is, in fact, a substrate of the proteasome in sparsely growing cells.

3.6. NFκB and JAK are required for the cell to cell adhesion-mediated, Stat3 activation

Early data showed that Rac1 activates NFκB [46]. To examine whether NFκB may be required for the cell to cell adhesion-mediated Stat3 activation, sparsely growing Balb/c3T3 cells were trypsinized and plated at a high density (3×10^6 cells/3 cm petri). Following attachment, cells were treated with the IKK-inhibitor-III (BMS-345541) or the DMSO carrier alone, for 48 h. As shown in Fig. 5A, treatment of Balb/c3T3 cells for 48 h with this inhibitor caused a clear reduction in Stat3-ptyr705 levels (lane 2 *vs* 1), while Rac1 levels were unaffected. Similar results were obtained with caffeic acid phenethyl ester (CAPE), another extensively employed NFκB inhibitor (not shown). These data indicate that the density-mediated increase in Stat3-tyr705 phosphorylation requires NFκB.

The role of the JAK kinases in the confluence-induced, Stat3 activation was examined next. Balb/c3T3 cells were grown to a density of 1 day after confluence and treated with the pan-JAK inhibitor, JAK inhibitor-1 [37]. As shown in Fig. 5B, there was a dramatic reduction in Stat3-ptyr705 levels, while Rac1 protein levels remained unaffected. Similar results were obtained with the AG490 JAK inhibitor ([47]). These data suggest that the JAK kinases are required for the cell to cell-adhesion-mediated increase in Stat3-ptyr705 levels in mouse Balb/c3T3 fibroblasts.

3.7. Cell to cell adhesion triggers cytokine gene expression in mouse Balb/c3T3 fibroblasts

In order to examine the possibility that the cell density-mediated, Stat3 activation might occur through secretion of soluble factors, a quantitative RT-PCR array for mRNA of 86 cytokines was performed, by comparing sparsely growing cells to cells grown as dense cultures. The results revealed an increase in mRNA levels of a number of cytokines, including the IL6 family, known to act through the common gp130 subunit, shared by a number of Stat3 activating cytokines, such as IL6, LIF, Ct1 and IL27 (32-fold for IL6 mRNA, see Supplementary Table S1) [48]. To examine whether these cytokines are indeed required for the Stat3 activation observed in confluent cultures, the levels of gp130, the common subunit of the family were reduced through expression of shRNA with a retroviral vector (see Materials and methods). As shown in Fig. 5 (C and D), gp130 knockdown caused a dramatic reduction in Stat3-ptyr705 levels (Fig. 5D, lanes 1–3 *vs* 4–6), indicating that gp130 activation is at least partly responsible for the Stat3-ptyr705 increase.

3.8. Cadherin-11 engagement does not allow Erk1/2 activation by IL6

Besides Stat3, IL6 stimulation was shown to activate the Erk1/2 (Erk) kinase by triggering its phosphorylation at a TEY sequence [49]. However, our present data demonstrate that levels of doubly-phosphorylated, p-Erk1/2 remained unaffected by cell density (Fig. 1B), or direct cadherin engagement (Fig. 2), although Stat3-ptyr705 levels were dramatically increased. To solve this apparent paradox, we examined the ability of IL6 itself, whose synthesis is induced upon cadherin engagement and is the trigger of Stat3 upregulation, to activate Erk as a function of cell density. Balb/c3T3 cells were grown to 50% or 2 days postconfluence, serum-starved and, following IL6 stimulation, cell extracts were probed for p-Erk or Stat3-ptyr705. As shown in Fig. 5E, at a confluence of 50%, IL6 addition caused a dramatic increase in both Stat3-ptyr705 (upper panel) and p-Erk (lower panel) as expected, based on the published literature [49]. As previously documented, cell density *per se* caused an increase in Stat3-ptyr705 levels (Fig. 5E, upper panel lanes 1–3 *vs* 4–6), and IL6 caused a further activation at both densities (lanes 1 *vs* 3 and 4 *vs* 6). Interestingly however, in densely growing cultures IL6 was unable to bring about an increase in p-Erk levels (Fig. 5E, lower panel, lanes 4 and 5), hinting at the possibility of a profound effect of confluence on the response of Balb/c3T3 cells to IL6 addition. To investigate whether this might be due to cadherin function *per se*, the same experiment was conducted with the Balb-shCad11 cells, which are deficient in cadherin-11. As shown in Fig. 5F, in sharp contrast to the parental Balb/c3T3 cells, IL6 could stimulate Erk in densely growing, cadherin-11 deficient, Balb-shCad11 cells (Fig. 5F, lower panel, lanes 3 *vs* 4), clearly indicating that it is indeed cadherin-11 engagement that prevents Erk activation by IL6.

3.9. Cadherin-11 plays a positive role in cell division, survival and migration of Balb/c3T3 fibroblasts

Previous results have shown that Stat3 signalling contributes to the induction of anti-apoptotic genes, such as *Bcl-xL* and *mcl-1* [50,51], while it downregulates the p53 promotor [52], thus protecting tumor cells from apoptosis. To examine the functional consequences of the cadherin-11 mediated, Stat3 activation, we examined the effect of cadherin-11 knockdown in Balb/c3T3 cells. Apoptosis was examined in Balb-shCad11 cells and the parental Balb/c3T3 by terminal deoxynucleotidyl transferase dUTP nick end labeling (TUNEL) staining as before [35]. As shown in Fig. 6A, cadherin-11 deficient, Balb/c3T3 cells succumbed to apoptosis when confluent (panel b), while no apoptosis was noted in the parental Balb/c3T3, even at high densities (panel d), indicating that cadherin-11 plays a positive role in cell survival signalling.

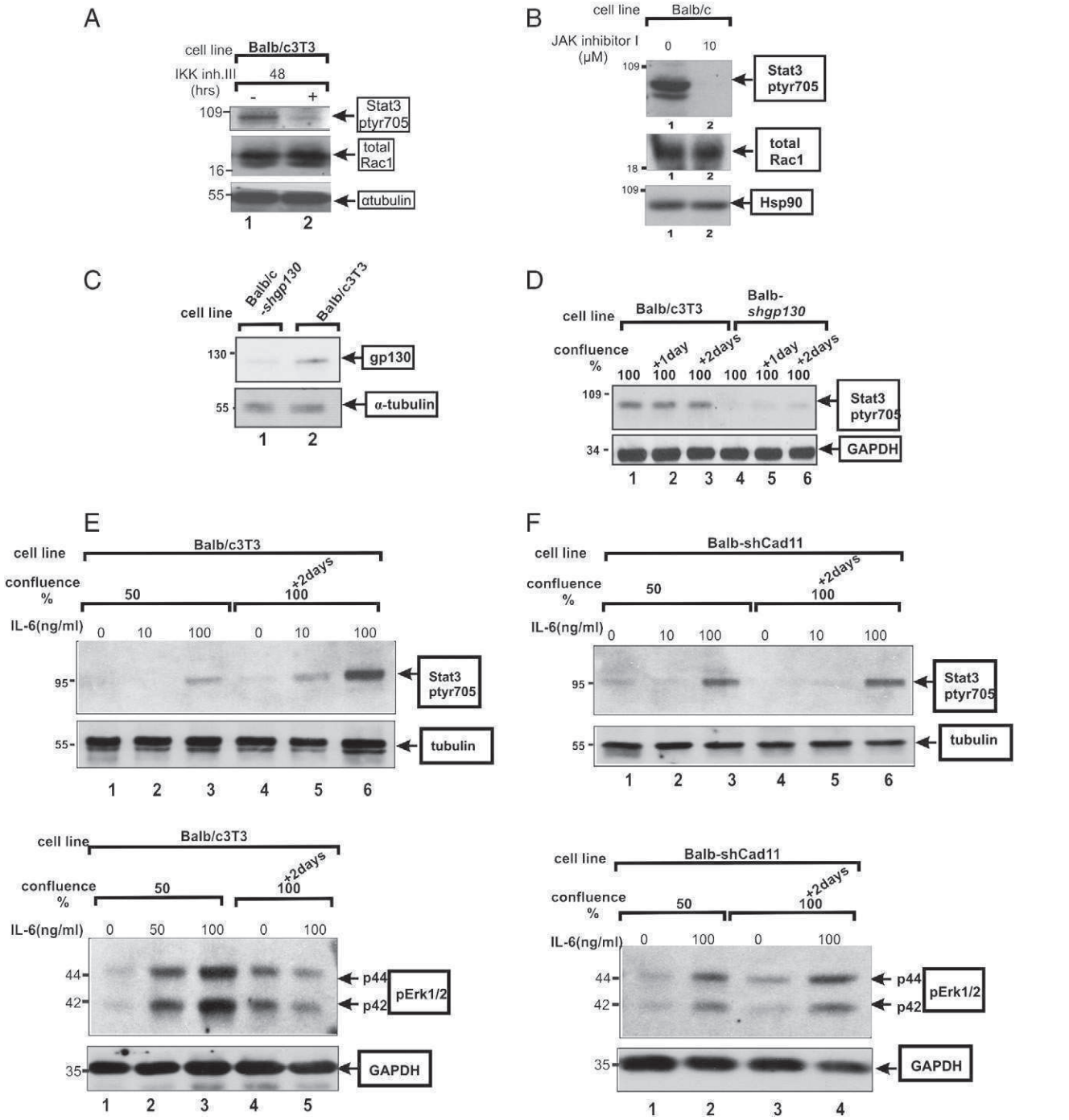

Fig. 5. A: The IKK inhibitor III inhibits the density-mediated, Rac1 activation in Balb/c3T3 cells. Balb/c3T3 cells were trypsinized and plated at a high density (10^6 cells/3 cm plate) and treated with IKK inhibitor III (lane 2), or the DMSO carrier (lane 1). Cell extracts were probed for Stat3-ptyr705, Rac1 or α-tubulin as a loading standard. B: JAK inhibitor 1 reduces the density-dependent, Stat3-tyr705 phosphorylation. Balb/c3T3 cells were trypsinized and plated at a high density and treated with 0 (lane 1), or 10 (lane 2) μg/ml JAK inhibitor 1. Cell lysates were probed for Stat3-ptyr705, Rac1 or Hsp90 as a loading standard. C–D: Gp130 knockdown causes a dramatic reduction in Stat3-ptyr705. C: Extracts from Balb/c3T3 cells before (lane 2) or after (lane 1) gp130 knockdown were probed for gp130 or Hsp90 as a loading control. D: Extracts from Balb/c3T3 cells before (lanes 1–3) or after (lanes 4–6) gp130 knockdown were probed for Stat3-ptyr705 or Hsp90 as a loading control. E: IL6 activates Stat3, but not Erk, at high densities in Balb/c3T3 cells. IL6 was added at 0, 10, 50 or 100 ng/ml for 15 min to Balb/c3T3 cells grown to 50% (lanes 1–3), or 2 days postconfluence as indicated and cell extracts probed for Stat3-ptyr705 (upper panel) or Hsp90 as a loading control. Note the absence of Erk activation at high densities (lower panel, lanes 4 and 5). F: IL6 activates Stat3 and Erk in the absence of cadherin-11. Same as above, cadherin11-deficient, Balb-shCad11 cells. Note the Erk activation at high densities (lower panel, lanes 3 and 4).

We next evaluated the effect of cadherin-11 downregulation upon the rate of cell growth. As shown in Fig. 6B, cadherin-11 knockdown cells had a doubling time of 35 h, while the doubling time of the parental Balb/c3T3 was 24 h, indicating that cadherin-11 plays an important, positive role in cell proliferation.

Extensive evidence has indicated that Rac1 is required for cell motility, through the formation of lamellipodia at the leading edge of cells in a wound healing assay [53]. Since cadherin-11 leads to Rac1 activation, we examined the effect of cadherin-11 knockdown upon cell migration. Balb-shCad11 cells were plated in plastic petri dishes. Two days post-confluence, a scratch-wound was introduced to the monolayer using a plastic pipette tip, and the cells allowed to migrate into the gap. As shown in Fig. 6C, 16 h later the parental Balb/c3T3 cells had moved to close the wound (b), while in Balb-shCad11 cells a substantial amount

of space was still remaining (d). Although the parental Balb/c3T3 cells grow faster than Balb-shCad11, the difference in growth rate cannot account for the increase in rate of migration and gap closure, within 16 h. Downregulation of Stat3 through shRNA knockdown [54], or treatment with the CPA7 inhibitor [55] caused a similar decrease in cell migration of Balb/c3T3 cells (not shown), as previously reported in other systems [Arulanandam 2010][56]. Taken together, the above findings indicate that cadherin-11 is an essential factor necessary for survival, proliferation and migration of Balb/c3T3 cells.

4. Discussion

Unlike cells cultured in two dimensions, cells in a tissue have extensive opportunities for adhesion to their neighbors. These interactions are mediated mostly by the cadherin transmembrane protein family members, which trigger homotypic adhesion between adjacent cells. In addition to this structural role, cadherins profoundly influence signalling events leading to mitogenesis, survival and migration. In fact, previous data showed that E-cadherin may often act as a tumor suppressor molecule; it is frequently down-regulated in carcinomas [18], while in cultured, human colon carcinoma and mammary carcinoma cell lines, E-cadherin plays a negative role in cell proliferation [57]. In sharp contrast, cadherin-11 and N-cadherin are aberrantly expressed in certain cancer cells of epithelial lineage, such as breast carcinomas with a more invasive phenotype and increased metastatic ability [20,28,29,31], and in prostate cancer, where it promotes metastasis specifically to the bone [30]. In the present communication we demonstrate that homophilic interactions of cadherin-11 and N-cadherin upregulate Stat3 and this leads to cell proliferation, survival and migration.

These findings raise important questions: (1), is there a common mechanism of Stat3 activation following engagement of classical, type I and II cadherins? (2), what is the functional significance of the Stat3 activation, which is mediated both by cadherins that largely inhibit metastasis, such as E-cadherin, as well as cadherins that play a

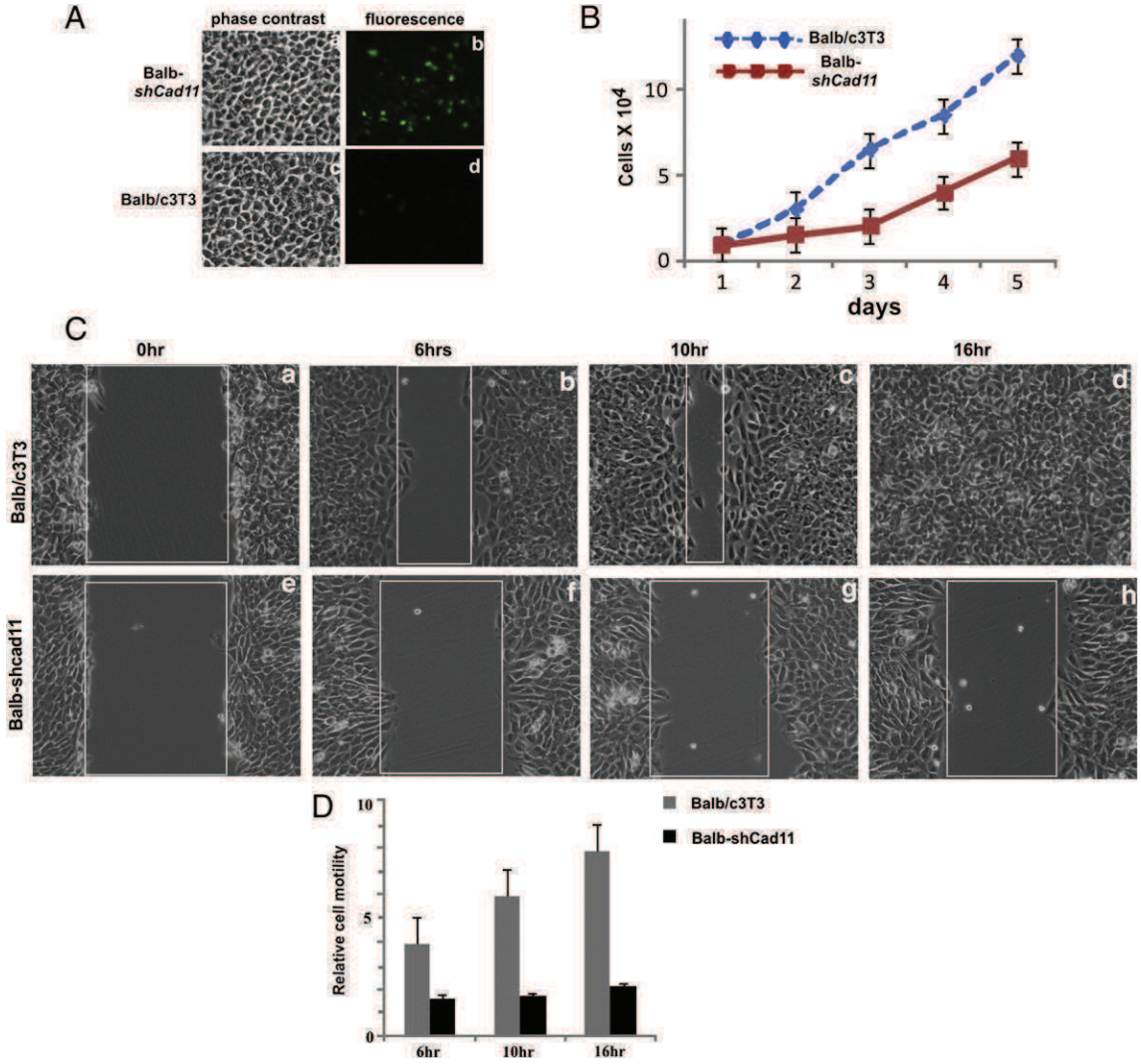

Fig. 6. Cadherin-11 engagement promotes survival, proliferation and migration. A: Balb/c3T3 or Balb-shCad11 cells were grown to densities of two days post-confluence and TUNEL-stained for apoptosis assessment (b, d) (see Materials and methods). a, c: Same fields as in b, d, photographed under phase contrast illumination. B: Cell proliferation: Balb/c3T3 or Balb-shCad11 cells were grown in petri dishes in 10% serum and cell numbers obtained over several days, as indicated. Values represent averages of 3 independent experiments. C–D: Cell migration. C: Balb/c3T3 (panels a–d) or Balb-shCad11 (panels e–h) cells were cultured to confluence in 10% fetal calf serum, then the monolayer was wounded. Spontaneous wound closure at each of eight marked wound sites for each line, in two independent experiments was monitored by phase contrast microscopy. Representative fields, photographed at 0 (panels a, e), 6 (panels b, f), 10 (panels c, g) or 16 h (panels d, h) are shown. Magnification: 140×. D: Histogram showing relative cell motility for each clone, calculated as area of wound closure at 6, 10 and 16 h, compared to t = 0. Values represent mean ± SD of 4 sites per line, in each of two independent experiments.

positive role in it, such as cadherin-11 or N-cadherin? These are crucial questions in the context of fundamental molecular mechanisms of cadherin-mediated adhesion and cell and tissue survival.

4.1. Cadherin-11 engagement inhibits the proteasomal degradation of Rac1 and Cdc42

We previously demonstrated that E-cadherin activates Rac1 and this leads to Stat3 activation [37]. In the present communication, we examined the effect of cadherin-11 upon Rac and Cdc42 activity, using Balb/c3T3 cells which naturally express high amounts of this cadherin [27]. Our results demonstrate a dramatic increase in Rac1 and Cdc42 activity with cell density. In addition, we also demonstrate that plating Balb/c3T3 cells on surfaces coated with a cadherin-11 fragment encompassing the two outermost extracellular domains of cadherin-11 caused a dramatic increase in Rac1 activity levels, indicating that cadherin-11 can *directly* upregulate Rac1, in the absence of cell to cell contact. These results are at variance with previous data on mouse L cells which do not naturally express cadherins, where transfection with cadherin-11 was found to *reduce* Rac1 activity [58]. It follows that data on cadherin signalling should be interpreted in the appropriate cellular context. Our data, using cell lines which naturally express cadherin-11, demonstrate that Rac1 is upregulated following cadherin homophilic ligation.

Our findings also reveal that in addition to this cadherin-induced activation of Rac1, there is a dramatic increase in *total* Rac1 protein levels with confluence, without an increase in mRNA levels, leading to a further increase in activity. Plating cells on surfaces coated with the 11/EC12 fragment showed that this is a direct effect of cadherin engagement. We further demonstrate that the Rac1 activation could be due to inhibition of proteasome-mediated degradation of Rac1 upon cadherin-11 engagement. Conversely, cadherin-11 knockdown caused a dramatic reduction in Rac1 levels and activity. These findings are consistent with previous data indicating that epithelial cell scattering brought about by the Hepatocyte growth factor (HGF) induces the proteasomal degradation of Rac1 [43] and demonstrate that Rac1 turnover mechanisms may operate in cells of mesenchymal origin as well. A similar mechanism could hold true for Cdc42, which mirrored Rac1 activity and protein levels at all densities examined.

4.2. Cadherin-11 mediated, Rac1 upregulation activates the gp130/Stat3 axis

We previously demonstrated that mutationally activated, $Rac1^{V12}$ or $Cdc42^{Val12}$ can lead to Stat3 activation ([59], reviewed in [42]). Our results now indicate that activation of Rac1/Cdc42 through cadherin-11 engagement causes a dramatic surge in mRNA levels of cytokines of the IL6 family. The fact that downregulation of gp130, the common subunit of the family, abolished the cell density-mediated, Stat3 activation strongly suggests that this subunit is actually required.

During developmental processes changes in the cells' cadherin complement occur, to allow different cell types to segregate from one another, to form tissues and organs (cadherin switching). This is recapitulated in tumor cells and promotes metastasis [2]. The fact that cadherin-11 knockdown did achieve a dramatic reduction in Rac1 and Stat3-ptyr705 indicates that if cadherin switching is operating, it is not able to maintain the high Rac1 and Stat3-ptyr705 levels observed in the parental Balb/c3T3 cells at high densities.

Our results also demonstrate that, besides cadherin-11, N-cadherin activates Stat3 in a similar manner. Previous data demonstrated that N-cadherin (but not E-cadherin) activates the Fibroblast Growth Factor receptor (FGF-R), a weak Stat3 activator [60], by direct binding of their extracellular domains. This interaction stabilizes the FGF-R by reducing its internalization [61–63]. Similar results were later published with cadherin-11, although the effect was less pronounced [64]. In any event, no increase in total FGF-R or FGFR-ptyr654/653 with cell density was noted in Balb/c3T3 cells (not shown). The fact that gp130 knockdown prevented Stat3 activation triggered by the engagement of three different cadherins further underscores the importance of the IL6 family, rather than FGF-R, in Stat3 activation. Overall, our findings obtained with different cadherins of the type I or type II classical families, and different cell lines derived from different tissues indicate that cadherins function to activate Stat3, by a mechanism involving a surge in Rac1/Cdc42 levels and activity and IL6 family upregulation, likely through upregulation of NFκB and Jak.

4.3. Cadherin-11 engagement inhibits Erk activation by IL6

Our results demonstrate that cadherin-11 engagement triggers the production of cytokines of the IL6 family, which were previously documented to activate the Erk pathway [49]. Surprisingly however, IL6 was found to be unable to activate Erk in Balb/c3T3 cells grown to high densities. We further demonstrate that cadherin-11 knockdown in Balb/c3T3 cells allowed Erk activation by IL6, which indicates that it is cadherin-11 engagement that inhibits Erk activation by IL6.

The reasons for the Stat3 specificity are at present unclear. It is conceivable that Erk-specific phosphatases such as Cdc25A [65] may be activated at high densities. However, we previously showed that other growth factors such as EGF or PDGF *can* activate Erk in densely growing, mouse fibroblasts [66], which argues against a blanket Erk inhibition by cadherin engagement. The possibility that adaptors specific to IL6/gp130-mediated, Erk activation might be downregulated following cadherin engagement is currently under investigation. It is tempting to speculate that cadherin engagement stimulates IL6 secretion in dense tissues in order to counteract apoptotic death signals, through Stat3 activation. On the other hand, Erk would promote mainly cell division, which is absent in contact-inhibited cells. These data are in keeping with results from HC11 cells, which express E-cadherin [37]. In any event, taken together, our findings demonstrate a *specific* Stat3 response of cells to engagement of three different cadherins, despite the fact that the two pathways, Erk and Stat3, have been reported to be coordinately regulated by cytokine receptors.

4.4. Cadherin-11 engagement increases cell proliferation, survival and motility through Stat3 activation

Previous results [29] indicated that cadherin-11 expression in the SKBR3, breast cancer line, which normally expresses no known cadherins caused a slight increase in cell proliferation, although cadherin-11 expression alone did not transform the cells to anchorage independence. On the other hand, cadherin-11 downregulation in PC3, prostate carcinoma cells had no detectable effect upon cell proliferation [30]. We now demonstrate that cadherin-11 knockdown in normal Balb/c3T3 fibroblasts reduced the rate of cell proliferation and led to apoptosis, especially at high densities. Since the effect of density upon Stat3 activity had not been investigated in the lines previously examined, it is conceivable that expression of other cadherins, or other factors activating Stat3 in the above lines might account for these apparent discrepancies. Our findings are in keeping with previous data indicating that direct Stat3 inhibition using cell permeable peptides [34] or peptidomimetics blocking the Stat3-SH2 domain [67], pharmacological inhibitors, or genetic ablation [35,37], in densely growing cultures induces apoptosis in mouse fibroblasts and epithelial cells.

Cadherin-mediated, cell to cell adhesion was previously shown to activate the PI3 kinase, a potent survival factor [68]. However, although Rac1/Cdc42 is dramatically increased following engagement of E- or N-cadherin or cadherin-11, no increase in Akt-p473 phosphorylation was seen with density in cells expressing any of these three cadherins (Fig. 1). The fact that Stat3 and not PI3k/Akt is the survival factor activated by cadherin engagement, underscores Stat3's importance in survival signalling.

5. Conclusion

The three cadherins described so far, E-cadherin [37], N-cadherin and cadherin-11, classical, type I and type II cadherins, in various combinations are present in essentially all tissues.

The fact that all activate the same Stat3 pathway, points to a central importance of this pathway in cellular survival and may explain the presence of at least one cadherin in all cells of the organism during embryonic development and homeostasis. For tumor tissues, the demonstration that N-cadherin and cadherin-11 may actually activate Stat3, despite the fact that, contrary to E-cadherin, they promote migration and metastasis [28], may point to Stat3 as a central survival, rather than metastasis, factor. Most importantly, inhibition of these cadherins would induce apoptosis (through Stat3 inhibition) in metastatic cells specifically, while normal cells expressing E-cadherin would be spared.

Supplementary data to this article can be found online at http://dx.doi.org/10.1016/j.bbamcr.2013.03.014.

Acknowledgements

We thank Dr. Richard Jove and Dr. James Turkson for useful discussions. We also thank Dr. Olivier Courjean for purification of cadherin fragments; Dr. Frank Beier and Maike Bossert for advice and help with the Rac1/Cdc42, RT-PCR experiments; Drs. Doug Gray and Harvey Ozer for the ts20 cell line; Dr. Bruce Elliott for numerous reagents; and Dr. Harriet Feilotter and Xiao Zhang of the Queen's University Laboratory for Molecular Pathology/Microarray Facility for RT-PCR array analysis.

The financial assistance of the Canadian Institutes of Health Research (CIHR), the Canadian Breast Cancer Foundation (CBCF- Ontario Chapter), the Natural Sciences and Engineering Research Council of Canada (NSERC), the Ontario Centers of Excellence, the Breast Cancer Action Kingston and the Clare Nelson bequest fund and the Canadian Breast Cancer Research Alliance (LR), the Fondation pour la Recherche Médicale, Région Aquitaine, the Association pour la Recherche contre le Cancer and the Ligue Contre le Cancer Comité de Dordogne, and Cnano GSO (HF) and the Instituto de Salud Carlos III in Sara Borell program (BS), is gratefully acknowledged. LL was supported by the Ligue Nationale contre le cancer (equipe labelisée) and INCa. RA was supported by a Canada Graduate Scholarships Doctoral award from CIHR, the Ontario Women's Health Scholars Award from the Ontario Council on Graduate Studies and a Queen's University Graduate Award (QGA). MG was supported by a postdoctoral fellowship from the US army Breast Cancer Program (#BC087586), the Ministry of Research and Innovation of the Province of Ontario and the Advisory Research Committee of Queen's University.

References

[1] M.P. Stemmler, Cadherins in development and cancer, Mol. Biosyst. 4 (2008) 835–850.
[2] M.J. Wheelock, Y. Shintani, M. Maeda, Y. Fukumoto, K.R. Johnson, Cadherin switching, J. Cell Sci. 121 (2008) 727–735.
[3] M. Takeichi, Morphogenetic roles of classic cadherins, Curr. Opin. Cell Biol. 7 (1995) 619–627.
[4] L. Larue, C. Antos, S. Butz, O. Huber, V. Delmas, M. Dominis, R. Kemler, A role for cadherins in tissue formation, Development 122 (1996) 3185–3194.
[5] S.D. Patel, C.P. Chen, F. Bahna, B. Honig, L. Shapiro, Cadherin-mediated cell–cell adhesion: sticking together as a family, Curr. Opin. Struct. Biol. 13 (2003) 690–698.
[6] P. Hulpiau, F. van Roy, Molecular evolution of the cadherin superfamily, Int. J. Biochem. Cell Biol. 41 (2009) 349–369.
[7] A.W. Koch, S. Pokutta, A. Lustig, J. Engel, Calcium binding and homoassociation of E-cadherin domains, Biochemistry 36 (1997) 7697–7705.
[8] O. Courjean, G. Chevreux, E. Perret, A. Morel, S. Sanglier, N. Potier, J. Engel, A. van Dorsselaer, H. Feracci, Modulation of E-cadherin monomer folding by cooperative binding of calcium ions, Biochemistry 47 (2008) 2339–2349.
[9] J.M. Halbleib, W.J. Nelson, Cadherins in development: cell adhesion, sorting, and tissue morphogenesis, Genes Dev. 20 (2006) 3199–3214.
[10] F. Nollet, P. Kools, F. van Roy, Phylogenetic analysis of the cadherin superfamily allows identification of six major subfamilies besides several solitary members, J. Mol. Biol. 299 (2000) 551–572.
[11] Y.S. Chu, O. Eder, W.A. Thomas, I. Simcha, F. Pincet, A. Ben-Ze'ev, E. Perez, J.P. Thiery, S. Dufour, Prototypical type I E-cadherin and type II cadherin-7 mediate very distinct adhesiveness through their extracellular domains, J. Biol. Chem. 281 (2006) 2901–2910.
[12] A. Pierres, H. Feracci, V. Delmas, A.M. Benoliel, J.P. Thiery, P. Bongrand, Experimental study of the interaction range and association rate of surface-attached cadherin 11, Proc. Natl. Acad. Sci. U. S. A. 95 (1998) 9256–9261.
[13] E. Perret, A.M. Benoliel, P. Nassoy, A. Pierres, V. Delmas, J.P. Thiery, P. Bongrand, H. Feracci, Fast dissociation kinetics between individual E-cadherin fragments revealed by flow chamber analysis, EMBO J. 21 (2002) 2537–2546.
[14] S.D. Patel, C. Ciatto, C.P. Chen, F. Bahna, M. Rajebhosale, N. Arkus, I. Schieren, T.M. Jessell, B. Honig, S.R. Price, L. Shapiro, Type II cadherin ectodomain structures: implications for classical cadherin specificity, Cell 124 (2006) 1255–1268.
[15] A. Jeanes, C.J. Gottardi, A.S. Yap, Cadherins and cancer: how does cadherin dysfunction promote tumor progression? Oncogene 27 (2008) 6920–6929.
[16] H. Oka, H. Shiozaki, K. Kobayashi, M. Inoue, H. Tahara, T. Kobayashi, Y. Takatsuka, N. Matsuyoshi, S. Hirano, M. Takeichi, Expression of E-cadherin cell adhesion molecules in human breast cancer tissues and its relationship to metastasis, Cancer Res. 53 (1993) 1696–1701.
[17] A.M. Gonzalez-Angulo, A. Sahin, S. Krishnamurthy, Y. Yang, S.W. Kau, G.N. Hortobagyi, M. Cristofanilli, Biologic markers in axillary node-negative breast cancer: differential expression in invasive ductal carcinoma *versus* invasive lobular carcinoma, Clin. Breast Cancer 7 (2006) 396–400.
[18] C.J. Gottardi, E. Wong, B.M. Gumbiner, E-cadherin suppresses cellular transformation by inhibiting beta-catenin signaling in an adhesion-independent manner, J. Cell Biol. 153 (2001) 1049–1060.
[19] G. Berx, F. van Roy, Involvement of members of the cadherin superfamily in cancer, Cold Spring Harb. Perspect. Biol. 1 (2009) a003129.
[20] R.B. Hazan, R. Qiao, R. Keren, I. Badano, K. Suyama, Cadherin switch in tumor progression, Ann. N. Y. Acad. Sci. 1014 (2004) 155–163.
[21] R.B. Hazan, G.R. Phillips, R.F. Qiao, L. Norton, S.A. Aaronson, Exogenous expression of N-cadherin in breast cancer cells induces cell migration, invasion, and metastasis, J. Cell Biol. 148 (2000) 779–790.
[22] G. Li, K. Satyamoorthy, M. Herlyn, N-cadherin-mediated intercellular interactions promote survival and migration of melanoma cells, Cancer Res. 61 (2001) 3819–3825.
[23] S. Islam, T.E. Carey, G.T. Wolf, M.J. Wheelock, K.R. Johnson, Expression of N-cadherin by human squamous carcinoma cells induces a scattered fibroblastic phenotype with disrupted cell–cell adhesion, J. Cell Biol. 135 (1996) 1643–1654.
[24] M.T. Nieman, R.S. Prudoff, K.R. Johnson, M.J. Wheelock, N-cadherin promotes motility in human breast cancer cells regardless of their E-cadherin expression, J. Cell Biol. 147 (1999) 631–644.
[25] M. Okazaki, S. Takeshita, S. Kawai, R. Kikuno, A. Tsujimura, A. Kudo, E. Amann, Molecular cloning and characterization of OB-cadherin, a new member of cadherin family expressed in osteoblasts, J. Biol. Chem. 269 (1994) 12092–12098.
[26] I. Hoffmann, R. Balling, Cloning and expression analysis of a novel mesodermally expressed cadherin, Dev. Biol. 169 (1995) 337–346.
[27] M. Orlandini, S. Oliviero, In fibroblasts Vegf-D expression is induced by cell–cell contact mediated by cadherin-11, J. Biol. Chem. 276 (2001) 6576–6581.
[28] M.J. Pishvaian, C.M. Feltes, P. Thompson, M.J. Bussemakers, J.A. Schalken, S.W. Byers, Cadherin-11 is expressed in invasive breast cancer cell lines, Cancer Res. 59 (1999) 947–952.
[29] C.M. Feltes, A. Kudo, O. Blaschuk, S.W. Byers, An alternatively spliced cadherin-11 enhances human breast cancer cell invasion, Cancer Res. 62 (2002) 6688–6697.
[30] K. Chu, C.J. Cheng, X. Ye, Y.C. Lee, A.J. Zurita, D.T. Chen, L.Y. Yu-Lee, S. Zhang, E.T. Yeh, M.C. Hu, C.J. Logothetis, S.H. Lin, Cadherin-11 promotes the metastasis of prostate cancer cells to bone, Mol. Cancer Res. 6 (2008) 1259–1267.
[31] K. Tomita, A. van Bokhoven, G.J. van Leenders, E.T. Ruijter, C.F. Jansen, M.J. Bussemakers, J.A. Schalken, Cadherin switching in human prostate cancer progression, Cancer Res. 60 (2000) 3650–3654.
[32] D.A. Frank, STAT3 as a central mediator of neoplastic cellular transformation, Cancer Lett. 251 (2007) 199–210.
[33] H. Yu, D. Pardoll, R. Jove, STATs in cancer inflammation and immunity: a leading role for STAT3, Nat. Rev. Cancer 9 (2009) 798–809.
[34] A. Vultur, J. Cao, R. Arulanandam, J. Turkson, R. Jove, P. Greer, A. Craig, B.E. Elliott, L. Raptis, Cell to cell adhesion modulates Stat3 activity in normal and breast carcinoma cells, Oncogene 23 (2004) 2600–2616.
[35] A. Vultur, R. Arulanandam, J. Turkson, G. Niu, R. Jove, L. Raptis, Stat3 is required for full neoplastic transformation by the Simian Virus 40 Large Tumor antigen, Mol. Biol. Cell 16 (2005) 3832–3846.
[36] L. Raptis, R. Arulanandam, A. Vultur, M. Geletu, S. Chevalier, H. Feracci, Beyond structure, to survival: Stat3 activation by cadherin engagement, Biochem. Cell Biol. 87 (2009) 835–843.
[37] R. Arulanandam, A. Vultur, J. Cao, E. Carefoot, P. Truesdell, B. Elliott, L. Larue, H. Feracci, L. Raptis, Cadherin–cadherin engagement promotes survival via Rac/Cdc42 and Stat3, Mol. Cancer Res. 17 (2009) 1310–1327.
[38] H. Mak, A. Naba, S. Varma, C. Schick, A. Day, S.K. SenGupta, M. Arpin, B.E. Elliott, Ezrin phosphorylation on tyrosine 477 regulates invasion and metastasis of breast cancer cells, BMC Cancer 12 (2012) 82.
[39] S. Greer, R. Honeywell, M. Geletu, R. Arulanandam, L. Raptis, Housekeeping gene products; levels may change with confluence of cultured cells, J. Immunol. Methods 355 (2010) 76–79.
[40] M. Narimatsu, H. Maeda, S. Itoh, T. Atsumi, T. Ohtani, K. Nishida, M. Itoh, D. Kamimura, S.J. Park, K. Mizuno, J. Miyazaki, M. Hibi, K. Ishihara, K. Nakajima, T. Hirano, Tissue-specific autoregulation of the stat3 gene and its role in interleukin-6-induced survival signals in T cells, Mol. Cell. Biol. 21 (2001) 6615–6625.

[41] T. Gritsko, A. Williams, J. Turkson, S. Kaneko, T. Bowman, M. Huang, S. Nam, I. Eweis, N. Diaz, D. Sullivan, S. Yoder, S. Enkemann, S. Eschrich, J.H. Lee, C.A. Beam, J. Cheng, S. Minton, C.A. Muro-Cacho, R. Jove, Persistent activation of stat3 signaling induces survivin gene expression and confers resistance to apoptosis in human breast cancer cells, Clin. Cancer Res. 12 (2006) 11–19.
[42] L. Raptis, R. Arulanandam, M. Geletu, J. Turkson, The R(h)oads to Stat3: Stat3 activation by the Rho GTPases, Exp. Cell Res. 317 (2011) 1787–1795.
[43] E.A. Lynch, J. Stall, G. Schmidt, P. Chavrier, C. D'Souza-Schorey, Proteasome-mediated degradation of Rac1-GTP during epithelial cell scattering, Mol. Biol. Cell 17 (2006) 2236–2242.
[44] Q. Zhu, G. Wani, J. Yao, S. Patnaik, Q.E. Wang, M.A. El Mahdy, M. Praetorius-Ibba, A.A. Wani, The ubiquitin-proteasome system regulates p53-mediated transcription at p21waf1 promoter, Oncogene 26 (2007) 4199–4208.
[45] D.R. Chowdary, J.J. Dermody, K.K. Jha, H.L. Ozer, Accumulation of p53 in a mutant cell line defective in the ubiquitin pathway, Mol. Cell. Biol. 14 (1994) 1997–2003.
[46] D.J. Sulciner, K. Irani, Z.X. Yu, V.J. Ferrans, P. Goldschmidt-Clermont, T. Finkel, rac1 regulates a cytokine-stimulated, redox-dependent pathway necessary for NF-kappaB activation, Mol. Cell. Biol. 16 (1996) 7115–7121.
[47] Y. Zhang, J. Turkson, C. Carter-Su, T. Smithgall, A. Levitzki, A. Kraker, J.J. Krolewski, P. Medveczky, R. Jove, Activation of Stat3 in v-Src transformed fibroblasts requires cooperation of Jak1 kinase activity, J. Biol. Chem. 275 (2000) 24935–24944.
[48] P. Fischer, D. Hilfiker-Kleiner, Survival pathways in hypertrophy and heart failure: the gp130-STAT axis, Basic Res. Cardiol. 102 (2007) 393–411.
[49] P. Fischer, D. Hilfiker-Kleiner, Role of gp130-mediated signalling pathways in the heart and its impact on potential therapeutic aspects, Br. J. Pharmacol. 153 (Suppl. 1) (2008) S414–S427.
[50] J.R. Grandis, S.D. Drenning, Q. Zeng, S.C. Watkins, M.F. Melhem, S. Endo, D.E. Johnson, L. Huang, Y. He, J.D. Kim, Constitutive activation of Stat3 signaling abrogates apoptosis in squamous cell carcinogenesis *in vivo*, Proc. Natl. Acad. Sci. U. S. A. 97 (2000) 4227–4232.
[51] P.K. Epling-Burnette, J.H. Liu, R. Catlett-Falcone, J. Turkson, M. Oshiro, R. Kothapalli, Y. Li, J.M. Wang, H.F. Yang-Yen, J. Karras, R. Jove, T.P. Loughran Jr., Inhibition of STAT3 signaling leads to apoptosis of leukemic large granular lymphocytes and decreased Mcl-1 expression, J. Clin. Invest. 107 (2001) 351–362.
[52] G. Niu, K.L. Wright, Y. Ma, G.M. Wright, M. Huang, R. Irby, J. Briggs, J. Karras, W.D. Cress, D. Pardoll, R. Jove, J. Chen, H. Yu, Role of Stat3 in regulating p53 expression and function, Mol. Cell. Biol. 25 (2005) 7432–7440.
[53] C.D. Nobes, A. Hall, Rho GTPases control polarity, protrusion, and adhesion during cell movement, J. Cell Biol. 144 (1999) 1235–1244.
[54] M. Geletu, C. Chaize, R. Arulanandam, A. Vultur, C. Kowolik, A. Anagnostopoulou, R. Jove, L. Raptis, Stat3 activity is required for gap junctional permeability in normal epithelial cells and fibroblasts, DNA Cell Biol. 28 (2009) 319–327.
[55] S.L. Littlefield, M.C. Baird, A. Anagnostopoulou, L. Raptis, Synthesis, characterization and Stat3 inhibitory properties of the prototypical platinum(IV) anticancer drug, [PtCl3(NO2)(NH3)2] (CPA-7), Inorg. Chem. 47 (2008) 2798–2804.
[56] M. Debidda, L. Wang, H. Zang, V. Poli, Y. Zheng, A role of STAT3 in Rho GTPase-regulated cell migration and proliferation, J. Biol. Chem. 280 (2005) 17275–17285.
[57] M. Perrais, X. Chen, M. Perez-Moreno, B.M. Gumbiner, E-cadherin homophilic ligation inhibits cell growth and epidermal growth factor receptor signaling independently of other cell interactions, Mol. Biol. Cell 18 (2007) 2013–2025.
[58] H.P. Kiener, C.S. Stipp, P.G. Allen, J.M. Higgins, M.B. Brenner, The cadherin-11 cytoplasmic juxtamembrane domain promotes alpha-catenin turnover at adherens junctions and intercellular motility, Mol. Biol. Cell 17 (2006) 2366–2376.
[59] R. Arulanandam, M. Geletu, H. Feracci, L. Raptis, RacV12 requires gp130 for Stat3 activation, cell proliferation and migration, Exp. Cell Res. 316 (2010) 875–886.
[60] A.A. Dudka, S.M. Sweet, J.K. Heath, Signal transducers and activators of transcription-3 binding to the fibroblast growth factor receptor is activated by receptor amplification, Cancer Res. 70 (2010) 3391–3401.
[61] J. Hulit, K. Suyama, S. Chung, R. Keren, G. Agiostratidou, W. Shan, X. Dong, T.M. Williams, M.P. Lisanti, K. Knudsen, R.B. Hazan, N-cadherin signaling potentiates mammary tumor metastasis via enhanced extracellular signal-regulated kinase activation, Cancer Res. 67 (2007) 3106–3116.
[62] J.B. Kim, S. Islam, Y.J. Kim, R.S. Prudoff, K.M. Sass, M.J. Wheelock, K.R. Johnson, N-Cadherin extracellular repeat 4 mediates epithelial to mesenchymal transition and increased motility, J. Cell Biol. 151 (2000) 1193–1206.
[63] S. Chung, J. Yao, K. Suyama, S. Bajaj, X. Qian, O.D. Loudig, E.A. Eugenin, G.R. Phillips, R.B. Hazan, N-cadherin regulates mammary tumor cell migration through Akt3 suppression, Oncogene 32 (2013) 422–430.
[64] C. Boscher, R.M. Mege, Cadherin-11 interacts with the FGF receptor and induces neurite outgrowth through associated downstream signalling, Cell. Signal. 20 (2008) 1061–1072.
[65] J.S. Lazo, K. Nemoto, K.E. Pestell, K. Cooley, E.C. Southwick, D.A. Mitchell, W. Furey, R. Gussio, D.W. Zaharevitz, B. Joo, P. Wipf, Identification of a potent and selective pharmacophore for Cdc25 dual specificity phosphatase inhibitors, Mol. Pharmacol. 61 (2002) 720–728.
[66] L. Raptis, H.L. Brownell, A.M. Vultur, G. Ross, E. Tremblay, B.E. Elliott, Specific inhibition of growth factor-stimulated ERK1/2 activation in intact cells by electroporation of a Grb2-SH2 binding peptide, Cell Growth Differ. 11 (2000) 293–303.
[67] A. Anagnostopoulou, A. Vultur, R. Arulanandam, J. Cao, J. Turkson, R. Jove, J.S. Kim, M. Glenn, A.D. Hamilton, L. Raptis, Differential effects of Stat3 inhibition in sparse *vs* confluent normal and breast cancer cells, Cancer Lett. 242 (2006) 120–132.
[68] C. Murga, M. Zohar, H. Teramoto, J.S. Gutkind, Rac1 and RhoG promote cell survival by the activation of PI3K and Akt, independently of their ability to stimulate JNK and NF-kappaB, Oncogene 21 (2002) 207–216.

BMC Cancer

RESEARCH ARTICLE Open Access

Stat3 is a positive regulator of gap junctional intercellular communication in cultured, human lung carcinoma cells

Mulu Geletu[1], Rozanne Arulanandam[1,2], Samantha Greer[1,3], Aaron Trotman-Grant[1], Evangelia Tomai[1,4] and Leda Raptis[1*]

Abstract

Background: Neoplastic transformation of cultured cells by a number of oncogenes such as *src* suppresses gap junctional, intercellular communication (GJIC); however, the role of Src and its effector Signal transducer and activator of transcription-3 (Stat3) upon GJIC in non small cell lung cancer (NSCLC) has not been defined. Immunohistochemical analysis revealed high Src activity in NSCLC biopsy samples compared to normal tissues. Here we explored the potential effect of Src and Stat3 upon GJIC, by assessing the levels of tyr418-phosphorylated Src and tyr705-phosphorylated Stat3, respectively, in a panel of NSCLC cell lines.

Methods: Gap junctional communication was examined by electroporating the fluorescent dye Lucifer yellow into cells grown on a transparent electrode, followed by observation of the migration of the dye to the adjacent, non-electroporated cells under fluorescence illumination.

Results: An inverse relationship between Src activity levels and GJIC was noted; in five lines with high Src activity GJIC was absent, while two lines with extensive GJIC (QU-DB and SK-LuCi6) had low Src levels, similar to a non-transformed, immortalised lung epithelial cell line. Interestingly, examination of the mechanism indicated that Stat3 inhibition in any of the NSCLC lines expressing high endogenous Src activity levels, or in cells where Src was exogenously transduced, did not restore GJIC. On the contrary, Stat3 downregulation in immortalised lung epithelial cells or in the NSCLC lines displaying extensive GJIC actually suppressed junctional permeability.

Conclusions: Our findings demonstrate that although Stat3 is generally growth promoting and in an activated form it can act as an oncogene, it is actually ***required*** for gap junctional communication both in nontransformed lung epithelial cells and in certain lung cancer lines that retain extensive GJIC.

Keywords: Stat3, Electroporation, Indium-Tin oxide, Gap junctions, Src, Cell to cell adhesion, Lung cancer

Background

Gap junctions are plasma membrane channels that provide a path of direct communication between the interiors of neighboring cells and are formed by the connexin (Cx) family of proteins. An increase in cell proliferation correlates with a reduction in gap junctional, intercellular communication (GJIC [1]). In fact, a number of oncogene products such as v-Src [2], the polyoma virus middle Tumor antigen, an oncogene which acts by activating Src family kinases (mT [3,4]), the chaperone Hsp90N [5], vRas [6,7] and others have been shown to interrupt junctional communication.

Extensive evidence has indicated that expression of the Src tyrosine kinase leads to gap junction closure, through phosphorylation of the ubiquitous connexin, Cx43. Src exerts its effect either through direct tyrosine phosphorylation of Cx43, or indirectly, through activation of the serine/threonine, Erk1/2 or protein kinase C family kinases [8]. Examination of levels of tyr-418 phosphorylated, ie activated Src in a number of Non Small Cell Lung Cancer (NSCLC) biopsies previously showed the presence of higher Src activity than the surrounding, non-tumor lung tissue

* Correspondence: raptisl@queensu.ca
[1]Departments of Microbiology and Immunology and Pathology, Queen's University, Kingston, Ontario, K7L3N6, Canada
Full list of author information is available at the end of the article

[9,10]. However, Src's contribution to GJIC suppression in NSCLC lines and primary cells which may express other oncogenes in addition to Src, or different levels of Src effectors, remains to be determined.

The Signal Transducer and Activator of transcription-3 (Stat3), an important Src downstream effector, is a cytoplasmic transcription factor. Following phosphorylation on tyr-705 by Src, as well as by growth factor or cytokine receptors such as the IL6 family, Stat3 normally dimerises through a reciprocal SH2 domain-phosphotyrosine interaction and translocates to the nucleus, where it induces the transcription of specific genes [11]. The effect of Src upon Stat3 activation in NSCLC lines is at present unclear. Examination of Stat3 levels in certain NSCLC lines demonstrated that Src is a major Stat3 activator, transducing signals from EGFR and IL6 that lead to apoptosis inhibition [12], while in another report [13] Src inhibition in different NSCLC lines was found to actually ***increase*** Stat3-ptyr705. However, we and others previously demonstrated that cell-to-cell adhesion, as observed at confluence of cultured cells, causes a dramatic increase in Stat3 activity levels in a number of cellular systems ([14-16] reviewed in [17]); for this reason, cell density must be taken into account in the examination of the effect of different factors such as Src upon Stat3 activity levels. In the present report this was achieved by measuring Stat3-ptyr705 phosphorylation and activity levels at a range of densities.

We previously assessed GJIC in a number of lung cancer lines [18]. In the present work GJIC was examined using an apparatus where cells were grown on a glass slide, half of which was coated with electrically conductive, optically transparent, indium-tin oxide. An electrode was placed on top of the cells and an electrical pulse, which opens transient pores on the plasma membrane, was applied in the presence of the fluorescent dye, Lucifer yellow. Although this technique is adequate for a number of lines, the turbulence generated as the electrode is removed can cause cell detachment, which makes GJIC examination problematic. Here, we revisited the question of GJIC levels in lung cancer lines using an improved technique, where the upper electrode is eliminated. This approach is valuable for the electroporation of tumor-derived lines especially at high densities, where cell adhesion to the substratum may be weak. Interestingly, the results revealed that cell density *per se* triggers a dramatic increase in both Cx43 levels and GJIC. Two NSCLC lines, QU-DB and SK-LuCi6 were found to have extensive GJIC, similar to control, nontransformed lung epithelial cells, while GJIC in five other lines was very low or undetectable. Investigation of the mechanism of gap junction closure revealed an inverse relation between Src activity levels and GJIC. Further studies led to the discovery that, unlike Ras inhibition in Src-transformed fibroblasts [19], Stat3 inhibition in NSCLC lines with high Src activity does not restore GJIC. On the contrary, Stat3 inhibition in lines displaying extensive GJIC (QU-DB, SK-LuCi6) suppressed junctional permeability, indicating that Stat3 activity is actually ***required*** for the maintenance of gap junction function in these lung cancer lines.

Results

Cell density upregulates GJIC and connexin-43 protein levels

A number of reports showed that gap junction function is dependent upon cell to cell contact and the assembly of adherens junctions [20,21]. Since the opportunity for engagement of cadherins, key components of adherens junctions, is expected to increase with cell density, we examined the effect of cell density upon GJIC. To this effect, we took advantage of the nontransformed mouse lung epithelial type II line, E10 that has extensive GJIC, an even and flat morphology and good adhesion to the substratum even at high densities [22] (Figure 1A). In addition, unlike nontransformed human lung lines such as NL-20 [23], E10 cells can be grown in the absence of growth factors that could affect GJIC. Cells were plated in electroporation chambers and when 90% confluent or at 3 days post-confluence Lucifer yellow was electroporated and the movement of the dye through gap junctions observed under fluorescence and phase contrast illumination (see Methods). The results are presented as the average number of cells where dye transfered, per cell loaded with the dye by electroporation (GJIC). As shown in Figure 1B, ***a-c***, although cells at 90% confluence did display some gap junction transfer (GJIC ~1.5), GJIC increased to ~6 at 3 days post-confluence (Figure 1B, ***d-f***), indicating that cell density causes a dramatic increase in GJIC (Table 1,A).

We next examined the levels of Cx43, a widely expressed gap junction protein, at different cell densities. Cells were plated in plastic petri dishes at a confluence of 80% and at different times up to 5 days post confluence, total protein extracts were probed for Cx43 by Western blotting. As shown in Figure 1C, cell density caused a dramatic increase in Cx43 levels, which plateaued at ~3 days post-confluence (lane 1 *vs* 5).

GJIC and connexin-43 in NSCLC lines and freshly explanted tumor cells

In light of the above findings, we examined GJIC levels at different densities up to 4 days post-confluence in a panel of human lung cancer lines [18]. Two NSCLC lines, QU-DB (Figure 2A, ***a-c***) and SK-LuCi6 (Table 1,A) displayed extensive GJIC at their peak density, while five NSCLC lines had very low GJIC (e.g. A549, Figure 2B, ***a-c,*** and Table 1,B). In addition, primary cells explanted and cultured from a moderately differentiated adenosquamous carcinoma

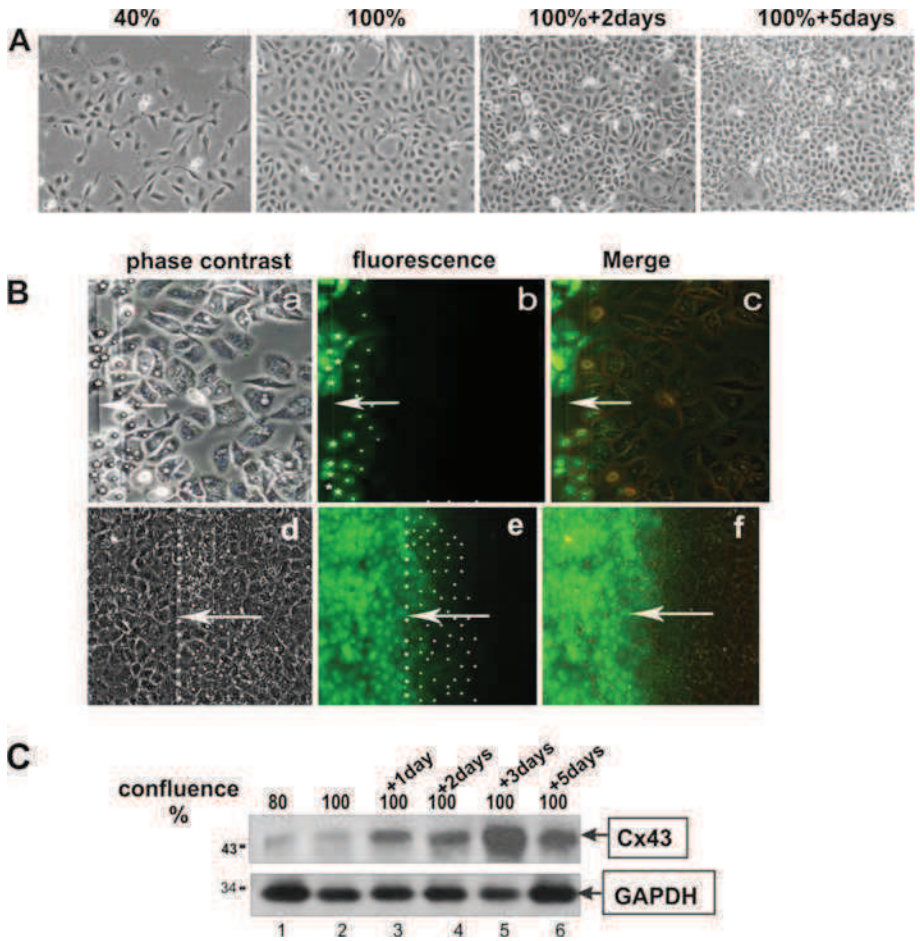

Figure 1 Cell density increases GJIC and Cx43 levels. A. Immortalised lung epithelial E10 cells were plated in 3 cm plastic petri dishes, grown to different densities and photographed under phase-contrast illumination. Magnification: 240x. **B**. E10 cells were plated in electroporation chambers and subjected to a pulse in the presence of Lucifer yellow when 90% confluent (***a-c***) or 3 days after confluence (***d-f***) and photographed under phase-contrast (***a, d***), fluorescence (***b, e***) or combined (***c, f***) illumination (see Methods, Figure 7). Arrows point to the position of the edge of the electroporated area. In ***a***, ***b***, ***d*** and ***e***, stars mark cells loaded with the dye at the edge of the electroporated area and dots mark cells into which the dye was transferred through gap junctions. Magnification: 240x **C**. E10 cells were seeded in plastic petri dishes and when they reached the indicated densities, detergent cell extracts were probed for Cx43 (top) or GAPDH (bottom) as a control.

(Figure 3, ***a-b***), a poorly differentiated adenocarcinoma, and an adenocarcinoma (Table 2) had no GJIC.

Examination of Cx43 levels showed that QU-DB cells had levels similar to E10, which increased dramatically with cell density, while Cx43 levels in A549 cells were almost undetectable, at any cell density (Figure 4A). SK-LuCi6 cells had levels similar to QU-DB, while all other NSCLC lines examined had very low Cx43 levels at all densities tested (not shown). The above data taken together indicate that, besides nontransformed epithelial cells, cell density causes a dramatic increase in GJIC and Cx43 protein levels in two lung carcinoma lines which display extensive GJIC. Nevertheless, the majority of lung cancer lines examined (5/7) had very low or no detectable gap junctional communication, even at high cell densities (Table 1,B).

Src activity and GJIC suppression in NSCLC lines

We next examined Src-tyr418 phosphorylation, as an indication of Src activity. As shown in Figure 5A and C, A549 cells displayed high Src-ptyr418 levels, similar to the levels in SK-LuCi6 or E10 cells expressing activated Src by retroviral transduction (lines SK-LuCi6-***Src***, E10-***Src***, respectively, Figure 5C, lanes 1 *vs* 3 and Table 1,B), while Src-ptyr418 levels in QU-DB cells were low (Figure 5A, lanes 5-8), similar to E10 (Figure 5B, lanes 5 and 6). Lines CALU-1, SW-900, CALU-6 and SK-Lu1 had Src-ptyr418 levels comparable to SK-LuCi6-***Src*** (Figure 5B, lanes 1-3 *vs* 7 and Table 1,B), while SK-LuCi6 had low levels, similar to QU-DB (Figure 5B, lanes 4-5). Examination of gap junctional communication revealed that five lines with high Src-ptyr418 (A549, CALU-1, SW-900, CALU-6, LuCi-1) had very low or no detectable GJIC (Figure 2B,

Table 1 Effect of Stat3 downregulation upon GJIC

A. Cells with extensive junctional communication						
Cell line	**Treatment[α]**	**Src[β](%)**	**Stat3[β] (%)**		**GJIC[γ]**	
			50%	**100+3d**	**90%**	**100+3d**
E10	**-**	6±1	9±3	26±9	1.5±0.5	6.0±1
"	**DMSO**	6±1	9±3	30±8	-	6.0±1
"	**CPA7**	5±1	2±1.1	3±1	-	0.2±0.1
"	**sh-Stat3**	N/A	6±1.1	8±2	-	1.0±0.2
QU-DB	**-**	7±1	10±2	20±4	1±0.2	6.3±1
"	**DMSO**	7±1	10±2	22±3	-	6.3±1
"	**CPA7**	5±1	2±0.5	2±0.5	-	0.2±0.1
"	**sh-Stat3**	N/A	5±3	8±2	-	0.8±0.2
SK-LuCi6	**-**	5±1	8±2	21±4	1.8±0.2	6.5±1
"	**DMSO**	5±1	8±2	20±5	-	6.5±1
"	**CPA7**	5±1.2	2.8±1.25	3±1	-	0.3±0.1
"	**sh-Stat3**	N/A	6±2	4±0.5	-	1±0.2
"	**Jak inhib.1**	5.2±0.3	4.2±1.1	5±0.5	-	0.5±0.2
"	**Stat3C**	5.1±1	22±9	97±10	-	8±1
B. Cells expressing activated Src						
A549	**-**	95±11	93±12	320±32	0.1 ±0.1	0.3 ±0.1
"	**DMSO**	95±11	93±12	320±32	-	0.3 ±0.1
"	**CPA7**	93±10	8±1	12±2	-	0.1 ±0.1
"	**sh-Stat3**	N/A	12±3	11±4	-	0.1±0.1
E10-*Src*	**DMSO**	98±12	98±15	350±28	-	0.4 ±0.2
"	**CPA7**	95±11	5±1	15±4	-	0.1 ±0.1
"	**sh-Stat3**	N/A	9±3	20±3	-	0.1±0.1
SK-LuCi6-*Src*	**DMSO**	100±12	100±12	420±33	-	0.2±0.1
"	**CPA7**	98±10	3±1	9±1	-	0.1 ±0.1
"	**sh-Stat3**	N/A	11±3	17±3	-	0.3±0.1
"	**sh-Stat3+Das.**	4±1	6±1.1	14±3	-	0.2±0.1
SK-Lu-1	**DMSO**	85±5	90±11	311±23	-	1±0.2
"	**CPA7**	82±4	6±1	8±3	-	0.1 ±0.1
CALU-1	**DMSO**	96±9	100±10	290±12	-	0.1 ±0.1
"	**CPA7**	90±12	8±2	6±1	-	0.1 ±0.1
SW-900	**DMSO**	100±13	100±12	405±21	-	0.1 ±0.1
"	**CPA7**	96±11	12±1	11±2	-	0.1 ±0.1
CALU-6	**DMSO**	95±11	93±10	300±18	-	0.1 ±0.1
"	**CPA7**	93±10	10±1	15±5	-	0.1 ±0.1

[α]For Stat3 inhibition, cells were treated with 50 μM CPA7, or the DMSO carrier for 24 hrs, or infected with a lentivirus vector expressing a Stat3-specific, shRNA [37]. For Stat3 upregulation, cells were infected with a retroviral vector containing Stat3C. Jak inhibitor-1 was used at 5μM [16].

[β] Stat3-tyr705 or Src-ptyr418 levels were measured by Western blotting. Numbers represent relative values obtained by quantitation analysis. Averages of at least three experiments ±SEM are shown. For Stat3, data from cells grown to 50% confluence or 3 days after confluence are presented [15], with the average of the values for DMSO-treated, Src-transduced, SK-LuCi6-***Src*** cells grown to 50% confluence taken as 100%. The transcriptional activity values obtained paralleled the Stat3-705 phosphorylation levels indicated (Figure 4C and D, see Methods).

[γ]GJIC was assessed by *in situ* electroporation at the indicated confluences (see Methods, Figure 8). Quantitation was achieved by dividing the number of cells into which the dye had transferred through gap junctions (denoted by dots, Figure 1B and 2A), by the number of cells at the edge of the electroporated area (denoted by stars). Numbers are averages ±SEM of at least three experiments, where transfer from more than 200 cells was examined.

N/A: Not applicable.

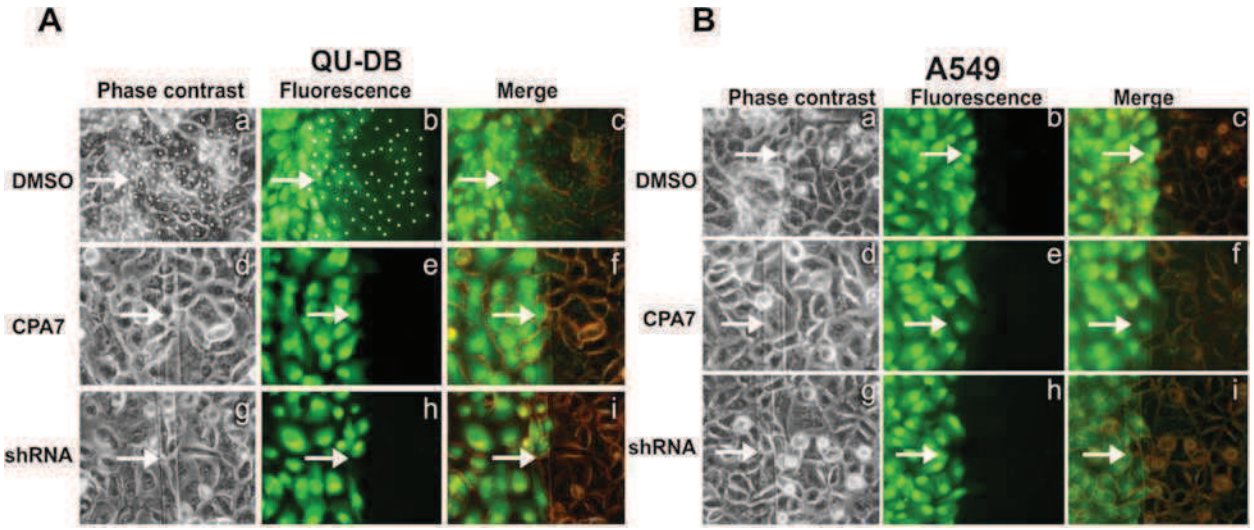

Figure 2 A. Stat3 downregulation eliminates gap junctional permeability in human lung carcinoma QU-DB cells. QU-DB cells were plated in electroporation chambers and subjected to a pulse in the presence of Lucifer yellow, following treatment with the DMSO carrier alone (***a-c***), or CPA7 (***d-f***), or infection with the sh-Stat3 lentiviral vector (***g-i***) (see Methods, Figure 8). After washing away the unincorporated dye, cells from the same field were photographed under fluorescence (***b, e, h***) or phase contrast (***a, d, g***) illumination. Cells at the edge of the conductive area which were loaded with LY through electroporation were marked with a star, and cells at the non-electroporated area which received LY through gap junctions were marked with a dot [4]. Arrows point to the edge of the electroporated area. ***c, f, i***: Overlay of phase-contrast and fluorescence. Magnification: 240 x. Note the extensive gap junctional communication in (***b***). **B. Stat3 downregulation does not increase gap junctional permeability in human lung carcinoma A549 cells.** Same as above, A549 cells. Note the absence of GJIC, even after Stat3 downregulation (***e, h***).

a-c and Table 1,B). In addition, Src expression in SK-LuCi6 or E10 cells eliminated junctional permeability (E10-***Src*** and SK-LuCi6-***Src***, Table 1, B), in agreement with the known Src effect of GJIC suppression. Conversely, the two lines with low Src-ptyr418 levels (QU-DB and SK-LuCi6), had high GJIC, especially at high densities (Figure 2A and Table 1, A). Primary cells from the three tumor specimens were found to have higher Src activity than the E10, consistent with previous results from biopsy tissues (Figure 3, bottom panel). Taken together, these data point to an inverse relationship between Src activity levels and GJIC in these NSCLC lines.

Stat3 is a positive regulator of GJIC in NSCLC lines

Stat3 is a prominent effector of the non-receptor tyrosine kinase Src [24]. However, Stat3 can be activated by cytokine and membrane tyrosine kinase receptors, which can act in a Src-independent manner [11]. Therefore, to assess the specific contribution of Src to Stat3 activation in the lung cancer lines, we at first examined the correlation between Src-ptyr418 and Stat3-ptyr705 levels. As shown before for a number of cell types (reviewed in [17]), high cell density caused an increase in Stat3-ptyr705 levels in all lines (e.g. Figure 5A, lanes 1-4 and 5-8), therefore Stat3-ptyr705 levels were assessed at a confluence of 50% for this experiment (see Methods). The results showed elevated Stat3-ptyr705 levels in the five lines with high Src-ptyr418 at all cell densities, comparable to SK-LuCi6-***Src*** cells (e.g. A549 *vs* QU-DB, Figure 5A, lanes 1-4 *vs* 5-8 and Figure 5B and Table 1,B). At the same time, QU-DB and SK-LuCi6 cells had low levels of both Src-ptyr418 and Stat3-ptyr705 (Figure 5B). The above data point to a correlation between Src and Stat3 activity levels in the NSCLC lines. We next examined the effect of Src inhibition upon Stat3-ptyr705 in the lines found to have high Src-ptyr418. The results showed that treatment with the Src inhibitor Dasatinib caused a dramatic reduction in Stat3-ptyr705 (e.g. line A549, Figure 5C, and Additional file 1: Additional data, Table Add-I). Similar results were obtained with the PD180970 and SU6656 Src inhibitors (see Methods). These findings indicate that Src may, in fact, be an important Stat3 activator in these cells.

The effect of Stat3 inhibition upon GJIC in the 5 lines with high Src activity was examined next. As shown in Figure 3C and D treatment with the Stat3 inhibitor, CPA7 for 15 hrs [25], or knockdown with a Stat3-specific, shRNA, essentially eliminated Stat3, tyr705 phosphorylation and activity in A549 cells. However, CPA7 treatment (Figure 2B, ***d-f***), or Stat3 knockdown (Figure 2B, ***g-i***) did not increase junctional permeability in A549 cells. Similar results were obtained with SK-Lu1, CALU-1, SW-900 and CALU-6 lines (Table 1,B). The above data taken together indicate that the high Stat3 activity, which could be, at least in part, due to high Src activity in these lines, cannot be responsible

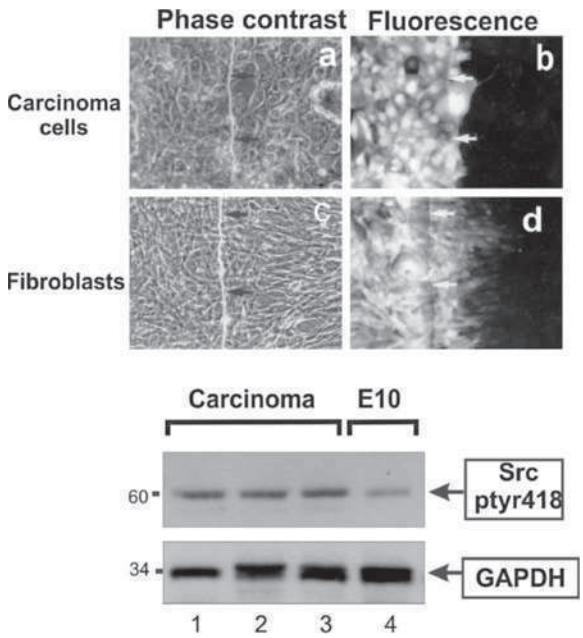

Figure 3 Primary lung carcinoma cells display low gap junctional, intercellular communication. a and **b**: Cells cultured from a freshly explanted lung tumor specimen were grown in electroporation chambers and Lucifer yellow introduced with an electrical pulse (Figure 7, [42]). Arrows point to the edge of the electroporated area. Note the absence of gap junctional communication. Magnification: 240x. **c** and **d**: Following growth of the cells for 10 weeks, fibroblasts present in the original cell suspension predominated. They were plated in electroporation chambers and Lucifer yellow introduced with an electrical pulse. Note the extensive communication through gap junctions. **Lower panel** Extracts of cells cultured from a moderately differentiated adenosquamous carcinoma, a poorly differentiated adenocarcinoma, and adenocarcinoma, respectively (lanes 1–3), or E10 cells (lane 4), were probed for Src-ptyr418 or GAPDH as a loading control, as indicated.

for the lack of junctional communication in the lung carcinoma lines examined.

Since the lung cancer lines might express other oncogenes besides Src, we examined the role of Stat3 in the Src-triggered GJIC suppression specifically, using the Src-transduced, SK-LuCi6-***Src*** line. As expected, Src expression disrupted gap junctional permeability. Interestingly, subsequent Stat3 inhibition with CPA7 or shRNA did not restore GJIC (Table 1,B). Taken together, the above findings indicate that Stat3 cannot be part of a pathway leading to Src-induced, gap junction closure in SK-LuCi6-***Src*** cells.

We then examined the possibility that Stat3 might play a ***positive*** role in the maintenance of gap junctional permeability, by assessing the effect of Stat3 inhibition upon GJIC levels in QU-DB cells which have low Src activity and extensive GJIC. As shown in Figure 2A (***d-f***), Stat3 downregulation through CPA7 treatment essentially ***abolished*** GJIC in QU-DB cells. Reduction of Stat3 levels through infection with the sh-Stat3 lentivirus vector gave similar results (Figure 2A, ***g-i***). Similarly, Stat3 downregulation in SK-LuCi6 or E10 cells caused a dramatic decrease in GJIC (Table 1,A). Conversely, expression of the constitutively active form of Stat3, Stat3C [26], increased the already extensive gap junctional communication in SK-LuCi6 cells (Table 1,A).

Examination of Cx43 levels following sh-Stat3 expression revealed a dramatic reduction (Figure 4B), indicating that Stat3 is required for the maintenance of Cx43 protein levels. TUNEL staining revealed that Stat3 inhibition by CPA7 treatment caused an increase in apoptosis in SK-LuCi6 cells (Figure 6A). In addition, CPA7 treatment caused an increase in PARP cleavage in these cells, even at a confluence of 50% (Figure 6B, lane 2). At 3 days post confluence, the time of GJIC examination, PARP cleavage was greater (lane 4), in agreement with previous results indicating that Stat3 inhibition causes apoptosis which is more pronounced in confluent cultures [27]. This finding hints at a link between GJIC reduction and apoptosis induced by Stat3 inhibition.

We next examined whether Stat3 inhibition might also affect Cx43 mRNA levels, through quatitative RT-PCR analysis [28]. The results showed that Stat3 inhibition by CPA7 treatment, or downregulation through shRNA expression brought about a substantial reduction in Cx43 mRNA levels, indicating an effect of Stat3 upon Cx43 gene transcription as well. In any event, taken together, our data reveal that, rather than increasing junctional permeability as might have been expected based on the well documented ability of Stat3 to act as a Src effector, Stat3 inhibition eliminates GJIC, indicating that Stat3 activity is actually ***required*** for gap junction function in two cultured lung carcinoma lines which display extensive GJIC.

Table 2 GJIC in primary lung carcinoma cells[α]

	Cells[β]	GJIC[α]
Adenosquamous carcinoma, moderately differentiated	**carcinoma cells**	0.1 ±0.1
	fibroblasts	5.8±1.2
Adenocarcinoma, poorly differentiated	**carcinoma cells**	0.1 ±0.1
Adenocarcinoma	**carcinoma cells**	0.1 ±0.1

[α]Immediately after surgery, cells were placed in culture and GJIC examined (see Methods, Figure 7). After 8-10 weeks in culture, most of the tumor cells had died while the fibroblasts present in the initial suspension predominated. These cells did not express cytokeratins, contrary to tumor cells [18]. The fibroblasts shown were derived from the moderately differentiated adenosquamous carcinoma tumor above (Figure 3, *c-d*). GJIC was examined as in Table I, at 3 days after confluence.

Discussion

Extensive data from our group and others demonstrated that oncogenes such as mT, Src or Ras can suppress gap junctional, intercellular communication [3,6]. Moreover,

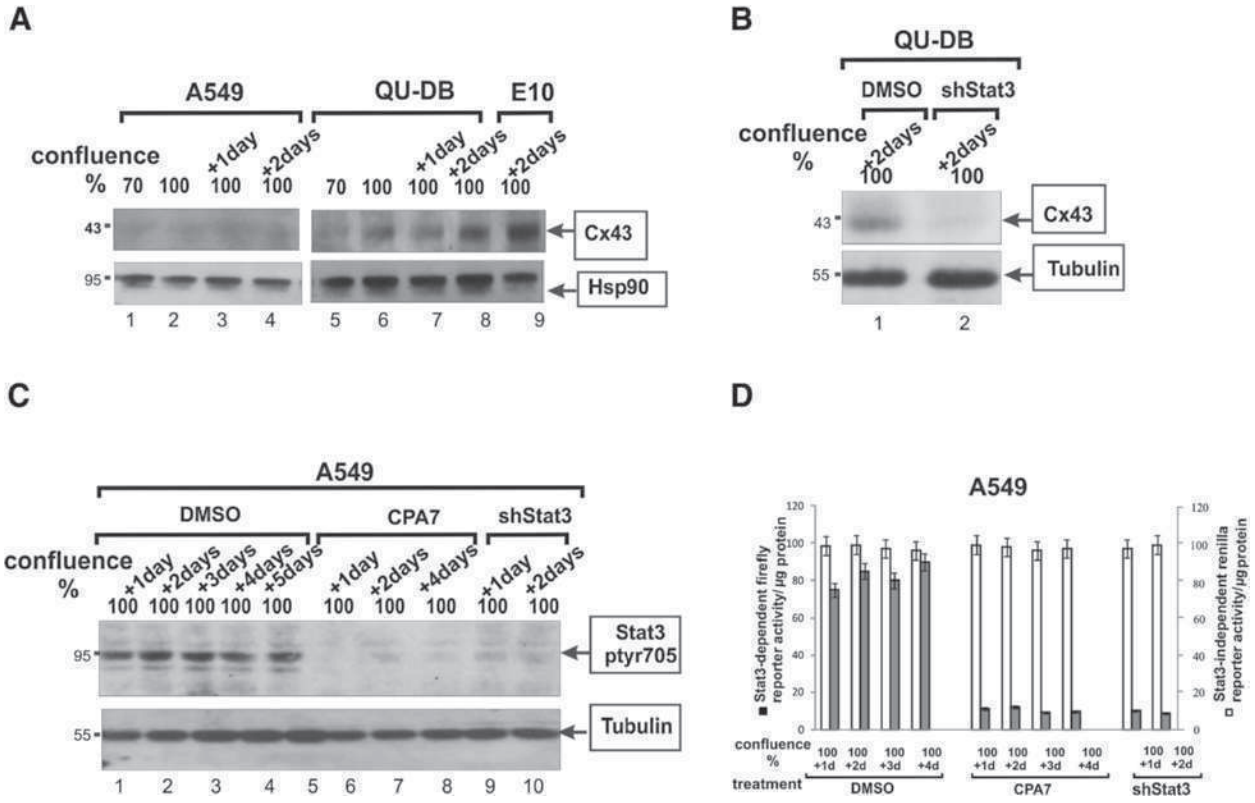

Figure 4 A: Cell density causes a dramatic increase in Cx43 levels in QU-DB cells. QU-DB (lanes 5-8) or A549 (lanes 1-4) or nontransformed E10 (lane 9) cells were grown to different densities as indicated and extracts probed for Cx43 or Hsp90 as a loading control. Note the absence of Cx43 in A549 cells and the increase in Cx43 with density in QUDB. **B: Stat3 knockdown reduces Cx43 levels.** QU-DB cells infected with the lentiviral vector carrying the Stat3-specific shRNA (lane 2) or not infected (lane 1) were grown to 2 days post-confluence and lysates probed for Cx43 or Hsp90 as a loading control. **C: CPA7 or Stat3-knockdown with shRNA reduce Stat3-ptyr705 levels in A549 cells.** A549 cells were grown to increasing densities and treated with the Stat3 inhibitor, CPA7 (lanes 6-8) or the DMSO carrier (lanes 1-5) for 15 hrs and cell extracts probed for Stat3-ptyr705 or tubulin as a loading control. Parallel cultures were infected with a vector expressing a Stat3-specific, shRNA [37], and cell extracts from stable lines produced were probed as above. **D: CPA7 or Stat3-knockdown with shRNA reduce Stat3 transcriptional activity in A549 cells.** A549 cells were transfected with a plasmid expressing a firefly luciferase gene under control of a Stat3-responsive promotor (▪) and a Stat3-independent promotor driving a *Renilla* luciferase gene (□) (see Methods). After transfection, cells were plated to different densities and treated with CPA7 or the DMSO carrier alone for 24 hrs, at which time firefly and *Renilla* luciferase activities were determined. Parallel cultures expressing the sh-Stat3 construct were transfected with the plasmids and firefly and *Renilla* luciferase activities determined.

it was shown that lower levels of these gene products were sufficient to eliminate gap junction function than the levels necessary for full transformation [4,29], indicating that a decrease in GJIC may be an early event in neoplastic conversion. In this communication we used an improved procedure to examine GJIC in lung cancer lines as well as in primary lung tumor cells. All cell lines had been established from NSCLC tumors which were known to be metastatic [18], except QU-DB, which was derived from a patient that was a long term survivor [30]. Our results reveal that GJIC was low in the majority of cases, except in the QU-DB and SK-LuCi6 lines. Assuming that the establishment process did not bring about an ***increase*** in GJIC, the existence of extensive GJIC in line SK-LuCi6 which was established from a rapidly metastatic tumor [31] indicates that intercellular communication does not necessarily inhibit metastasis; other factors may supercede potential growth inhibitory effects of intercellular communication and may be responsible for tumor growth and metastasis.

We next examined the mechanism of GJIC suppression by assessing the role of Src and its effector Stat3. Our results revealed an inverse relationship between Src-tyr418 phosphorylation levels and GJIC in a number of lines. Since Src is known to suppress gap junctional communication in cultured cells such as rodent fibroblasts and epithelial cells, it is tempting to speculate that Src may be responsible, at least in part, for gap junction closure in these lines. However, repeated attempts to reinstate GJIC by reducing Src activity levels through treatment with the Src kinase family-selective, pharmacological inhibitors

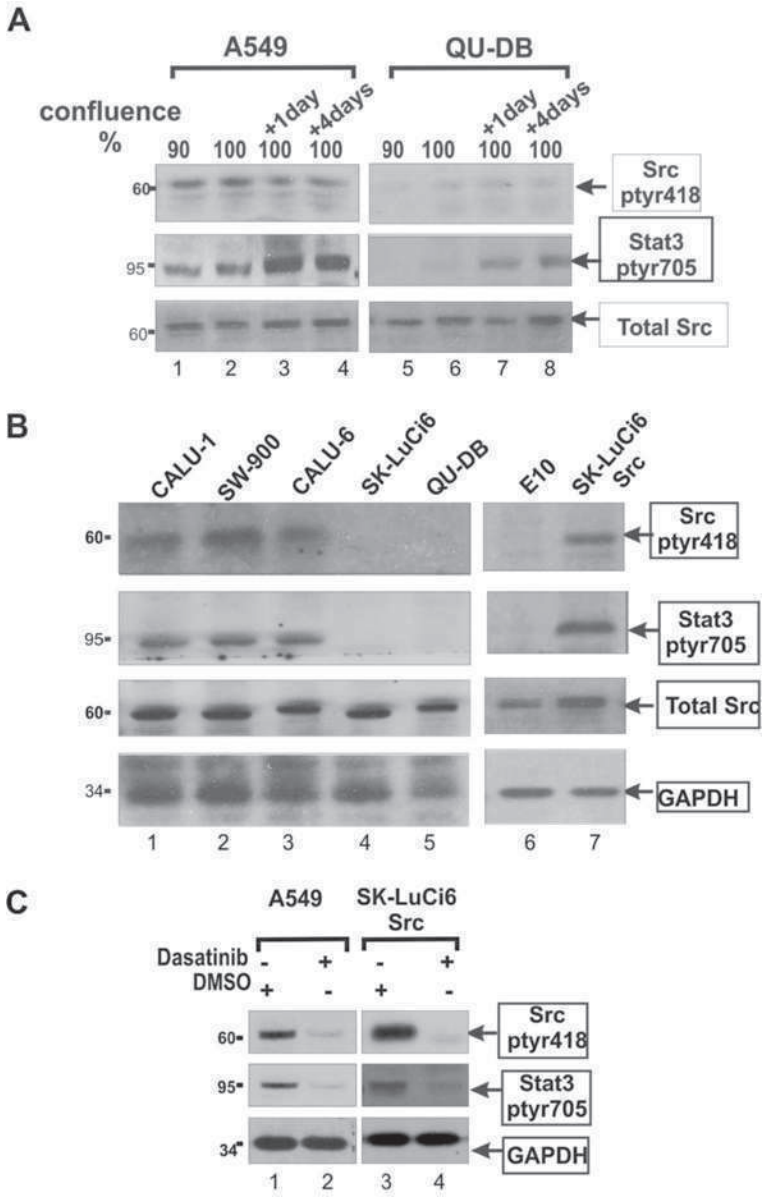

Figure 5 A: A549 cells have high Src-ptyr418 levels. QU-DB (lanes 5-8) or A549 (lanes 1-4) cells were grown to different densities as indicated and extracts probed for Src-ptyr418, Stat3-ptyr705 or total Src. Note the low levels of Src-ptyr418 in QU-DB cells. **B: Src-ptyr418 and Stat3-ptyr705 in NSCLC lines.** The indicated cell lines were grown to 50% confluence and extracts probed for Src-ptyr418, Stat3-ptyr705, total Src or GAPDH as a loading control. **C: Dasatinib reduces Stat3-ptyr705 levels in A459 cells:** A549 or SK-LuCi6-*Src* cells were grown to subconfluence and treated with the Src-selective inhibitor, Dasatinib (1μM) or the DMSO carrier alone and cell extracts probed for Src-ptyr418, Stat3-ptyr705 or GAPDH as a loading control, as indicated.

Dasatinib, PD180970 or SU6656, or infection with Adenoviral vectors expressing a Src dominant-negative mutant or c-Src kinase [15] in A549 cells which have high Src-ptyr418 were unsuccessful (not shown). Possibly other oncoproteins besides Src, or other factors may be important contributors to GJIC suppression in these lines. Alternatively, since low levels of activated Src were previously shown to be sufficient for GJIC suppression in mouse fibroblasts [3,4], the possibility that the residual Src activity in treated cells might be sufficient to interrupt gap junctional communication cannot be excluded. Dasatinib treatment of SK-LuCi6-***Src*** cells did cause a partial restoration of GJIC, although the high levels of SK-LuCi6 were not attained, possibly due to the high Src activity levels in this line.

We also examined GJIC in freshly explanted, primary cells from 3 NSCLC specimens. Since the

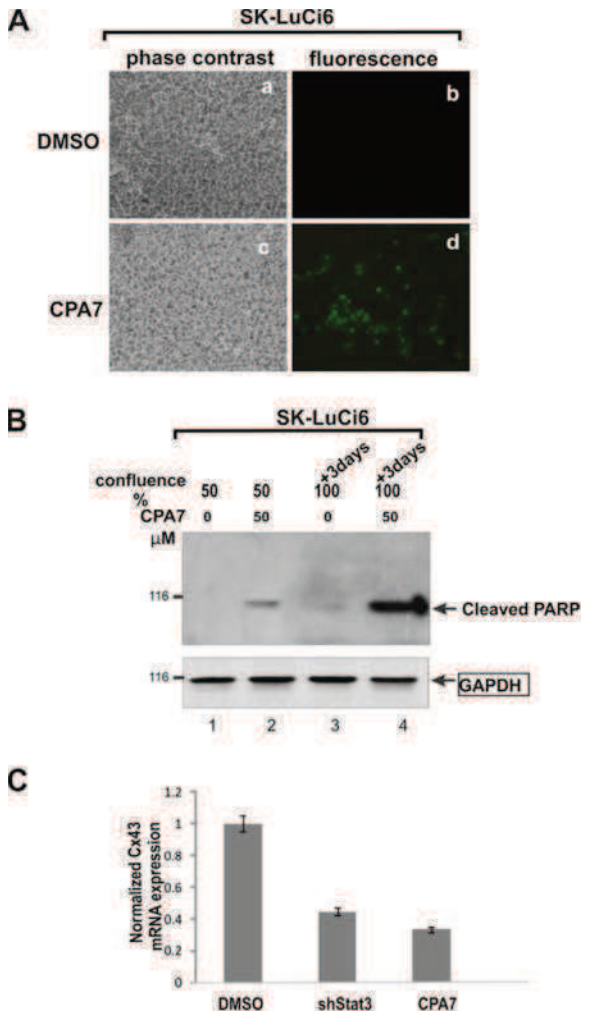

Figure 6 A, B: Stat3 inhibition induces apoptosis A: SK-LuCi6 cells without (***a,b***) or with (***c,d***) CPA7 treatment were fixed and stained for TUNEL using FITC-coupled, nucleotide triphosphates (see Methods). **B**: Extracts from SK-LuCi6 cells grown to 50% confluence or 3 days post-confluence, without (lanes 1,3) or with (lanes 2,4) treatment with 50 μM CPA7 for 15 hrs as indicated, were probed for cleaved PARP, with Hsp90 as a loading control (lower panel). **C: Stat3 inhibition reduces Cx43 mRNA.** Total RNA from SK-LuCi6 cells treated with the CPA7, Stat3 inhibitor, or the DMSO carrier alone, or stably expressing shStat3 as indicated, was subjected to quantitative RT-PCR analysis (see Methods).

senescence process can reduce GJIC [32], cells were plated in electroporation chambers immediately after surgery at densities of ~80%, so that they would reach confluence within 1–2 days, and GJIC examined every day for up to 10 days. No gap junctional communication was ever detected in any of the preparations, although fibroblasts from the same tissue had extensive GJIC (Figure 3, ***c-d***). Src-418 levels were relatively high in cells from all three tumor specimens, indicating that Src may have played a role in GJIC suppression. However, the possibility that the initiation of the senescence process even a day after surgery may have affected GJIC cannot be excluded.

Stat3 does not transmit Src signals to gap junction closure

Several signal transducers besides Stat3 are known to be downstream effectors of the Src kinase such as Ras/Raf/Erk, PI3k/Akt, the Crk-associated substrate (Cas) and others [33]. Constitutively active Ras is neoplastically transforming and can suppress GJIC [6,29]. Examination of the mechanism of Src-mediated, GJIC suppression previously indicated that inhibition of Ras in Src-transformed, rat fibroblasts reinstated gap junctional communication [19]. Conversely, mT expression in Ras-deficient cells did not suppress GJIC [34]. These data taken together underline the importance of the Ras pathway in GJIC reduction by activated Src. It was also shown later that Cas is required for the Src-induced, reduction in gap junctional communication [35]. In sharp contrast, our present data with Src-transduced, SK-LuCi6-***Src*** cells demonstrate that Stat3 inhibition does not restore GJIC, indicating that a role of Stat3 in the Src-induced, GJIC suppression in these cells is unlikely, despite the fact that constitutively active Stat3 can act as an oncogene and transform established lines [36].

Stat3 plays a *positive* role in gap junctional communication

The fact that cell density upregulates Stat3 concomitant with an increase in both Cx43 and GJIC prompted us to explore a potential positive role of Stat3 upon GJIC. Interestingly, Stat3 inhibition in two NSCLC lines which exhibit extensive junctional communication (QU-DB, SK-LuCi6) abolished GJIC, indicating that Stat3 does in fact play a positive role in the maintenance of gap junction function. This conclusion is in agreement with a previous report indicating that Stat3 inhibition eliminated GJIC in nontransformed rat liver epithelial cells as well [37].

Results from a number of labs demonstrated that Stat3 activates a number of anti-apoptotic genes, such as BcL-xL, Mcl1 and Akt1 [11]. Global induction of apoptosis with etoposide, cycloheximide or puromycin was shown to lead to a loss of cell coupling, probably due to caspase-3-mediated degradation of Cx43, in primary bovine lens epithelial and mouse NIH3T3 fibroblasts [38]. Interestingly, we previously demonstrated that Stat3 inhibition in cells transformed by Src or the Large Tumor antigen of Simian Virus 40 leads to apoptosis [15,39], possibly due to activation of the transcription factor E2F family, potent apoptosis inducers, by these oncogenes. Therefore, apoptosis induced by Stat3 downregulation in cells with high Src may have triggered gap junction closure.

We previously demonstrated that while Stat3 inhibition in sparsely growing, normal mouse fibroblasts causes

growth retardation, at high densities, such as needed for optimal gap junction formation, Stat3 inhibition leads to apoptosis [27]. Therefore, apoptosis induction through a reduction in Stat3 levels or activity could explain the dramatic reduction in Cx43 and GJIC upon Stat3 pharmacological or genetic inhibition, in lines with low Src activity. Still, our results also demonstrate a substantial reduction in Cx43 mRNA levels upon Stat3 inhibition, pointing to a transcriptional effect of Stat3 upon the Cx43 promotor in these NSCLC lines, as previously demonstrated in other cell types [28,40,41].

Conclusions

Our results demonstrate that Stat3 is not transmitting Src signals leading to gap junction closure in the NSCLC cell lines examined. In the contrary, although Stat3 is generally growth promoting and in an activated form it can act as an oncogene, we show for the first time that Stat3 is actually ***required*** for gap junctional communication both in normal epithelial cells and in certain tumor cell lines that retain GJIC. This novel role of Stat3 in gap junction function may be an important regulatory step in progression of tumours that exploit such a pathway.

Methods

Examination of gap junctional communication

To examine gap junctional communication by *in situ* electroporation, it is important to be able to reliably distinguish cells that were loaded with Lucifer yellow directly by electroporation, from cells that received the dye from neighbouring cells by diffusion through gap junctions. This was achieved using a slide where a 3 mm-wide strip of ITO had been removed by etching with acids, leaving two co-planar electrodes, supported by the same glass slide substrate (Figure 7) [42].

In a further improvement (Figure 8), the coating was removed from the glass surface in ~20 μm wide lines, to define electrode and non-conducting regions. Etching was done using a laser beam, so that the nonconductive glass underneath is exposed. It was important to ensure that only the 800Å coating was removed, without affecting the glass, so that cell growth would be unaffected across the line. This was achieved with a UV laser operating at a 355 nm wavelength using approximately 1 Watt of output power with 60% of the energy delivered to the surface of the glass. The beam was manipulated by mirrors on a pair of galvanometers to produce the desired pattern.

To form the two electrodes, the coating was removed in a straight line in the middle (**2**). A dam of nonconductive plastic (**3**) was bonded onto this line, to divert the current upwards, thus creating a sharp transition in electric field intensity between electroporated and non-electroporated sections. To provide areas where the cells are not electroporated, the ITO was also removed in two parallel lines

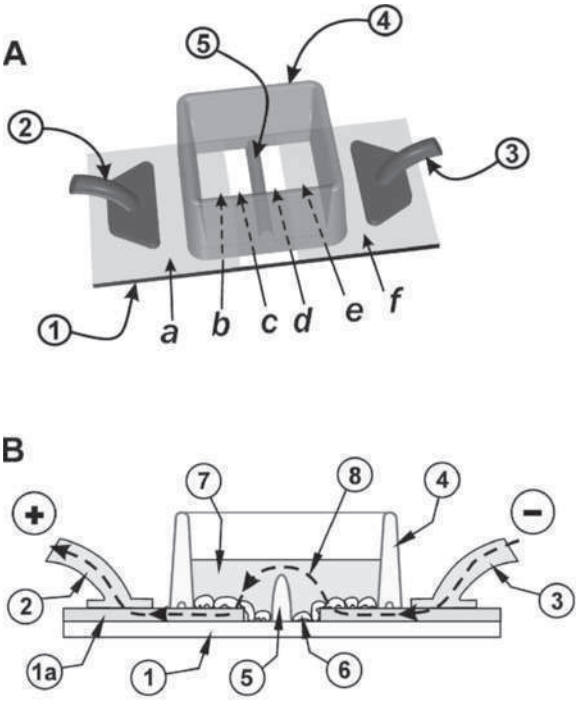

Figure 7 Electroporation on two co-planar ITO electrodes, formed by removing the ITO coating by chemical etching **A: Top view.** Cells were grown on an ITO-coated slide from which the coating was removed in a strip as shown. The two conductive sides (***a, f***), serving as electrodes, were connected to the positive and negative poles of the pulse generator (**2**) and (**3**). A nonconductive barrier (**5**) divides the strip of bare glass in half and separates the chamber into two sections. **B: Side view.** The slide with the cells growing on the ITO coated and the bare glass regions is shown. When electroporation buffer is added to the chamber to a level above the height of the barrier (**5**) then an electrical path between the electrodes (***e*** and ***b***) is formed. Note that the ITO layer (1***a***) is shown with dramatically exaggerated thickness for clarity, although its actual thickness is much less than the thickness of the cells (from [42]).

[(**4**) **and** (**4*a***)]. A plastic chamber was bonded onto the slide, to form a container for the cells and electroporation solutions (**5**). Current flows inwards from each contact point (**6** and **6*a***), via a conductive highway under the well (**5**) electroporating cells in area (***d***) then over the barrier [(**8**), arrowheads] to the other side, in area (***a***). In this configuration, cells which acquired LY by electroporation [growing in (***a***) and (***d***)] and cells into which LY traveled through gap junctions [(***b***) and (***c***)] both grow on ITO, separated only by a laser-etched line of ~20 μm. Extensive experimentation showed that in this setup the electroporation intensity is uniform across the electroporated area (see Figure 1B and Figure 2).

Cells were plated in the chamber and when they reached the appropriate density (90% confluence, to 5 days post-confluence), the growth medium was replaced with Calcium-free DMEM supplemented with 5 mg/ml Lucifer yellow (**7**). The slide/chamber was placed into a

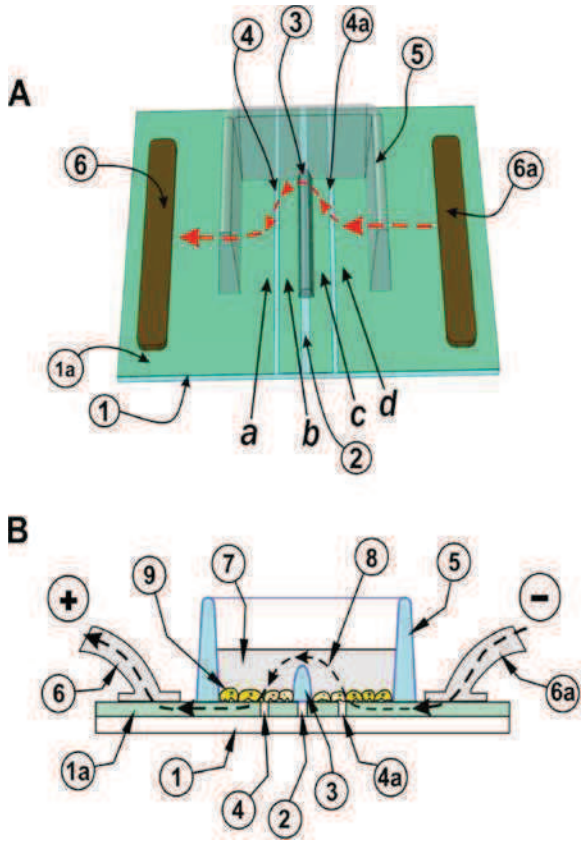

Figure 8 Electroporation on two co-planar ITO electrodes, formed by removing the ITO coating by etching with Lasers. **A:** Top view. Cells are grown on a glass slide (**1**), coated with ITO (**1*a***). The coating is laser-etched in a straight line in the middle (**2**), essentially forming two electrodes. A dam of Teflon (**3**) is used to divert the current upwards, thus creating a sharp transition in electric field intensity. A plastic chamber is bonded onto the slide, to form a container for the cells and LY (**5**). To provide areas where the cells are not electroporated, the ITO was also removed in two parallel lines [(**4**), (**4a**)]. Current from a pulse generator flows inwards from each contact point (**6** and **6*a***) to area (***d***) then over the barrier [(**3**), arrowheads] to the other side, electroporating cells in area (***a***). For clarity, the front part of the chamber is removed. **B: Side view.** The slide (**1**) with the cells growing on the ITO coated [(**1*a***), light green] and etched, bare glass regions is shown. When electroporation medium (**7**) is added to the chamber to a level above the height of the dam (**3**) then an electrical path (arrowheads) between the electrodes (**6**) and (**6*a***) and the cells (**9**) growing in this area is formed. Note that the size of the cells and the ITO layer (**1*a***) are shown exaggerated for clarity although the actual thickness of the ITO (800 Å) is much lower than the thickness of the cells.

holder where electrical contacts were established and a set of electrical pulses delivered to the cells. Extensive experimentation indicated that 10 pulse pairs, each pulse of 18 Volts peak value, 100 μs length and spaced 0.5 seconds apart, with one of each pair having a polarity opposite to that of its partner gave optimal results. Following a 5 min incubation at 37°C, the unincorporated dye was washed away with Calcium-free DMEM supplemented with 10% dialysed fetal calf serum and cells observed and photographed under fluorescence and phase contrast illumination. Communication is expressed as the number of cells into which the dye has transferred per cell loaded with the dye by electroporation at the edge of the electroporated area. All experiments were conducted at least three times, with at least 5 slides each time, and the results are presented as average GJIC±SEM where the transfer from at least 200 cells is assessed.

The equipment (*Insitu* Porator) was supplied by Cell Projects Ltd UK.

Cell lines, culture techniques and Stat3 activity measurement

All cells were grown in DMEM with 10% fetal calf serum. Extra care was taken to ensure that cell seeding was uniform, by passing cells at subconfluence, when cell to cell adhesion was low. Confluence was estimated visually and quantitated by imaging analysis of live cells under phase contrast [14]. To ensure that the growth medium was not depleted of nutrients, it was changed every day.

Cells were cultured from surgically explanted tumors as previously described [18].

Stat3C and activated Src were expressed in SK-LuCi-6 cells through infection with the culture supernatant from a Phoenix amphotropic packaging line transfected with a pBabe-puro-Stat3C plasmid [26]. shStat3 was expressed by retroviral vector infection as described [16].

Stat3 transcriptional activity was measured as described, by transient transfection of the p*Luc*TKS3 construct [24]. As a control, cells were co-transfected with the reporter pRLSRE, which contains two copies of the serum response element (SRE) of the c-fos promoter, subcloned into the *Renilla* luciferase reporter, pRL-null (Promega) [15]. Following transfection, cells were plated to different densities and luciferase activity determined.

For Stat3 immunostaining, SK-LuCi6 cells were fixed with 4% paraformaldehyde, permeabilized in 0.2% Triton-X100 and probed with a Stat3 antibody (Cell Signalling, #9132 diluted at 1:100) followed by AlexaFluor-coupled, goat anti-rabbit IgG (Invitrogen #A11008, used at 1:400).

Inhibitors

Stat3 was inactivated using two approaches: **(1).** Treatment with 50 μM CPA7 [$PtCl_3(NO_2)(NH_3)_2$] [25] overnight, or **(2).** Expression of shRNA, delivered with a lentivirus vector as described [37]. Jak inhibitor-1 was from EMD Biosciences (5 μM [16]).

Src was inactivated using 3 pharmacological inhibitors: Dasatinib (0.5 or 1 μM, up to 72h), PD180970 (0.2 μM with redosing every 12h for a total of 24h), or SU6656 (5μM for 24h) [15].

Western blotting

It was conducted on proteins extracted from cell pellets [43], using antibodies to Cx43 (Cell Signalling, #3512, used at a 1:500 dilution), Stat3-ptyr705 (Cell Signalling, #9131, 1:1,000), Src-ptyr418 (Invitrogen, #44-660G , 1:1,000) or total Src (rabbit monoclonal 36D10, Cell Signalling, #2109, 1:1,000), followed by secondary antibodies and ECL reagents (Biosource). Alpha-Tubulin (Cell Signalling #2125, 1:5,000), GAPDH (BD Transduction, #14C10, 1:5,000) or Hsp90 (Assay designs, #SPA-830, 1:5,000) served as loading controls.

qRT-PCR

SK-LuCi6 cells were treated with CPA7 for 15 hrs. The RNeasy Mini Kit (Qiagen, Hilden Germany, cat. #74104) was used for the purification of RNA. cDNA synthesis from 1μg of total RNA was performed using the iScript cDNA synthesis kit (Bio-RAD Laboratories, Hercules, CA). qRT-PCR was performed using iQ SYBR Green Supermix (Bio-RAD Laboratories, Hercules, CA) and 20μM primer. Primer sequences were [28]:

Cx43: Forward: 5′-GCCTGAACTTGCCTTTTCAT-3′,

Reverse: 5′- CTCCAGTCACCCATGTTGC-3′, [28] to generate a product of 500 bp [40].

As internal reference genes we used GAPDH: (forward: 5′-AATGCATCCTGCACCACCAA-3′, Reverse: 5′-GTAGCCATATTCATTGTCATA-3′) [40] and 18S RNA [16]. mRNA from SK-LuCi6 cells where Stat3 was downregulated with sh-Stat3 was analysed in a similar manner. Results from 3 independent experiments, each conducted in triplicate were averaged out and SEM calculated.

Additional file

Additional file 1: Additional data.

Abbreviations

Cx43: Connexin-43; GJIC: Gap junctional, intercellular communication; NSCLC: Non-small cell lung cancer.

Competing interests

The corresponding author received a royalty from PARTEQ, the intellectual property arm of Queen's University, for a patent where she is a co-inventor of the apparatus used in this work. PARTEQ had no involvement whatsoever in the content of this paper.

Authors' contributions

MG did the bulk of the benchwork. SG and RA conducted some of the initial experiments. Aaron Trotman-Grant did the Stat3C experiments. ET obtained the results on the primary lung carcinoma cells. LR conceived of the study, designed and coordinated it and drafted the manuscript. All authors read and approve of the manuscript.

Authors' information

MG is a postdoctoral fellow, funded by the US Army breast cancer program. RA and ET were graduate students. ATG is currently doing a project. LR is a professor at Queen's University, Kingston, Canada.

Acknowledgements

We would like to thank Dr. Mike Baird and Shallyn Littlefield for CPA7 synthesis, Dr. Jackie Bromberg for the pBabe-puro-Stat3C plasmid, Kevin Firth, P.Eng., of Ask Sciences products, Kingston, Ontario for engineering design, Dr. Christopher Nicol for advice and help with qRT-PCR assays, Drs Bruce Banfield and Renee Finnen for fluorescent microscopy and Dr. Andrew Craig for the NL20 line. We are grateful to Dr. Elissavet Kardami (University of Manitoba, Canada) for a generous gift of connexin-43 antibody. The financial assistance of the Canadian Institutes of Health Research (CIHR), the Canadian Breast Cancer Foundation (Ontario Chapter), the Natural Sciences and Engineering Research Council of Canada (NSERC), the Canadian Breast Cancer Research Alliance, the Ontario Centers of Excellence, the Breast Cancer Action Kingston and the Clare Nelson bequest fund through grants to LR is gratefully acknowledged. RA was supported by a Canada Graduate Scholarships Doctoral award from CIHR, the Ontario Women's Health Scholars Award from the Ontario Council on Graduate Studies and a Queen's University Graduate Award. ET was the recipient of an OGSST award. SG was the recipient of an NSERC summer studentship. MG was supported by a postdoctoral fellowship from the US army Breast Cancer Program, the Ministry of Research and Innovation of the Province of Ontario and the Advisory Research Committee of Queen's University.

Author details

[1]Departments of Microbiology and Immunology and Pathology, Queen's University, Kingston, Ontario, K7L3N6, Canada. [2]Present address: Center for Innovative Cancer Research, Ottawa Hospital Research Institute, 501 Smyth Road, Ottawa, ON K1H 8L6, Canada. [3]Present address: Department of Laboratory Medicine and Pathobiology, University of Toronto, Toronto, Ontario, Canada M5S1A8. [4]Present address: Institute for Physiology and Pathophysiology, Medical Faculty, University of Heidelberg, Im Neuenheimer Feld 326, D-69120, Germany.

Received: 12 April 2012 Accepted: 13 December 2012
Published: 18 December 2012

References

1. Vinken M, Vanhaecke T, Papeleu P, Snykers S, Henkens T, Rogiers V: **Connexins and their channels in cell growth and cell death.** *Cell Signal* 2006, **18:**592–600.
2. Lin R, Martyn KD, Guyette CV, Lau AF, Warn-Cramer BJ: **v-Src tyrosine phosphorylation of connexin43: regulation of gap junction communication and effects on cell transformation.** *Cell Commun Adhes* 2006, **13:**199–216.
3. Azarnia R, Loewenstein WR: **Polyomavirus middle t antigen downregulates junctional cell-to-cell communication.** *Mol Cell Biol* 1987, **7:**946–950.
4. Raptis L, Brownell HL, Firth KL, MacKenzie LW: **A novel technique for the study of intercellular, junctional communication; electroporation of adherent cells on a partly conductive slide.** *DNA Cell Biol* 1994, **13:**963–975.
5. Grammatikakis N, Vultur A, Ramana CV, Siganou A, Schweinfest CW, Raptis L: **The role of Hsp90N, a new member of the Hsp90 family, in signal transduction and neoplastic transformation.** *J Biol Chem* 2002, **277:**8312–8320.
6. Brownell HL, Narsimhan R, Corbley MJ, Mann VM, Whitfield JF, Raptis L: **Ras is involved in gap junction closure in mouse fibroblasts or preadipocytes but not in differentiated adipocytes.** *DNA Cell Biol* 1996, **15:**443–451.
7. Atkinson MM, Sheridan JD: **Altered junctional permeability between cells transformed by v-ras, v-mos, or v-src.** *Am J Physiol* 1988, **255:**C674–C683.
8. Pahujaa M, Anikin M, Goldberg GS: **Phosphorylation of connexin43 induced by Src: regulation of gap junctional communication between transformed cells.** *Exp Cell Res* 2007, **313:**4083–4090.
9. Masaki T, Igarashi K, Tokuda M, Yukimasa S, Han F, Jin YJ, *et al*: **pp60c-src activation in lung adenocarcinoma.** *Eur J Cancer* 2003, **39:**1447–1455.
10. Zhang J, Kalyankrishna S, Wislez M, Thilaganathan N, Saigal B, Wei W, *et al*: **SRC-family kinases are activated in non-small cell lung cancer and promote the survival of epidermal growth factor receptor-dependent cell lines.** *Am J Pathol* 2007, **170:**366–376.
11. Yu H, Pardoll D, Jove R: **STATs in cancer inflammation and immunity: a leading role for STAT3.** *Nat Rev Cancer* 2009, **9:**798–809.

12. Song L, Turkson J, Karras JG, Jove R, Haura EB: **Activation of Stat3 by receptor tyrosine kinases and cytokines regulates survival in human non-small cell carcinoma cells.** *Oncogene* 2003, **22:**4150–4165.
13. Byers LA, Sen B, Saigal B, Diao L, Wang J, Nanjundan M, *et al*: **Reciprocal regulation of c-Src and STAT3 in non-small cell lung cancer.** *Clin Cancer Res* 2009, **15:**6852–6861.
14. Vultur A, Cao J, Arulanandam R, Turkson J, Jove R, Greer P, *et al*: **Cell to cell adhesion modulates Stat3 activity in normal and breast carcinoma cells.** *Oncogene* 2004, **23:**2600–2616.
15. Vultur A, Arulanandam R, Turkson J, Niu G, Jove R, Raptis L: **Stat3 is required for full neoplastic transformation by the Simian Virus 40 Large Tumor antigen.** *Mol Biol Cell* 2005, **16:**3832–3846.
16. Arulanandam R, Vultur A, Cao J, Carefoot E, Truesdell P, Elliott B, *et al*: **Cadherin-cadherin engagement promotes survival via Rac/Cdc42 and Stat3.** *Mol Cancer Res* 2009, **17:**1310–1327.
17. Raptis L, Arulanandam R, Vultur A, Geletu M, Chevalier S, Feracci H: **Beyond structure, to survival: Stat3 activation by cadherin engagement.** *Biochem Cell Biol* 2009, **87:**835–843.
18. Tomai E, Brownell HL, Tufescu T, Reid K, Raptis L: **Gap junctional communication in lung carcinoma cells.** *Lung Cancer* 1999, **23:**223–231.
19. Ito S, Ito Y, Senga T, Hattori S, Matsuo S, Hamaguchi M: **v-Src requires Ras signaling for the suppression of gap junctional intercellular communication.** *Oncogene* 2006, **25:**2420–2424.
20. Wei CJ, Francis R, Xu X, Lo CW: **Connexin43 associated with an N-cadherin-containing multiprotein complex is required for gap junction formation in NIH3T3 cells.** *J Biol Chem* 2005, **280:**19925–19936.
21. Frenzel EM, Johnson RG: **Gap junction formation between cultured embryonic lens cells is inhibited by antibody to N-cadherin.** *Dev Biol* 1996, **179:**1–16.
22. Vultur A, Tomai E, Peebles K, Malkinson AM, Grammatikakis N, Forkert PG, *et al*: **Gap junctional, intercellular communication in cells from urethane-induced tumors in A/J mice.** *DNA Cell Biol* 2003, **22:**33–40.
23. Schiller J, Sabatini L, Bittner G, Pinkerman C, Mayotte J, Levitt M, *et al*: **Phenotypic, molecular and genetic-characterization of transformed human bronchial epithelial-cell strains.** *Int J Oncol* 1994, **4:**461–470.
24. Turkson J, Bowman T, Garcia R, Caldenhoven E, de Groot RP, Jove R: **Stat3 activation by Src induces specific gene regulation and is required for cell transformation.** *Mol Cell Biol* 1998, **18:**2545–2552.
25. Littlefield SL, Baird MC, Anagnostopoulou A, Raptis L: **Synthesis, characterization and Stat3 inhibitory properties of the prototypical platinum(IV) anticancer drug, [PtCl3(NO2)(NH3)2] (CPA-7).** *Inorg Chem* 2008, **47:**2798–2804.
26. Bromberg JF, Wrzeszczynska MH, Devgan G, Zhao Y, Pestell RG, Albanese C, *et al*: **Stat3 as an oncogene.** *Cell* 1999, **98:**295–303.
27. Anagnostopoulou A, Vultur A, Arulanandam R, Cao J, Turkson J, Jove R, *et al*: **Differential effects of Stat3 inhibition in sparse vs confluent normal and breast cancer cells.** *Cancer Lett* 2006, **242:**120–132.
28. Andersson H, Brittebo E: **Proangiogenic effects of environmentally relevant levels of bisphenol A in human primary endothelial cells.** *Arch Toxicol* 2012, **86:**465–474.
29. Brownell HL, Whitfield JF, Raptis L: **Elimination of intercellular junctional communication requires lower Ras^{leu61} levels than stimulation of anchorage-independent proliferation.** *Cancer Detect Prev* 1997, **21:**289–294.
30. Cole SP, Campling BG, Dexter DF, Holden JJ, Roder JC: **Establishment of a human large cell lung tumor line (QU-DB) with metastatic properties in athymic mice.** *Cancer* 1986, **58:**917–923.
31. Anger B, Bockman R, Andreeff M, Erlandson R, Jhanwar S, Kameya T, *et al*: **Characterization of two newly established human cell lines from patients with large-cell anaplastic lung carcinoma.** *Cancer* 1982, **50:**1518–1529.
32. Xie HQ, Huang R, Hu VW: **Intercellular communication through gap junctions is reduced in senescent cells.** *Biophys J* 1992, **62:**45–47.
33. Aleshin A, Finn RS: **SRC: a century of science brought to the clinic.** *Neoplasia* 2010, **12:**599–607.
34. Brownell HL, Whitfield JF, Raptis L: **Cellular Ras partly mediates gap junction closure by the polyoma virus middle Tumor antigen.** *Cancer Lett* 1996, **103:**99–106.
35. Shen Y, Khusial PR, Li X, Ichikawa H, Moreno AP, Goldberg GS: **SRC utilizes Cas to block gap junctional communication mediated by connexin43.** *J Biol Chem* 2007, **282:**18914–18921.
36. McLemore ML, Grewal S, Liu F, Archambault A, Poursine-Laurent J, Haug J, *et al*: **STAT-3 activation is required for normal G-CSF-dependent proliferation and granulocytic differentiation.** *Immunity* 2001, **14:**193–204.
37. Geletu M, Chaize C, Arulanandam R, Vultur A, Kowolik C, Anagnostopoulou A, *et al*: **Stat3 activity is required for gap junctional permeability in normal epithelial cells and fibroblasts.** *DNA Cell Biol* 2009, **28:**319–327.
38. Theiss C, Mazur A, Meller K, Mannherz HG: **Changes in gap junction organization and decreased coupling during induced apoptosis in lens epithelial and NIH-3T3 cells.** *Exp Cell Res* 2007, **313:**38–52.
39. Anagnostopoulou A, Vultur A, Arulanandam R, Cao J, Turkson J, Jove R, *et al*: **Role of Stat3 in normal and SV40 transformed cells.** *Research Trends - Trends in Cancer Research* 2006, **2:**93–103.
40. Ozog MA, Bernier SM, Bates DC, Chatterjee B, Lo CW, Naus CC: **The complex of ciliary neurotrophic factor-ciliary neurotrophic factor receptor alpha up-regulates connexin43 and intercellular coupling in astrocytes via the Janus tyrosine kinase/signal transducer and activator of transcription pathway.** *Mol Biol Cell* 2004, **15:**4761–4774.
41. Rajasingh J, Bord E, Hamada H, Lambers E, Qin G, Losordo DW, *et al*: **STAT3-dependent mouse embryonic stem cell differentiation into cardiomyocytes: analysis of molecular signaling and therapeutic efficacy of cardiomyocyte precommitted mES transplantation in a mouse model of myocardial infarction.** *Circ Res* 2007, **101:**910–918.
42. Anagnostopoulou A, Cao J, Vultur A, Firth KL, Raptis L: **Examination of gap junctional, intercellular communication by *in situ* electroporation on two co-planar indium-tin oxide electrodes.** *Mol Oncol* 2007, **1:**226–231.
43. Greer S, Honeywell R, Geletu M, Arulanandam R, Raptis L: **housekeeping gene products; levels may change with confluence of cultured cells.** *J Immunol Methods* 2010, **355:**76–79.

doi:10.1186/1471-2407-12-605
Cite this article as: Geletu *et al.*: Stat3 is a positive regulator of gap junctional intercellular communication in cultured, human lung carcinoma cells. *BMC Cancer* 2012 **12**:605.

The Simian Virus 40 Large Tumor Antigen Activates cSrc and Requires cSrc for Full Neoplastic Transformation

ROZANNE ARULANANDAM, MULU GELETU and LEDA RAPTIS

Departments of Microbiology and Immunology and Pathology, Queen's University, Kingston, Ontario, K7L 3N6, Canada

Abstract. *Aim: To investigate the role of the cellular protooncogene product, cSrc, in neoplastic transformation by the large tumor antigen of simian virus 40 (TAg), the ability of TAg to increase cSrc activity was examined. Materials and Methods: cSrc activity was measured in cells expressing wild-type or mutant TAg and compared to the parental line. Results: The results indicated that TAg expression in mouse 3T3 fibroblasts causes a dramatic increase in cSrc activity, a finding which establishes TAg as a cSrc activator. This ability depended upon a TAg, intact retinoblastoma-susceptibility gene product (Rb) family-binding site. In addition, genetic ablation of pRb in mouse fibroblasts increased cSrc activity, suggesting that pRb inactivation by TAg might be responsible for the observed cSrc activation. Furthermore, down-regulation or genetic ablation of cSrc alone, or together with the Src family members, Yes and Fyn, caused a dramatic reduction in the ability of TAg to transform mouse fibroblasts. Conclusion: Taken together, these findings suggest for the first time that cSrc is part of an important pathway emanating from TAg and leading to neoplastic conversion.*

The simian virus 40 large tumor antigen (TAg) is a viral oncogene which is able to elicit neoplastic transformation in a variety of mammalian cell types by targeting a number of proteins to override cellular growth controls. Prominent among the latter are two tumor-suppressor proteins, p53 and the retinoblastoma-susceptibility gene product family (pRb, p107, p130, reviewed in (1)). The interaction with the Rb family is through an LXCXE motif (residues 103-107), and mutants where this motif is altered are defective for transformation in nearly all assay systems (2, 3).

Correspondence to: Leda Raptis, Department of Microbiology and Immunology, Queen's University, Botterell Hall, Rm. 713, Kingston, Ontario, K7L3N6, Canada. Tel: +16135332462, Fax: +16135336796, e-mail: raptisl@queensu.ca

Key Words: cSrc, Simian Virus 40 Large Tumor antigen, retinoblastoma susceptibility gene product, neoplastic transformation, rodent fibroblasts, signal transduction.

The effects of TAg on the Rb family proteins are thought to be exerted by regulating the activity of the E2F transcription factors. There are eight known E2F proteins (E2F1-8), all of which possess a DNA-binding domain that governs their interactions with a common consensus sequence present in the promoters of a number of genes (reviewed in (4, 5)). In quiescent cells, E2F-regulated genes are not expressed because their promoters are occupied primarily by p130/E2F4 complexes which repress transcription. Following receptor stimulation, Rb proteins are inactivated through phosphorylation by the cyclin-dependent kinases and this results in the replacement of the p130/E2F4 complexes by the 'activating' E2F1-3. This leads to the transcription of E2F-regulated genes, many of which encode proteins required for DNA replication, nucleotide metabolism, DNA repair and cell cycle progression. Large T antigen short-circuits this pathway by binding Rb proteins thereby blocking their ability to down-regulate E2Fs. Thus, TAg disrupts repressive Rb-E2F complexes, allowing transcription of E2F-dependent genes and progression of cells into the S-phase. In addition, the amino-terminus of TAg has a DNA-J domain function, which can recruit the heat-shock protein hsc70 to aid in the disruption of the Rb/E2F complex (reviewed in (6)).

Previous results demonstrated that TAg activates the Ras/Raf/extracellular signal regulated kinase (Erk) and signal transducer and activator of transcription-3 (Stat3) pathways (7-9), thus establishing a link between a viral oncogene known to have mainly nuclear targets, and the membrane signalling apparatus. However, the role of the cellular Src protooncogene product (cSrc), a signal transducer also often activated by membrane growth factor receptors, in TAg signalling is unclear (10). In the present communication, we attempted to examine the role of cSrc in transformation by TAg.

Materials and Methods

Cell lines, culture techniques and gene expression. Tissue culture medium (Dulbecco's modified Eagle's medium, DMEM) was from ICN (Aurora, Ohio) and calf serum from Life Technologies Inc. (Burlington, ON, Canada). 3T3 fibroblasts were previously described (11) and were grown in plastic dishes in DMEM supplemented with 10% calf serum, in a 7% CO_2 incubator. The SYF, SYF-Src and Src++ cells (12) were obtained from ATCC

(Manassas, VA, USA) and grown in DMEM supplemented with 10% fetal calf serum.

TAg expression was achieved through a pBabe-Hygro-based retroviral vector system as described elsewhere (8). The K1 mutant, which is defective in pRb binding, was expressed with a pBabe-puro retroviral vector (a gift of Drs. Thomas Roberts and Ole Gjoerup). In each case, 3T3 fibroblasts were infected, selected for hygromycin resistance and a number of independent clones picked and tested for TAg levels. Representative clones were chosen for further study. The adenovirus vectors expressing the dominant-negative Src mutant (DN-Src) and the C-terminal Src kinase (Ad-Csk) which phosphorylates Src, Fyn and Yes kinases were a generous gift of Dr. D. R. Kaplan. They were amplified in 293 cells as elsewhere (9). Both vectors also express a green fluorescence protein (GFP) from a separate cytomegalovirus (CMV) promotor, which allows for easy identification of infected cells. High titer virus stocks were produced and the virus purified by CsCl centrifugation and titrated on 293 cells. Cells were infected with the vectors or the control pAdTrack (Stratagene, La Jolla, CA, USA) lacking an insert, at 300 pfu/ml in the presence of poly-lysine (13), and lysed 48 hours later for Western blotting, or for agar assays. In both cases, infection rates were more than 95%, as determined by fluorescence microscopy of the GFP protein (14). For growth rate assessment, cells were reinfected 4 days later.

To examine the cells' ability for anchorage-independent proliferation, approximately 10^4 cells were suspended in 2 ml of 0.33% Agarose (Sigma, Oakville, ON, Canada)-containing DMEM supplemented with 15% fetal calf serum on top of a feeder layer of the same medium containing 0.7% agarose, in 6 cm petri dishes (8). Growth was recorded and photographs taken 10 days later under phase-contrast illumination. For foci formation, 200 3T3, 3T3-TAg, 3T3-TAg-DNSrc, SYF, SYF-Src or Src++ cells were plated together with 2×10^4 normal 3T3 cells. Foci appeared 10 days later and were stained and photographed.

Western blotting. Cells were grown to different densities from 10% to 2 days after confluence, at which times total proteins were extracted. In initial experiments, cells were lysed directly on the plate and protein determination conducted on extracts clarified by centrifugation. However, a significant amount of serum proteins present in the growth medium was found to attach nonspecifically to the plastic petri dish and be eluted with the detergent-containing extraction buffer, which could disturb the determination of protein concentration in the lysate significantly, especially at lower cell densities (15). To avoid this problem, cells were scraped in ice-cold phosphate-buffered saline (PBS), transferred into microcentrifuge tubes, washed once in PBS and the extraction buffer [50 mM Hepes, pH 7.4, 150 mM NaCl, 10 mM EDTA, 10 mM $Na_4P_2O_7$, 100 mM NaF, 2 mM Na_3VO_4, 0.5 mM phenylmethylsulphonyl fluoride (PMSF), 10 μg/ml aprotinin, 10 μg/ml leupeptin, and 1% Triton X-100 (16)] added to cell pellets for 10 minutes with vigorous pipetting. Subsequently, 30 μg of clarified cell extract were resolved on a 10% polyacrylamide-SDS gel and transferred to a nitrocellulose membrane (Bio-Rad, Mississauga, ON, Canada). Immunodetection was performed using antibodies against TAg (clone 108, a gift of Dr. Gurney), Src418 (#44-660G, Biosource, Carlsbad, CA, USA), total Src (36D10; Cell Signaling, Danvers, MA, USA, #2109), focal adhesion kinase (FAK) ptyr861 (#44-626G, Biosource) and α-tubulin (Cell Signalling), followed by alkaline phosphatase-conjugated goat secondary antibodies (#ALI 4405, Biosource,). The bands were visualized using enhanced chemiluminescence (ECL), according to the manufacturer's instructions (PerkinElmer Life Sciences, Waltham, MA, USA). Quantification was achieved by fluorimager analysis using the FluorChem program (AlphaInnotech Corp, San Leandro, CA, USA), with the values obtained normalized for α-tubulin.

Results

Cell density does not up-regulate cSrc activity in mouse 3T3 fibroblasts. We previously demonstrated that cell confluence alone increases the activity of a number of proteins, such as the Jak kinases [(17), reviewed in (18)]. Therefore, to examine the role of Src in TAg-mediated transformation, we at first investigated the effect of cell density upon the levels of cSrc tyr418 phosphorylation (Src418) which correlates with its activity, in newly established mouse embryo 3T3 fibroblasts. As a control for protein loading, the same extracts were probed for α-tubulin (see Materials and Methods). As shown in Figure 1 (lanes 1-4), cell density had no effect upon Src418 or total Src protein levels, indicating that, unlike the Jak kinases (17), density does *not* affect cSrc activity.

TAg triggers cSrc activation. Previous results indicated that TAg can activate the Ras/Raf/Erk pathway, a finding which provided a link between a nuclear oncogene and the membrane signalling apparatus (7, 8). Since cSrc is also often activated by membrane-bound, growth factor receptors, we examined the ability of TAg to activate cSrc in mouse fibroblasts. To this effect, we used established mouse 3T3 fibroblasts expressing TAg with a retroviral vector (3T3-TAg), with cells infected with the same vector lacking an insert serving as negative controls [3T3 (8)]. As shown in Figure 1A, TAg expression caused a dramatic increase in Src418 levels, while total cSrc levels remained unchanged (lanes 1-4 *vs*. 5-8). To ensure that cell density did not affect TAg expression itself, TAg levels were also examined at different densities and found to be unchanged (Figure 1A, top panel). As a control for specificity of the TAg-mediated Src418 increase, Src418 levels were examined in 3T3 cells stably expressing activated Ras^{leu61} (19) and found to have the same levels as the parental line (lanes 9-10), indicating that Src418 phosphorylation is not simply a general outcome of the transformed state. The above data taken together indicate that TAg expression results in stimulation of Src418 in cultured mouse fibroblasts.

One of the major Src substrates is FAK, which is phosphorylated by activated Src at tyr861 (20). To examine whether the increase in Src418 translates into an increase in Src activity, Western blots from TAg-expressing cells were probed with an antibody specific for FAK ptyr861 (21). The results (Figure 1A, right panel) revealed a dramatic increase in FAK ptyr861 upon TAg expression, indicating that TAg does indeed increase cSrc activity.

TAg requires cSrc activity for neoplastic transformation. To examine the cSrc requirement for TAg-induced transformation, cSrc activity was reduced in 3T3-TAg cells through infection

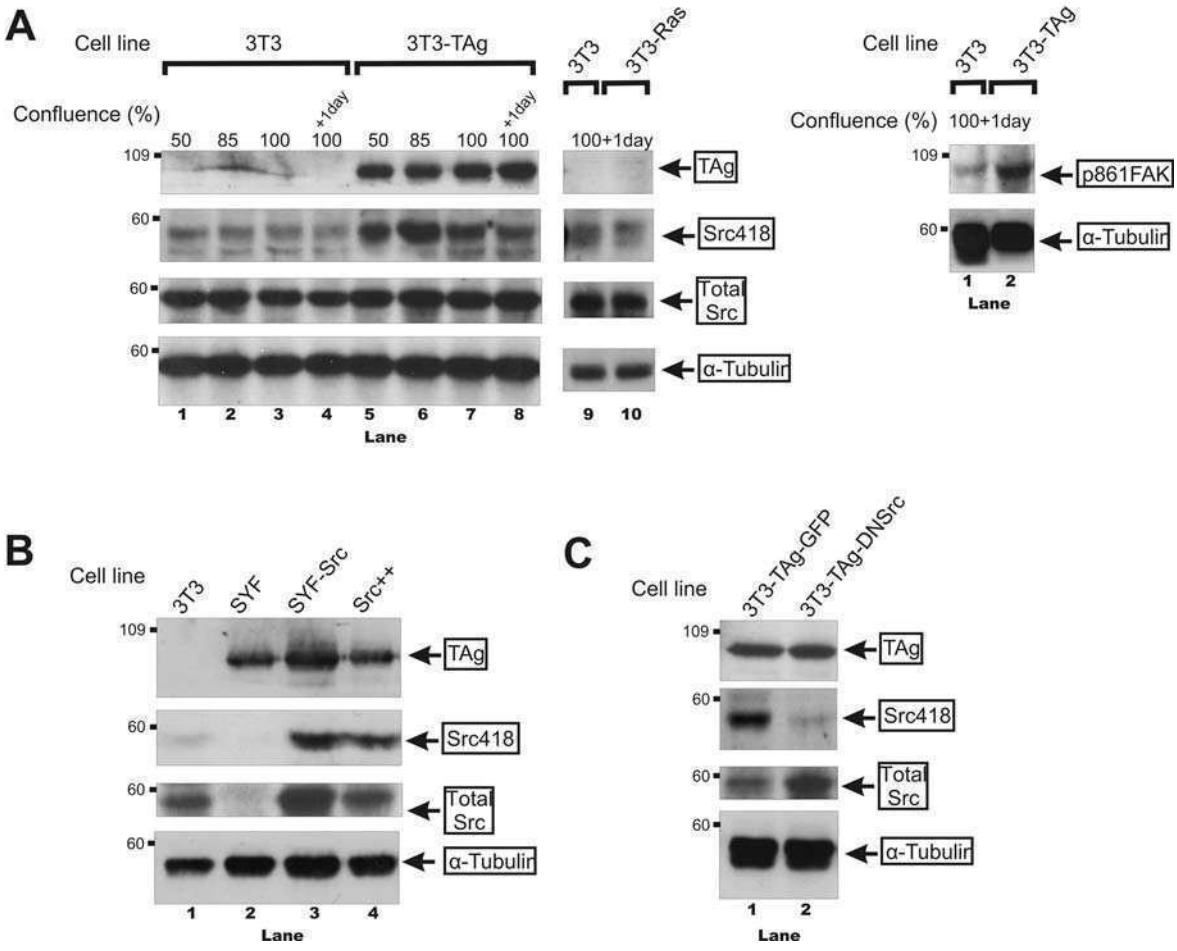

Figure 1. *TAg triggers cSrc activation. A, TAg activates cSrc in mouse 3T3 fibroblasts. Left panel: Control 3T3 fibroblasts infected with a blank vector (3T3, lanes 1-4) or their TAg-transformed counterparts (lanes 5-8) were grown to different densities as indicated and detergent lysates probed for TAg, Src418, total Src, and α-tubulin as a loading control, as indicated. As a negative control, detergent extracts from Ras-transformed 3T3 cells were probed for the same proteins (lanes 9-10). Numbers at the left refer to molecular weight markers. Right panel: Extracts from 3T3 or 3T3-TAg cells grown to one day post-confluence were probed for FAK p861, and α-tubulin as a loading control, as indicated. Numbers at the left refer to molecular weight markers. B, Src and TAg levels in SYF cells and their derivatives. Extracts from 3T3 fibroblasts (lane 1), cells where the Src, Fyn, Yes genes were ablated (SYF cells) before (lane 2) or after re-expression of Src (lane 3), or cells where Fyn and Yes only were ablated (Src++ cells, lane 4) were probed for TAg, Src418, total Src and α-tubulin as a loading control, as indicated. Numbers at the left refer to molecular weight markers. C, Src down-regulation following expression of DN-Src. 3T3-TAg cells were infected with an adenovirus vector containing DNSrc (lane 2), or the control vector expressing GFP alone (lane 1). Detergent cells lysates were were probed for TAg, Src418, and α-tubulin as a loading control, as indicated. Numbers at the left refer to molecular weight markers.*

with an adenovirus vector expressing a dominant-negative cSrc mutant (DNSrc, K297R, see Materials and Methods). As a control, cells were infected with the same vector expressing GFP alone. Western blotting 48 hours post infection indicated that Src418 levels were effectively reduced upon infection with this vector (Figure 1C). 3T3, 3T3-TAg and 3T3-TAg-DNSrc cells were subsequently tested for transformation-related parameters, such as morphological transformation, growth rate in monolayer culture and anchorage independence (see Materials and Methods). As shown in Figure 2A, 3T3-TAg cells were able to grow in agar and had a higher growth rate than the parental 3T3 cells. However, expression of the DNSrc mutant reduced the ability of 3T3-TAg cells to grow in agar, as well as their growth rate on plastic (Figure 2A). Similar results were obtained with cells infected with a vector expressing the cSrc kinase (CSK, not shown). The above findings taken together indicate that cSrc down-regulation reduces the ability of TAg to transform established mouse 3T3 fibroblasts.

To definitively demonstrate the requirement for Src, as well as the Src-related proteins, Fyn and Yes in TAg-mediated transformation, we made use of mouse fibroblasts where these genes had been genetically ablated (SYF cells). TAg had been previously expressed in these cells in order to establish them in culture from mouse E9.5 embryos. In addition, to examine

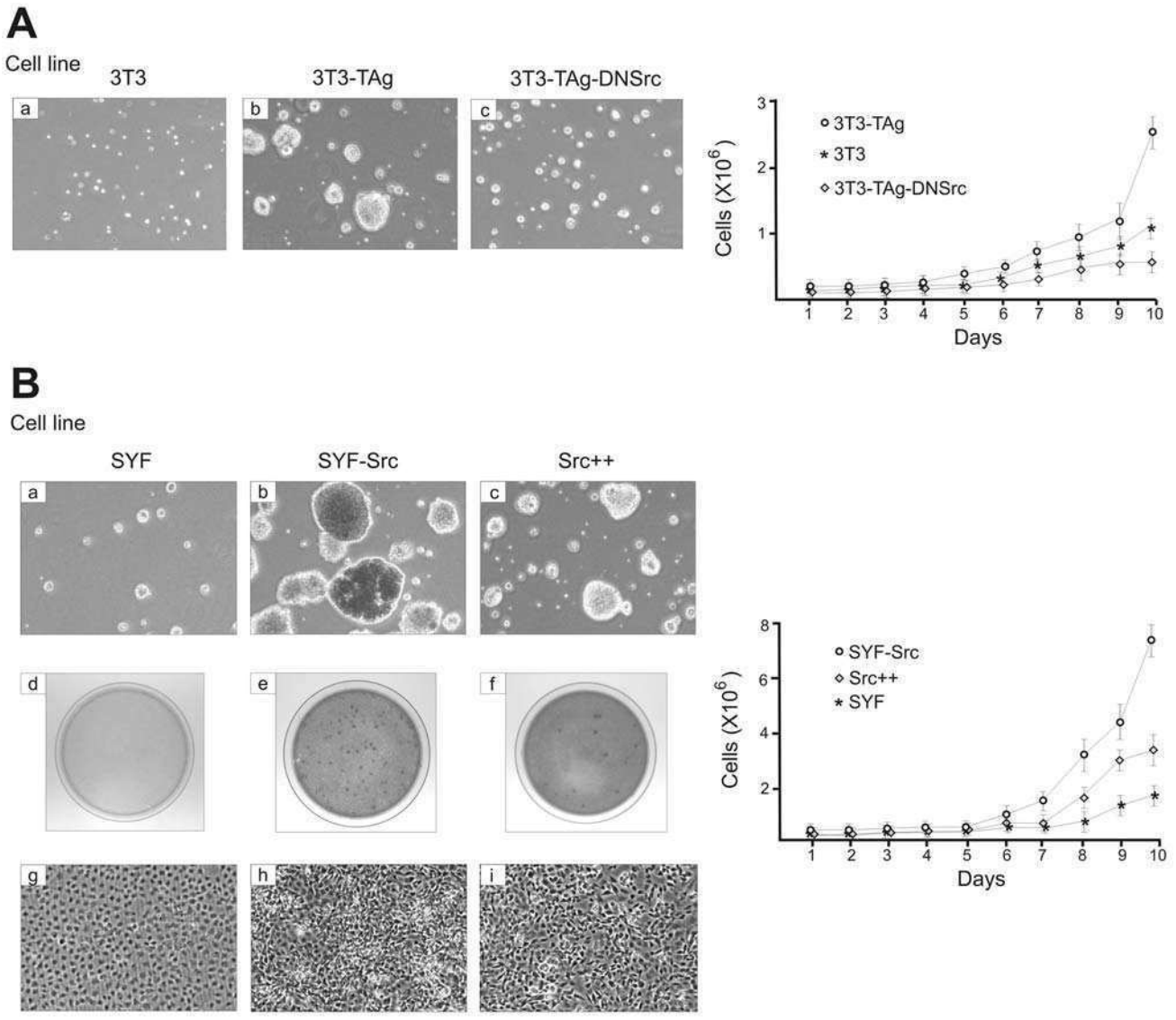

Figure 2. *Src deficiency prevents TAg-mediated transformation. A. Left panel: Anchorage-independent growth. (a) 3T3, (b) 3T3-TAg (c) 3T3-TAg-DNSrc cells were suspended in soft agarose. Twenty days later cells were photographed under phase contrast illumination. Magnification: ×40. Right panel: Growth rate on plastic. Src deficiency reduces the growth rate of 3T3-TAg cells. The indicated cell lines were plated in plastic, 6 cm petri dishes and cell numbers determined for several days, as indicated. B, Left panel: a-c: Agar assays. SYF, SYF-Src and Src++ cells were suspended in soft agarose. Twenty days later cells were photographed under phase-contrast illumination. Magnification: ×40. d-f: Formation of foci. Two hundred, SYF (a), SYF-Src (b), and Src++ (c) cells were plated in 6 cm petri dishes together with 10,000 normal 3T3 cells. Cells were fixed, stained with Coomassie blue and photographed 10 days later. g-i: Morphology on plastic. SYF, SYF-Src and Src++ cells were photographed under phase-contrast illumination. Magnification: ×140. Right panel: Growth rate on plastic. Src deficiency reduces the growth rate of 3T3-TAg cells. The indicated cell lines were plated in plastic, 6 cm petri dishes and cell numbers determined for several days, as indicated.*

the potential requirement for the Src family proteins, Fyn and Yes alone, we used established fibroblasts where the cSrc gene had been added back to SYF cells through retroviral vector infection (SYF-Src cells), and Src++ cells, where only Fyn and Yes were ablated (12). Western blotting indicated that all three lines expressed similar levels of TAg (Figure 1B, top panel). However, SYF-Src cells expressed slightly higher cSrc levels than Src++ or 3T3 cells due to the fact that cSrc was added back in these cells by retroviral vector infection (12). Examination of the cellular phenotype regarding transformation-associated properties indicated that while SYF-Src cells displayed a transformed morphology on plastic and were able to grow in agar and to form foci overgrowing a monolayer of normal cells, in a manner indistinguishable from

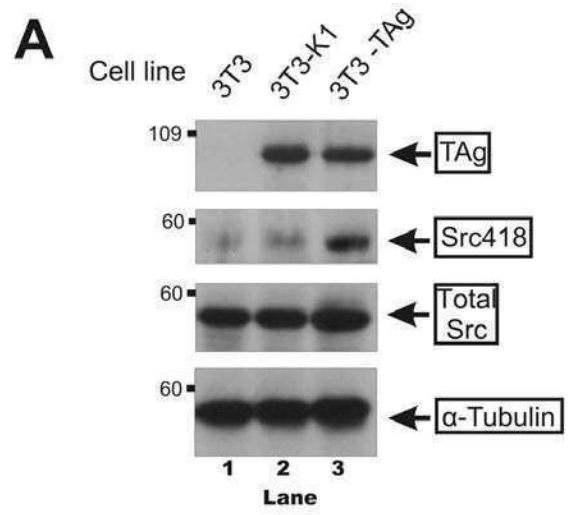

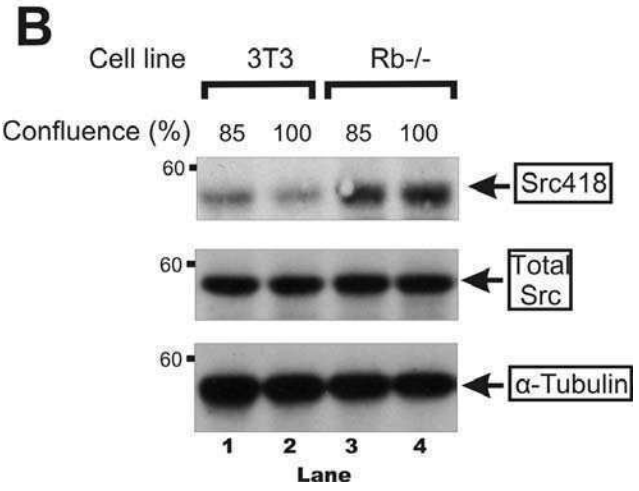

Figure 3. *pRb inactivation leads to cSrc activation. A, pRb binding by TAg is required for Src-tyr418 phosphorylation. Lysates from control 3T3 cells (lane 1) and 3T3 cells expressing the K1 TAg mutant which is defective in pRb binding (lane 2), or wt TAg (lane 3) were grown to different densities and Western immunoblots probed for TAg, Src418, total Src and or α-tubulin as a loading control, as indicated. Numbers at the left refer to molecular weight markers (see Materials and Methods). B, pRb ablation leads to cSrc, tyr418 phosphorylation. Lysates from 3T3 (lanes 1 and 2), and pRb-/- cells were probed for Src418, total Src and α-tubulin as a loading control, as indicated. Numbers at the left refer to molecular weight markers.*

3T3-TAg cells, the SYF cells had a slower growth rate, a flat morphology and were unable to grow as foci or in an anchorage-independent manner (Figure 2B), indicating that cSrc alone, in the absence of Fyn and Yes is sufficient to promote TAg-mediated transformation. The above results taken together indicate that cSrc is an integral component of the pathway whereby TAg transforms mouse fibroblasts. *pRb binding is required for cSrc activation by TAg*. One of the TAg targets is the retinoblastoma-susceptibility gene product (pRb). To investigate the importance of pRb binding to and inactivation by TAg, for TAg-induced cSrc activation and neoplasia, we examined the ability of the non-transforming TAg mutant K1 (E107K), which is unable to bind pRb family proteins, to increase Src activity levels. As shown in Figure 3A, Src activity levels in K1-expressing 3T3 cells were low, similar to that of the parental 3T3 line (lanes 1 and 2, respectively), indicating that Src activation is associated with the ability of TAg to bind pRb and neoplastically transform rodent fibroblasts.

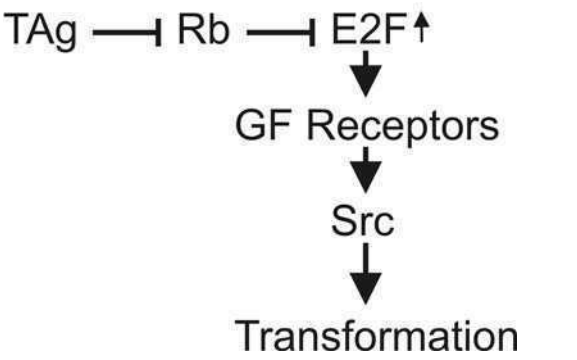

Figure 4. *Role of cSrc in transformation by TAg. TAg activates the transcription factor E2F through binding to and inactivation of pRb. E2F may then transcriptionally activate a number of receptor tyrosine kinases which could activate cSrc, leading to neoplastic conversion. GR, Growth Factor.*

To definitively demonstrate the role of pRb inactivation in Src activation by TAg, we measured Src418 levels in cells established from knockout mice where the pRb gene had been genetically ablated ($pRb^{-/-}$ cells) (11). pRb deletion in these cells liberates the activating E2F transcription factors and abrogates the G_1 restriction point. As shown in Figure 3B, the $pRb^{-/-}$ cells had high Src418 levels compared to their wild-type counterparts (lanes 3-4, *vs*. 1-2). The above data taken together point to the possibility that inactivation of pRb by TAg may induce the observed Src 418 phosphorylation and activation, leading to neoplastic conversion.

Discussion

We examined the role of the cellular Src protooncogene product in transformation by TAg. The results demonstrated that TAg expression causes a dramatic increase in Src418 phosphorylation and activity, measured by FAK tyr861 phosphorylation, in the absence of an increase in total cSrc protein. In addition, down-regulation of cSrc activity through expression of a dominant-negative mutant, expression of the cSrc kinase or genetic ablation reduced the cells' growth rate, focus formation ability and anchorage-independence, pointing to a requirement for Src

function in TAg-mediated transformation. Thus, albeit predominantly nuclear and thought to affect mostly nuclear targets, TAg requires the activity of the membrane-bound cSrc to induce full neoplastic conversion.

We and others previously demonstrated that cell to cell adhesion dramatically increases the levels and activity of a number of proteins, such as Rac (22), connexin-43 (23) as well as Stat3 [reviewed in (18)]. Since Src is an important Stat3 activator, we examined the effect of cell density upon Src tyr418 phosphorylation, previously shown to correlate with activity. Our results demonstrated the absence of an increase in Src 418 phosphorylation with cell density. This finding is consistent with previous results demonstrating that the cell density-dependent Stat3 activation is independent of Src action (17). In fact, cadherin engagement, as brought about through confluence of cultured cells triggers a dramatic increase in the levels of interleukin-6 (IL6), which leads to Stat3 ptyr705 phosphorylation and activation through the Jak kinases, rather than Src (22). Consistent with this observation, IL-6 addition did not increase Src418 levels in any of our cellular systems (not shown), as previously documented by others (24).

The cSrc protein is composed of a *C*-terminal tail containing a negative regulatory tyrosine residue (tyr529), which interacts with the cSrc SH2 domain. In addition, the SH3 domain interacts with the kinase domain and this causes the cSrc molecule to assume a closed configuration that covers the kinase domain and reduces the potential for substrate interaction (25). The tyr529 phosphorylation is conducted by CSK kinase (26). Conversely, the phosphate residue on tyr529 can be removed by several phosphatases that are potent cSrc activators. One of them is the protein tyrosine phosphatase 1b (PTP1b), the first phosphatase to be identified and cloned (27). Upon overexpression in breast cancer lines, PTP1b was shown to depho-sphosphorylate Src ptyr529 and activate cSrc (28). However, using PTP1b knockout lines, rather than overexpression experiments, it was later shown that PTP1b can dephosphorylate and activate cSrc in mouse fibroblasts, but only when the cells are kept in suspension (29). Since however, TAg expression leads to a dramatic increase in PTP1b levels (29), the possibility remains that TAg-mediated PTP1b activation might be a significant contributor to cSrc activation.

The pRb family of anti-oncogenes are important TAg targets (1), and the TAg–Rb interaction is required for transformation, even by cytoplasmic TAg mutants (30). Current models of pRb function indicate that the TAg–pRb association, in turn, inhibits pRb binding to the E2F family of transcription factors, which are important cell cycle regulators (5). In fact, a detailed examination of E2F-activated genes indicated that E2F1 has many targets, among which is a number of membrane receptor tyrosine kinases and their ligands, including known Src activators (31), such as epidermal growth factor receptor (EGFR) (32), platelet-derived growth factor α receptor (PDGFαR) (33, 34), fibroblast growth factor receptor (35), colony-stimulating factor 1 (36), and hepatocyte growth factor (37). These can induce cSrc activity, probably by disrupting the intramolecular interactions that hold cSrc in a closed configuration. Such an induction of growth factor or receptor genes by E2F following TAg expression would explain the observed cSrc activation. The fact that, like TAg levels, cSrc activity does *not* increase with cell density in TAg-expressing cells (Figure 1A, lanes 5-8) is consistent with this observation. Furthermore, the fact that the pRb-binding site is required both for transformation by TAg and for cSrc activation highlights the importance of cSrc in TAg action (Figure 4). This conclusion is further reinforced by the fact that pRb inactivation by genetic ablation also leads to cSrc activation. Thus, it appears that pRb inactivation is an important factor both for TAg-mediated cSrc activation and neoplastic transformation. The present report presents evidence for cSrc as an integral component of the signaling pathways from the primarily nuclear TAg oncogene.

Acknowledgements

We would like to thank Dr. Dave Kaplan (Toronto Sick Kids Hospital) for the gift of the adenovirus vectors, Drs Thomas Roberts and Ole Gjoerup for the TAg retroviral vectors and Dr. E.G. Gurney for the anti-TAg hybridoma line.

The financial assistance of the Canadian Institutes of Health Research (CIHR), the Canadian Breast Cancer Foundation (Ontario Chapter), the Natural Sciences and Engineering Research Council of Canada (NSERC), the Ontario Centers of Excellence, the Canadian Breast Cancer Research Alliance, the Breast Cancer Action Kingston and the Clare Nelson bequest fund (LR) is gratefully acknowledged. RA was supported by a Canada Graduate Scholarships Doctoral award from CIHR, the Ontario Women's Health Scholar's Award from the Ontario Council of Graduate Studies and a Queen's University Graduate Award (QGA). MG was supported by a postdoctoral fellowship from the US Department of Defense Breast Cancer Research Program (BCRP-CDMRP), a postdoctoral fellowship from the Ministry of Research and Innovation of the Province of Ontario and the Advisory Research Committee of Queen's University.

References

1 Ahuja D, Saenz-Robles MT and Pipas JM: SV40 large T antigen targets multiple cellular pathways to elicit cellular transformation. Oncogene *24*: 7729-7745, 2005.

2 Chen S and Paucha E: Identification of a region of simian virus 40 large T antigen required for cell transformation. J Virol *64*: 3350-3357, 1990.

3 Zalvide J and DeCaprio JA: Role of pRb-related proteins in simian virus 40 large-T-antigen- mediated transformation. Mol Cell Biol *15*: 5800-5810, 1995.

4 Attwooll C, Lazzerini DE and Helin K: The E2F family: specific functions and overlapping interests. EMBO J *23*: 4709-4716, 2004.

5 Dimova DK and Dyson NJ: The E2F transcriptional network: old acquaintances with new faces. Oncogene *24*: 2810-2826, 2005.

6 Sullivan CS and Pipas JM: T antigens of simian virus 40: molecular chaperones for viral replication and tumorigenesis. Microbiol Mol Biol Rev *66*: 179-202, 2002.
7 Grammatikakis N, Jaronczyk K, Grammatikakis A, Vultur A, Brownell HL, Benzaquen M, Rausch C, Lapointe R, Gjoerup O, Roberts TM and Raptis L: Simian virus 40 large tumor antigen modulates the Raf signaling pathway. J Biol Chem *276*: 27840-27845, 2001.
8 Raptis L, Brownell HL, Wood K, Corbley M, Wang D and Haliotis T: Cellular ras gene activity is required for full neoplastic transformation by simian virus 40. Cell Growth Differ *8*: 891-901, 1997.
9 Vultur A, Arulanandam R, Turkson J, Niu G, Jove R and Raptis L: Stat3 is required for full neoplastic transformation by the simian virus 40 large tumor antigen. Mol Biol Cell *16*: 3832-3846, 2005.
10 Broome MA and Courtneidge SA: No requirement for src family kinases for PDGF signaling in fibroblasts expressing SV40 large T antigen. Oncogene *19*: 2867-2869, 2000.
11 Sage J, Mulligan GJ, Attardi LD, Miller A, Chen S, Williams B, Theodorou E and Jacks T: Targeted disruption of the three Rb-related genes leads to loss of G(1) control and immortalization. Genes Dev *14*: 3037-3050, 2000.
12 Klinghoffer RA, Sachsenmaier C, Cooper JA and Soriano P: Src family kinases are required for integrin but not PDGFR signal transduction. EMBO J *18*: 2459-2471, 1999.
13 Orlicky DJ and Schaack J: Adenovirus transduction of 3T3-L1 cells. J Lipid Res *42*: 460-466, 2001.
14 Angers-Loustau A, Hering R, Werbowetski TE, Kaplan DR and Del Maestro RF: SRC regulates actin dynamics and invasion of malignant glial cells in three dimensions. Mol Cancer Res *2*: 595-605, 2004.
15 Greer S, Honeywell R, Geletu M, Arulanandam R and Raptis L: housekeeping gene products; levels may change with confluence of cultured cells. Journal of Immunological Methods JIM-D-09-00266: 2009.
16 Raptis L, Brownell HL, Vultur AM, Ross G, Tremblay E and Elliott BE: Specific inhibition of growth factor-stimulated ERK1/2 activation in intact cells by electroporation of a Grb2-SH2 binding peptide. Cell Growth Differ *11*: 293-303, 2000.
17 Vultur A, Cao J, Arulanandam R, Turkson J, Jove R, Greer P, Craig A, Elliott BE and Raptis L: Cell to cell adhesion modulates Stat3 activity in normal and breast carcinoma cells. Oncogene *23*: 2600-2616, 2004.
18 Raptis L, Arulanandam R, Vultur A, Geletu M, Chevalier S and Feracci H: Beyond structure, to survival: Stat3 activation by cadherin engagement. Biochem Cell Biol *87*: 835-851, 2009.
19 Raptis L, Yang J, Brownell HL, Lai J, Preston T, Corbley MJ, Narsimhan RP and Haliotis T: Rasleu61 blocks differentiation of transformable 3T3 L1 and C3HT1/2-derived preadipocytes in a dose- and time-dependent manner. Cell Growth Differ *8*: 11-21, 1997.
20 Calalb MB, Zhang X, Polte TR and Hanks SK: Focal adhesion kinase tyrosine-861 is a major site of phosphorylation by Src. Biochem Biophys Res Commun *228*: 662-668, 1996.
21 Gabarra-Niecko V, Schaller MD and Dunty JM: FAK regulates biological processes important for the pathogenesis of cancer. Cancer Metastasis Rev *22*: 359-374, 2003.
22 Arulanandam R, Vultur A, Cao J, Carefoot E, Truesdell P, Elliott B, Larue L, Feracci H and Raptis L: Cadherin engagement promotes survival *via* Rac/Cdc42 and Stat3. Mol Cancer Res *7*: 1310-1327, 2009.
23 Geletu M, Chaize C, Arulanandam R, Vultur A, Kowolik C, Anagnostopoulou A, Jove R and Raptis L: Stat3 activity is required for gap junctional permeability in normal epithelial cells and fibroblasts. DNA Cell Biol *28*: 319-327, 2009.
24 Fischer P and Hilfiker-Kleiner D: Role of gp130-mediated signalling pathways in the heart and its impact on potential therapeutic aspects. Br J Pharmacol *153(Suppl 1)*: S414-S427, 2008.
25 Yeatman TJ: A renaissance for SRC. Nat Rev Cancer *4*: 470-480, 2004.
26 Cooper JA, Gould KL, Cartwright CA and Hunter T: Tyr 527 is phosphorylated in pp60c-src: Implications for regulation. Science *231*: 1431-1434, 1986.
27 Chernoff J, Schievella AR, Jost CA, Erikson RL and Neel BG: Cloning of a cDNA for a major human protein-tyrosine phosphatase. Proc Natl Acad Sci USA *87*: 2735-2739, 1990.
28 Bjorge JD, Pang A and Fujita DJ: Identification of protein-tyrosine phosphatase 1B as the major tyrosine phosphatase activity capable of dephosphorylating and activating c-Src in several human breast cancer cell lines. J Biol Chem *275*: 41439-41446, 2000.
29 Cheng A, Bal GS, Kennedy BP and Tremblay ML: Attenuation of adhesion-dependent signaling and cell spreading in transformed fibroblasts lacking protein tyrosine phosphatase-1B. J Biol Chem *276*: 25848-25855, 2001.
30 Tedesco D, Fischer-Fantuzzi L and Vesco C: Limits of transforming competence of SV40 nuclear and cytoplasmic large T mutants with altered Rb binding sequences. Oncogene *8*: 549-557, 1993.
31 Young AP, Nagarajan R and Longmore GD: Mechanisms of transcriptional regulation by Rb-E2F segregate by biological pathway. Oncogene *22*: 7209-7217, 2003.
32 Tice DA, Biscardi JS, Nickles AL and Parsons SJ: Mechanism of biological synergy between cellular Src and epidermal growth factor receptor. Proc Natl Acad Sci USA *96*: 1415-1420, 1999.
33 DeMali KA, Godwin SL, Soltoff SP and Kazlauskas A: Multiple roles for Src in a PDGF-stimulated cell. Exp Cell Res *253*: 271-279, 1999.
34 Bowman T, Broome MA, Sinibaldi D, Wharton W, Pledger WJ, Sedivy JM, Irby R, Yeatman T, Courtneidge SA and Jove R: Stat3-mediated Myc expression is required for Src transformation and PDGF-induced mitogenesis. Proc Nat Acad Sci USA *98*: 7319-7324, 2001.
35 Landgren E, Blume-Jensen P, Courtneidge SA and Claesson-Welsh L: Fibroblast growth factor receptor-1 regulation of Src family kinases. Oncogene *10*: 2027-2035, 1995.
36 Courtneidge SA, Dhand R, Pilat D, Twamley GM, Waterfield MD and Roussel MF: Activation of Src family kinases by colony stimulating factor-1, and their association with its receptor. EMBO J *12*: 943-950, 1993.
37 Mao W, Irby R, Coppola D, Fu L, Wloch M, Turner J, Yu H, Garcia R, Jove R and Yeatman TJ: Activation of c-Src by receptor tyrosine kinases in human colon cancer cells with high metastatic potential. Oncogene *15*: 3083-3090, 1997.

Received October 6, 2009
Revised December 8, 2009
Accepted December 9, 2009

Mini Review

Mind the Gap; Regulation of Gap Junctional, Intercellular Communication by the Src Oncogene Product and its Effectors

MULU GELETU, AARON TROTMAN-GRANT and LEDA RAPTIS*

Department of Biomedical and Molecular Sciences and Department of Pathology and Molecular Medicine, Queen's University, Kingston, ON, Canada

Abstract. *Gap junctions are channels that connect the interiors of neighboring cells and are formed by the connexin (Cx) proteins. A reduction in gap junctional, intercellular communication (GJIC) often correlates with increased growth and neoplastic transformation. Cx43 is a widely expressed connexin which can be phosphorylated by the Src oncoprotein tyrosine kinase on tyr247 and -265, and this reduces communication. However, Src activates multiple signalling pathways such as the Ras/Raf/Erk and PLCγ/protein kinase C, which can also phosphorylate Cx43 and interrupt communication. In addition, the Src effector Cas, which has an adaptor function, binds Cx43 to suppress gap junctional communication. In sharp contrast, activation of a different Src effector, the cytoplasmic transcription factor Signal transducer and activator of transcription-3 (Stat3) is not required for the Src-mediated, GJIC suppression. In fact, Stat3 is actually required for the maintenance of gap junctional communication in normal cells with high GJIC.*

Contrary to unicellular organisms, cells in multicellular metazoa must divide under strict control. Thus, intercellular communication is crucial in the regulation of cellular functions and it often occurs indirectly through the release of diffusible growth factors by certain cells that initiate the signal through receptors on target cells. Communication between cells can also be achieved directly, through the gap junctions, *i.e.* channels running through the membrane which allow the passage of ions and other molecules between the interiors of adjacent cells. Gap junctions consist of transmembrane proteins, termed connexins, a family of at least 20 members, as described in mammals. They are often designated with a suffix referring to their molecular weight. Gap junctions are formed by the aggregation of two hemi-channels of six connexons each, contributed by the two neighboring cells. This structure forms an aqueous channel through the two plasma membranes, that permits the passage of small-molecules such as ions, nucleotides, aminoacids, short-peptides or even RNA (24), between adjacent cells (46).

Results from a number of labs indicated that an increase in cell proliferation correlates with a reduction in gap junctional, intercellular communication (GJIC). In fact, a number of oncogene products such as the transforming protein of the Rous sarcoma virus, vSrc (29), the polyoma virus middle Tumor antigen (mT (4, 35)), the activated chaperone Hsp90N (18), vRas (3, 8), tumor promotors such as the 12-O-Tetradecanoylphorbol-13-acetate and others, have been shown to interrupt junctional communication.

src is an oncogene with a high clinical relevance and one of the best-studied targets for cancer therapy (reviewed in (1)). src encodes a potent oncoprotein with high tyrosine kinase activity (Src). Src can affect the activity of Cx43 by multiple mechanisms, namely by direct phosphorylation on tyrosine residues, but also by its direct downstream effector kinase pathways, Ras/Raf/Erk and the phosphatidylinositol-3 kinase (PI3k)/Akt which phosphorylate Cx43 on serine residues. In addition, Src may indirectly activate the ser/thr kinase, protein kinase C that can phosphorylate Cx43 and block gap junctions, as well as other kinases (5, 26, 33, 38). Besides activating kinase pathways, Src can make use of the adaptor protein Cas (Crk-associated substrate), that binds Cx43 to suppress gap junctional communication (39). Src is also a potent activator of the cytoplasmic transcription factor, Signal

Correspondence to: Leda Raptis, Department of Biomedical and Molecular Sciences and Department of Pathology and Molecular Medicine, Queen's University, Kingston, Ontario, Canada K7L3N6, Tel: +1 613 5332462 (office/lab), +1 613 5332450 (secretary), e-mail: raptisl@queensu.ca

Key Words: src oncogene, Cx43, gap junctional intercellular communication.

transducer and activator of transcription-3 (Stat3). In this short communication we review the prevailing evidence on the role of Src and its effector pathways upon Cx43 and GJIC.

Phosphorylation of Cx43 on tyrosine by the Src kinase

A reduction in gap junctional communication of Src-transformed cells was reported for the first time in 1966 (31). Subsequent cloning of Cx43 enabled a molecular characterisation of the mechanism whereby Src affects Cx43 function, and this led to fundamental studies on Cx43 regulation. A combination of genetic and biochemical evidence indicated that Src can phosphorylate Cx43 directly: At first the SH3 domain of Src binds a proline-rich area between P274 and P284 of Cx43. This brings the Src kinase domain in close proximity to Y265, which is then phosphorylated by Src (Figure 1). The phosphorylated Y265 offers a docking site for the Src, Src-homology-2 (SH2) domain and this enhanced interaction causes the phosphorylation of Y247 of Cx43, which may contribute to GJIC reduction (10, 30, 43). In fact, vSrc co-expression with a Cx43 mutant, where tyr247 and tyr265 were replaced by phenylalanine in *Cx43*-knockout cells, was unable to interrupt communication, indicating that tyr247 and ty265 are important for GJIC suppression by the Src kinase (30). However, expression of the same Cx43 mutants in Xenopus oocytes can result in the formation of gap junctions, but these gap junctions can be disrupted by Src, indicating that the sites of direct phosphorylation by Src are not required for GJIC suppression in this setting (29). This led to the hypothesis that Src effectors may play a role upon GJIC suppression.

Effect of Src effectors upon GJIC suppression

The Ras/Raf/Erk pathway. Prominent among the signalling cascades initiated by the Src kinase to effect neoplastic conversion is the Ras/Raf/Mek/Erk. Src activates the Ras GTPase, which triggers the translocation of the ser/thr kinase Raf to the membrane, leading to Raf activation. Raf then activates Mek, a dual-specificity kinase, which, in turn, activates Erk (37), through phosphorylation on both thr and tyr in a ^{P}TE^{P}Y motif. Activated Ras was shown to suppress GJIC (8), and the Ras function is also required by *mT*, an oncogene which induces neoplastic conversion by binding to and activating cSrc, to reduce gap junctional communication (9).

Erk can phosphorylate Cx43 at S255, S279 and S282 (50). In fact, expression of Cx43 mutants with all Erk phosphorylation sites mutated to alanine, induces gap junction formation, but these gap junctions are not disrupted by Src expression, indicating that phosphorylation by Erk is important for GJIC suppression by vSrc. In addition, pharmacological inhibition of Erk eliminates Src's ability to interrupt gap junctional communication (54) and it was recently shown that ser- residues of Cx43 were phosphorylated in vSrc- transformed cells (40). Taken together, these data suggest that Erk activation by Src may be important in GJIC suppression. However, in addition to the direct phosphorylation of Cx43 by the Erk kinase, Ras may also act through other effectors to down-regulate GJIC, such as RalGDS, p120GAP, AG6 and others (22).

PI3k/Akt. One of the Src downstream effectors is the phosphatidylinositol-3 (PI3) kinase. Work from a number of laboratories has shown that activated-Src activates class I, PI3K, which phosphorylates phosphatidylinositol-4,5-bisphosphate (PIP2) and phosphatidylinositol-4-phosphate (PIP), to generate phosphatidylinositol-3,4,5-trisphosphate (PIP3) and PI(3,4)P2, respectively, in a reaction which can be reversed by the tumor suppressor PIP3 phosphatase, PTEN. The ser/thr kinase Akt binds to PIP3 at the membrane, by virtue of an amino-terminal plekstrin homology domain. Then the PDK1 kinase, also bound to PIP3 at the membrane, phosphorylates the activation loop of Akt at thr308 (Akt1 numbering). Another complex activated by RTK's, the mammalian target of rapamycin complex-2 (mTORC2) phosphorylates Akt1 on the carboxylterminal, hydrophobic domain, at ser473. Akt is thus transiently localised to the plasma membrane during activation and once activated, it phosphorylates substrates throughout the cell to regulate for multiple cellular functions, including growth modulation, survival, proliferation and metabolism. Three isoforms have been described, Akt1, Akt2, Akt3, and studies from knockout mice documented distinct functions for each isoform (reviewed in (16,32)).

The effect of Src-mediated, PI3K/Akt activation upon GJIC is complex. Akt1 was shown to phosphorylate Cx43 at ser373 and ser369 (34). It was recently demonstrated that Akt is essential for the disruption of gap junctional communication by Src, while the expression of a constitutively active Akt1, but not Akt2 or Akt3 was sufficient to suppress GJIC in rat fibroblasts (21). However, results from osteoblasts indicated that PI3K/Akt is necessary for the maintenance of the steady-state expression of Cx43 through an effect on post-transcriptional mRNA stability (6). Given the large variety of substrates of the different Akt isoforms, it is possible that the effect of Akt activation by Src may be different in different settings.

PKC. Protein kinase C (PKC) is a Src- effector serine/threonine kinase (17). Src activates PKC through activation of phospholipase Cγ, but also through direct phosphorylation (19). PKC phosphorylates Cx43 at S368 and S372 (12, 27, 28). These phosphorylation events reduce coupling, since PKC activation with 12-O-Tetradecanoylphorbol-13-Acetate (TPA)

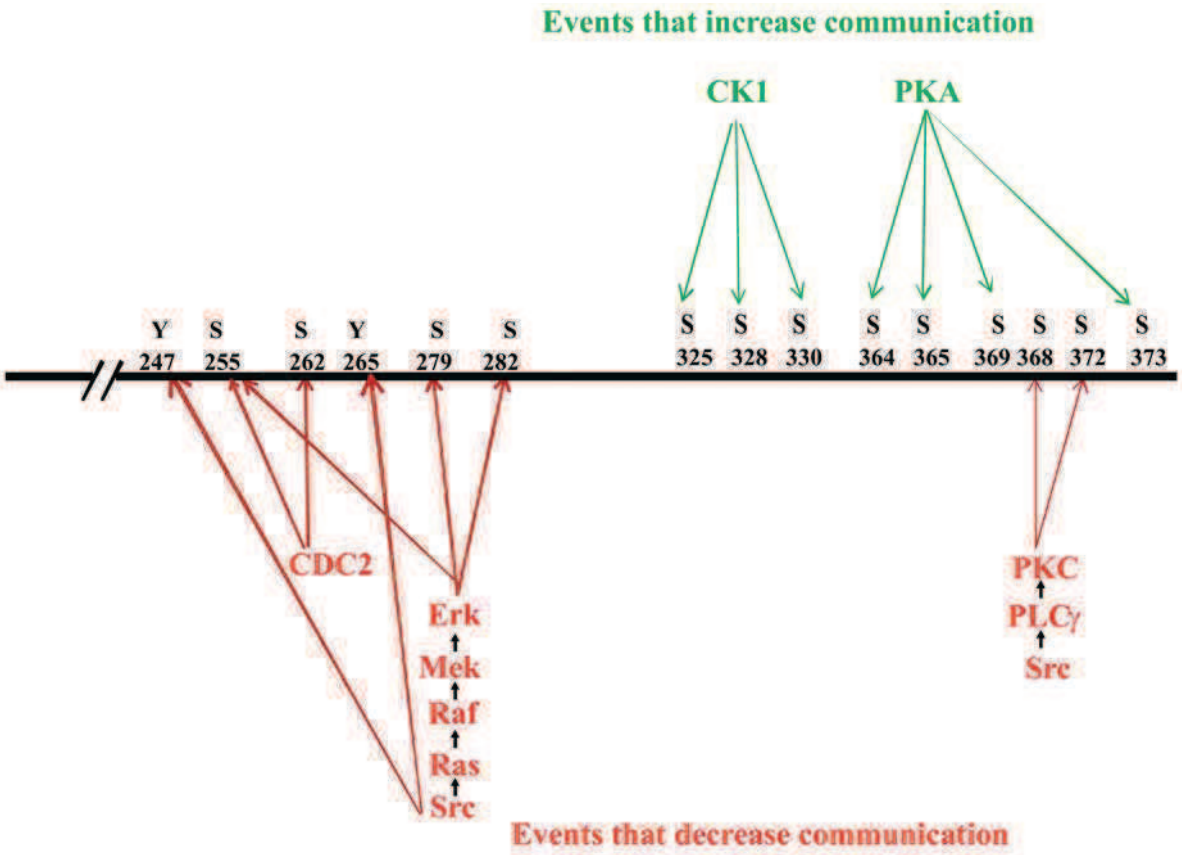

Figure 1. *Cx43 phosphorylations that affect gap junctional communication. Cx43 is shown with the phosphorylation sites targeted by Src and its effector kinases, Ras/Erk, and PKC, by aminoacid number and phosphorylating kinase. Sites phosphorylated by other kinases, such as protein kinase A (PKA) and caseine kinase 1 (Ck1) that increase communication, and the cell division cycle-2 ($p34^{Cdc2}$) kinase that decreases it are also indicated (23, 25, 44). Although the interplay between Src and these kinases has not been firmly established, it is possible that in addition to activating kinases that inhibit GJIC, Src may also suppress the activity of kinases that are required for communication (33). In red are events that decrease communication, in green events that increase it.*

leads to a reduction in GJIC (5, 26). Inhibition experiments indicated that the PKCγ isoform reduces GJIC in lens epithelial cells (49), while PKCα, β or δ can disrupt coupling between fibroblasts (11).

Stat3. The signal transducer and activator of transcription-3 (Stat3), is latent in the cytoplasm in unstimulated cells and is activated by cytokine receptors of the IL6 family, as well as by tyrosine kinase receptors such as EGF-R and PDGF-R (52). Ligand-induced assembly of cell surface receptor complexes causes receptor activation. Subsequent tyrosine phosphorylation of the receptor cytoplasmic tail by the receptor itself or by the associated Jak or Src tyrosine kinases, creates docking sites for recruiting latent, unphosphorylated Stat3 *via* its Src homology 2 (SH2) domain. The receptor-bound Stat3 becomes a substrate for phosphorylation at a critical tyrosine (tyr705). This activates Stat3 by stabilizing the association of two monomers through reciprocal SH2-phosphotyrosine interactions. The Stat3 dimer then binds to specific target sequences in the nucleus, leading to the transcriptional activation of genes which play a role in cell proliferation and survival, such as myc, cyclin D, Bcl-xL, survivin, hepatocyte growth factor (VEGF) (20), Vascular Endothelial Growth Factor and others (13, 52). Activated-Src also activates Stat3 and this is required for Src transformation. It was shown that the process requires the activity of the Jak1 kinase as well, while wild-type or kinase-inactive PDGF-receptor enhances Stat3 activation by vSrc, serving a scaffolding function (53). Stat3 is found to be hyperactive in a number of cancers (15), and the fact that a constitutively active form of Stat3 alone is sufficient to induce neoplastic transformation (7), points to an etiological role for Stat3 in neoplasia.

Stat3 down-regulation does not restore GJIC in Src-transformed cells. Previous results from our lab and others demonstrated that engagement of E-cadherin, as brought

about by confluence of adherent, cultured cells causes a dramatic increase in Stat3, ptyr705 phosphorylation and activity (41, 42, 47, 48), therefore the density must be taken into account when assessing the effect of inhibitors upon Stat3 activity. To examine the effect of Stat3 down-regulation upon GJIC, Stat3 activity was reduced using the pharmacological inhibitor CPA7 (2), or by infection with a retroviral vector carrying a Stat3-specific, siRNA (14). For these experiments, GJIC was examined using an apparatus of electroporation *in situ*, on a partly-conductive slide (36). The fluorescent dye, Lucifer yellow, was electroporated into cells grown on electrically- conductive, optically-transparent, indium-tin oxide, followed by observation of the migration of the dye to the adjacent, non-electroporated cells under fluorescence illumination. The results demonstrated that, contrary to inhibition of the Ras/Erk pathway, Stat3 inhibition in cells expressing activated-Src does not restore GJIC, indicating that Stat3 is not part of a pathway of Src-induced, GJIC suppression (14).

Stat3 is required for the maintenance of gap junctional communication in normal epithelial cells and fibroblasts. Since *Stat3*-knockdown did not restore GJIC in Src-expressing cells, the possibility that *Stat3*-might have a positive role upon GJIC was explored. In fact, Stat3 knockdown in normal rat liver epithelial T51B cells which have extensive GJIC (14), or certain lung cancer lines that retain GJIC (Geletu *et al*., submitted), abolished junctional communication and caused a dramatic reduction in Cx43 levels. That is, rather than increasing communication, Stat3 inhibition eliminates GJIC, indicating that Stat3 activity is, in fact, required for the maintenance of gap junction function in normal cells with extensive GJIC. This could be related to Stat3's ability to prevent apoptosis, since apoptotic death induction through cycloheximide, etoposide or puromycin caused a rapid loss of coupling, due to caspase-3-mediated degradation of Cx43 (45). Whether a similar mechanism might apply to GJIC suppression following Stat3 inhibition remains to be determined. In any event, current evidence demonstrates that Stat3, although it is generally growth-promoting and in an activated form can act as an oncogene, its function is actually required for the maintenance of junctional permeability.

Final remarks. Besides *src*, a variety of oncogenes and growth factors are known to cause gap junction closure. Although the effects of neoplastic transformation upon GJIC are clear, the mechanisms whereby this leads to tumor growth and progression are not well-defined. A better understanding of the relationship between Src and Cx43 will offer useful insights on the paths leading to carcinogenesis. Since Src also plays an important role in other cellular functions, this will also unveil mechanisms involved in processes such as development and homeostasis (51).

Acknowledgements

The financial support from the Canadian Institutes of Health Research, the Canadian Breast Cancer Foundation (Ontario Chapter), the Natural Sciences and Engineering Research Council of Canada, the Canadian Breast Cancer Research Alliance, the Ontario Centers of Excellence, the Breast Cancer Action Kingston and the Clare Nelson bequest fund through grants to LR, are gratefully acknowledged. MG was supported by a post-doctoral fellowship from the US army Breast Cancer Program (#BC087586), the Ministry of Research and Innovation of the Province of Ontario and the Advisory Research Committee of Queen's University.

References

1 Aleshin A and Finn RS: SRC: a century of science brought to the clinic. Neoplasia *12*: 599-607, 2010.
2 Anagnostopoulou A, Vultur A, Arulanandam R, Cao J, Turkson J, Jove R, Kim JS, Glenn M, Hamilton AD and Raptis L: Differential effects of Stat3 inhibition in sparse vs confluent normal and breast cancer cells. Cancer Lett *242*: 120-132, 2006.
3 Atkinson MM and Sheridan JD: Altered junctional permeability between cells transformed by v-ras, v-mos, or v-src. American Journal of Physiology *255*: C674-C683, 1988.
4 Azarnia R and Loewenstein WR: Polyomavirus middle t antigen downregulates junctional cell-to-cell communication. Mol Cell Biol *7*: 946-950, 1987.
5 Bao X, Reuss L and Altenberg GA: Regulation of purified and reconstituted connexin 43 hemichannels by protein kinase C-mediated phosphorylation of Serine 368. J Biol Chem *279*: 20058-20066, 2004.
6 Bhattacharjee R, Kaneda M, Nakahama K and Morita I: The steady-state expression of connexin43 is maintained by the PI3K/Akt in osteoblasts. Biochem Biophys Res Commun *382*: 440-444, 2009.
7 Bromberg JF, Wrzeszczynska MH, Devgan G, Zhao Y, Pestell RG, Albanese C and Darnell JE Jr.: Stat3 as an oncogene. Cell *98*: 295-303, 1999.
8 Brownell HL, Narsimhan R, Corbley MJ, Mann VM, Whitfield JF, and Raptis L: Ras is involved in gap junction closure in mouse fibroblasts or preadipocytes but not in differentiated adipocytes. DNA & Cell Biol *15*: 443-451, 1996.
9 Brownell HL, Whitfield JF and Raptis L: Cellular Ras partly mediates gap junction closure by the polyoma virus middle Tumor antigen. Cancer Lett *103*: 99-106, 1996.
10 Crow DS, Beyer EC, Paul DL, Kobe SS and Lau AF: Phosphorylation of connexin43 gap junction protein in uninfected and rous sarcoma virus-transformed mammalian fibroblasts. Mol Cell Biol *10*: 1754-1763, 1990.
11 Cruciani V, Husoy T and Mikalsen SO: Pharmacological evidence for system-dependent involvement of protein kinase C isoenzymes in phorbol ester-suppressed gap junctional communication. Exp Cell Res *268*: 150-161, 2001.
12 Doble BW, Ping P and Kardami E: The epsilon subtype of protein kinase C is required for cardiomyocyte connexin-43 phosphorylation. Circ Res *86*: 293-301, 2000.
13 Frank DA: STAT3 as a central mediator of neoplastic cellular transformation. Cancer Lett *251*: 199-210, 2007.

14 Geletu M, Chaize C, Arulanandam R, Vultur A, Kowolik C, Anagnostopoulou A, Jove R and Raptis L: Stat3 activity is required for gap junctional permeability in normal epithelial cells and fibroblasts. DNA & Cell Biol *28*: 319-327, 2009.
15 Germain D and Frank DA: Targeting the cytoplasmic and nuclear functions of signal transducers and activators of transcription 3 for cancer therapy. Clin Cancer Res *13*: 5665-5669, 2007.
16 Gonzalez E and McGraw TE: The Akt kinases: isoform specificity in metabolism and cancer. Cell Cycle *8*: 2502-2508, 2009.
17 Gould KL, Woodgett JR, Cooper JA, Buss JE, Shalloway D, and Hunter T: Protein kinase C phosphorylates pp60c-src at a novel site. Cell *42*: 849-857, 1985.
18 Grammatikakis N, Vultur A, Ramana CV, Siganou A, Schweinfest CW and Raptis L: The role of Hsp90N, a new member of the Hsp90 family, in signal transduction and neoplastic transformation. J Biol Chem *277*: 8312-8320, 2002.
19 Griner EM and Kazanietz MG: Protein kinase C and other diacylglycerol effectors in cancer. Nat Rev Cancer *7*: 281-294, 2007.
20 Hung W and Elliott B: Co-operative effect of c-Src tyrosine kinase and Stat3 in activation of hepatocyte growth factor expression in mammary carcinoma cells. J Biol Chem *276*: 12395-12403, 2001.
21 Ito S, Hyodo T, Hasegawa H, Yuan H, Hamaguchi M and Senga T: PI3K/Akt signaling is involved in the disruption of gap junctional communication caused by v-Src and TNF-alpha. Biochem Biophys Res Commun *400*: 230-235, 2010.
22 Ito S, Ito Y, Senga T, Hattori S, Matsuo S and Hamaguchi M: v-Src requires Ras signaling for the suppression of gap junctional intercellular communication. Oncogene *25*: 2420-2424, 2006.
23 Kanemitsu MY, Jiang W and Eckhart W: Cdc2-mediated phosphorylation of the gap junction protein, connexin43, during mitosis. Cell Growth Differ *9*: 13-21, 1998.
24 Katakowski M, Buller B, Wang X, Rogers T and Chopp M: Functional microRNA is transferred between glioma cells. Cancer Res *70*: 8259-8263, 2010.
25 Lampe PD, Kurata WE, Warn-Cramer BJ and Lau AF: Formation of a distinct connexin43 phosphoisoform in mitotic cells is dependent upon p34cdc2 kinase. J Cell Sci *111(Pt 6)*: 833-841, 1998.
26 Lampe PD, TenBroek EM, Burt JM, Kurata WE, Johnson RG and Lau AF: Phosphorylation of connexin43 on serine368 by protein kinase C regulates gap junctional communication. J Cell Biol *149*: 1503-1512, 2000.
27 Lin D, Boyle DL, and Takemoto DJ: IGF-I-induced phosphorylation of connexin 43 by PKCgamma: regulation of gap junctions in rabbit lens epithelial cells. Invest Ophthalmol Vis Sci *44*: 1160-1168, 2003.
28 Lin D, Zhou J, Zelenka PS and Takemoto DJ: Protein kinase Cgamma regulation of gap junction activity through caveolin-1-containing lipid rafts. Invest Ophthalmol Vis Sci *44*: 5259-5268, 2003.
29 Lin R, Martyn KD, Guyette CV, Lau AF and Warn-Cramer BJ: v-Src tyrosine phosphorylation of connexin43: regulation of gap junction communication and effects on cell transformation. Cell Commun Adhes *13*: 199-216, 2006.
30 Lin R, Warn-Cramer BJ, Kurata WE and Lau AF: v-Src phosphorylation of connexin 43 on Tyr247 and Tyr265 disrupts gap junctional communication. J Cell Biol *154*: 815-827, 2001.
31 Loewenstein WR and Kanno Y: Intercellular communication and the control of tissue growth: lack of communication between cancer cells. Nature *209*: 1248-1249, 1966.
32 Manning BD and Cantley LC: AKT/PKB signaling: navigating downstream. Cell *129*: 1261-1274, 2007.
33 Pahujaa M, Anikin M and Goldberg GS: Phosphorylation of connexin43 induced by Src: regulation of gap junctional communication between transformed cells. Exp Cell Res *313*: 4083-4090, 2007.
34 Park DJ, Wallick CJ, Martyn KD, Lau AF, Jin C and Warn-Cramer BJ: Akt phosphorylates Connexin43 on Ser373, a "mode-1" binding site for 14-3-3. Cell Commun Adhes *14*: 211-226, 2007.
35 Raptis L, Brownell HL, Firth KL and MacKenzie LW: A novel technique for the study of intercellular, junctional communication; electroporation of adherent cells on a partly conductive slide. DNA & Cell Biol *13*: 963-975, 1994.
36 Raptis L and Firth KL: Electrode assemblies used for electroporation of cultured cells. *In*: Electroporation protocols (Li S ed). Humana Press, pp. 58-73, 2008.
37 Roberts PJ and Der CJ: Targeting the Raf-MEK-ERK mitogen-activated protein kinase cascade for the treatment of cancer. Oncogene *26*: 3291-3310, 2007.
38 Shah MM, Martinez AM and Fletcher WH: The connexin43 gap junction protein is phosphorylated by protein kinase A and protein kinase C: *in vivo* and *in vitro* studies. Mol Cell Biochem *238*: 57-68, 2002.
39 Shen Y, Khusial PR, Li X, Ichikawa H, Moreno AP and Goldberg GS: SRC utilizes Cas to block gap junctional communication mediated by connexin43. J Biol Chem *282*: 18914-18921, 2007.
40 Solan JL and Lampe PD: Connexin 43 in LA-25 cells with active v-src is phosphorylated on Y247, Y265, S262, S279/282, and S368 *via* multiple signaling pathways. Cell Commun Adhes *15*: 75-84, 2008.
41 Steinman RA, Wentzel A, Lu Y, Stehle C and Grandis JR: Activation of Stat3 by cell confluence reveals negative regulation of Stat3 by cdk2. Oncogene *22*: 3608-3615, 2003.
42 Su HW, Yeh HH, Wang SW, Shen MR, Chen TL, Kiela PR, Ghishan FK and Tang MJ: Cell confluence-induced activation of signal transducer and activator of transcription-3 (Stat3) triggers epithelial dome formation *via* augmentation of sodium hydrogen exchanger-3 (NHE3) expression. J Biol Chem *282*: 9883-9894, 2007.
43 Swenson LI, Piwnica-Worms H, McNamee H and Paul DL: Tyrosine phosphorylation of the gap junction protein connexin43 is required for the pp60v-src-induced inhibition of communication. Cell Regul *1*: 989-1002, 1990.
44 TenBroek EM, Lampe PD, Solan JL, Reynhout JK and Johnson RG: Ser364 of connexin43 and the up-regulation of gap junction assembly by cAMP. J Cell Biol *155*: 1307-1318, 2001.
45 Theiss C, Mazur A, Meller K and Mannherz HG: Changes in gap junction organization and decreased coupling during induced apoptosis in lens epithelial and NIH-3T3 cells. Exp Cell Res *313*: 38-52, 2007.
46 Vinken M, Vanhaecke T, Papeleu P, Snykers S, Henkens T and Rogiers V: Connexins and their channels in cell growth and cell death. Cell Signal *18*: 592-600, 2006.
47 Vultur A, Arulanandam R, Turkson J, Niu G, Jove R and Raptis L: Stat3 is required for full neoplastic transformation by the Simian Virus 40 Large Tumor antigen. Molecular Biology of the Cell *16*: 3832-3846, 2005.

48 Vultur A, Cao J, Arulanandam R, Turkson J, Jove R, Greer P, Craig A, Elliott BE and Raptis L: Cell to cell adhesion modulates Stat3 activity in normal and breast carcinoma cells. Oncogene *23*: 2600-2616, 2004.

49 Wagner LM, Saleh SM, Boyle DJ and Takemoto DJ: Effect of protein kinase Cgamma on gap junction disassembly in lens epithelial cells and retinal cells in culture. Mol Vis *8*: 59-66, 2002.

50 Warn-Cramer BJ, Lampe PD, Kurata WE, Kanemitsu MY, Loo LW, Eckhart W and Lau AF: Characterization of the mitogen-activated protein kinase phosphorylation sites on the connexin-43 gap junction protein. J Biol Chem *271*: 3779-3786, 1996.

51 White TW and Paul DL: Genetic diseases and gene knockouts reveal diverse connexin functions. Annu Rev Physiol *61*: 283-310, 1999.

52 Yu H, Pardoll D and Jove R: STATs in cancer inflammation and immunity: a leading role for STAT3. Nat Rev Cancer *9*: 798-809, 2009.

53 Zhang Y, Turkson J, Carter-Su C, Smithgall T, Levitzki A, Kraker A, Krolewski JJ, Medveczky P and Jove R: Activation of Stat3 in v-Src transformed fibroblasts requires cooperation of Jak1 kinase activity. J Biol Chem *275*: 24935-24944, 2000.

54 Zhou L, Kasperek EM and Nicholson BJ: Dissection of the molecular basis of pp60(v-src) induced gating of connexin 43 gap junction channels. J Cell Biol *144*: 1033-1045, 1999.

Received July 24, 2012
Accepted August 20, 2012

EXPERIMENTAL CELL RESEARCH 317 (2011) 1787–1795

available at www.sciencedirect.com

ScienceDirect

www.elsevier.com/locate/yexcr

Review Article

The R(h)oads to Stat3: Stat3 activation by the Rho GTPases

Leda Raptis[a,*], *Rozanne Arulanandam*[a,1], *Mulu Geletu*[a], *James Turkson*[b]

[a] *Department of Microbiology and Immunology and Pathology, Queen's University, Kingston, Ontario, Canada K7L 3N6*
[b] *Burnett School of Biomedical Sciences, College of Medicine, University of Central Florida, Orlando, FL 32827, USA*

ARTICLE INFORMATION

Article Chronology:
Received 8 March 2011
Revised version received 9 May 2011
Accepted 10 May 2011
Available online 18 May 2011

Keywords:
Rho GTPases
MgcRacGAP
Stat3

ABSTRACT

The signal transducer and activator of transcription-3 (Stat3) is a member of the STAT family of cytoplasmic transcription factors. Overactivation of Stat3 is detected with high frequency in human cancer and is considered a molecular abnormality that supports the tumor phenotype. Despite concerted investigative efforts, the molecular mechanisms leading to the aberrant Stat3 activation and Stat3-mediated transformation and tumorigenesis are still not clearly defined. Recent evidence reveals a crosstalk close relationship between Stat3 signaling and members of the Rho family of small GTPases, including Rac1, Cdc42 and RhoA. Specifically, Rac1, acting in a complex with the MgcRacGAP (male germ cell RacGAP), promotes tyrosine phosphorylation of Stat3 by the IL6-receptor family/Jak kinase complex, as well as its translocation to the nucleus. Studies have further revealed that the mutational activation of Rac1 and Cdc42 results in Stat3 activation, which occurs in part through the upregulation of IL6 family cytokines that in turn stimulates Stat3 through the Jak kinases. Interestingly, evidence also shows that the engagement of cadherins, cell to cell adhesion molecules, specifically induces a striking increase in Rac1 and Cdc42 protein levels and activity, which in turn results in Stat3 activation. In this review we integrate recent findings clarifying the role of the Rho family GTPases in Stat3 activation in the context of malignant progression.

Contents

* *Corresponding author at:* Department of Microbiology and Immunology, Queen's University, Botterell Hall, Room 713, Kingston, Ontario, Canada K7L 3N6. Fax: +1 613 533 6796.
E-mail address: raptisl@queensu.ca (L. Raptis).

Abbreviations: STATs, signal transducers and activators of transcription; MgcRacGAP, male germ cell RacGAP; E-cadherin, epithelial cadherin; MDCK, Madin–Darby canine kidney cells; Rho, Ras homologous GTPases, Rho; Ras, Rat sarcoma; GEF, guanine nucleotide exchange factor; GAP, GTPase activating proteins; GDI, guanine nucleotide dissociation inhibitor; CRIB, Cdc42/Rac interactive binding domain; REM, Rho effector homology domain; PAK, p21-activated kinase; ROCK, Rho-associated coiled-coil domain kinases; ROS, reactive oxygen species; LMwtPTPase, low-molecular-weight phosphatase; Cool-2, cloned out of library-2; Tiam-1, T-cell lymphoma invasion and metastasis-1; PI3-kinase, phosphatidylinositol −3 kinase; APRF, acute phase response factor; IL6, interleukin-6; EGFR, epidermal growth factor receptor; HGF, hepatocyte growth factor; VEGF, vascular endothelial growth factor; ptyr, phosphorylated tyrosine; NLS, nuclear localisation signal; Erk, extracellular-signal activated kinase 1/2; SH2, Src homology 2; JAKs, Janus kinases; NFκB, nuclear factor-kappaB.

[1] Present address: Center for Innovative Cancer Research, 3rd Floor, The Ottawa Hospital General Campus, 503 Smyth Road, Ottawa, Ontario, Canada K1H 1C4.

0014-4827/$ – see front matter © 2011 Elsevier Inc. All rights reserved.
doi:10.1016/j.yexcr.2011.05.008

Introduction

Normal or tumor tissues consist of cells which are in constant contact with their neighbors in a three-dimensional structure, and recent findings revealed that cell to cell adhesion may influence fundamental cellular processes such as cell division, differentiation and apoptosis [6,47]. In this context, recent studies have shown that the engagement of cadherins, calcium-dependent cell to cell adhesion molecules, causes a dramatic increase in the levels and activity of the signal transducer and activator of transcription-3 (Stat3), a member of the STAT family of cytoplasmic transcription factors, known to play a key role in a variety of cancers. Despite extensive efforts, the molecular mechanisms of Stat3 activation that lead to tumorigenesis are poorly understood. A family of molecules that are dramatically affected by the engagement of cadherins is the Rho, small GTPases (Rho). It has been demonstrated that mutationally activated forms of the Rac1, Cdc42 or RhoA members of this family, which are known to be important for transformation by oncogenes such as Src and Ras [21,26,45], directly or indirectly promote the phosphorylation and activation of Stat3 [13,17,54]. Recent studies further showed that cadherin engagement causes a dramatic increase in the levels and activity of both mutant and wild-type Rac1 and Cdc42, which in turn leads to Stat3 activation [2,4]. Thus, there is compelling evidence to support the notion that members of the Rho family represent critical sources of signals that promote events leading to Stat3 activation in the context of malignant progression. The Rho family of small GTPases and their role in neoplasia have been recently reviewed [16,21,26,27,45] and will not be discussed here. In this review we summarize the prevailing evidence on the mechanism of Stat3 upregulation and neoplastic transformation following activation of wild-type or mutant members of the Rho family of small GTPases.

Cadherins activate Rho GTPases

Cadherin family of cell to cell adhesion receptors

The formation of cell–cell adhesion junctions is primarily modulated by the calcium-dependent family of cadherin receptors. These plasma membrane glycoproteins control the organization, specificity and dynamics of cell adhesion, which is crucial for the development and maintenance of tissue architecture. Classical, type I cadherins include the epithelial (E)-cadherin and neuronal cadherin, which are found in most tissues [56]. Type I cadherins share low amino acid homology with type II cadherins, e.g., cadherin-11. Classical cadherins consist of three domains, an extracellular, a single-pass transmembrane and an intracellular domain (Fig. 1A). The ectodomain consists of five modules of ~100 amino acids each with internal sequence homology [23]. In the presence of calcium, the extracellular segments expressed on the surface of opposing cells interact to form the cell to cell adherens junctions, which are stabilized by cytoskeletal elements inside the cell, through a homologous carboxy-terminal, cytoplasmic region for binding to β- or γ-catenin proteins, which are linked to actin filaments [6].

The Rho GTPases

The small GTPases of the Ras (Rat sarcoma) superfamily (Ras, Rho, Arf, Rab and Ran) are ~21 kDa proteins that function as molecular switches in signaling pathways which are initiated by a variety of membrane triggers [21]. The Rho (Ras homologous) proteins are a subfamily of the Ras superfamily which are highly conserved from lower eucaryotes to plants and mammals [7]. They differ from other members of the group by the presence of a Rho-specific insert in the GTPase domain (Rac1 amino acids, 123–135), which has been suggested to be involved in the recognition of downstream effector proteins. Over 20 Rho GTPases are known, and 3 members, RhoA, Rac1 and Cdc42, are ubiquitously expressed, can stimulate cell cycle progression [41] and are crucial for Ras-induced transformation [46], while Rac1 was shown to be required for transformation by oncogenes such as Src [53,62] and Ras [33].

The Rho GTPases are best known as master regulators of the actin cytoskeleton: Rac1 and Cdc42 remodel the actin cytoskeleton at the leading edge of the cell, resulting in filopodial (Cdc42) or lamellipodial (Rac1) protrusions. RhoA, B and C on the other hand are largely responsible for orchestrating focal adhesion assembly and actomyosin-mediated cell contraction at the rear of the cell, thus permitting cell movement across these adhesive contacts and subsequent detachment by the trailing end of the cell [67]. Increases in the levels of Rho family proteins have been observed in a number of cancers [16,26].

Like Ras, most Rho family proteins act as molecular switches cycling between a GTP-bound, active form and a GDP-bound,

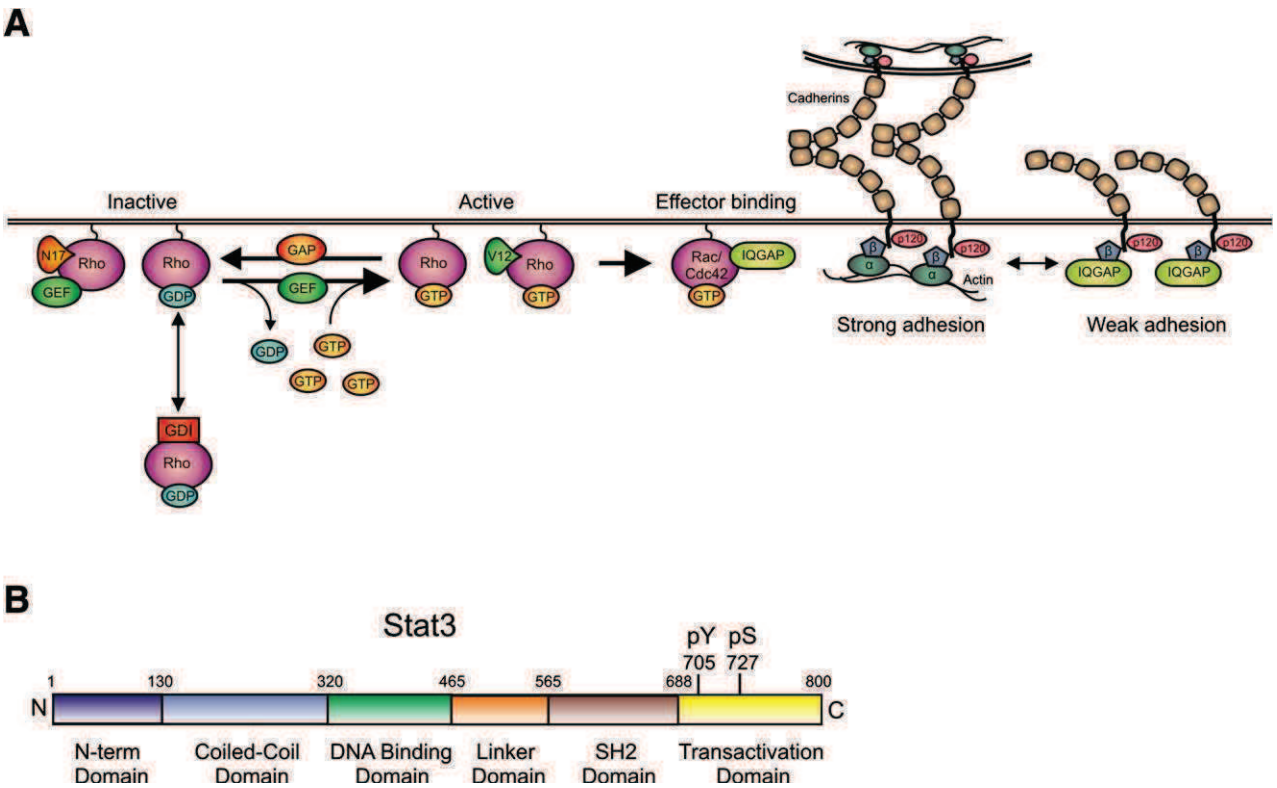

Fig. 1 – Activation of Rho GTPases (A) and Stat3 (B). (A) Rho GTPases are inactive when complexed to GDP and one of three known Rho-GDIs. Upon stimulation by extracellular factors, Rho is released from Rho-GDI and associates with the membrane through its C-terminal prenyl group. Rho-GEFs promote Rho-GTP exchange leading to the activation of various effector proteins. A Rho-GAP will then catalyze GTP hydrolysis and Rho-GDI will extract the GTPase from the membrane locking it once again in an inactive state. A substitution mutation of Thr for Asn at position 17 (Rac1 numbering) allows binding to GEF's but inhibits interactions with effectors, so that the mutant titrates out GEFs and acts as dominant-negative. On the other hand, mutation to V12 or L61 cannot hydrolyse GTP and is constitutively active. IQGAP, a Rac1 and Cdc42 effector, negatively regulates adhesion by binding to β-catenin which causes β-catenin to dissociate from the β-catenin/α-catenin complex. Activated Rac1 or Cdc42 bind IQGAP and force it to release β-catenin thus strengthening cell to cell adhesion. (B) Structure of the Stat3 transcription factor. The N-terminal, coiled-coil, DNA binding, SH2 and transactivation domains are shown, along with the tyr705 and ser727 phosphorylation sites.

inactive state [24]. GTP binding induces conformational changes which are localized within two surface loops (switch I and switch II, Rac1 amino acids 25–49 and 59–76, respectively [27]), which play an important role in GTP catalysis (Fig. 1A). The activity of Rho family proteins is regulated by three classes of proteins: guanine nucleotide exchange factors (GEFs), GTPase activating proteins (GAPs) and guanine nucleotide dissociation inhibitors (GDIs). GEFs catalyze the release of GDP from the Rho GTPases, which is the rate-limiting step in Rho activation. The free GTPase then associates with GTP, which alters the conformation of the switch regions of the enzyme to increase its affinity for the effectors (Fig. 1A). To date, over 70 Rho-GEFs have been described in humans. A substitution mutation of Thr for Asn at position 17 (Rac1 numbering) allows binding to GEFs but inhibits interactions with downstream effectors, so that these mutants titrate out the GEFs and act as dominant-negative [18]. In contrast to GEFs, the GAP proteins enhance the inherently low, intrinsic ability of the GTPases to hydrolyse the bound GTP to GDP. Therefore, GAPs promote inactivation and reverse the binding of effectors. There are over 80 mammalian Rho GAP proteins identified so far. Constitutively active mutants (e.g. Leu^{61} or Val^{12}) cannot hydrolyse GTP; therefore, they signal continuously to their effectors.

The Rho family members invariably have a C-terminal sequence ending with a -CAAX motif. Lipid modification at the C-terminus such as farnesylation, geranylgeranylation or palmitoylation promotes their membrane attachment, where they can be activated by GEFs. The GDI proteins (3 members) are cytosolic proteins that form a complex with GDP-bound Rho GTPases, so that they inhibit attachment to the membrane, hence activation by GEFs. GDIs are also able to associate with the active form and prevent binding to downstream effectors [14]. Therefore, the activation state of a given Rho family GTPase is tightly regulated and occurs in a cell-type and pathway-dependent manner, depending upon the balance of these regulators at any given moment, and this determines its downstream signaling.

Rho family proteins do not usually exert their effects directly, but instead operate through a multitude of effector proteins. The main region of Rho binding to its effectors is switch I, although regions outside switch I have been implicated in the binding of certain effectors. Over 70 effectors have been described [11]. Most Rac1 and Cdc42 effectors contain a conserved, GTPase-binding consensus site (Cdc42/Rac interactive binding or CRIB domain), while many RhoA, B, and C effectors possess an N-terminal Rho effector homology domain (REM). Many effector molecules are

serine/threonine kinases. The best characterised Rac1 and Cdc42 effectors are the p21-activated kinases (PAKs [22]), while the Rho-associated coiled-coil domain kinases (ROCK-I and II) represent the best characterised RhoA effectors [49].

It is interesting to note that the small GTPases can regulate each other's activity via crosstalk. For example, oncogenic Ras needs to activate both Raf and Rac1 to transform [46]; the Tiam1, Rac1 GEF binds the Ras effector domain to activate Rac1 [33]. Similar to Tiam1, Cool-2 is activated by binding the Cdc42 effector domain, to act as a GEF for Rac1, while in a feedback loop, Rac-GTP inhibits the GEF activity of Cool-2 [19]. An additional mechanism whereby Rac1 downregulates Rho activity is through Rac1-mediated production of reactive oxygen species (ROS). ROS inhibit the low-molecular-weight phosphatase (LMwtPTPase) which normally dephosphorylates and inhibits the p190RhoGAP. Consequently, Rac1 activation reduces the activity of RhoA [40].

Cadherin engagement increases Rac1 and Cdc42 protein levels and activity

In addition to providing structure and integrity to the cell, cadherin adhesive engagement initiates intracellular signals that are communicated through the conserved cadherin tail domain to different cytoplasmic pathways. In fact, results from a number of labs indicated that Cdc42 and Rac1 are required for E-cadherin-mediated, cell–cell adhesion in MDCK cells [20], and are believed to contribute to the stability of cell–cell adhesion via their effect on cytoskeletal organization [9]: Expression of activated $Rac1^{val12}$ in canine epithelial MDCK cells induces the accumulation of E-cadherin, β-catenin and actin filaments at sites of cell–cell contact, whereas overexpression of the dominant-negative, $Rac1^{N17}$ mutant reduces their accumulation [59]. Rac1 and Cdc42 can regulate E-cadherin activity through their effector, IQGAP. IQGAP is localized to sites of cell–cell contact and negatively regulates adhesion by binding to β-catenin, which causes β-catenin to dissociate from α-catenin [32]. Rac1 and Cdc42 bind IQGAP and remove it from the β-catenin/α-catenin complex. As a result, activated Rac1 inhibits cell dissociation and scattering, and strengthens cell–cell adhesion. Interestingly, in a positive feedback mechanism, E-cadherin engagement also results in the rapid activation of Rac1 and Cdc42, in part through a PI3-kinase-mediated mechanism, while, as expected, it inhibits RhoA, through the production of ROS by Rac1 [25].

In addition to E-cadherin-mediated activation of Rac1 and Cdc42, previous reports revealed another mechanism of Rac1 regulation involving protein stability, namely, degradation through the proteasome pathway [36,44]. In fact, cadherin engagement, e.g., achieved by high cell density, led to a dramatic increase in Rac1/Cdc42 protein levels through inhibition of proteasomal degradation [2,4]. Conversely, epithelial cell scattering brought about by hepatocyte growth factor (HGF) can induce the proteasome-mediated degradation of Rac1 [36]. Moreover, a mutational analysis further indicated that constitutive activation of Rac1, as well as binding of effectors, which might be acting as ubiquitin E3 ligases, are necessary for Rac1 degradation [44]. Still, results by Arulanandam et al. indicated that although permanently activated by mutation, protein levels of $Rac1^{V12}$ and $Rac1^{L61}$ are increased dramatically with cell density [2], indicating that cell density can overcome the degradative effect of activation. The effect of cadherin engagement upon Rac1/Cdc42 levels was found to be independent from direct cell to cell contact; plating HC11 mouse breast epithelial cells sparsely on surfaces coated with a fragment encompassing the two outermost domains of E-cadherin caused a dramatic increase in Rac1 protein levels and activity, compared to cells growing on plastic [4], indicating that E-cadherin engagement per se is responsible for the increase in Rac1 and Cdc42 levels. Such a mechanism could hold true for Cdc42, which mirrored Rac1 levels and stability increases with cell density. Similarly, cadherin-11 and N-cadherin were also found to activate Rac1 in different cell lines (Arulanandam et al., in preparation). The above data taken together indicate that cadherin engagement can abolish Rac1/Cdc42 proteasomal degradation, which leads to a dramatic increase in their levels and consequently their activity, even in the absence of direct cell to cell contact.

Rho GTPases activate Stat3

The Stat3 pathway in neoplasia

Stat3 was originally discovered as the acute phase response factor (APRF) that mediates the acute phase response in the liver via the induction of the C-reactive protein [50,71]. Stat3 is activated not only by cytokine receptors, such as the receptor for the interleukin-6 (IL6) family cytokines, but also growth receptor tyrosine kinases, such as the EGFR family including Her2/Neu, and non-receptor tyrosine kinases such as Src and Abl [63], and is also activated in response to stimulation of G-protein-coupled receptors [43]. Classically, the receptor stimulation by ligand induces Stat3 binding to phosphotyrosine residues of activated receptors through its SH2 domain and its phosphorylation on a critical tyr705 residue by the receptor itself, or by associated Janus kinase (JAK, Jak1-3, Tyk2) or Src family tyrosine kinases [68], and the phosphorylation is known to mediate dimerization between two Stat3 monomers through reciprocal SH2 domain–ptyr interactions [68]. However, studies have also identified pre-existing complexes between non-phosphorylated Stat3 monomers [51]. Stat3:Stat3 dimers translocate to the nucleus where they bind to target sequences in specific promoters, although Stat3 monomers have also been detected in the nucleus. Known Stat3 upregulated genes include *Bcl-xL*, *Mcl1*, *survivin*, *Akt*, *vascular endothelial growth factor* (*VEGF*), *HGF*, *myc*, *cyclinD*, and *HIF1*, while the *p53* tumor suppressor is downregulated by Stat3 activity [69].

In contrast to normal Stat3 signaling, which is transient, hyperactive Stat3 is associated with malignant transformation and tumorigenesis. Constitutively active Stat3 is present in a large number of cancers, and studies show that aberrant Stat3 activity promotes tumor cell growth and survival, tumor angiogenesis and metastasis, and induces tumor immune evasion [68]. It was also shown that a constitutively active form of Stat3, Stat3C, is able to transform cultured cells, which further points to an etiologic role for Stat3 in cancer [10]. Of therapeutic importance, disruption of hyperactive Stat3 signaling in tumor xenografts induces tumor cell apoptosis and tumor regression with little effect upon normal tissues [65,68,70], which points to Stat3 as an important player in tumor progression.

Rac1 and MgcRacGAP mediate Stat3 ptyr705 phosphorylation and nuclear transport

Emerging evidence suggests a more complex mechanism for Stat3 activation than initially thought; recent studies indicate that Rac1

plays an important role in Stat3 (as well as Stat5) tyrosine phosphorylation and nuclear translocation:

The male germ cell RacGAP (MgcRacGAP) is an evolutionarily conserved protein which binds directly to and serves as a GAP against Rac1, Rac2 and Cdc42 in vitro [61]. Studies in murine M1 leukemia cells, which differentiate into macrophages upon IL6 stimulation, show that MgcRacGAP can bind through its cysteine-rich and GAP domains to the DNA binding domain of Stat3 (aa 338–362), and that the MgcRacGAP-Stat3 association is required for Stat3, tyr705 phosphorylation following cytokine stimulation. That is, besides having Rac1-GAP activity, the MgcRacGAP, GAP domain is required for IL6-induced, Stat3 ptyr705 phosphorylation, acting as an effector of Rac1. Although MgcRacGAP is constitutively associated with Rac1, the association with Stat3 is increased upon IL6 stimulation [60]. In addition, MgcRacGAP phosphorylation at ser-387 was implicated in transformation by Src, although the exact mechanism is unclear [15].

Following their synthesis in the cytoplasm, transcription factors such as the STAT proteins have to cross the nuclear envelope in order to enter the nucleus. The exact mechanism of Stat3 translocation to the nucleus is just now beginning to emerge. Recent evidence suggests that, besides tyr705 phosphorylation, the Rac1/MgcRacGAP complex may be involved in Stat3 translocation. As a general mechanism for nuclear import, proteins larger than ~50 kDa require specific sequences, the nuclear localisation signals (NLS), or binding to NLS-containing chaperones. The best characterised NLS is the mono- or bi-partite, polybasic NLS, which is usually recognized by a family of proteins, the importin-α carriers. These associate with importin-β which docks the complex to the nuclear pore, so that the complex can migrate into the nucleus. The small GTPase, Ran-GTP, then binds importin-β, and the complex is disassembled inside the nucleus [12]. In the case of Stat1 it was recognized that it must be phosphorylated first on tyr701 and dimerized, in order to reveal a conditional NLS which can associate with importin-α5 [48]. Despite the initial assumption, however, that all STATs need to be phosphorylated to enter the nucleus, Stat3 was found to be nuclear and to shuttle between nucleus and cytoplasm, independent of tyrosine phosphorylation. Nevertheless, phosphorylation is still required to bind to specific DNA target sites [35]. It was further demonstrated that a sequence within the coiled-coil domain of Stat3 (amino acids 150–162) is necessary for nuclear translocation and is critical for the recognition of unphosphorylated as well as phosphorylated Stat3 by importins α3 and α6 [29,30,35]. However, although the 150–162 sequence was found to be indispensable for nuclear translocation of full-length Stat3, substitution of the basic amino acid cluster in this sequence did not hamper nuclear accumulation, indicating that aa 150–162 may only be part of a conformational structure that is required for nuclear import rather than a bona fide NLS [35].

In addition to this mechanism, recent evidence brought forth the role of MgcRacGAP as a nuclear chaperone for translocation of Stat3 (as well as Stat5) to the nucleus. In fact, the ternary complex between ptyrStat3, Rac1-GTP and MgcRacGAP facilitates the association with importin-α/β and nuclear translocation; mutation of the polybasic region of the MgcRacGAP NLS inhibited the nuclear translocation and transcriptional activity of Stat3 and Stat5 [28]. Therefore, Rac1 is emerging as an important regulator of Stat3 phosphorylation, nuclear import and function, acting through the MgcRacGAP/Rac/Stat3 complex (Fig. 2).

Mutationally activated Rho GTPases activate Stat3 through IL6 secretion

Data from a number of labs have demonstrated a functional role for the Rho GTPases in the activation of Stat3. An earlier study first implicated RhoA in the phosphorylation of Stat3 on ser727 in Src-transformed cells. Moreover, in vitro kinase assays using purified Stat3 as the substrate revealed that both p38 and JNK kinases, which can be activated by the Rho GTPases, phosphorylate Stat3 on ser727, while inhibition of p38 activity suppressed Stat3 activation and vSrc-mediated transformation [62]. In a subsequent report, mutationally activated RhoA was shown to activate Stat3 (but not Stat1) through phosphorylation at both tyr705 and ser727 in human cells, while this Stat3 activation, mediated by the ROCK effector, is required for RhoA-mediated transformation [5]. Further results similarly demonstrated Stat3 activation by mutationally activated forms of Rac1, Cdc42 and RhoA [13,17,54].

Despite extensive efforts, the exact mechanism of Stat3 activation by Rho's has been a matter of controversy. Simon et al. reported a direct binding between Rac1 and Stat3 in transiently transfected, Cos1 cells, while $Rac1^{N17}$ inhibited EGF-mediated, Stat3 activation [54]. On the other hand, using neutralising antibodies to inhibit IL6 binding, Faruqi et al. showed that Rac1 activates Stat3 indirectly through autocrine induction of IL-6 [17]. These results were contradicted in a later study where, using Stat3 null cells, it was demonstrated that Stat3 activation by the Rho GTPases could occur without the formation of a stable complex, and in the absence of IL6 secretion [13]. Notably, a recent report indicated that the engagement of E-cadherin, by growing the mouse breast epithelial HC11 cells to high densities, causes a dramatic increase in the levels and activity of Rac/Cdc42 ([4], see next section). Cell density was not taken into account previously, but would significantly impact studies the observations regarding the effect of Rho GTPases upon Stat3 activity. Stat3 ptyr705 levels in HC11 mouse breast epithelial cells over-expressing activated Rac^{V12} (or Rac^{Leu61}) or $Cdc42^{V12}$ mutants were compared to the parental HC11 line, both grown to different densities (from 50% confluence to 5 days post-confluence), and found to be higher at all cell densities, indicating that the activated forms of the GTPases promoted the activation of Stat3, in agreement with previous data [13,17,54]. In a similar experiment, activated $RhoA^{V13}$ was also found to activate Stat3, although to a lesser extent than $Rac1^{V12}$ or $Cdc42^{V12}$ (Arulanandam et al., unpublished). Inhibition experiments indicated that Stat3 activation by Rac^{V12}/$Cdc42^{V12}$ required NFκB and Jak activity [2]. Further examination of the mechanism showed that the addition of medium conditioned by Rac^{V12}-expressing cells to the parental line caused an increase in Stat3 activity, suggesting the presence of autocrine factor (s) that in turn promote Stat3 activation. Screening for mRNA of 86 cytokines by RT-PCR in Rac^{V12}-expressing cells indicated a significant increase in at least 3 cytokines of the IL6 family compared to untransfected HC11 cells. Furthermore, downregulation of the gp130, common receptor subunit of the family, blocked the induction of Stat3 activity in Rac^{V12}-expressing cells, indicating an important role for this family in Stat3 activation [2,4] (Fig. 2). The fact that more than one cytokine of the IL6 family appears to be involved explains the previous results where addition of neutralising antibodies to IL6 alone did not block Stat3 activation by Rac^{V12}[13]. The above results taken together demonstrate that activated forms of members of the Rho family can activate Stat3 through nuclear factor (NF)κB, gp130 and JAKs and provides a basis to explain the apparent discrepancy in the potential that Rho family GTPases promote Stat3 activation.

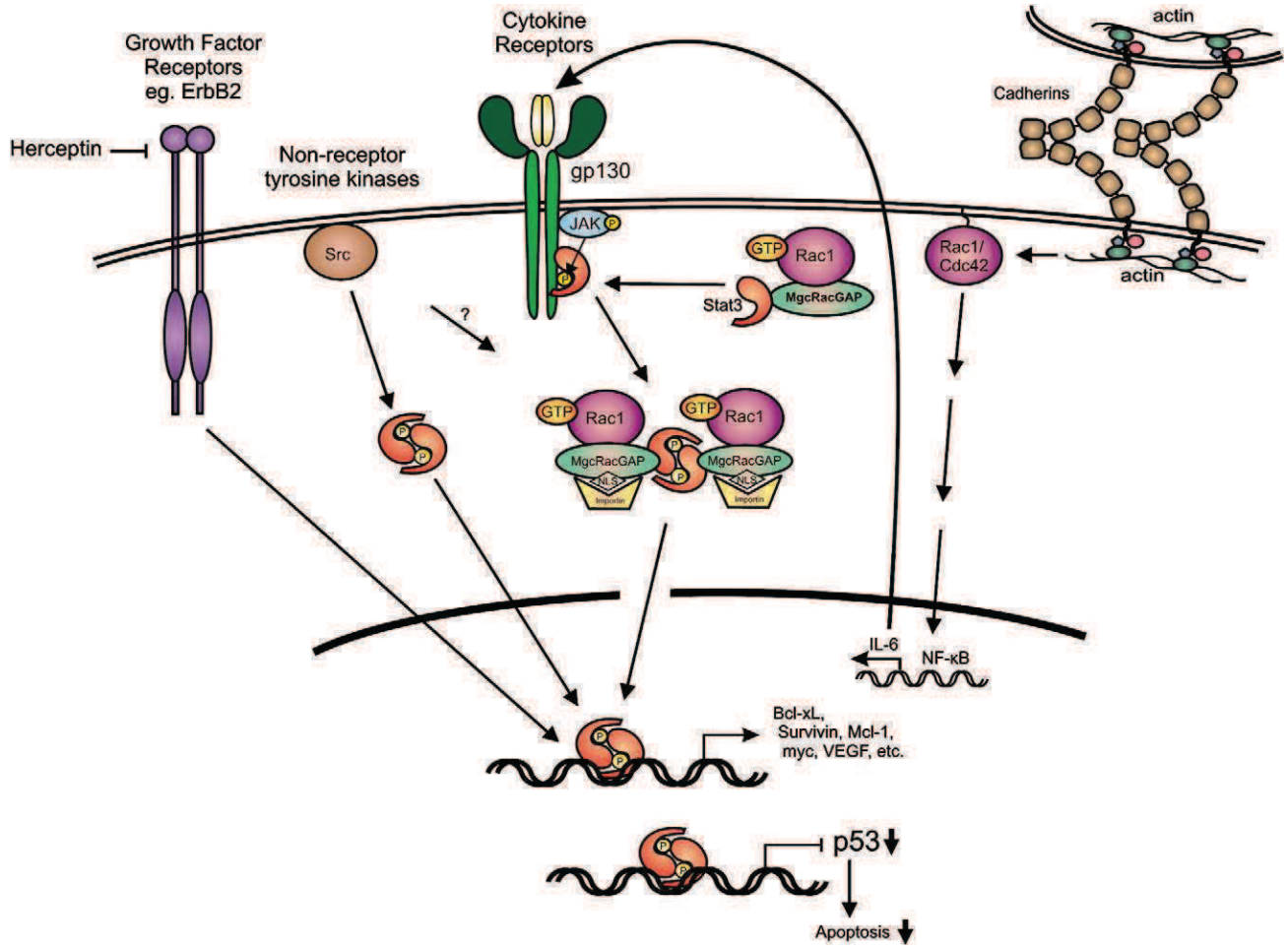

Fig. 2 – Stat3 is activated by growth factor receptors such as Her2/ErbB2 (that can be inhibited by drugs such as Herceptin), non-receptor tyrosine kinases such as Src and cytokine receptors such as the IL6 family. Activated Rac1-GTP, in a complex with MgcRacGAP and Stat3, facilitates Stat3 phosphorylation by the IL6-R/Jak complex, which results in targeting of the complex to the nuclear envelope, driven by the NLS of MgcRacGAP. The Stat3 dimer then binds specific DNA sequences to initiate transcription of Stat3 responsive genes or downregulation of other genes such as the p53 anti-oncogene. MgcRacGAP may also play a role in Stat3 activation by Src. In addition to this mechanism, cadherin engagement was shown to cause a dramatic increase in the levels of Rac1 and Cdc42 proteins and activity, which results in a transcriptional activation of IL6 through NFκB, hence Stat3 activation.

Cadherin engagement activates Stat3 through Rac1/Cdc42 and IL6

The dramatic activation of Rac1/Cdc42 following cadherin engagement [4], coupled with the ability of Rac1/Cdc42 to activate Stat3 [2], leads to the conclusion that cadherin engagement may activate Stat3 through an increase in activity of the Rho GTPases. In fact, results from a number of labs revealed that cell density causes a striking increase in the activity of Stat3 in breast carcinoma [67], melanoma [31], head and neck squamous cell carcinoma [42,55], as well as normal epithelial cells [4,57,58] and fibroblasts ([67], reviewed in [47]). Although tumor cells or cells transformed by Src or other oncogenes had higher Stat3 activity than their normal counterparts when sparse, cell density caused a further Stat3 activation [66,67]. Moreover, growing HC11 mouse breast epithelial cells on surfaces coated with E-cadherin caused a dramatic increase in Stat3 activity, demonstrating that E-cadherin engagement is sufficient to directly activate Stat3, in the absence of cell to cell contact [4]. The density-dependent Stat3 activation was strikingly greater than that brought about by serum or EGF stimulation and was not affected by inhibition or ablation of the cellular Src, Fyn, Yes, Abl, EGFR, Fer or IGF1-R kinases. As expected, this Stat3 activation is triggered by a dramatic increase in the levels of the Rac1 and Cdc42, Rho family GTPases, brought about by inhibition of proteasomal degradation [2], and a corresponding increase in their activity, following E-cadherin engagement [4]. The Rac1/Cdc42 upregulation, in turn, causes a dramatic increase in the expression of a number of cytokines of the IL6 family, which are responsible for the Stat3 activation observed.

Specificity of Stat3 activation

A key question is how and why cadherin engagement would promote the activation of Stat3, but not other pathways, such as Erk1/2. Notably, although IL-6/IL-6R typically activates extracellular-signal activated kinase 1/2 (Erk) in subconfluent cells, post-

confluent cultures do not respond with Erk activation upon IL6 stimulation [4]. In the same vein, E-cadherin engagement does not lead to Erk activation. This demonstrates a rather specific Stat3 response of cells to E-cadherin engagement, despite the fact that the two pathways, Erk and Stat3, are often coordinately regulated by oncogenes and growth factor or cytokine receptors including IL-6 [4]. It is conceivable that Erk-specific phosphatases such as Cdc25A [34] may be activated at high densities or that other adaptors required for Erk activation by IL6 might be down-regulated following cadherin engagement. It is interesting to note in this context that cell density also increases Stat5, tyr694 phosphorylation and activity in K562 human chronic myelogenous leukemia cells, although the role of Rho GTPases or cadherins in this is unknown [39].

Phenotypic effects of activated Rho GTPases require Stat3

Rac1 activation was shown to stimulate survival signals through activation of the PI3k/Akt pathway [37]. However, although Rac1/Cdc42 activity is dramatically increased following cadherin engagement, no increase in Akt-473 phosphorylation was seen with cell density in HC11 cells (Arulanandam et al., unpublished results). In sharp contrast, Stat3 is dramatically upregulated at high densities and known to provide a major survival mechanism to cultured epithelial cells and fibroblasts [47,66,67]. Given the propensity of over-confluent cells to undergo growth arrest and apoptosis, it is conceivable that the Stat3 activation serves to provide a survival signal as a last effort to rescue from an impending apoptosis. Interestingly, Stat3 also enhances the resistance of tumor cells to chemotherapeutic agents [8]. The observations that cells are more resistant to inhibition of Src [1] and to chemotherapy when grown to high densities [38] are consistent with the induction of Stat3 signaling at post-confluence, which would provide a survival mechanism.

Stat3 could mediate the proliferative and migration signals provided by activated Rac1, consistent with the known function of Stat3. Thus, expression of activated $Rac1^{V12}$ or $Cdc42^{V12}$ mutants in epithelial cells was shown to increase cell migration in a "wound-healing," cell culture assay, and this process was found to require Stat3 [13] and gp130 [2]. In the same vein, Stat3 is required for the neoplastic conversion of HEK-293T cells expressing activated RhoA to anchorage independence [5].

Conclusions

In summary, while the mechanisms continue to be investigated, there is strong evidence that certain Rho GTPases are important Stat3 activators. (1) Mutational activation of Rac1, RhoA and Cdc42 leads to Stat3 activation. (2) Rac1 and Cdc42 mediate the cadherin signal that leads to activation of Stat3 through NFκB and gp130. (3) Rac1 binds MgcRacGAP and Stat3 and this complex promotes interaction with the IL6 receptor for tyr705 phosphorylation and the activation of the MgcRacGAP - NLS, thereby facilitating nuclear translocation for Stat3-mediated transcription of specific genes (Fig. 2).

The importance of cadherin engagement upon levels and activity of proteins such as Rho and Stat3 is just beginning to emerge. Cadherin engagement was also shown to activate Jak1, which is required for Stat3 activation [67]. In sharp contrast, Src was not required for Stat3 activation following cadherin engagement and its activity was unaffected by cell density [3].

Overall, the potential for the Rho GTPases to promote the pro-survival Stat3 signaling in the context of malignant transformation underscores the importance of cell–cell interactions in the tumor microenvironment in facilitating tumor progression. Due to the generally higher level of expression of E2F transcription factors which are potent apoptosis inducers [52], many tumor cells may have higher requirements for survival signals, such as provided by the cadherin/Rac1/gp130 axis. The increased dependence on Stat3 for survival would explain the increased sensitivity of cells transformed by oncogenes such as Src [64] or the large tumor antigen of simian virus 40 [66] to Stat3 inhibition, a finding which could have significant therapeutic implications.

Acknowledgments

Special thanks are due to Dr. Richard Jove for valuable advice. The financial assistance of the Canadian Institutes of Health Research (CIHR), the Canadian Breast Cancer Foundation (Ontario Chapter), the Natural Sciences and Engineering Research Council of Canada (NSERC), the Ontario Centers of Excellence, the Breast Cancer Action Kingston, the Clare Nelson bequest fund and the Canadian Breast Cancer Research Alliance (L.R.) is gratefully acknowledged. R.A. was supported by a Canada Graduate Scholarships Doctoral award from CIHR, the Ontario Women's Health Scholars Award from the Ontario Council of Graduate Studies, a Queen's University Graduate Award and a MITACS Elevate Postdoctoral fellowship. M.G. was supported by a postdoctoral fellowship from the Ministry of Research and Innovation, a postdoctoral award from the province of Ontario, and a US Army breast cancer program. JT was supported by a grant from the National Cancer Institute (CA128865).

REFERENCES

[1] A. Anagnostopoulou, A. Vultur, R. Arulanandam, J. Cao, J. Turkson, R. Jove, J.S. Kim, M. Glenn, A.D. Hamilton, L. Raptis, Differential effects of Stat3 inhibition in sparse vs confluent normal and breast cancer cells, Cancer Lett. 242 (2006) 120–132.
[2] R. Arulanandam, M. Geletu, H. Feracci, L. Raptis, RacV12 requires gp130 for Stat3 activation, cell proliferation and migration, Exp. Cell Res. 316 (2010) 875–886.
[3] R. Arulanandam, M. Geletu, L. Raptis, The simian virus 40 large tumor antigen activates cSrc and requires Src for full neoplastic transformation, Anticancer Res. 30 (2010) 47–54.
[4] R. Arulanandam, A. Vultur, J. Cao, E. Carefoot, P. Truesdell, B. Elliott, L. Larue, H. Feracci, L. Raptis, Cadherin–cadherin engagement promotes survival via Rac/Cdc42 and Stat3, Mol. Cancer Res. 17 (2009) 1310–1327.
[5] S. Aznar, P.F. Valeron, S.V. del Rincon, L.F. Perez, R. Perona, J.C. Lacal, Simultaneous tyrosine and serine phosphorylation of STAT3 transcription factor is involved in Rho A GTPase oncogenic transformation, Mol. Biol. Cell 12 (2001) 3282–3294.
[6] J.M. Benjamin, W.J. Nelson, Bench to bedside and back again: molecular mechanisms of alpha-catenin function and roles in tumorigenesis, Semin. Cancer Biol. 18 (2008) 53–64.
[7] A. Boureux, E. Vignal, S. Faure, P. Fort, Evolution of the Rho family of ras-like GTPases in eukaryotes, Mol. Biol. Evol. 24 (2007) 203–216.
[8] L.Y. Bourguignon, K. Peyrollier, W. Xia, E. Gilad, Hyaluronan–CD44 interaction activates stem cell marker Nanog, Stat-3-mediated MDR1 gene expression, and ankyrin-regulated multidrug efflux in breast and ovarian tumor cells, J. Biol. Chem. 283 (2008) 17635–17651.

[9] V.M. Braga, A. Del Maschio, L. Machesky, E. DeJana, Regulation of cadherin function by Rho and Rac: modulation by junction maturation and cellular context, Mol. Biol. Cell 10 (1999) 9–22.
[10] J.F. Bromberg, M.H. Wrzeszczynska, G. Devgan, Y. Zhao, R.G. Pestell, C. Albanese, J.E. Darnell Jr., Stat3 as an oncogene, Cell 98 (1999) 295–303.
[11] X.R. Bustelo, V. Sauzeau, I.M. Berenjeno, GTP-binding proteins of the Rho/Rac family: regulation, effectors and functions in vivo, Bioessays 29 (2007) 356–370.
[12] A. Cook, F. Bono, M. Jinek, E. Conti, Structural biology of nucleocytoplasmic transport, Annu. Rev. Biochem. 76 (2007) 647–671.
[13] M. Debidda, L. Wang, H. Zang, V. Poli, Y. Zheng, A role of STAT3 in Rho GTPase-regulated cell migration and proliferation, J. Biol. Chem. 280 (2005) 17275–17285.
[14] C. DerMardirossian, G.M. Bokoch, GDIs: central regulatory molecules in Rho GTPase activation, Trends Cell Biol. 15 (2005) 356–363.
[15] N. Doki, T. Kawashima, Y. Nomura, A. Tsuchiya, C. Oneyama, T. Akagi, Y. Nojima, T. Kitamura, Constitutive phosphorylation of a Rac GAP MgcRacGAP is implicated in v-Src-induced transformation of NIH3T3 cells, Cancer Sci. 100 (2009) 1675–1679.
[16] S.I. Ellenbroek, J.G. Collard, Rho GTPases: functions and association with cancer, Clin. Exp. Metastasis 24 (2007) 657–672.
[17] T.R. Faruqi, D. Gomez, X.R. Bustelo, D. Bar-Sagi, N.C. Reich, Rac1 mediates STAT3 activation by autocrine IL-6, Proc. Natl Acad. Sci. USA 98 (2001) 9014–9019.
[18] L.A. Feig, Tools of the trade: use of dominant-inhibitory mutants of Ras-family GTPases, Nat. Cell Biol. 1 (1999) E25–E27.
[19] Q. Feng, D. Baird, X. Peng, J. Wang, T. Ly, J.L. Guan, R.A. Cerione, Cool-1 functions as an essential regulatory node for EGF receptor- and Src-mediated cell growth, Nat. Cell Biol. 8 (2006) 945–956.
[20] M. Fukata, K. Kaibuchi, Rho-family GTPases in cadherin-mediated cell–cell adhesion, Nat. Rev. Mol. Cell Biol. 2 (2001) 887–897.
[21] S.J. Heasman, A.J. Ridley, Mammalian Rho GTPases: new insights into their functions from in vivo studies, Nat. Rev. Mol. Cell Biol. 9 (2008) 690–701.
[22] C. Hofmann, M. Shepelev, J. Chernoff, The genetics of Pak, J. Cell Sci. 117 (2004) 4343–4354.
[23] P. Hulpiau, F. van Roy, Molecular evolution of the cadherin superfamily, Int. J. Biochem. Cell Biol. 41 (2009) 349–369.
[24] A.B. Jaffe, A. Hall, Rho GTPases: biochemistry and biology, Annu. Rev. Cell Dev. Biol. 21 (2005) 247–269.
[25] Z.M. Jaffer, J. Chernoff, The cross Rho'ds of cell–cell adhesion, J. Biol. Chem. 279 (2004) 35123–35126.
[26] R. Karlsson, E.D. Pedersen, Z. Wang, C. Brakebusch, Rho GTPase function in tumorigenesis, Biochim. Biophys. Acta 1796 (2009) 91–98.
[27] A.E. Karnoub, M. Symons, S.L. Campbell, C.J. Der, Molecular basis for Rho GTPase signaling specificity, Breast Cancer Res. Treat. 84 (2004) 61–71.
[28] T. Kawashima, Y.C. Bao, Y. Minoshima, Y. Nomura, T. Hatori, T. Hori, T. Fukagawa, T. Fukada, N. Takahashi, T. Nosaka, M. Inoue, T. Sato, M. Kukimoto-Niino, M. Shirouzu, S. Yokoyama, T. Kitamura, A Rac GTPase-activating protein, MgcRacGAP, is a nuclear localizing signal-containing nuclear chaperone in the activation of STAT transcription factors, Mol. Cell. Biol. 29 (2009) 1796–1813.
[29] M. Kohler, S. Ansieau, S. Prehn, A. Leutz, H. Haller, E. Hartmann, Cloning of two novel human importin-alpha subunits and analysis of the expression pattern of the importin-alpha protein family, FEBS Lett. 417 (1997) 104–108.
[30] M. Kohler, C. Speck, M. Christiansen, F.R. Bischoff, S. Prehn, H. Haller, D. Gorlich, E. Hartmann, Evidence for distinct substrate specificities of importin alpha family members in nuclear protein import, Mol. Cell. Biol. 19 (1999) 7782–7791.
[31] S. Kreis, G.A. Munz, S. Haan, P.C. Heinrich, I. Behrmann, Cell density dependent increase of constitutive signal transducers and activators of transcription 3 activity in melanoma cells is mediated by Janus kinases, Mol. Cancer Res. 5 (2007) 1331–1341.
[32] S. Kuroda, M. Fukata, M. Nakagawa, K. Fujii, T. Nakamura, T. Ookubo, I. Izawa, T. Nagase, N. Nomura, H. Tani, I. Shoji, Y. Matsuura, S. Yonehara, K. Kaibuchi, Role of IQGAP1, a target of the small GTPases Cdc42 and Rac1, in regulation of E-cadherin- mediated cell–cell adhesion, Science 281 (1998) 832–835.
[33] J.M. Lambert, Q.T. Lambert, G.W. Reuther, A. Malliri, D.P. Siderovski, J. Sondek, J.G. Collard, C.J. Der, Tiam1 mediates Ras activation of Rac by a PI(3)K-independent mechanism, Nat. Cell Biol. 4 (2002) 621–625.
[34] J.S. Lazo, K. Nemoto, K.E. Pestell, K. Cooley, E.C. Southwick, D.A. Mitchell, W. Furey, R. Gussio, D.W. Zaharevitz, B. Joo, P. Wipf, Identification of a potent and selective pharmacophore for Cdc25 dual specificity phosphatase inhibitors, Mol. Pharmacol. 61 (2002) 720–728.
[35] L. Liu, K.M. McBride, N.C. Reich, STAT3 nuclear import is independent of tyrosine phosphorylation and mediated by importin-alpha3, Proc. Natl Acad. Sci. USA 102 (2005) 8150–8155.
[36] E.A. Lynch, J. Stall, G. Schmidt, P. Chavrier, C. D'Souza-Schorey, Proteasome-mediated degradation of Rac1-GTP during epithelial cell scattering, Mol. Biol. Cell 17 (2006) 2236–2242.
[37] C. Murga, M. Zohar, H. Teramoto, J.S. Gutkind, Rac1 and RhoG promote cell survival by the activation of PI3K and Akt, independently of their ability to stimulate JNK and NF-kappaB, Oncogene 21 (2002) 207–216.
[38] T. Nakamura, Y. Kato, H. Fuji, T. Horiuchi, Y. Chiba, K. Tanaka, E-cadherin-dependent intercellular adhesion enhances chemoresistance, Int. J. Mol. Med. 12 (2003) 693–700.
[39] S. Nam, A. Williams, A. Vultur, A. List, K. Bhalla, D. Smith, F.Y. Lee, R. Jove, Dasatinib (BMS-354825) inhibits Stat5 signaling associated with apoptosis in chronic myelogenous leukemia cells, Mol. Cancer Ther. 6 (2007) 1400–1405.
[40] A.S. Nimnual, L.J. Taylor, D. Bar-Sagi, Redox-dependent downregulation of Rho by Rac, Nat. Cell Biol. 5 (2003) 236–241.
[41] M.F. Olson, A. Ashworth, A. Hall, An essential role for Rho, Rac, and Cdc42 GTPases in cell cycle progression through G1, Science 269 (1995) 1270–1272.
[42] A. Onishi, Q. Chen, J.O. Humtsoe, R.H. Kramer, STAT3 signaling is induced by intercellular adhesion in squamous cell carcinoma cells, Exp. Cell Res. 314 (2008) 377–386.
[43] S. Pelletier, F. Duhamel, P. Coulombe, M.R. Popoff, S. Meloche, Rho family GTPases are required for activation of Jak/STAT signaling by G protein-coupled receptors, Mol. Cell. Biol. 23 (2003) 1316–1333.
[44] M. Pop, K. Aktories, G. Schmidt, Isotype-specific degradation of Rac activated by the cytotoxic necrotizing factor 1, J. Biol. Chem. 279 (2004) 35840–35848.
[45] M.R. Popoff, B. Geny, Multifaceted role of Rho, Rac, Cdc42 and Ras in intercellular junctions, lessons from toxins, Biochim. Biophys. Acta 1788 (2009) 797–812.
[46] R.G. Qiu, J. Chen, D. Kirn, F. McCormick, M. Symons, An essential role for Rac in Ras transformation, Nature 374 (1995) 457–459.
[47] L. Raptis, R. Arulanandam, A. Vultur, M. Geletu, S. Chevalier, H. Feracci, Beyond structure, to survival: Stat3 activation by cadherin engagement, Biochem. Cell Biol. 87 (2009) 835–843.
[48] N.C. Reich, L. Liu, Tracking STAT nuclear traffic, Nat. Rev. Immunol. 6 (2006) 602–612.
[49] K. Riento, A.J. Ridley, Rocks: multifunctional kinases in cell behaviour, Nat. Rev. Mol. Cell Biol. 4 (2003) 446–456.
[50] J.A. Ripperger, S. Fritz, K. Richter, G.M. Hocke, F. Lottspeich, G.H. Fey, Transcription factors Stat3 and Stat5b are present in rat liver nuclei late in an acute phase response and bind interleukin-6 response elements, J. Biol. Chem. 270 (1995) 29998–30006.
[51] M. Schroder, K.M. Kroeger, H.D. Volk, K.A. Eidne, G. Grutz, Preassociation of nonactivated STAT3 molecules demonstrated in living cells using bioluminescence resonance energy transfer: a new model of STAT activation? J. Leukoc. Biol. 75 (2004) 792–797.
[52] R.C. Sears, J.R. Nevins, Signaling networks that link cell proliferation and cell fate, J. Biol. Chem. 277 (2002) 11617–11620.

[53] J.M. Servitja, M.J. Marinissen, A. Sodhi, X.R. Bustelo, J.S. Gutkind, Rac1 function is required for Src-induced transformation. Evidence of a role for Tiam1 and Vav2 in Rac activation by Src, J. Biol. Chem. 278 (2003) 34339–34346.
[54] A.R. Simon, H.G. Vikis, S. Stewart, B.L. Fanburg, B.H. Cochran, K.L. Guan, Regulation of STAT3 by direct binding to the Rac1 GTPase, Science 290 (2000) 144–147.
[55] R.A. Steinman, A. Wentzel, Y. Lu, C. Stehle, J.R. Grandis, Activation of Stat3 by cell confluence reveals negative regulation of Stat3 by cdk2, Oncogene 22 (2003) 3608–3615.
[56] M.P. Stemmler, Cadherins in development and cancer, Mol. Biosyst. 4 (2008) 835–850.
[57] H.W. Su, S.W. Wang, F.K. Ghishan, P.R. Kiela, M.J. Tang, Cell confluency-induced Stat3 activation regulates NHE3 expression by recruiting Sp1 and Sp3 to the proximal NHE3 promoter region during epithelial dome formation, Am. J. Physiol. Cell Physiol. 296 (2009) C13–C24.
[58] H.W. Su, H.H. Yeh, S.W. Wang, M.R. Shen, T.L. Chen, P.R. Kiela, F.K. Ghishan, M.J. Tang, Cell confluence-induced activation of signal transducer and activator of transcription-3 (Stat3) triggers epithelial dome formation via augmentation of sodium hydrogen exchanger-3 (NHE3) expression, J. Biol. Chem. 282 (2007) 9883–9894.
[59] K. Takaishi, T. Sasaki, H. Kotani, H. Nishioka, Y. Takai, Regulation of cell–cell adhesion by rac and rho small G proteins in MDCK cells, J. Cell Biol. 139 (1997) 1047–1059.
[60] Y. Tonozuka, Y. Minoshima, Y.C. Bao, Y. Moon, Y. Tsubono, T. Hatori, H. Nakajima, T. Nosaka, T. Kawashima, T. Kitamura, A GTPase-activating protein binds STAT3 and is required for IL-6-induced STAT3 activation and for differentiation of a leukemic cell line, Blood 104 (2004) 3550–3557.
[61] A. Toure, O. Dorseuil, L. Morin, P. Timmons, B. Jegou, L. Reibel, G. Gacon, MgcRacGAP, a new human GTPase-activating protein for Rac and Cdc42 similar to Drosophila rotundRacGAP gene product, is expressed in male germ cells, J. Biol. Chem. 273 (1998) 6019–6023.
[62] J. Turkson, T. Bowman, J. Adnane, Y. Zhang, J.Y. Djeu, M. Sekharam, D.A. Frank, L.B. Holzman, J. Wu, S. Sebti, R. Jove, Requirement for Ras/Rac1-mediated p38 and c-Jun N-terminal kinase signaling in Stat3 transcriptional activity induced by the Src oncoprotein, Mol. Cell. Biol. 19 (1999) 7519–7528.
[63] J. Turkson, T. Bowman, R. Garcia, E. Caldenhoven, R.P. de Groot, R. Jove, Stat3 activation by Src induces specific gene regulation and is required for cell transformation, Mol. Cell. Biol. 18 (1998) 2545–2552.
[64] J. Turkson, S. Zhang, L.B. Mora, A. Burns, S. Sebti, R. Jove, A novel platinum compound that inhibits constitutive Stat3 signaling and induces cell cycle arrest and apoptosis of malignant cells, J. Biol. Chem. 280 (2005) 32979–32988.
[65] J. Turkson, S. Zhang, J. Palmer, H. Kay, J. Stanko, L.B. Mora, S. Sebti, H. Yu, R. Jove, Inhibition of constitutive signal transducer and activator of transcription 3 activation by novel platinum complexes with potent antitumor activity, Mol. Cancer Ther. 3 (2004) 1533–1542.
[66] A. Vultur, R. Arulanandam, J. Turkson, G. Niu, R. Jove, L. Raptis, Stat3 is required for full neoplastic transformation by the Simian Virus 40 Large Tumor antigen, Mol. Biol. Cell 16 (2005) 3832–3846.
[67] A. Vultur, J. Cao, R. Arulanandam, J. Turkson, R. Jove, P. Greer, A. Craig, B.E. Elliott, L. Raptis, Cell to cell adhesion modulates Stat3 activity in normal and breast carcinoma cells, Oncogene 23 (2004) 2600–2616.
[68] H. Yu, R. Jove, The STATs of cancer—new molecular targets come of age, Nat. Rev. Cancer 4 (2004) 97–105.
[69] H. Yu, D. Pardoll, R. Jove, STATs in cancer inflammation and immunity: a leading role for STAT3, Nat. Rev. Cancer 9 (2009) 798–809.
[70] P. Yue, J. Turkson, Targeting STAT3 in cancer: how successful are we? Expert Opin. Investig. Drugs 18 (2009) 45–56.
[71] D. Zhang, M. Sun, D. Samols, I. Kushner, STAT3 participates in transcriptional activation of the C-reactive protein gene by interleukin-6, J. Biol. Chem. 271 (1996) 9503–9509.

EXPERIMENTAL CELL RESEARCH 316 (2010) 875–886

available at www.sciencedirect.com

ScienceDirect

www.elsevier.com/locate/yexcr

Research Article

Activated Rac1 requires gp130 for Stat3 activation, cell proliferation and migration

Rozanne Arulanandam[a], *Mulu Geletu*[a], *Hélène Feracci*[b], *Leda Raptis*[a,*]

[a] *Departments of Microbiology and Immunology and Pathology and Molecular Medicine, and Queen's University Cancer Institute, Queen's University, Botterell Hall, Rm. 713, Kingston, Ontario, Canada K7L 3N6*

[b] *Université Bordeaux 1, Centre de Recherche Paul Pascal, CNRS UPR 8641, 33600 Pessac, France*

ARTICLE INFORMATION

Article Chronology:
Received 31 August 2009
Revised version received
15 October 2009
Accepted 16 October 2009
Available online 21 October 2009

Keywords:
Rac/Cdc42
Stat3
IL6
gp130
Erk1/2
Cell migration

ABSTRACT

Rac1 (Rac) is a member of the Rho family of small GTPases which controls cell migration by regulating the organization of actin filaments. Previous results suggested that mutationally activated forms of the Rho GTPases can activate the Signal Transducer and Activator of Transcription-3 (Stat3), but the exact mechanism is a matter of controversy. We recently demonstrated that Stat3 activity of cultured cells increases dramatically following E-cadherin engagement. To better understand this pathway, we now compared Stat3 activity levels in mouse HC11 cells before and after expression of the mutationally activated Rac1 (Rac^{V12}), at different cell densities. The results revealed for the first time a dramatic increase in protein levels and activity of both the endogenous Rac and Rac^{V12} with cell density, which was due to inhibition of proteasomal degradation. In addition, Rac^{V12}-expressing cells had higher Stat3, tyrosine-705 phosphorylation and activity levels at all densities, indicating that Rac^{V12} is able to activate Stat3. Further examination of the mechanism of Stat3 activation showed that Rac^{V12} expression caused a surge in mRNA of Interleukin-6 (IL6) family cytokines, known potent Stat3 activators. Knockdown of gp130, the common subunit of this family reduced Stat3 activity, indicating that these cytokines may be responsible for the Stat3 activation by Rac^{V12}. The upregulation of IL6 family cytokines was required for cell migration and proliferation induced by Rac^{V12}, as shown by gp130 knockdown experiments, thus demonstrating that the gp130/Stat3 axis represents an essential effector of activated Rac for the regulation of key cellular functions.

Introduction

Rho family GTPases are intracellular molecular switches cycling between the active, GTP-bound state and the inactive, GDP-bound form [1]. Upon activation, the Rho GTPases can activate a distinct panel of effectors to regulate cellular functions. In fact, the Rho family members RhoA, Rac1 and Cdc42 are best known as master regulators of the actin cytoskeleton, promoting the formation of stress fibers, lamellipodia or filopodia, respectively. In addition, Rho GTPases are known growth stimulators that act by modulating key cell cycle regulators, such as cyclin D1 and the transcription factor Nuclear Factor-kappaB (NFkB), at the transcriptional level [2,3].

The Signal Transducers and Activators of Transcription (STATs) were discovered as latent cytoplasmic transcription factors that are activated by a number of cytokines and growth factors. Among

* *Corresponding author.* Fax: +1 613 533 6796.
E-mail address: raptisl@queensu.ca (L. Raptis).

Abbreviations: STATs, Signal Transducers and Activators of Transcription; IL6, Interleukin-6; ptyr, phosphorylated tyrosine; Erk, Extracellular-signal activated kinase; SH2, Src homology 2; JAKs, Janus kinases; Hsp90, Heat shock protein 90; NFkB, Nuclear Factor-kappaB; IKK, IkappaB kinase

0014-4827/$ – see front matter © 2009 Elsevier Inc. All rights reserved.
doi:10.1016/j.yexcr.2009.10.017

seven mammalian STAT genes identified, Stat3 is found to be overexpressed in a number of tumor cell lines and carcinomas [4]. The fact that a constitutively active form of Stat3 alone is sufficient to transform cultured fibroblasts to anchorage-independence and tumorigenicity points to an etiological role for Stat3 in neoplasia [5]. Like other STAT proteins, Stat3 is latent in the cytoplasm in an unstimulated cell. Following ligand engagement and receptor phosphorylation, Stat3 binds the activated receptor through its Src homology 2 (SH2) domain and is activated through phosphorylation by the receptor itself or by the associated JAKs (Janus kinases) or Src family kinases. Phosphorylation at a critical tyrosine, tyr-705 activates Stat3 by stabilizing the association of two monomers through reciprocal SH2-phosphotyrosine interactions. The Stat3 dimer then migrates to the nucleus where it binds to target sequences, leading to the transcriptional activation of specific genes, such as myc, Bcl-xL, cyclin D, survivin, Hepatocyte Growth Factor [6] and to the downregulation of the p53 antioncogene [7,8].

Previous results suggested a functional link between the Rho GTPases and Stat3 but the mechanism is still unclear. Indeed, while in one study it was reported that mutationally activated Rac1 can directly interact with Stat3 in co-immunoprecipitation assays [9], other data showed that Rac1 indirectly activates Stat3 through autocrine induction of interleukin-6 (IL-6) [10], while another group reported that the Rho GTPases can activate Stat3 independent from IL6 action [11]. We and others recently demonstrated a dramatic increase in the activity of Stat3 triggered by cell to cell contact in a variety of cell lines [12–16]. For this reason, the modulation of Stat3-ptyr705 levels by cell density must be taken into account in experiments assessing the effect of proto-oncogenes such as the Rho GTPases upon Stat3 function.

In this communication, we revisited the question of the mechanism of Stat3 activation by Rac1 and Cdc42, in light of the above findings. The results indicate that cell density alone causes a dramatic increase in protein levels and activity of both the endogenous cRac1 (Rac) and Cdc42, and the mutationally activated Rac1 (Rac^{V12}) and $Cdc42^{V12}$ in mouse HC11 epithelial cells, through inhibition of proteasomal degradation. Furthermore, lines expressing activated Rac^{V12} had higher Stat3 activity levels at all cell densities examined, indicating that Rac^{V12} is, in fact, able to activate Stat3. The Stat3 increase was mediated through the expression of IL6 family cytokines, as shown through knockdown of the gp130, common subunit of the family. Gp130 function and Stat3 activation were required for cell migration and increase in proliferation induced by mutationally activated Rac and Cdc42, as shown by genetic knockdown experiments, thus demonstrating that the gp130/Stat3 axis represents an essential effector of activated Rac in the regulation of both of these essential cellular functions.

Materials and methods

Cell lines, culture techniques and gene expression

The normal mouse mammary epithelial line HC11 is a prolactin-responsive cell clone originally isolated from the COMMA-1D mouse mammary epithelial cell line derived from a female Balb/c mouse in mid-gestation [17]. Cell confluence was estimated visually and quantitated by imaging analysis of live cells under phase contrast using a Leitz Diaplan microscope and the MCID-elite software (Imaging Research, St. Catharine's Ont.).

For NFkB inhibition, cells were treated with 20 μM IKK-inhibitorIII (BMS-345541) or 20 μM/ml CAPE (EMD Biosciences). JAK-inhibitor-1 (EMD Biosciences) or MG132 (Sigma) were added at the indicated concentrations. Treatment with the JAK-inhibitor-1 was for 24 h and with MG132 for 8 h. The CPA7, platinum Stat3 inhibitor was prepared as described [18] and used at a 50 μM concentration. Cell viability was assessed by trypan blue exclusion and by replating cells in medium lacking the inhibitors. IL6 was purchased from Invitrogen.

For gp130 knockdown, a mouse pSM2 retroviral target gene shRNA set (Cat#. RMM4530-NM_010560, Supplementary Table S1) was purchased from Open Biosystems. V2MM-70734 was the most efficient. Infected cells were selected for puromycin resistance. Rac^{V12} was expressed with a retroviral vector (a gift of Dr John Collard, [19]). Rac^{L61}, $Cdc42^{V12}$ and wtRac1 were expressed through plasmid transfection under control of the CMV promotor (plasmids were a gift of Dr. Graham Côté, Queen's University). Transient transfections for wtRac1 and Rac^{L61} expression were performed with Lipofectamine Plus (Invitrogen). To effectively compare the consequences of wtRac1 vs. Rac^{L61} expression upon Stat3 activity, HC11 cells were transfected with each of their respective plasmids and the next day plated at 3×10^6 cells/3 cm petri, equivalent to 2 days post-confluence, as before [20]. 24 h later, cell extracts were prepared and Western blots probed with the indicated antibodies.

For neutralisation of IL6 the #ab6672 antibody (Abcam) was used, while for neutralisation of LIF we used the antibody #L9152 (Sigma), at concentrations of 0.425 μM/ml and 1 ng/ml, respectively, according to the manufacturers' protocols.

Western blotting and immunoprecipitation

Detergent cell extracts were prepared as described [12]. Following a careful protein determination (BCA-1 Protein assay kit, Sigma), 30 or 100 μg of clarified cell extract were submitted to SDS-PAGE, as indicated. Blots were cut into strips and probed with antibodies specific for the tyr-705 phosphorylated Stat3 (Cell Signalling), total Stat3 (Cell Signalling), the dually phosphorylated form of Extracellular-signal activated kinase Erk1/2 (Biosource), survivin (Cell Signalling), p21 (Biosource), gp130 (Sigma) or Heat shock protein 90 (Hsp90, Stressgen) followed by alkaline phosphatase, or Horseradish Peroxidase-conjugated secondary antibodies (Jackson Labs). Rac1 and Cdc42 antibodies (BD Transduction Labs) recognised both the endogenous and mutant Rac or Cdc42, respectively. To examine the degree of Rac ubiquitination, extracts were immunoprecipitated with anti-ubiquitin antibodies (Biomol) and blotted against Rac1 or myc-tag (for Rac^{L61}, antibody 9E10, Sigma). In all cases, bands were visualized using enhanced chemiluminescence (PerkinElmer Life Sciences), or SuperSignal West Femto Maximum Sensitivity Substrate (Pierce). Quantitation was achieved by fluorimager analysis using the FluorChem program (AlphaInnotech Corp). In all cases Stat3-ptyr705 band intensities were normalized to Hsp90 levels of the same samples. Jak1 phosphorylation was examined by immunoprecipitation against total Jak1, followed by blotting with a Jak-ptyr1022/1023 antibody (Cell Signalling).

Rac/Cdc42 activation assays were performed using GST-PAK pull-down assays with the Rac/Cdc42 activation assay kit

(Cytoskeleton, #BK035). Briefly, the beads were coated with glutathione-S-transferase (GST) fused to the binding domain of p21-activated kinase, PAK (PAK-PBD) in pulldown assays. Adding twice the amount of PBD-coated beads did not increase the signal, indicating that the amount of binding partner used in the detection was not limiting.

Photoshop (Adobe) or Corel Draw software were used for the organization of non-adjusted, original images and blots.

qRT-PCR assays

For quantitative RT-PCR, the delta ct (Dct) value was calculated from the given ct value by the formula: $Dct = (ct_{sample} - ct_{control})$. For the qRT-PCR cytokine array, we used the PAMM-021A kit (SA Biosciences) with an RT-PCR for IL6 run in parallel, according to the manufacturer's protocol.

Results

Cell density inhibits cRac1 proteasomal degradation

We recently demonstrated that cell–cell contacts through E-cadherin engagement in HC11, normal mouse breast epithelial cells causes a dramatic increase in the cellular Rac1 (Rac) and Cdc42 protein levels [20]. To explore the possibility that the increase in Rac/Cdc42 with cell density (Figs. 1A and B, lanes 1–7) might be due to inhibition of proteasome-mediated degradation, we at first made use of the MG132 proteasome inhibitor [21]. As shown in Fig. 2A, MG132 treatment of sparsely growing HC11 cells caused a substantial increase in Rac protein levels, as well as the $p21^{CIP/WAF}$, p53 substrate serving as a positive control [22]. This observation points to a role for the proteasome in Rac degradation. At the same time, the levels of phosphorylated, i.e. activated extracellular-signal activated kinase (Erk1/2) remained unchanged following MG132 treatment, suggesting that Rac may be selectively degraded by the proteasome.

We next examined the effect of ubiquitin overexpression upon Rac protein levels, by transfecting HC11 cells with a plasmid consisting of a CMV promotor driving the transcription of an mRNA encoding a multimeric precursor molecule composed of eight, NH2-terminal hexa-histidine tagged ubiquitin units [23]. The results revealed that ubiquitin overexpression caused a reduction in Rac total protein levels which was more pronounced at lower cell densities, while pErk1/2 levels remained unaffected (Fig. 2B).

To further investigate whether Rac itself might be a substrate of the proteasome in sparsely growing cells, we examined whether Rac is modified by ubiquitin tagging. To this effect, we searched for the presence of Rac in the pool of ubiquitinated proteins, by probing anti-ubiquitin immunoprecipitates from HC11 cells for Rac by Western blotting. As shown in Fig. 2C, a diffuse band of ubiquitin-tagged Rac, consistent with short chain polyubiquitination [24], was detected in immunoprecipitates from HC11 cells grown to 30% confluence (lane 5). This band was very weak at 100% confluence (lane 6), possibly due to inhibition of ubiquitination at high cell densities. When the anti-ubiquitin antibody was omitted (lane 1) or replaced with normal mouse IgG (lane 3) or an unrelated, control mouse monoclonal antibody (not shown), no Rac was found in the immunoprecipitates from 30% confluent cultures. The above data taken together indicate that Rac itself is, in fact, a substrate of the proteasome in sparsely growing HC11 cultures, and that cell confluence inhibits Rac ubiquitination and proteasomal degradation.

Cell density upregulates activated Rac^{V12} levels through inhibition of proteasomal degradation

It was previously shown that the active, GTP-bound form of Rac is preferentially degraded by the proteasome [25]. Therefore, to examine the impact of cell density upon the levels of mutationally activated Rac^{V12} or Rac^{L61}, the latter labelled with a myc-tag, these genes were stably expressed in HC11 cells (see Materials and methods). A number of colonies were picked and, since cell density affects Rac protein levels (Fig. 1), screening for total Rac or myc-Rac by Western blotting was performed at 40% confluence. Three clones from each, expressing high Rac levels (H-Rac^{V12} and H-Rac^{L61}) were used for further study. Cells were plated in 3 cm dishes and when 30% confluent and at different times thereafter, Rac protein levels were evaluated by Western blotting. As shown in Fig. 1A (lanes 8–14), the levels of Rac^{V12} increased dramatically with cell density (lane 8 vs. 14). H-Rac^{V12} cells had ~3× higher total Rac levels than the parental HC11, at all densities examined. Two other Rac^{V12} and three Rac^{L61}-expressing clones gave the same results (not shown). The above results taken together indicate that, similar to cRac1 [20], activated Rac^{V12} and Rac^{L61} are also subject to density-dependent upregulation.

The effect of cell density upon Rac^{V12} activity was examined next. Cells were plated in petri dishes and when ~30% confluent, and over several days thereafter, Rac activity was measured by assessing the binding between Rac-GTP and its effector p21-activated kinase (PAK) in cell extracts using pull-down assays (see Materials and methods). As shown in Fig. 1, there was a dramatic increase in Rac activity with cell density, in both the parental line (lanes 1–7), and in Rac^{V12}-expressing, H-Rac^{V12} cells, at all densities examined (lanes 8–14), in parallel with Rac protein levels. Clones expressing the mutationally activated, $Cdc42^{V12}$ gave similar results (Fig. 1B). The above findings taken together indicate that cell density, besides an increase in total Rac/Cdc42 protein levels, it also causes a dramatic increase in both Rac/Cdc42 and Rac^{V12}/$Cdc42^{V12}$ activity. It follows that, cell density has to be taken into account when the effect of Rac^{V12} upon Stat3 is examined.

To better control the degree of cell–cell contact, irrespective of differences in cell growth patterns, we repeated the experiments by plating different numbers of HC11 or H-Rac^{V12} cells (0.4×10^6, 0.7×10^6, 1.0×10^6, 1.3×10^6, 1.8×10^6 or 2.5×10^6 per 3 cm petri, respectively), so that they would reach the same densities as above within 24 h [20]. At that time, cells were lysed and Rac protein levels and activity analysed as above. In all cases, very similar results were obtained, indicating that it is the extent of cell–cell contact, regardless of time in culture beyond 24 h, that is responsible for the increase in Rac protein and activity (not shown).

The potential role of ubiquitination upon the levels of the mutationally activated, Rac^{V12} was examined next. As for Rac in HC11 cells (Fig. 2C, lanes 5 and 6), anti-ubiquitin immunoprecipitates of Rac^{V12}-expressing cells grown to different densities were probed with an anti-Rac1 antibody. As shown in Fig. 2C (lane 8), a diffuse band of ubiquitin-tagged Rac [24], was detected in immunoprecipitates from cells grown to 30% confluence. Cells grown to 100% confluence on the other hand, had very low levels

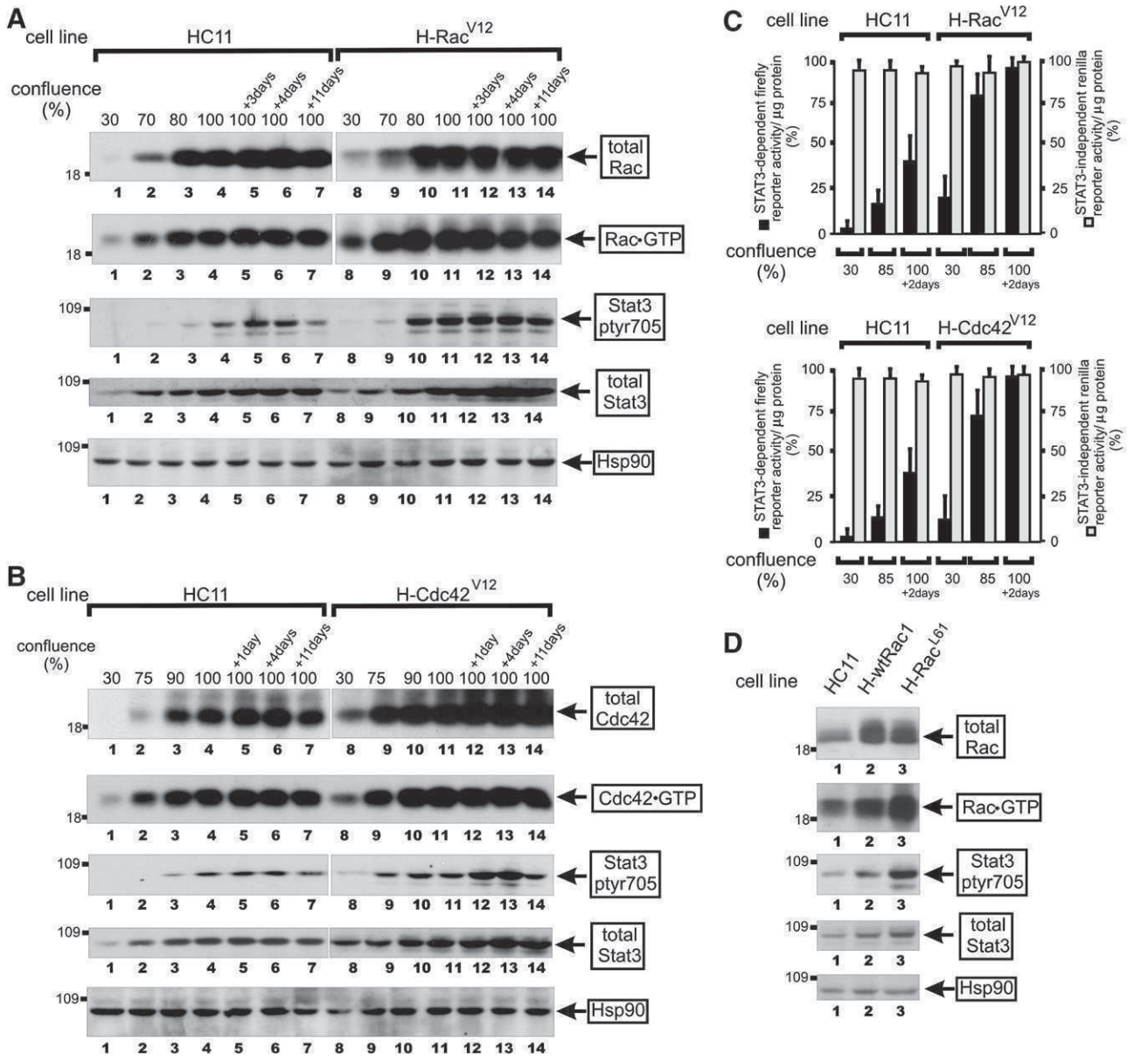

Fig. 1 – Rac^{V12} and Cdc42^{V12} activate Stat3 in HC11 cells at all cell densities. (A) Both endogenous and mutant Rac^{V12} protein levels and activity are dramatically increased by cell density, while Rac^{V12} expression increases Stat3-ptyr705 levels at all cell densities. HC11 cells (lanes 1–7) or their counterparts stably expressing activated Rac^{V12} (lanes 8–14) were grown to increasing densities, up to 11 days post-confluence. Detergent cell lysates were probed for total Rac, active Rac-GTP, Stat3-ptyr705, total Stat3 or Hsp90 as a loading control, as indicated (see Materials and methods). Numbers at the left refer to molecular weight markers. (B) Both endogenous and mutant Cdc42^{V12} protein levels and activity are dramatically increased by cell density, while Cdc42^{V12} expression increases Stat3-ptyr705 levels at all cell densities. HC11 cells (lanes 1–7) or their counterparts stably expressing activated Cdc42^{V12} (lanes 8–14) were grown to increasing densities, up to 11 days post-confluence. Detergent cell lysates were probed for total Cdc42, active Cdc42-GTP, Stat3-ptyr705, total Stat3 or Hsp90 as a loading control, as indicated. (C) Rac^{V12} and Cdc42^{V12}-expression increases Stat3 transcriptional activity. HC11 and Rac^{V12} (top panel)- and Cdc42 ^{V12} (bottom panel)-expressing cells were transfected with the Stat3-dependent p*Luc*TKS3 and the Stat3-independent pRLSRE reporters and grown to the indicated densities. Firefly (■) or *Renilla* (□) luciferase activities were determined in detergent cell extracts [12]. Values shown represent luciferase units expressed as a percentage of the highest value obtained, means ± s.e.m. of at least 3 experiments, each performed in triplicate. (D) Rac^{L61} is more effective than wtRac1 at increasing Stat3-705 phosphorylation. HC11 cells (lane 1), or their counterparts transfected with wtRac1 (lane 2) or Rac^{L61} (lane 3) were plated at 3×10^6 cells/3 cm plate (see Materials and methods) and detergent cell lysates probed for total Rac, active Rac-GTP, Stat3-ptyr705, total Stat3 or Hsp90 as a loading control, as indicated. Numbers at the left refer to molecular weight markers.

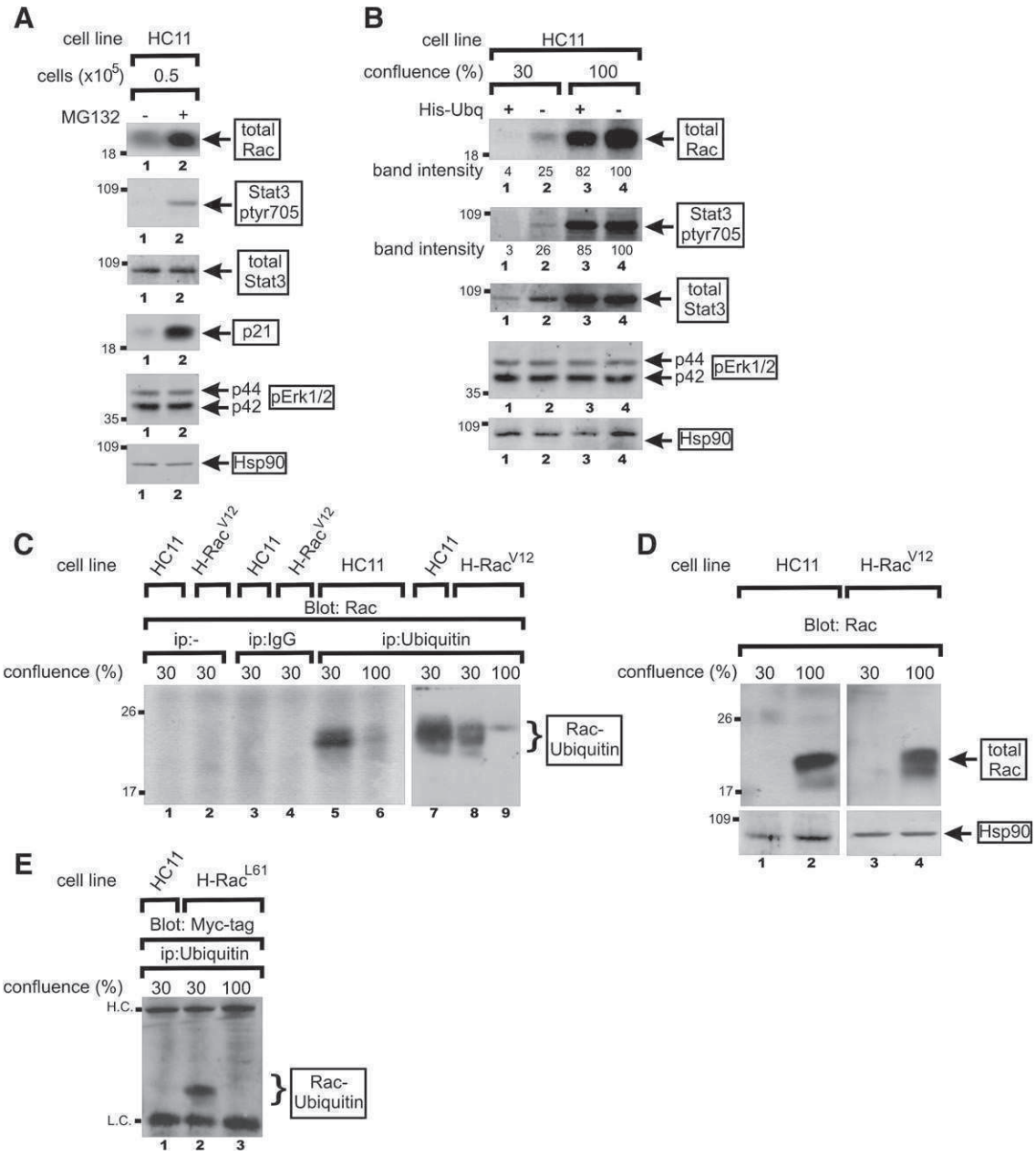

Fig. 2 – Cell density inhibits the proteasomal degradation of Rac. (A) The proteasome inhibitor, MG132 increases total Rac and Stat3-ptyr705 levels. Sparsely growing HC11 cells were treated with 10 mM of the proteasome inhibitor, MG132 (lane 2), or buffer alone (lane 1) for 8 h. Detergent cell extracts were probed for total Rac, Stat3-ptyr705, total Stat3, p21$^{CIP/WAF}$, pErk1/2 or Hsp90 as a loading control, as indicated. (B) Ubiquitin overexpression leads to Rac degradation. HC11 cells were transfected with a plasmid consisting of a CMV promotor driving the transcription of an mRNA encoding eight ubiquitin units with a his6 tag (His-Ubq, lanes 1 and 3) and grown to 30% (lanes 1 and 2) or 100% (lanes 3 and 4) confluence. Extracts were probed for Rac, Stat3-ptyr705, total Stat3, pErk1/2 or Hsp90, as indicated. Numbers under the lanes refer to total Rac or Stat3-ptyr705 band intensities obtained through quantitation by fluorimager analysis and normalized to Hsp90 levels, with the peak value of the control, HC11 cells grown to confluence (lane 4) taken as 100% (see Materials and methods). (C–E) Rac is ubiquitinated *in vivo*, at low cell densities. HC11 or H-Rac^{V12} cells were grown to 30% or 100% confluence and anti-ubiquitin immunoprecipitates of detergent cell extracts (lanes 5–9) blotted against Rac1. As a control, extracts from cells grown to 30% confluence were immunoprecipitated with normal rabbit serum (lanes 3–4) or buffer alone (lanes 1–2). Bracket points to the ubiquitinated Rac. (D) Extracts from HC11 or H-Rac^{V12} cells grown to 30% or 100% confluence were blotted against Rac1. (E) HC11 cells before (lane 1) or after (lanes 2 and 3) expression of a myc-tagged, L61 mutant were grown to 30% or 100% confluence and anti-ubiquitin immunoprecipitates of detergent cell extracts blotted against the myc-tag. H.C., L.C.: IgG heavy and light chains, respectively. Bracket points to the ubiquitinated Rac.

of ubiquitin-tagged Rac (lane 9), consistent with inhibition of ubiquitination at high cell densities. When the anti-ubiquitin antibody was omitted (lane 2) or replaced with normal mouse IgG (lane 4), no Rac^{V12} was detected in the immunoprecipitates. At the same time, total Rac protein levels were much higher at high densities, both in the HC11 and H-Rac^{V12} cell lines (Fig. 2D). Taken together, these data strongly suggest that Rac^{V12} itself is a substrate of the proteasome, in sparsely growing cells exclusively. To ensure that it is the mutationally activated Rac which is ubiquitinated, we made use of the myc-tagged, Rac^{L61}. As shown in Fig. 2E, blotting anti-ubiquitin immunoprecipitates from H-Rac^{L61} cells, expressing a myc-tagged Rac^{L61}, grown to 30% confluence, with an anti-myc-tag antibody, yielded a strong band (lane 2), while at 100% confluence no myc-tagged band was detected (lane 3). The above data taken together indicate that cell density can cause a dramatic increase in both Rac, and Rac^{V12} and RacL61 protein levels, through inhibition of proteasomal degradation.

Mutationally activated Rac^{V12} and $Cdc42^{V12}$ can activate Stat3

Previous results demonstrated that Rac^{V12} expression leads to activation of Stat3. However, the effect of cell density was not taken into account in any previous report, and this could be a source of apparently conflicting results [9–11]. To definitively demonstrate the effect of Rac^{V12} upon Stat3 activity, H-Rac^{V12} cells were plated in 3 cm dishes and at different times thereafter Stat3-ptyr705 levels measured by western blotting and compared to the parental HC11. As shown in Fig. 1A (lanes 8–14), H-Rac^{V12} cells had higher Stat3-ptyr705 levels at all cell densities examined. Similar results were obtained with Rac^{L61} (not shown), while overexpression of the cellular Rac1 (wtRac1, Fig. 1D) had a substantially reduced effect upon Stat3-ptyr705 levels, compared to Rac^{V12} or Rac^{L61}. Examination of the levels of total Stat3 protein revealed a modest increase with cell density, as previously reported [12], and with Rac^{V12} or $Cdc42^{V12}$ expression (Figs. 1A, B, D), possibly due to the fact that the Stat3 promotor itself is one of the Stat3 targets [26], although the differences were not as pronounced as the Stat3-tyr705 phosphorylation observed. Stat3 transcriptional activity also increased upon Rac^{V12} or $Cdc42^{V12}$ expression (Fig. 1C), following the pattern of Stat3-tyr705 phosphorylation (Figs. 1A and B).

The effect of Rac ubiquitination upon Stat3-ptyr705 levels was examined next. As shown in Fig. 2A, treatment with MG132, which increased Rac levels, also increased the levels of Stat3-ptyr705, while expression of his-ubiquitin, which reduced Rac levels, had a proportional effect upon Stat3-ptyr705 (Fig. 2B). $Cdc42^{V12}$ mirrored the effect of Rac^{V12} regarding Stat3 activation (Fig. 1B, lanes 8–14). The above results taken together indicate that mutationally activated forms of both Rho family GTPases are indeed able to activate Stat3, above and beyond the activation due to cell density.

NFkB and JAKs are required for the Rac^{V12}-mediated, Stat3 activation

Early data showed that Rac1 can activate NFkB [27]. To examine whether NFkB may be actually required for the Rac^{V12}-mediated Stat3 activation, sparsely growing HC11 cells were trypsinised and plated to a high density (2.5×10^6 cells/3 cm petri). Following attachment, cells were treated with the Ikappa Kinase (IKK)-inhibitor-III (BMS-345541) or the DMSO carrier alone, for 48 h. As shown in Fig. 3A, treatment with the inhibitor caused a dramatic reduction in Stat3-ptyr705 levels, in both the parental HC11 (lanes 3 vs. 2) and H-Rac^{V12} (lanes 5 vs. 4) cells. Similar results were obtained with caffeic acid phenethyl ester (CAPE), another known inhibitor of NFkB activity (not shown). These data indicate that both the cell density-mediated, and Rac^{V12}-mediated increase in Stat3-tyr705 phosphorylation requires NFkB. On the other hand, Rac levels were unaffected by NFkB inhibition (Fig. 3A), which further reinforces the conclusion that NFkB is downstream of Rac, i.e., it is required for the Rac-mediated, Stat3 activation exclusively.

To explore the role of Jak1 in the Rac^{V12}-mediated, Stat3 activation, we at first investigated whether Jak1 is activated by Rac^{V12}, by examining Jak1 phosphorylation at tyr1022/1023, shown to be important in the regulation of Jak1 activity [28,29]. Jak1 phosphorylation at 1022/1023 was measured by blotting lysates from H-Rac^{V12} and HC11 cells with a phospho-specific antibody (see Materials and methods). As shown in Fig. 3B, there was a ~2 fold increase in Jak1, 1022/1023 phosphorylation upon Rac^{V12} expression at 1 day after 100% confluence (lanes 3 vs. 4), which paralleled the phosphorylation of Stat3 at this density (Fig. 3A, lanes 2 vs. 4), while at 30% confluence the difference was more pronounced (Fig. 3B, lane 1 vs. 2). To examine whether Jak1 is actually required for the Rac^{V12}-mediated increase in Stat3 activity, HC11 cells grown to densities of 1 day post-confluence were treated with the pan-JAK inhibitor, JAK inhibitor 1. The results showed a dramatic reduction in Stat3-ptyr705 levels, which essentially plateaued at 2 μM of inhibitor, consistent with previous findings [20], while Rac levels remained unaffected (Fig. 3C, lanes 1–6). Similar results were obtained with the AG490 JAK inhibitor ([30], not shown). These findings suggest that the JAK kinases are required for the Rac^{V12}-mediated increase in Stat3-ptyr705 levels.

Rac^{V12} triggers cytokine gene expression and requires gp130 for Stat3 activation

To explore the possibility that the Rac^{V12}-induced, Stat3 activation may be mediated by autocrine factors, medium conditioned by sparsely growing, H-Rac^{V12} cells was added to the parental HC11 cells growing to a low density and Stat3-ptyr705 examined. The results revealed a 3-fold increase in Stat3-ptyr705, indicating the presence of autocrine factors (not shown). To explore the nature of the cytokines responsible, we conducted a quantitative RT-PCR array experiment for 86 cytokines, comparing mRNA levels in H-Rac^{V12} cells with levels in the parental HC11 line (see Materials and methods). Given the effect of density upon Stat3 levels, to examine the effect of Rac^{V12} *per se*, we compared cells expressing Rac^{V12} with the parental HC11, while both were grown to densities of 40%. The results revealed an increase in mRNA levels of two cytokines of the IL6 family, IL6 (18-fold) and Leukemia inhibitory factor (LIF) (~10-fold), known to act through the common gp130 subunit, shared by a number of Stat3 activating cytokines [31] (Supplementary Table S2). In fact, addition of neutralising antibodies against two members of the family, IL6 and LIF separately reduced Stat3-ptyr705 levels by approximately 30%, while a combination of the two caused a reduction of ~50% (Fig. 4A, top panel). To further demonstrate the requirement for IL6 family cytokines for the Rac^{V12}-mediated, Stat3 activation, the levels of gp130 were reduced through stable expression of a specific shRNA, using a retroviral vector (see

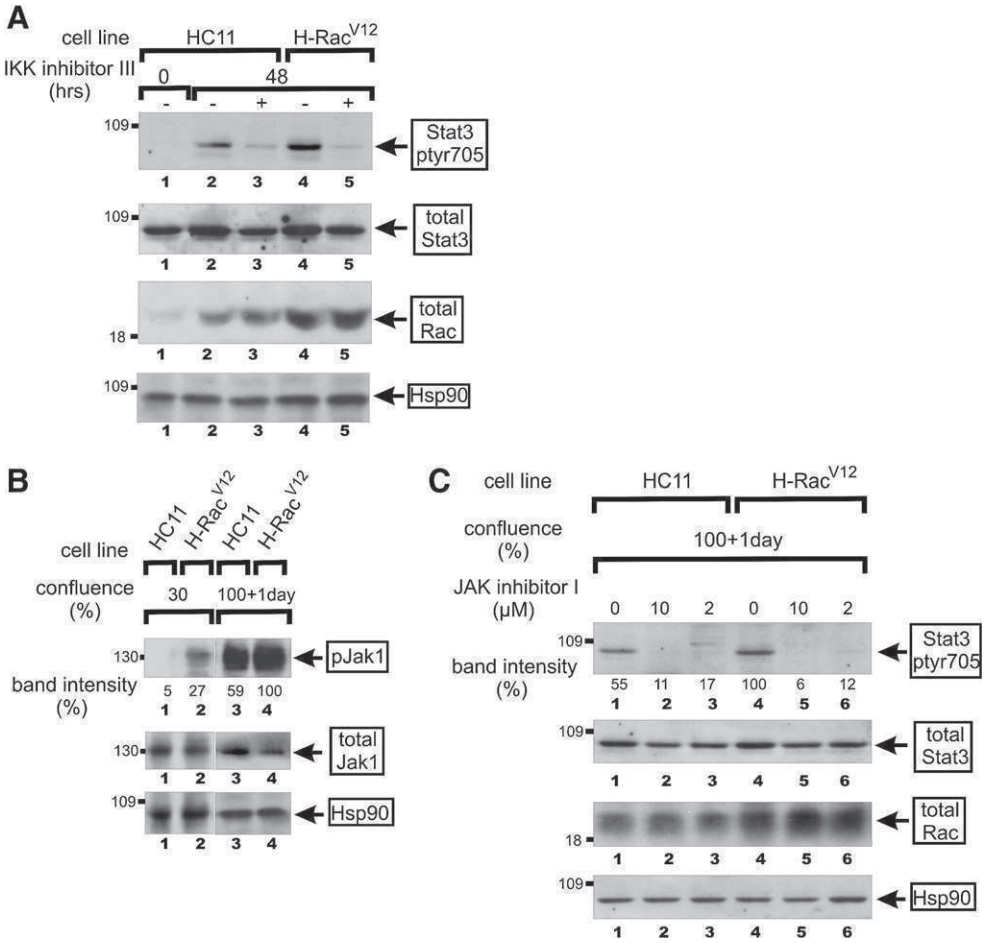

Fig. 3 – Rac^{V12}-dependent Stat3-ptyr705 phosphorylation requires JAK and NFkB. (A) The IKK inhibitor III inhibits the density-mediated, Stat3, tyr705 phosphorylation in both HC11 and H-Rac^{V12} cells. HC11 (lanes 1–3) or Rac^{V12} (lanes 4 and 5) cells were trypsinised and plated at a high density (2.5×10^6 cells/3 cm plate). Following attachment 30 min later, cells were treated with the IKK inhibitor III (lanes 3 and 5), or the DMSO carrier (lanes 2 and 4). Cell extracts were probed for Stat3-ptyr705, total Stat3, Rac or Hsp90, as a loading control. Lane 1: HC11 cells immediately after attachment to the plastic. (B) Rac^{V12}-expression increases Jak11022/1023 phosphorylation. Lysates from HC11 (lanes 1 and 3) or H-Rac^{V12} (lanes 2 and 4) cells were grown to 30% confluence (lanes 1 and 2), or 1 day after confluence (lanes 3 and 4) and probed for p-Jak1022/1023, total Jak1 or Hsp90 as a loading control, as indicated. (C) JAK inhibitor 1 reduces the Rac^{V12}-dependent, Stat3-tyr705 phosphorylation. HC11 (lanes 1–3) or Rac^{V12} (lanes 4–6) cells were grown to a high density and treated with 0 (lanes 1 and 4), 10 (lanes 2 and 5) or 2 (lanes 3 and 6) μg/ml JAK inhibitor 1. Cell lysates were probed for Stat3-ptyr705, total Stat3, Rac or Hsp90 as a loading control, as indicated.

Materials and methods). As shown in Fig. 4A, gp130 knockdown reduced Stat3-ptyr705 levels in H-Rac^{V12} cells (line H-Rac^{V12}-sh*gp130*) at all densities examined (lanes 1–3 vs. 4–6), pointing to the possibility that the two IL6 family cytokines play an important role in the activation of Stat3 by Rac^{V12}.

Rac^{V12}-induced IL6 upregulation is unable to activate Erk1/2 in confluent cultures

Results from a number of labs indicated that, in addition to Stat3, IL6 is able to activate the Erk1/2 kinase (Erk) [32]. Since Rac^{V12} expression leads to IL6 upregulation, we investigated whether Rac^{V12} can activate Erk. H-Rac^{V12} and HC11 cells were grown to 30% confluence, serum-starved for 24 h and levels of the dually phosphorylated, i.e. activated Erk1/2 (pErk) examined by Western immunoblotting. As shown in Fig. 4B, pErk levels were higher in H-Rac^{V12} cells when grown to 30% confluence than the parental HC11 (lane 2 vs. 1). At high density however, there was no Erk activity increase upon Rac^{V12} expression (lanes 4 vs. 3), although Stat3 phosphorylation was increased (Fig. 1A). To investigate whether the Erk activation by Rac^{V12} might be due to the IL6 family cytokines produced, pErk levels were examined in the gp130 knockdown cells. As shown in Fig. 4B (lanes 5–8), sh*gp130*-expressing cells had low pErk levels, even after Rac^{V12} expression (lane 6 vs. 2), indicating that IL6 activity is required for pErk upregulation by Rac^{V12}. To further verify the effect of IL6 upon Erk, we directly examined the role of density upon the activation of Erk by purified IL6. HC11 cells were grown to densities of 60% or 2 days after confluence, stimulated with IL6 for 15 min and Erk activity examined by probing for pErk (Fig. 4B, right panel). The results demonstrated that although IL6 could activate Erk in subconfluent cultures (lane 2 vs. 1), as previously reported [32], there was no Erk activity increase upon IL6 addition in cells grown to high confluence (lane 4). The above

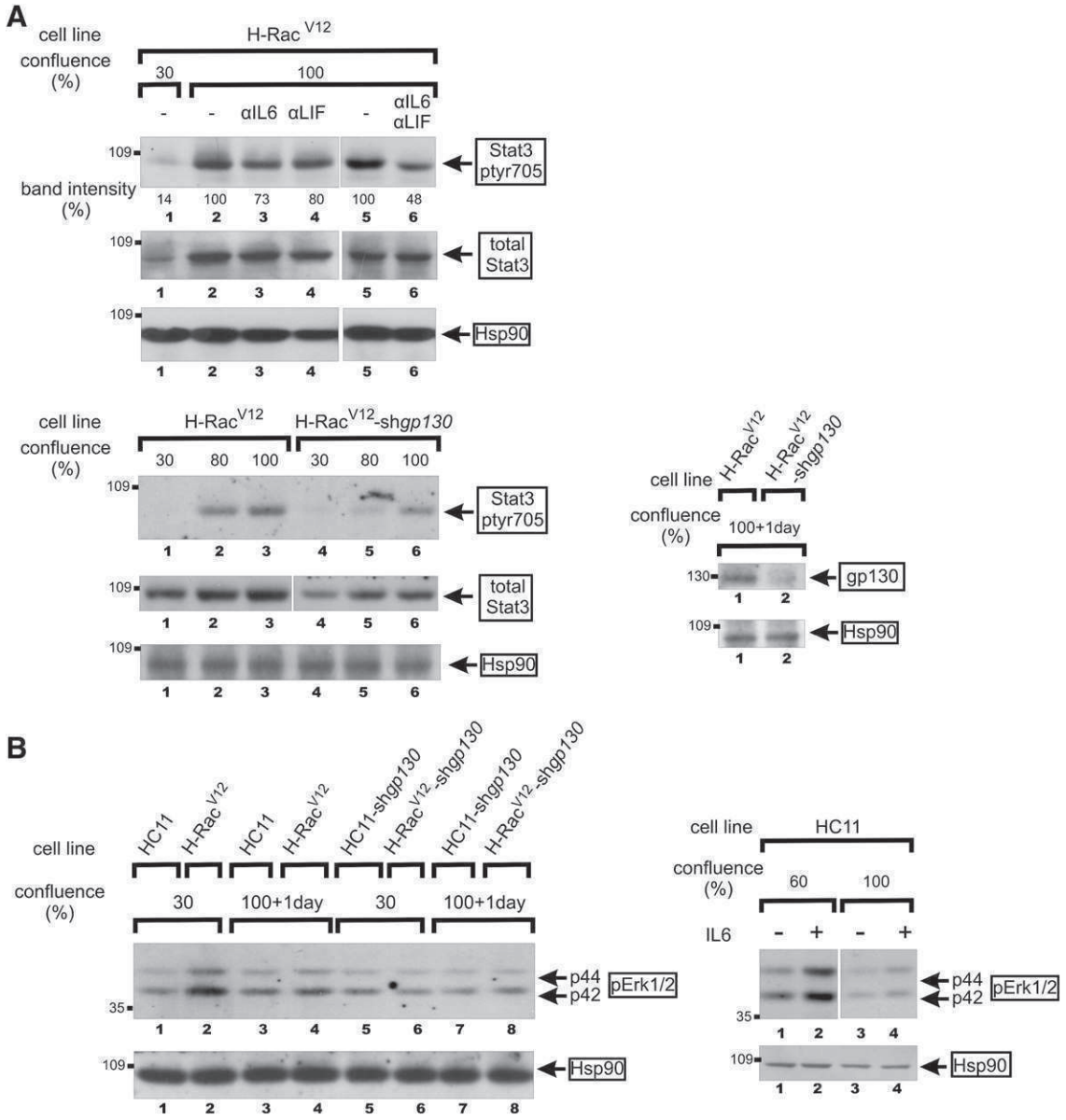

Fig. 4 – gp130 is required for the Rac^{V12}-mediated, Stat3 activation. (A) Top: reduction in Stat3-ptyr705 levels by neutralising antibodies to IL6 and LIF. Rac^{V12} cells were grown to 30% confluence (lane 1) or 1 day post-confluence and an antibody to IL6 (lane 3) or to LIF (lane 4), or a combination of the two (lane 6) added to the growth medium for 6 h. Detergent cell extracts were blotted for Stat3-ptyr705, total Stat3 or Hsp90 as a loading control. Lanes 2 and 5: control lanes, cells treated with buffer alone. Bottom panel: lysates from H-Rac^{V12} cells before (lanes 1–3) or after (lanes 4–6) expression of a gp130-specific, shRNA were probed for Stat3-ptyr705, total Stat3 or Hsp90 as a loading control, as indicated. Right panel: lysates from H-Rac^{V12} cells, before (lane 1) or after (lane 2) knockdown of gp130 were probed for gp130 or Hsp90 as a loading control, as indicated. (B) Rac^{V12} does not activate Erk at high cell densities. Left panel: extracts from the indicated cell lines, before (lanes 1–4) or after (lanes 5–8) expression of the gp130-specific, shRNA were probed for pErk1/2 or Hsp90 as a loading control, as indicated. Right panel: IL6 was added at 10 ng/ml for 15 min to HC11 cells grown to 60% (lane 2) or 100% (lane 4) confluence and cell extracts probed for Erk1/2 or Hsp90 as a loading control, as indicated.

findings clearly indicate that, although Rac^{V12} induces the expression of IL6, a known Erk activator, IL6 is unable to activate Erk in cells grown to high densities. This observation explains earlier data indicating that pErk levels are unaffected by confluence in a number of cellular systems [12], and reveals a profound effect of cell to cell adhesion upon the response of HC11 cells to IL6.

Rac^{V12}-induced cell proliferation and migration require IL6 family cytokines

The Rho family GTPases are known to play a role in the control of cell proliferation [33]. To examine the effect of IL6 family cytokines upon the Rac^{V12}-induced cell proliferation, HC11, H-*sh*gp130, H-Rac^{V12} and H-Rac^{V12}- sh*gp130* cells were plated in 3 cm dishes and their

growth rate determined. As shown in Fig. 5A, sh*gp130* expression caused a ~2.2 fold reduction in the growth rate of both H-Rac^{V12} cells and the parental HC11, indicating that gp130 is an essential component of a pathway leading to Rac-induced cell proliferation.

It is well established that increased Rac activity can increase cell motility through the formation of lamellipodia at the leading edge of cells in a wound healing assay [34]. To examine the role of the gp130 subunit in the Rac-induced cell migration, HC11, H-Rac^{V12}, H-sh*gp130* and H-Rac^{V12}-sh*gp130* cells were plated in plastic petri dishes. At 2 days post-confluence, a scratch-wound was introduced to the monolayer using a plastic pipette tip, and the cells allowed to migrate into the gap. As shown in Figs. 5B and C, Rac^{V12}-expressing cells were able to move faster to the open wound than the parental HC11 (panel f vs. b). However, gp130 downregulation abolished this effect (panel h), indicating that gp130 is an integral component of the Rac^{V12} pathway leading to the increase in cell migration. gp130 shRNA expression in the parental HC11 line also decreased cell migration (panel d). Although H-Rac^{V12} cells grow faster than H-Rac^{V12}-sh*gp130*, the accelerated growth rate cannot account for the increase in rate of migration and gap closure. Downregulation of Stat3 through shRNA knockdown [35], or treatment with the CPA7 inhibitor [18] caused a similar decrease in cell migration of H-Rac^{V12} cells (not shown), as previously reported in other systems [11]. These findings indicate that gp130 is required for cell migration triggered by the cellular Rac, and that expression of the mutationally activated Rac^{V12} cannot overcome the gp130 knockdown. Taken together, these results demonstrate that gp130 represents an essential effector of activated Rac in the regulation of both cell proliferation and migration.

Discussion

We previously demonstrated that cell to cell adhesion induces a dramatic increase in the levels of Stat3 activity, which peaks at

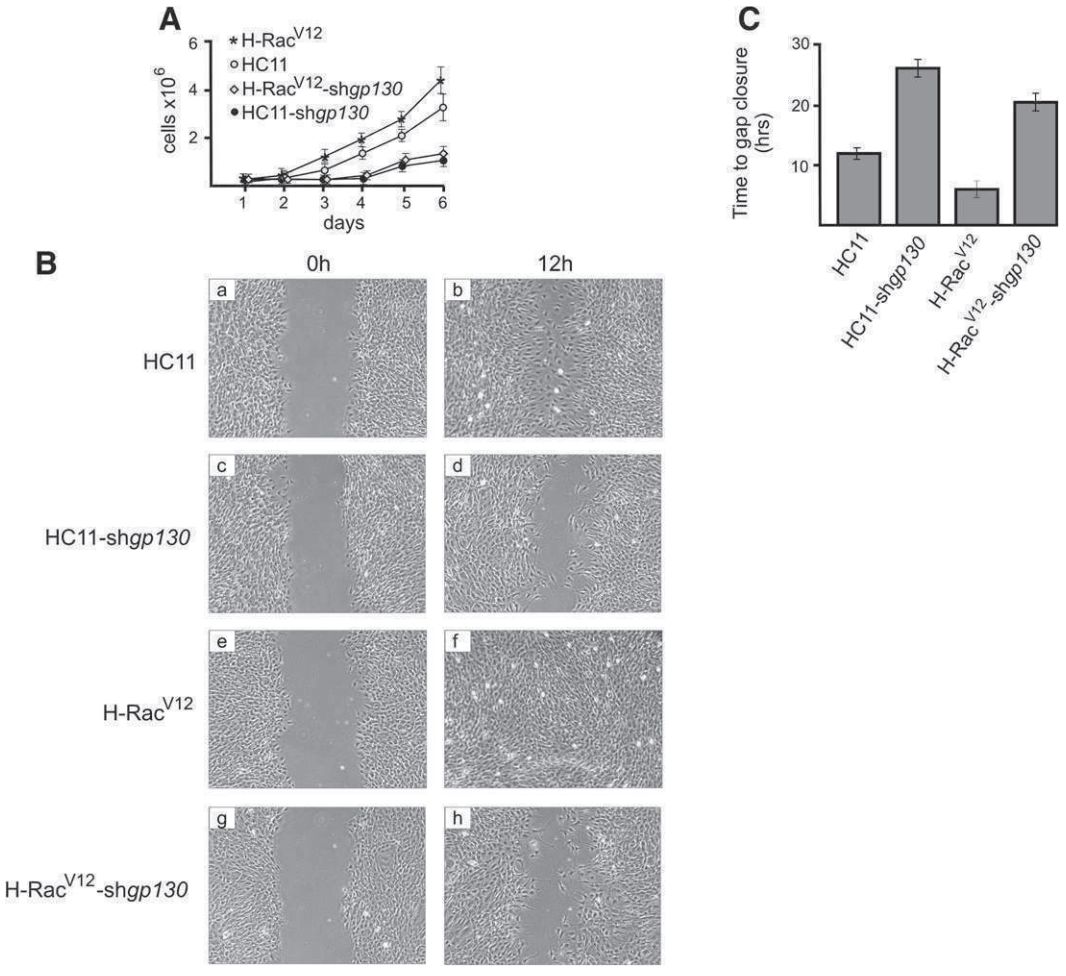

Fig. 5 – Rac-induced cell migration and proliferation require gp130. (A) Cell proliferation: HC11, H-sh*gp130*, H-Rac^{V12}, or H-Rac^{V12}-sh*gp130* cells were grown in Petri dishes in 10% serum and cell numbers obtained over several days, as indicated. Values represent averages of 3 independent experiments. (B) Cell migration: HC11, HC11-sh*gp130*, H-Rac^{V12} or H-Rac^{V12}-sh*gp130* cells were cultured to confluence before a scratch was made through the monolayer using a plastic pipette tip. Cells were photographed at 0 (panels a, c, e, g) or 24 h (panels b, d, f, h) after 12 h of culturing in 0.5% fetal calf serum. (C) Quantitation of the time (h) required by the different cell lines for gap junction closure. HC11, HC11-sh*gp130*, H-Rac^{V12} or H-Rac^{V12}-sh*gp130* cells were cultured to confluence before a scratch was made through the monolayer using a plastic pipette tip. The time taken for gap junction closure was determined by microscopic observation. Numbers represent averages of 3 independent experiments.

approximately 2 days after 100% confluence [12,36] (reviewed in [37]. An important piece of information that came out of these studies is that cell density must be taken into account in experiments to assess the effect of an oncogene upon Stat3 activity. Therefore, to investigate the effect of activated Rac upon Stat3, Stat3 activity levels were examined at different cell densities, following expression of two mutationally activated Rac constructs, Rac^{V12} and Rac^{L61}. The results revealed that Stat3 activity was increased with activated Rac expression at all cell densities examined, indicating that activated Rac can, in fact, activate Stat3, above and beyond the activation due to cell density.

These observations raise important questions: (1) What is the mechanism of increase in Rac and Rac^{V12} levels with cell density? (2) What is the mechanism of Stat3 activation by Rac^{V12}? (3) What is the functional significance of the Stat3 activation in Rac^{V12}-expressing cells?

Cell density inhibits the proteasomal degradation of Rac

We previously demonstrated that cell density increases Rac levels [20]. Our data now indicate that this increase could be due to inhibition of Rac proteasomal degradation with confluence. In fact, previous results indicated that Rac can be degraded through the proteasome pathway [25]. A mutational analysis further indicated that constitutive activation of Rac, as well as binding of effectors, which might be acting as ubiquitin E3 ligases, are necessary for Rac degradation [25]. Our results, demonstrating that, although activated, Rac^{V12} and Rac^{L61} protein levels are increased dramatically with cell density, indicate that cell density can overcome the degradative effect of activation. These findings extend and reinforce previous data indicating that epithelial cell scattering brought about by Hepatocyte Growth factor can induce the proteasome-mediated degradation of Rac1 [24]. A similar mechanism could hold true for Cdc42, which mirrored Rac levels and stability increases with cell density.

IL6 family cytokines transmit the signal from activated Rac^{V12} to Stat3

Although earlier reports [9] indicated that Rac can directly interact with Stat3 in co-expression/co-immunoprecipitation assays, later findings unequivocally demonstrated that Stat3 activation by the Rho GTPases can occur without the formation of a stable complex ([11] and data not shown). In addition, data by Faruqi et al. [10] demonstrated that Rac^{V12} could indirectly activate Stat3 through autocrine induction of IL6. However, through the use of specific antibodies added to the medium it was later demonstrated that Stat3 activation can occur independently of IL6 stimulation [11]. To resolve this apparent controversy, we examined mRNA levels for 86 cytokines in an array analysis. The results revealed an increase in two cytokines of the IL6 family (IL6 and LIF), indicating that this family may be involved in Stat3 activation by mutationally activated Rac. Furthermore, downregulation of gp130, the common subunit of the family, abolished the Rac^{V12}-mediated, Stat3 activation indicating that this subunit is actually required for Stat3 activation. The fact that the LIF also, rather than IL6 alone, is upregulated by Rac^{V12} explains earlier data indicating that IL6-specific antibodies did not reduce Stat3 activity [11], since these antibodies, directed against the unique extracellular subunit of IL6 would inhibit IL6 exclusively, while LIF would still be free to activate Stat3. In any event, these results demonstrate that the total Stat3 activity in the cell is the sum of effects of both cell to cell adhesion, plus the Stat3 activating, Rac^{V12} or $Cdc42^{V12}$ oncogene present.

Previous results indicated that IL6 activates Erk, as well as Stat3. Since Rac^{V12} causes the upregulation of IL6 family cytokines, it is expected that Rac^{V12} expression would activate Erk. However, although Rac^{V12}-expressing cells had higher pErk levels than the parental HC11, when sparsely grown, there was no pErk increase in H-Rac^{V12} cells grown to high densities. To solve this apparent paradox, HC11 cells were grown to different densities and stimulated with IL6. Indeed IL6 itself, although able to activate Erk in subconfluent cultures, was unable to do so once cells reached confluence (Fig. 4B), although Stat3 was still activated (Fig. 1). It is possible that Erk-specific phosphatases such as Cdc25A are activated at high cell densities [38], or that other adaptors required for Erk activation by IL6, or phosphorylation of IL6-R sites, are downregulated following cadherin engagement and establishment of cell to cell contacts. In any event, these results further demonstrate that, despite the fact that these two pathways are often both activated by oncogenes, cytokines or growth factors, they are not coordinately regulated by IL6 in densely growing cells.

Gp130 is required for Rac-mediated cell proliferation and migration

It is well established that Rac activation can increase cell motility, in part due to regulation of the actin cytoskeleton. However, the role of the IL6/Stat3 axis in this effect has not been examined. Our results showed that, as observed before [34], Rac^{V12}-expressing, HC11 cells were able to move faster into an open wound intro-

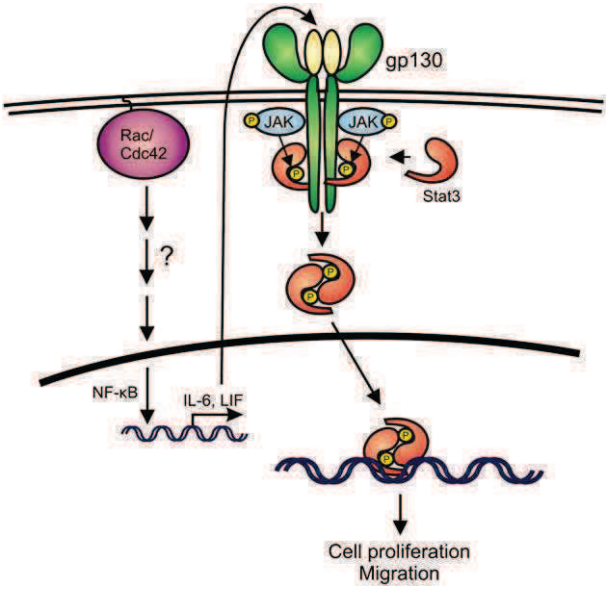

Fig. 6 – Proposed model for Rac/Cdc42-mediated, Stat3 activation. Constitutively active Rac/Cdc42 activates Stat3 through induction of IL6 family cytokines, such as IL6 and LIF which possess the common subunit, gp130. This leads to activation of their respective receptors, Jak activation and phosphorylation of Stat3, resulting in cell proliferation and migration.

duced with a plastic pipette tip into a cell monolayer than the parental line [1]. Furthermore, the Rac-mediated motility required the activity of IL6 family cytokines, since downregulation of the gp130, common subunit of the family, reduced the rate of migration. The fact that activated Rac^{V12} upregulates IL6 and Stat3, gives further credence to the model of Stat3 activation by cadherin engagement, *via* Rac and IL6 [20].

Conclusions

Our results definitively demonstrate that activated Rac/Cdc42 expression leads to Stat3 activation, by a mechanism requiring NFkB, gp130 and JAK. This pathway is required for cell proliferation and migration, that is the gp130/Stat3 axis represents an essential effector of activated Rac for the regulation of key cellular functions (Fig. 6).

Acknowledgments

Special thanks are due to Dr. Richard Jove and Dr. James Turkson for valuable advice. We would like to thank Dr. John Collard for the Rac^{V12} vector and Dr. Graham Côté for the Rac^{L61}, wtRac1 and $Cdc42^{V12}$ vectors and Dr. Harriet Feilotter and Xiao Zhang of the Queen's University Laboratory for Molecular Pathology/Microarray Facility for qRT-PCR array analysis.

The financial assistance of the Canadian Institutes of Health Research (CIHR), the Canadian Breast Cancer Foundation (Ontario Chapter), the Natural Sciences and Engineering Research Council of Canada (NSERC), the Ontario Centers of Excellence, the Canadian Breast Cancer Research Alliance, the Breast Cancer Action Kingston and the Clare Nelson bequest fund (LR) and the Fondation pour la Recherche Médicale, Région Aquitaine and the Association pour la Recherche contre le Cancer (HF), is gratefully acknowledged. RA was supported by a Canada Graduate Scholarships Doctoral award from CIHR, the Ontario Women's Health Scholars Award from the Ontario Council of Graduate Studies and a Queen's University Graduate Award (QGA). MG was supported by a postdoctoral fellowship from the US Department of Defense breast cancer research program (BCRP-CDMRP), a postdoctoral fellowship from the Ministry of Research and Innovation of the Province of Ontario and the Advisory Research Committee of Queen's University.

Appendix A. Supplementary data

Supplementary data associated with this article can be found, in the online version, at doi:10.1016/j.yexcr.2009.10.017.

REFERENCES

[1] S. Etienne-Manneville, A. Hall, Rho GTPases in cell biology, Nature 420 (2002) 629–635.
[2] R. Perona, S. Montaner, L. Saniger, I. Sanchez-Perez, R. Bravo, J.C. Lacal, Activation of the nuclear factor-kappaB by Rho, CDC42, and Rac-1 proteins, Genes Dev. 11 (1997) 463–475.
[3] D. Joyce, B. Bouzahzah, M. Fu, C. Albanese, M. D'Amico, J. Steer, J.U. Klein, R.J. Lee, J.E. Segall, J.K. Westwick, C.J. Der, R.G. Pestell, Integration of Rac-dependent regulation of cyclin D1 transcription through a nuclear factor-kappaB-dependent pathway, J. Biol. Chem. 274 (1999) 25245–25249.
[4] D.A. Frank, STAT3 as a central mediator of neoplastic cellular transformation, Cancer Lett. 251 (2007) 199–210.
[5] J.F. Bromberg, M.H. Wrzeszczynska, G. Devgan, Y. Zhao, R.G. Pestell, C. Albanese, J.E. Darnell Jr., Stat3 as an oncogene, Cell 98 (1999) 295–303.
[6] W. Hung, B. Elliott, Co-operative effect of c-Src tyrosine kinase and Stat3 in activation of hepatocyte growth factor expression in mammary carcinoma cells, J. Biol. Chem. 276 (2001) 12395–12403.
[7] G. Niu, K.L. Wright, Y. Ma, G.M. Wright, M. Huang, R. Irby, J. Briggs, J. Karras, W.D. Cress, D. Pardoll, R. Jove, J. Chen, H. Yu, Role of Stat3 in regulating p53 expression and function, Mol. Cell. Biol. 25 (2005) 7432–7440.
[8] H. Yu, R. Jove, The STATs of cancer—new molecular targets come of age, Nat. Rev., Cancer 4 (2004) 97–105.
[9] A.R. Simon, H.G. Vikis, S. Stewart, B.L. Fanburg, B.H. Cochran, K.L. Guan, Regulation of STAT3 by direct binding to the Rac1 GTPase, Science 290 (2000) 144–147.
[10] T.R. Faruqi, D. Gomez, X.R. Bustelo, D. Bar-Sagi, N.C. Reich, Rac1 mediates STAT3 activation by autocrine IL-6, Proc. Nat. Acad. Sci. U. S. A. 98 (2001) 9014–9019.
[11] M. Debidda, L. Wang, H. Zang, V. Poli, Y. Zheng, A role of STAT3 in Rho GTPase-regulated cell migration and proliferation, J. Biol. Chem. 280 (2005) 17275–17285.
[12] A. Vultur, J. Cao, R. Arulanandam, J. Turkson, R. Jove, P. Greer, A. Craig, B.E. Elliott, L. Raptis, Cell to cell adhesion modulates Stat3 activity in normal and breast carcinoma cells, Oncogene 23 (2004) 2600–2616.
[13] A. Onishi, Q. Chen, J.O. Humtsoe, R.H. Kramer, STAT3 signaling is induced by intercellular adhesion in squamous cell carcinoma cells, Exp. Cell Res. 314 (2008) 377–386.
[14] R.A. Steinman, A. Wentzel, Y. Lu, C. Stehle, J.R. Grandis, Activation of Stat3 by cell confluence reveals negative regulation of Stat3 by cdk2, Oncogene 22 (2003) 3608–3615.
[15] H.W. Su, H.H. Yeh, S.W. Wang, M.R. Shen, T.L. Chen, P.R. Kiela, F.K. Ghishan, M.J. Tang, Cell confluence-induced activation of signal transducer and activator of transcription-3 (Stat3) triggers epithelial dome formation via augmentation of sodium hydrogen exchanger-3 (NHE3) expression, J. Biol. Chem. 282 (2007) 9883–9894.
[16] S. Kreis, G.A. Munz, S. Haan, P.C. Heinrich, I. Behrmann, Cell density dependent increase of constitutive signal transducers and activators of transcription 3 activity in melanoma cells is mediated by Janus kinases, Mol. Cancer Res. 5 (2007) 1331–1341.
[17] R.K. Ball, R.R. Friis, C.A. Schoenenberger, W. Doppler, B. Groner, Prolactin regulation of beta-casein gene expression and of a cytosolic 120-kd protein in a cloned mouse mammary epithelial cell line, EMBO J. 7 (1988) 2089–2095.
[18] S.L. Littlefield, M.C. Baird, A. Anagnostopoulou, L. Raptis, Synthesis, characterization and Stat3 inhibitory properties of the prototypical platinum(IV) anticancer drug, [PtCl3(NO2)(NH3)2] (CPA-7), Inorg. Chem. 47 (2008) 2798–2804.
[19] E.E. Sander, S. van Delft, J.P. ten Klooster, T. Reid, R.A. van der Kammen, F. Michiels, J.G. Collard, Matrix-dependent Tiam1/Rac signaling in epithelial cells promotes either cell–cell adhesion or cell migration and is regulated by phosphatidylinositol 3-kinase, J. Cell Biol. 143 (1998) 1385–1398.
[20] R. Arulanandam, A. Vultur, J. Cao, E. Carefoot, P. Truesdell, B. Elliott, L. Larue, H. Feracci, L. Raptis, Cadherin–cadherin engagement promotes survival via Rac/Cdc42 and Stat3, Mol. Cancer Res. 17 (2009) 1310–1327.
[21] S. Tsubuki, Y. Saito, M. Tomioka, H. Ito, S. Kawashima, Differential inhibition of calpain and proteasome activities by peptidyl aldehydes of di-leucine and tri-leucine, J. Biochem. 119 (1996) 572–576.
[22] Q. Zhu, G. Wani, J. Yao, S. Patnaik, Q.E. Wang, M.A. El Mahdy, M. Praetorius-Ibba, A.A. Wani, The ubiquitin–proteasome system

regulates p53-mediated transcription at p21waf1 promoter, Oncogene 26 (2007) 4199–4208.
[23] M. Treier, L.M. Staszewski, D. Bohmann, Ubiquitin-dependent c-Jun degradation in vivo is mediated by the delta domain, Cell 78 (1994) 787–798.
[24] E.A. Lynch, J. Stall, G. Schmidt, P. Chavrier, C. D'Souza-Schorey, Proteasome-mediated degradation of Rac1-GTP during epithelial cell scattering, Mol. Biol. Cell 17 (2006) 2236–2242.
[25] M. Pop, K. Aktories, G. Schmidt, Isotype-specific degradation of Rac activated by the cytotoxic necrotizing factor 1, J. Biol. Chem. 279 (2004) 35840–35848.
[26] M. Narimatsu, H. Maeda, S. Itoh, T. Atsumi, T. Ohtani, K. Nishida, M. Itoh, D. Kamimura, S.J. Park, K. Mizuno, J. Miyazaki, M. Hibi, K. Ishihara, K. Nakajima, T. Hirano, Tissue-specific autoregulation of the stat3 gene and its role in interleukin-6-induced survival signals in T cells, Mol. Cell. Biol. 21 (2001) 6615–6625.
[27] D.J. Sulciner, K. Irani, Z.X. Yu, V.J. Ferrans, P. Goldschmidt-Clermont, T. Finkel, rac1 regulates a cytokine-stimulated, redox-dependent pathway necessary for NF-kappaB activation, Mol. Cell. Biol. 16 (1996) 7115–7121.
[28] M.C. Gauzzi, L. Velazquez, R. McKendry, K.E. Mogensen, M. Fellous, S. Pellegrini, Interferon-alpha-dependent activation of Tyk2 requires phosphorylation of positive regulatory tyrosines by another kinase, J. Biol. Chem. 271 (1996) 20494–20500.
[29] W.J. Leonard, J.J. O'Shea, Jaks and STATs: biological implications, Annu. Rev. Immunol. 16 (1998) 293–322.
[30] Y. Zhang, J. Turkson, C. Carter-Su, T. Smithgall, A. Levitzki, A. Kraker, J.J. Krolewski, P. Medveczky, R. Jove, Activation of Stat3 in v-Src transformed fibroblasts requires cooperation of Jak1 kinase activity, J. Biol. Chem. 275 (2000) 24935–24944.
[31] D. Hilfiker-Kleiner, A. Hilfiker, M. Fuchs, K. Kaminski, A. Schaefer, B. Schieffer, A. Hillmer, A. Schmiedl, Z. Ding, E. Podewski, E. Podewski, V. Poli, M.D. Schneider, R. Schulz, J.K. Park, K.C. Wollert, H. Drexler, Signal transducer and activator of transcription 3 is required for myocardial capillary growth, control of interstitial matrix deposition, and heart protection from ischemic injury, Circ. Res. 95 (2004) 187–195.
[32] P. Fischer, D. Hilfiker-Kleiner, Role of gp130-mediated signalling pathways in the heart and its impact on potential therapeutic aspects, Br. J. Pharmacol. 153 (Suppl. 1) (2008) S414–S427.
[33] F. Guo, Y. Zheng, Involvement of Rho family GTPases in p19Arf- and p53-mediated proliferation of primary mouse embryonic fibroblasts, Mol. Cell Biol. 24 (2004) 1426–1438.
[34] C.D. Nobes, A. Hall, Rho GTPases control polarity, protrusion, and adhesion during cell movement, J. Cell Biol. 144 (1999) 1235–1244.
[35] M. Geletu, C. Chaize, R. Arulanandam, A. Vultur, C. Kowolik, A. Anagnostopoulou, R. Jove, L. Raptis, Stat3 activity is required for gap junctional permeability in normal epithelial cells and fibroblasts, DNA Cell Biol. 28 (2009) 319–327.
[36] A. Vultur, R. Arulanandam, J. Turkson, G. Niu, R. Jove, L. Raptis, Stat3 is required for full neoplastic transformation by the Simian Virus 40 Large Tumor antigen, Mol. Biol. Cell 16 (2005) 3832–3846.
[37] L. Raptis, R. Arulanandam, A. Vultur, M. Geletu, S. Chevalier, H. Feracci, Beyond structure, to survival: Stat3 activation by cadherin engagement, Biochem. Cell Biol. 87 (2009) 835–843.
[38] J.S. Lazo, K. Nemoto, K.E. Pestell, K. Cooley, E.C. Southwick, D.A. Mitchell, W. Furey, R. Gussio, D.W. Zaharevitz, B. Joo, P. Wipf, Identification of a potent and selective pharmacophore for Cdc25 dual specificity phosphatase inhibitors, Mol. Pharmacol. 61 (2002) 720–728.

DNA AND CELL BIOLOGY
Volume 28, Number 7, 2009

Pp. 319–327
DOI: 10.1089/dna.2008.0833

Stat3 Activity Is Required for Gap Junctional Permeability in Normal Rat Liver Epithelial Cells

Mulu Geletu,[1,*] Chrystele Chaize,[1,*] Rozanne Arulanandam,[1] Adina Vultur,[2] Claudia Kowolik,[2] Aikaterini Anagnostopoulou,[1] Richard Jove,[2] and Leda Raptis[1]

Neoplastic transformation by oncogenes such as activated Src is known to suppress gap junctional, intercellular communication (GJIC). One of the Src effector pathways leading to GJIC suppression and transformation is the Ras/Raf/Mek/Erk, so that inhibition of this pathway in vSrc-transformed cells restores GJIC. A distinct Src downstream effector required for neoplasia is the signal transducer and activator of transcription-3 (Stat3). To examine the role of Stat3 upon the Src-mediated, GJIC suppression, Stat3 was downregulated in rat liver epithelial cells expressing activated Src through treatment with the CPA7, Stat3 inhibitor, or through infection with a retroviral vector expressing a Stat3-specific shRNA. GJIC was examined by electroporating the fluorescent dye, Lucifer yellow, into cells grown on two coplanar electrodes of electrically conductive, optically transparent, indium-tin oxide, followed by observation of the migration of the dye to the adjacent, nonelectroporated cells under fluorescence illumination. The results demonstrate that, contrary to inhibition of the Ras pathway, Stat3 inhibition in cells expressing activated Src does not restore GJIC. On the contrary, Stat3 inhibition in normal cells with high GJIC levels eliminated junctional permeability. Therefore, Stat3's function is actually required for the maintenance of junctional permeability, although Stat3 generally promotes growth and in an activated form can act as an oncogene.

Introduction

The signal transducer and activator of transcription-3 (Stat3) is a cytoplasmic protein that is activated by cytokines and receptor tyrosine kinases, as well as the nonreceptor tyrosine kinase Src (reviewed in Yu and Jove, 2004, and Frank, 2007). In an unstimulated cell, Stat3 is latent in the cytoplasm. Subsequent to binding to an activated receptor through its Src homology 2 domain, Stat3 becomes activated through phosphorylation at a critical tyrosine (tyr705). This activates Stat3 by stabilizing the association of two monomers through reciprocal Src homology 2-phosphotyrosine interactions. The Stat3 dimer then migrates to the nucleus, where it binds to target sequences, leading to the transcriptional activation of specific genes that play a role in cell proliferation and survival, such as *myc*, cyclin D, *Bcl-xL*, survivin, hepatocyte growth factor (Hung and Elliott, 2001), and others (Yu and Jove, 2004). The investigation of the role of Stat3 in neoplasia gained momentum when it was found to be activated in a number of tumor cell lines and carcinomas (Germain and Frank, 2007). The fact that a constitutively active form of Stat3 alone is sufficient to induce transformation (Bromberg *et al.*, 1999) points to an etiological role for Stat3 in neoplasia.

Gap junctions are plasma membrane channels that enable the passage of small molecules between the interiors of adjacent cells. A reduction in gap junctional, intercellular communication (GJIC) is believed to lead to an increase in cell proliferation (reviewed in Vinken *et al.*, 2006). In fact, a number of oncogenes such as v-Src (Lin *et al.*, 2006), the polyoma virus middle tumor antigen (Azarnia and Loewenstein, 1987; Raptis *et al.*, 1994), the simian virus 40 large tumor antigen (Khoo *et al.*, 1998), Hsp90N (Grammatikakis *et al.*, 2002), and vRas (Brownell *et al.*, 1996a; Atkinson and Sheridan, 1988) have been shown to interrupt junctional communication. Interestingly, a loss of GJIC also accompanies the cessation of proliferation and differentiation of murine preadipocytes (Azarnia and Russell, 1985; Brownell *et al.*, 1996a; Anagnostopoulou *et al.*, 2007) and apoptosis in bovine lens epithelial cells and mouse fibroblasts (Theiss *et al.*, 2007). Gap junctions are formed by the connexin (Cx) family of proteins that consists of at least 20 members in mammals (Vinken *et al.*, 2006). Oncogenes such as Src phosphorylate Cx43, both directly and indirectly, leading to

[1]Departments of Microbiology and Immunology and Pathology, Queen's University, Kingston, Canada.
[2]Molecular Medicine, City of Hope National Medical Center, Duarte, California.
*These two authors contributed equally to this work.

GJIC suppression (reviewed in Pahujaa *et al.*, 2007). Despite the extensive literature on the effect of viral or cellular oncogenes upon GJIC, the effect of Stat3 upon GJIC is at present unknown.

We previously reported on a technique where GJIC of adherent cells can be examined by *in situ* electroporation: Cells are grown on two coplanar electrodes, consisting of glass coated with conductive indium-tin oxide (ITO) (Anagnostopoulou *et al.*, 2007). The electrodes are separated by a barrier that diverts the electric field, rendering it vertical to the cell layer. An electric pulse is applied in the presence of the tracking dye, Lucifer yellow (LY). The pulse causes the introduction of LY into the cells growing on the electrodes by opening transient pores on the membrane, and the subsequent migration of the dye to adjacent, nonelectroporated cells growing on uncoated glass is microscopically observed under fluorescence illumination. Dye transfer through gap junctions can be precisely quantitated in this way, simultaneously and in a large number of cells, without any detectable disturbance to cellular metabolism (reviewed in Raptis *et al.*, 2008). Although this technique is adequate for many adherent cell lines, cells at the edge of the electrodes, adjacent to the nonconductive area, receive slightly higher amounts of current, which could result in cellular damage. In addition, slight differences in adhesion and growth of the cells on bare glass, as opposed to ITO, might create artifacts. To overcome these problems, we modified the geometry of the slide, so that both electroporated and nonelectroporated cells grow on conductive ITO, while the electric field intensity is essentially uniform over the entire electroporated area. This technique was used to examine the role of Stat3 upon GJIC levels in rat liver epithelial cells. The results demonstrate that, unlike Ras inhibition (Ito *et al.*, 2006), Stat3 inhibition in cells expressing activated Src does not increase GJIC. On the contrary, inhibition of Stat3 activity in cells with extensive GJIC causes a dramatic reduction in junctional communication, concomitant with apoptosis induction. Therefore, Stat3's function is actually required for the maintenance of junctional permeability, although Stat3 generally promotes growth and in an activated form can act as an oncogene.

Materials and Methods

Cell lines and culture techniques

Cells were grown in Dulbecco's modified Eagle's medium (DMEM) supplemented with 10% fetal calf serum (ICN; Biomedicals, Costa Mesa, CA). T51B is a normal rat liver epithelial line. Src was activated in this line by stable expression of a construct expressing the middle tumor antigen of polyoma virus (line T51B-Src) (Royal *et al.*, 1996). Confluence was estimated visually and quantitated by imaging analysis of live cells under phase contrast using a Leitz Diaplan microscope and the MCID-elite software (Imaging Research, St. Catharines, Canada).

For Stat3 downregulation, cells grown to different densities were treated with 50 μM CPA7, and diluted in growth medium from a 20 mM stock in 50% DMSO for 24 h. Control cells were treated with the same amount of the DMSO carrier (0.00125%) alone; however, no effect of DMSO was noted upon the activity of Stat3 or GJIC at this concentration. Apoptosis was assessed by morphological observation and poly-ADP-ribose polymerase (PARP)–cleavage analysis. For a more precise quantitation, cells were fixed with ethanol and stained with propidium iodide, and the percentage of cells with a subG1 DNA content was assessed by fluorescence-activated cell sorting (FACS) analysis (Vultur *et al.*, 2004).

Examination of gap junctional communication

The setup is described in Figure 1. Cells are grown and electroporated on a glass slide (1), coated with conductive and transparent ITO (1a) with a surface resistivity of 20 Ω/square (Colorado Concept Coatings, Loveland, CO) (Tomai *et al.*, 1998). The ITO was etched to define electrode and nonconducting regions, which were electrically isolated from each other by removing the ITO coating in lines of ~20 μm wide from the glass surface. It was important to ensure that only the 800 Å coating was removed, without affecting the glass, so that cell growth would be unaffected across the line. This was achieved with a UV laser operating at a 355 nm wavelength using 1 W of output power with 60% of the energy delivered to the surface of the glass. The spot size was 20 μm across with a spot overlap of 90%. The beam was manipulated by mirrors on a pair of galvanometers to produce the desired pattern. Waverunner™ software were used to define the pattern and control the system (Nutfield Technology, Inc., Windham, NH).

To form the two electrodes, the ITO coating was removed in a straight line in the middle (2). A dam of nonconductive Teflon (3) was used to divert the current upward, thus creating a sharp transition in electric field intensity. To provide areas where the cells are not electroporated, the ITO was also etched in two rectangles (4 and 4a). Current flows inward from each contact point (5 and 5a), via a conductive highway between the rectangles (red arrows), spreading in a direction parallel to the middle barrier, then over the barrier (arrowheads [6]) to the other side, electroporating cells in areas (7 and 7a). A polypropylene chamber is bonded onto the slide, to form a container for the cells and LY (9). Cells were plated in the chamber, and 2 days after confluence the growth medium was replaced with calcium-free DMEM containing 5 mg/mL LY. The slide/chamber was placed into a holder where electrical contacts were established, and a set of electrical pulses delivered to the cells. Extensive experimentation indicated that eight pulse pairs, each pulse of 24 V peak value, 300 μs length, and spaced 0.5 s apart, with one of each pair having a polarity opposite to that of its partner gave optimal results. After a 5-min incubation at 37°C, the unincorporated dye was washed with calcium-free DMEM, and cells were observed and photographed under fluorescence and phase contrast illumination. To better pin-point the position of the edge of the electroporated area, cells were also observed and photographed under combined fluorescence and phase-contrast illumination. In this configuration, cells that acquired LY by electroporation (growing in 7 and 7a) and cells into which LY traveled through gap junctions (8 and 8a) both grow on ITO, separated only by a laser-etched line of ~20 μm (Fig. 1B, C). The equipment is available from Cell Projects Ltd. (Harrietsham, United Kingdom).

Lentivirus vector production

293T cells were plated at a density of 4×10^6 cells per 10-cm culture dish. The cells were cotransfected by calcium phos-

phate coprecipitation with 15 μg of pLKO1-Stat3 shRNA (Sigma, St. Louis, MO) and 10 μg of pPACK packaging plasmid mix (SBI, Mountain View, CA). The culture medium was replaced with fresh medium after 6 h. The supernatant was collected 16 h after the transfection and stored at −80°C. To determine the vector titers, 10^5 HT1080 cells were seeded in a six-well plate and infected with various dilutions of the vector in the presence of 4 μg/mL polybrene. The culture medium was replaced 48 h later with fresh medium containing puromycin at a concentration of 1.5 μg/mL. Puromycin-resistant colonies were counted 10 days after transduction. To examine the efficiency of Stat3 downregulation, cells were infected at 5 pfu/cell and extracts probed for total Stat3 (Cell Signalling). For GJIC examination, cells were plated in electroporation chambers and infected with 5 pfu/cell at densities of ~80%. Two days after confluence, cells were electroporated with LY for GJIC examination as described above.

Western blotting

Cells were grown to different densities, and proteins extracted as described before (Raptis *et al.*, 2000). Fifty micrograms of clarified cell extract was resolved on a 10% polyacrylamide-SDS gel and transferred to a nitrocellulose membrane (Bio-Rad, Hercules, CA). The membranes were probed with antibodies against the tyrosine-705 phosphorylated form of Stat3 (Cell Signalling, Cat.# 9131L, used at a dilution of 1:2000), against anti-Cx43 (BD-Transduction, Cat.#610061 used at a dilution of 1:250), or PARP (Roche, Basel, Switzerland; Cat.# 1 835 238, used at 1:1000), followed by secondary antibodies: alkaline phosphatase-conjugated goat anti-mouse antibody (Biosource, Cat.#AMI3405, for anti-Cx43 and Hsp90) or goat anti-rabbit antibody (Biosource, Cat. #ALI4405, for tyr705 phosphorylated form of Stat3 [Stat3-ptyr705] and PARP), both used at a 1:10,000 dilution. The bands were viewed using enhanced chemiluminescence, according to the manufacturer's instructions (PerkinElmer Life Sciences, Cat.# NEL602). As a control for protein loading, parallel blots were routinely probed with a mouse monoclonal anti-Hsp90 antibody (Stressgen, Cat.# SPA-830, used at 1:5000), followed by a secondary antibody and enhanced chemiluminescence detection as above.

Luciferase assays for Stat3 transcriptional activity

Cells were transfected with a Stat3-specific reporter plasmid (p*Luc*TKS3) that harbors seven copies of a sequence corresponding to the Stat3-specific binding site in the C-reactive gene promoter (termed APRE, TTCCCGAA) upstream from a firefly luciferase coding sequence (Turkson *et al.*, 1998) and the pRLSRE plasmid that contains two copies of the serum response element of the *c-fos* promoter, subcloned into the *Renilla* luciferase reporter, pRL-null (Turkson

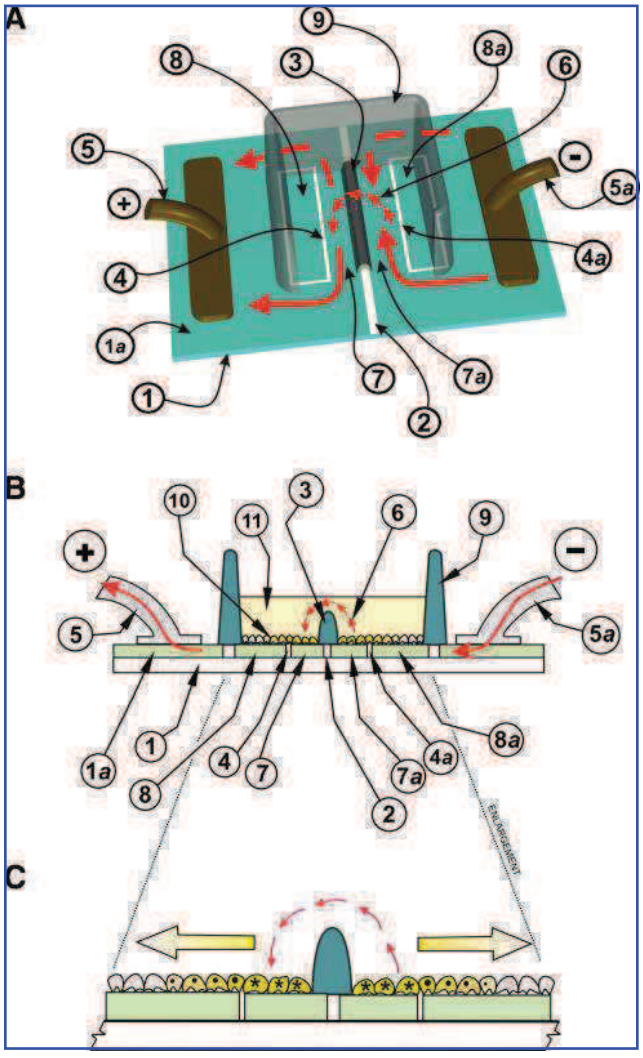

FIG. 1. The electroporation apparatus. (**A**) Top view. Cells are grown on a glass slide (1), coated with conductive and transparent indium-tin oxide (ITO, [1a]). The ITO coating is laser-etched in a straight line in the middle (2), essentially forming two electrodes. A dam of Teflon (3) is used to divert the current upward, thus creating a sharp transition in electric field intensity. To provide nonconductive areas, the ITO is also etched in two rectangles (4 and 4a). Current from a pulse generator flows inward from each contact point (5 and 5a), via a conductive highway between the rectangles (red arrows), spreading in a direction parallel to the middle barrier, then over the barrier (arrowheads [6]) to the other side, electroporating cells in areas 7 and 7a. A plastic chamber is bonded onto the slide, to form a container for the cells and Lucifer yellow (LY) (8). For clarity, the front part of the chamber is removed. (**B**) Side view. The slide (1) with the cells (10) growing on the ITO-coated (1a, light green) and etched bare glass regions (4 and 4a) is shown. When electroporation medium containing LY (11) is added to the chamber to a level above the height of the dam (3), an electrical path between the electrodes 7 and 7a and the cells (10) growing in this area is formed. Note that the ITO layer (1a) is shown with exaggerated thickness for clarity although its actual thickness (800 Å) is much less than the thickness of the cells. (**C**) The area of electroporated (7 and 7a) and nonelectroporated (8 and 8a) cells is shown enlarged. Stars denote cells (yellow) at the edge of the electroporated area that were loaded with LY by electroporation. Dots denote cells where the dye transferred through gap junctions. Large arrows show the direction of dye transfer through gap junctions. Note that the size and thickness of the cells are exaggerated for clarity. Color images available online at www.liebertonline.com/dna.

et al., 2001). Both luciferase activities were measured in total cell extracts according to the manufacturer's protocol (Promega, Cat. # E4030).

Results

Stat3 downregulation does not restore gap junctional communication in cells expressing activated Src

A body of evidence has indicated that the Src oncogene product downregulates gap junctional communication through a variety of mechanisms, including activation of the Ras/Raf/Mek/Erk pathway. As a result, inhibition of this pathway restores GJIC in vSrc-transformed cells (Ito *et al.*, 2006; Pahujaa *et al.*, 2007). Since Stat3 is also activated by and is required for transformation by vSrc (Turkson *et al.*, 1998), we used the rat liver epithelial line T51B transformed by activated Src (line T51B-Src) as a model to explore the possible role of Stat3 in suppressing gap junctional communication.

To examine gap junctional communication by *in situ* electroporation, it is important to be able to reliably distinguish cells that were loaded with LY by electroporation, from cells that received the dye from neighboring cells through gap junctions. That is, a sharp transition in electrical field intensity between electroporated and nonelectroporated areas must be established. This was achieved by etching the ITO in the pattern shown in Figure 1, and adding a dam to divert the electric field upward. To examine GJIC, cells were plated in the electroporation chambers (Fig. 1) and at 2 days postconfluence an electrical pulse was applied in the presence of the tracer, LY (see Materials and Methods). As shown in Figure 2, T51B cells have extensive GJIC (Fig. 2A, panels a and b), which is dramatically reduced after activated Src expression (Fig. 2B, panels a and b; Table 1).

To examine the effect of Stat3 downregulation, cells were treated with the platinum compound, CPA7, previously shown to be an effective Stat3 inhibitor (Turkson *et al.*, 2004; Littlefield *et al.*, 2008). The degree of Stat3 inactivation was assessed by probing Western blots with an antibody specific for the Stat3-ptyr705, as well as by measuring the reduction in Stat3 transcriptional activity. Since it was previously demonstrated that cell-to-cell adhesion dramatically activates Stat3 even in vSrc-transformed cells (Vultur *et al.*, 2004), tests were conducted at different densities; cells were plated in 3-cm Petri dishes at a confluence of 50%, and at different times thereafter, up to 5 days postconfluence, total protein extracts were probed for the Stat3-ptyr705 by Western blotting, using Hsp90 as a loading control (see Materials and Methods). To ensure that the growth medium was not depleted of nutrients, it was changed every day. As shown in Figure 3A, treatment of T51B-Src cells with 50 μM CPA7 for 24 h essentially eliminated Stat3-tyr705 phosphorylation at all cell densities examined (lanes 1–6 vs. 7–12). In addition, examination of Stat3 transcriptional activity in T51B-Src cells transfected with a luciferase gene construct under control of a Stat3-specific promoter (p*Luc*TKS3 plasmid; see Materials and Methods) revealed a dramatic decrease upon CPA7 treatment, while CPA7 did not affect Stat3-independent transcription from *c-fos*, serum response element promoter, indicating that this compound is selective for Stat3 (Fig. 3B) (Turkson *et al.*, 2004).

After Stat3 downregulation, GJIC was examined as above at 2 days postconfluence. Unexpectedly, the results showed that Stat3 inhibition did not reinstate GJIC in T51B-Src cells (Fig. 2B, panels c and d; Table 1). To further substantiate these findings, we downregulated Stat3 expression through infection with a lentivirus vector carrying an shRNA against Stat3 (sh-Stat3; see Materials and Methods). In addition, sh-Stat3 expression, which caused a reduction in Stat3-ptyr705 levels to 28% at all cell densities examined, did not increase GJIC (Fig. 2B, panels e and f; Table 1), in agreement with the CPA7 data. The above findings taken together indicate that, contrary to Ras, high Stat3 activity, which could be, at least in part, due to high Src activity levels, cannot be responsible for the lack of junctional communication in T51B-Src cells.

Stat3 is required for gap junctional communication

To further investigate whether Stat3 might, in fact, play a positive role upon gap junctional communication, we examined the effect of Stat3 inhibition in normal T51B cells that have extensive GJIC. Cells were plated in electroporation chambers and treated with 50 μM CPA7 or the DMSO carrier alone for 24 h, and gap junctional communication was examined through LY electroporation as above. Interestingly, the results showed that CPA7 treatment essentially abolished GJIC (Fig. 2A, panels c and d; Table 1). Similarly, reduction of Stat3 levels through infection with the sh-Stat3 lentivirus vector resulted in a dramatic reduction in GJIC in T51B cells (Fig. 2A, panels e and f; Table 1). The above data taken together reveal that, rather than increasing GJIC, Stat3 inhibition eliminates junctional permeability, indicating that Stat3 activity is required for gap junction function in normal epithelial cells that display extensive GJIC.

Stat3 inhibition leads to a reduction in Cx43 levels

Various reports showed that gap junction function is dependent upon cell-to-cell adhesion and the assembly of adherent junctions (Frenzel and Johnson, 1996; Wei *et al.*, 2005). Since the surface area of contact is expected to increase with cell density, we examined the effect of cell density upon the levels of Cx43, a widely expressed gap junction protein, in T51B cells. Cells were plated at a density of 50%, and at different times thereafter extracts were probed with an antibody against Cx43 (see Materials and Methods). The results revealed a dramatic increase in Cx43 levels, which plateaued at ~1–2 days after 100% confluence, indicating that cell-to-cell contact can cause a significant increase in Cx43 levels.

It was previously demonstrated that Cx43 has a short half-life (Beardslee *et al.*, 1998). To examine the effect of Stat3 inhibition upon Cx43 protein levels, lysates from T51B cells grown to different densities and treated with CPA7 were probed for Cx43 by Western blotting. As shown in Figure 4A (lanes 8–14), CPA7 treatment caused a dramatic reduction in Cx43 levels, at all densities examined, concomitant with GJIC reduction. These findings indicate that, besides GJIC, Stat3 activity is required for the maintenance of Cx43 levels as well.

Apoptosis of adherent cells causes cell rounding and a reduction in the area of cell to cell to contact. Since these morphological changes could affect GJIC, the cellular phenotype regarding apoptosis was examined after Stat3 inhibition. T51B cells were grown to 3 days postconfluence, and after Stat3 inhibition with CPA7, apoptosis was examined by PARP-cleavage analysis, and by examination of the percentage of cells with subG1 DNA content by FACS (see

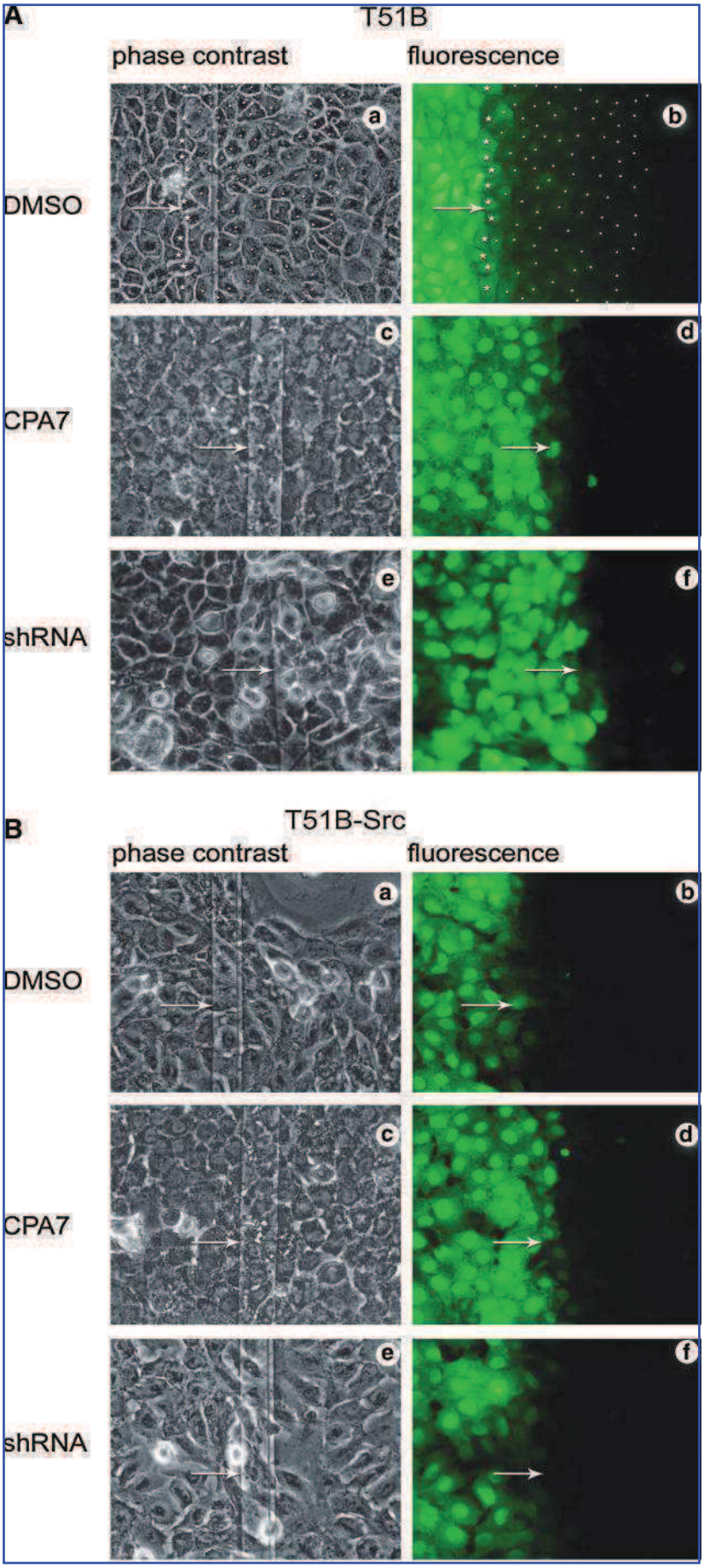

FIG. 2. (**A**) Stat3 downregulation eliminates gap junctional permeability in rat liver epithelial T51B cells. T51B cells were plated on conductive ITO-coated glass and LY electroporated after treatment with the DMSO carrier alone (**a**, **b**), or CPA7 (**c**, **d**), or infection with the sh-Stat3 lentiviral vector (**e**, **f**) (see Materials and Methods). After washing the unincorporated dye, cells from the same field were photographed under fluorescence (**b**, **d**, **f**) or phase contrast (**a**, **c**, **e**) illumination. Cells at the edge of the conductive area that were loaded with LY through electroporation were marked with a star (**a**, **b**), and cells at the nonelectroporated area that received LY through gap junctions were marked with a dot (Raptis *et al.*, 2006). Magnification, 240×. Note the extensive junctional communication in (**b**). (**B**) Stat3 downregulation does not increase gap junctional permeability in vSrc-transformed rat liver epithelial T51B cells. Same as above, T51B-Src cells. After pulse application, cells were photographed under phase contrast (**a**, **c**, **e**), or fluorescence (**b**, **d**, **f**) illumination. Magnification, 240×. Note the absence of communication, even after Stat3 downregulation (**d**, **f**). Color images available online at www.liebertonline.com/dna.

Table 1. Effect of Signal Transducer and Activator of Transcription-3 Downregulation upon Gap Junctional, Intercellular Communication

Cell line	*Treatment*[a]	*Stat3*[b] *(%)*	*GJIC*[c]	*Apoptosis % subG1*[d]
T51B	DMSO	52 ± 9	6.0 ± 2	2 ± 1
	CPA7	3 ± 2	0.2 ± 0.1	30 ± 11
	sh-Stat3	12 ± 3	0.9 ± 0.1	24 ± 9
T51B-Src	DMSO	100 ± 12	0.2 ± 0.1	5 ± 2
	CPA7	4 ± 1	0.1 ± 0.1	61 ± 12
	sh-Stat3	28 ± 3	0.1 ± 0.1	48 ± 14

[a]Cells were treated with 50 μM CPA7 or the DMSO carrier (0.00125%) for 24 h, or infected with a lentivirus vector expressing a Stat3-specific shRNA (see Materials and Methods).

[b]Stat3-ptyr705 levels were measured by Western blotting. Numbers represent relative values obtained by quantitation analysis, with the average of the values for v-Src-expressing T51B cells taken as 100%. Averages of at least three experiments ± SEM are shown. Data from sparsely growing cells are presented, but the relative increases were the same regardless of cell density (Vultur *et al.*, 2005). The transcriptional activity values obtained paralleled the Stat3-705 phosphorylation levels indicated (Fig. 3B; see Materials and Methods).

[c]GJIC was assessed by *in situ* electroporation 2 days after confluence, which was determined visually and by imaging analysis (Fig. 1; see Materials and Methods). Quantitation was achieved by dividing the number of cells into which dye had transferred through gap junctions (denoted by dots), by the number of cells at the edge of the electroporated area (denoted by stars, Fig. 2A, panels a and b). Numbers are averages of at least three experiments, where transfer from more than 200 cells was examined.

[d]After treatment, fixed cells were stained with propidium iodide and their subG1 profile was examined by fluorescence-activated cell sorting analysis (see Materials and Methods).

Materials and Methods). The results show that CPA7 treatment did result in an increase in PARP cleavage, indicating apoptosis (Fig. 4B). In addition, FACS analysis showed a substantial increase in cells with subG1 DNA content upon CPA7 treatment, or after infection with the sh-Stat3 lentivirus vector (Table 1). These findings indicate that Stat3 inhibition at high cell densities causes apoptosis, consistent with previous data regarding mouse fibroblasts and breast cancer lines (Anagnostopoulou *et al.*, 2006a, 2006b), and hint at a possible link between GJIC reduction and apoptosis induced by Stat3 inhibition.

Discussion

Results from a number of labs indicated that, constitutively active forms of Ras can suppress GJIC (Atkinson and Sheridan, 1988; Brownell *et al.*, 1996a). Moreover, this reduction in junctional permeability could be effected at lower levels than the levels required for full neoplastic conversion by this oncogene (Brownell *et al.*, 1997). Similarly, oncogenes such as the activated form of the Hsp90 chaperone, Hsp90N, which can activate the Raf protooncogene product, although unable to fully transform, can eliminate junctional permeability in normal rat F111 fibroblasts (Grammatikakis *et al.*, 2002), which stresses the role of oncogenes as GJIC suppressors. The prototype oncogene vSrc also suppresses GJIC, through direct phosphorylation of Cx43 at tyr247 and tyr265 (Lampe and Lau, 2004; Warn-Cramer and Lau, 2004), or indirectly through activation of the Protein kinase C or the Ras/Raf/Mek/Erk pathways (Zhou *et al.*, 1999; Lampe *et al.*, 2000; Shah *et al.*, 2002; Bao *et al.*, 2004; Griner and Kazanietz, 2007). It was further demonstrated that the suppression of gap junctional permeability by vSrc or middle tumor antigen, an oncogene whose function depends upon binding to and activation of cSrc (Dilworth, 2002), requires cRas signaling (Brownell *et al.*, 1996b), and independent from Erk action

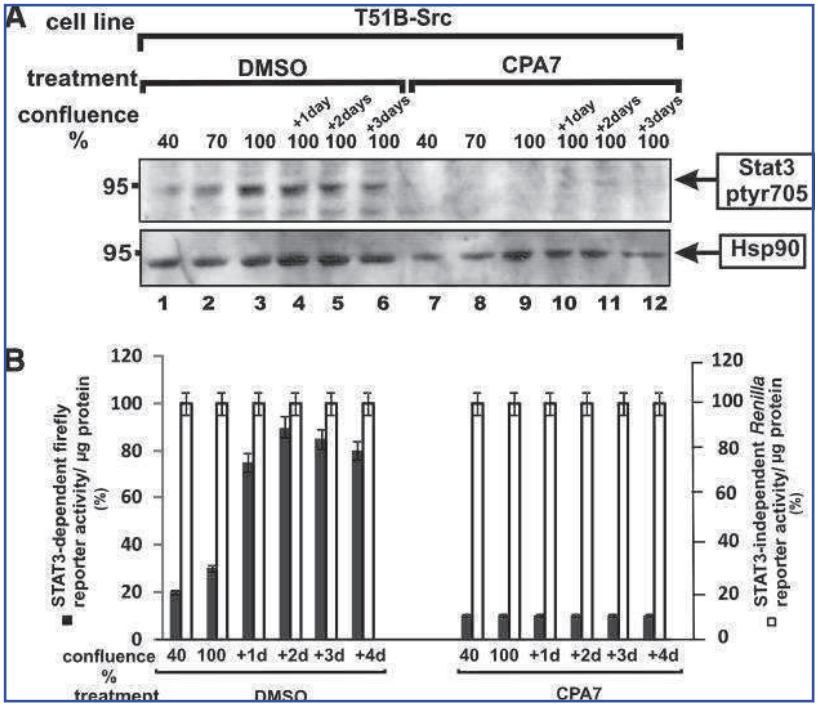

FIG. 3. CPA7 treatment eliminates Stat3-tyr705 phosphorylation and transcriptional activity in T51B-Src cells. (**A**) T51B-Src cells were grown to different densities from 40% confluence to 3 days postconfluence as indicated and treated with 50 μM CPA7 (lanes 7–12) or the DMSO carrier alone (0.00125%, lanes 1–7) for 24 h, at which time cell extracts were probed for Stat3-ptyr705 or Hsp90 as a loading control. (**B**) T51B-Src cells were transfected with a plasmid expressing a firefly luciferase gene under control of a Stat3 responsive promoter (■), and a Stat3 independent promoter driving a *Renilla* luciferase gene (□) (see Materials and Methods). After transfection, cells were plated to different densities and treated with CPA7 or the DMSO carrier alone for 24 h, at which time firefly and *Renilla* luciferase activities were determined.

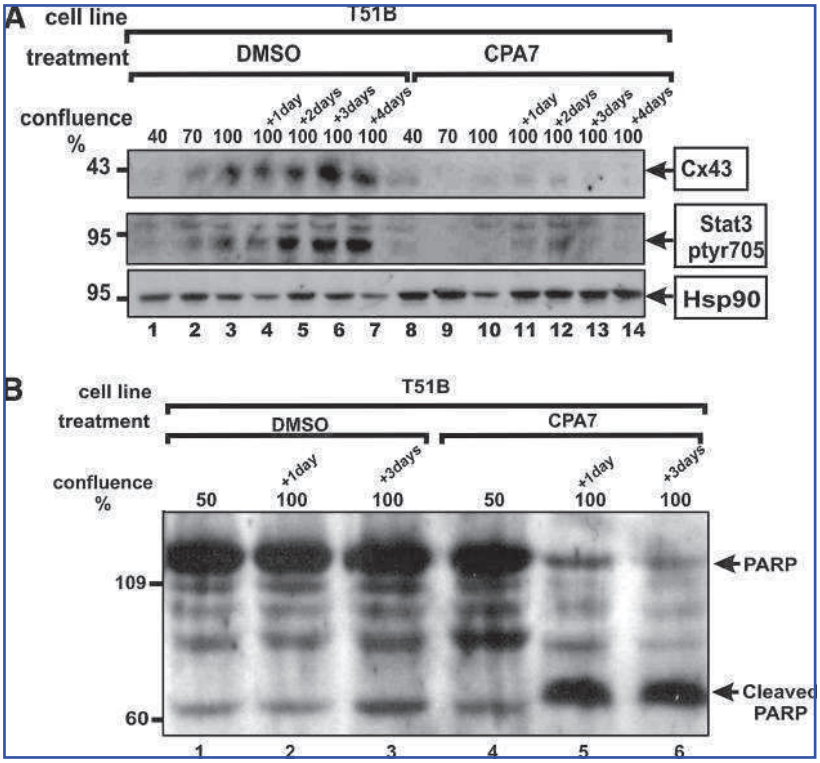

FIG. 4. (**A**) Stat3 inhibition reduces Cx43 levels. T51B cells were plated in 3-cm Petri dishes, grown to different densities and treated with CPA7 (lanes 8–14) or the DMSO carrier (0.00125%) alone (lanes 1–7), as indicated. Cell extracts were probed for Cx43 (top), Stat3 (middle), or Hsp90 as a loading control. Arrows point to the position of Cx43, Stat3-ptyr705, or Hsp90, respectively. (**B**) PARP-cleavage analysis: to assess apoptosis induction, T51B cells were grown to different densities and treated with CPA7 (lanes 4–6) or the DMSO carrier (0.00125%) alone (lanes 1–3) as indicated, and cell extracts probed with an antibody to PARP. Arrows point to the position of PARP (113 kDa) and cleaved PARP (89 kDa), respectively.

(Ito *et al.*, 2006). Since the Ras and Stat3 pathways are often coordinately regulated by growth factors or oncogenes, we looked for a possible role of Stat3 in the suppression of junctional communication. Unexpectedly, our findings indicated that, contrary to Ras downregulation, Stat3 inhibition does not restore junctional permeability in T51B cells transformed by activated Src. On the contrary, our results revealed that Stat3 inhibition eliminated GJIC in normal fibroblasts and epithelial cells that have extensive GJIC. These findings stress the role of Stat3 as a positive regulator of gap junctional communication. This is in sharp contrast to the effect of cRas, which was shown to cause gap junction closure in normal fibroblasts (Brownell *et al.*, 1996a). Therefore, Src has a dual role upon GJIC—acting as an inhibitor through direct or indirect phosphorylation of Cx43, and an activator through activation of Stat3. In the presence of high Src activity the former prevails, so that the net effect is gap junction closure.

Besides its role in promoting growth, Stat3 activates a number of antiapoptotic genes, such as survivin (Gritsko *et al.*, 2006), *Bcl-xL*, and *Mcl-1* (Yu and Jove, 2004). Apoptotic death is accompanied by dramatic shape changes, such as rounding, which force the cell to give up all its intercellular contacts, including the gap junctions. In fact, it was recently demonstrated that induction of apoptosis by cycloheximide, etoposide, or puromycin led to a rapid loss of cell coupling, most probably due to caspase-3-mediated degradation of Cx43, in primary bovine lens epithelial cells and NIH3T3 fibroblasts (Theiss *et al.*, 2007). Our results show that Stat3 inhibition, which in densely growing cells induces apoptosis (Anagnostopoulou *et al.*, 2006a), results in a dramatic reduction in Cx43 levels and GJIC, which is consistent with the above observations. In any event, our findings demonstrate that the function of Stat3, although it is generally growth promoting and in an activated form can act as an oncogene, is actually required for the maintenance of junctional permeability. The interruption of gap junctional communication upon Stat3 inhibition would therefore confine the apoptotic event to single cells, and this might be essential for the maintenance of tissue integrity.

Acknowledgments

We would like to thank Dr. Mike Baird and Shalyn Littlefield for CPA7 synthesis, the Center for Manufacturing of Advanced Ceramics and Nanomaterials of Queen's University for laser etching services, Dr. Elissavet Kardami for a generous gift of Cx43 antibody, and Kevin Firth, P.Eng., Ask Sciences products, Kingston, Ontario, for engineering design. The financial assistance of the Canadian Institutes of Health Research, the Canadian Breast Cancer Foundation (Ontario Chapter), the Natural Sciences and Engineering Research Council of Canada, the Canadian Breast Cancer Research Alliance, the Ontario Centers of Excellence, the Breast Cancer Action Kingston, and the Clare Nelson bequest fund through grants to LR is gratefully acknowledged. RA was supported by a Canada Graduate Scholarships Doctoral award from the Canadian Institutes of Health Research, an Ontario Women's Health Scholars Award from the Ontario Council on Graduate Studies, and a Queen's University Graduate Award. AV was supported by studentships and a postdoctoral fellowship from NSERC, the Ontario Graduate Studentship Program, and a Queen's University Graduate Award. MG was supported by postdoctoral fellowships from the U.S. Army Breast Cancer Program and from the Ministry of Research and Innovation of the Province of Ontario and the Advisory Research Committee of Queen's University. AA was supported by a traineeship from the U.S. Army Breast Cancer Program.

Disclosure Statement

The authors do not have any conflict of interest.

References

Anagnostopoulou, A., Cao, J., Vultur, A., Firth, K.L., and Raptis, L. (2007). Examination of gap junctional, intercellular communication by *in situ* electroporation on two co-planar indium-tin oxide electrodes. Mol Oncol **1,** 226–231.

Anagnostopoulou, A., Vultur, A., Arulanandam, R., Cao, J., Turkson, J., Jove, R., Kim, J.S., Glenn, M., Hamilton, A.D., and Raptis, L. (2006a). Differential effects of Stat3 inhibition in sparse vs confluent normal and breast cancer cells. Cancer Lett **242,** 120–132.

Anagnostopoulou, A., Vultur, A., Arulanandam, R., Cao, J., Turkson, J., Jove, R., Kim, J.S., Glenn, M., Hamilton, A.D., and Raptis, L. (2006b). Role of Stat3 in normal and SV40 transformed cells. Trends in Cancer Res **2,** 93–103.

Atkinson, M.M., and Sheridan, J.D. (1988). Altered junctional permeability between cells transformed by v-ras, v-mos, or v-src. Am J Physiol **255,** C674–C683.

Azarnia, R., and Loewenstein, W.R. (1987). Polyomavirus middle t antigen downregulates junctional cell-to-cell communication. Mol Cell Biol **7,** 946–950.

Azarnia, R., and Russell, T.R. (1985). Cyclic AMP effects on cell-to-cell junctional membrane permeability during adipocytic differentiation of 3T3-L1 fibroblasts. J Cell Biol **100,** 265–269.

Bao, X., Reuss, L., and Altenberg, G.A. (2004). Regulation of purified and reconstituted connexin 43 hemichannels by protein kinase C-mediated phosphorylation of Serine 368. J Biol Chem **279,** 20058–20066.

Beardslee, M.A., Laing, J.G., Beyer, E.C., and Saffitz, J.E. (1998). Rapid turnover of connexin43 in the adult rat heart. Circ Res **83,** 629–635.

Bromberg, J.F., Wrzeszczynska, M.H., Devgan, G., Zhao, Y., Pestell, R.G., Albanese, C., and Darnell, J.E., Jr. (1999). Stat3 as an oncogene. Cell **98,** 295–303.

Brownell, H.L., Narsimhan, R., Corbley, M.J., Mann, V.M., Whitfield, J.F., and Raptis, L. (1996a). Ras is involved in gap junction closure in mouse fibroblasts or preadipocytes but not in differentiated adipocytes. DNA Cell Biol **15,** 443–451.

Brownell, H.L., Whitfield, J.F., and Raptis, L. (1996b). Cellular Ras partly mediates gap junction closure by the polyoma virus middle tumor antigen. Cancer Lett **103,** 99–106.

Brownell, H.L., Whitfield, J.F., and Raptis, L. (1997). Elimination of intercellular junctional communication requires lower Ras^{leu61} levels than stimulation of anchorage-independent proliferation. Cancer Detect Prev **21,** 289–294.

Dilworth, S.M. (2002). Polyoma virus middle T antigen and its role in identifying cancer-related molecules. Nat Rev Cancer **2,** 951–956.

Frank, D.A. (2007). Stat3 as a central mediator of neoplastic cellular transformation. Cancer Lett **251,** 199–210.

Frenzel, E.M., and Johnson, R.G. (1996). Gap junction formation between cultured embryonic lens cells is inhibited by antibody to N-cadherin. Dev Biol **179,** 1–16.

Germain, D., and Frank, D.A. (2007). Targeting the cytoplasmic and nuclear functions of signal transducers and activators of transcription 3 for cancer therapy. Clin Cancer Res **13,** 5665–5669.

Grammatikakis, N., Vultur, A., Ramana, C.V., Siganou, A., Schweinfest, C.W., and Raptis, L. (2002). The role of Hsp90N, a new member of the Hsp90 family, in signal transduction and neoplastic transformation. J Biol Chem **277,** 8312–8320.

Griner, E.M., and Kazanietz, M.G. (2007). Protein kinase C and other diacylglycerol effectors in cancer. Nat Rev Cancer **7,** 281–294.

Gritsko, T., Williams, A., Turkson, J., Kaneko, S., Bowman, T., Huang, M., Nam, S., Eweis, I., Diaz, N., Sullivan, D., Yoder, S., Enkemann, S., Eschrich, S., Lee, J.H., Beam, C.A., Cheng, J., Minton, S., Muro-Cacho, C.A., and Jove, R. (2006). Persistent activation of Stat3 signaling induces survivin gene expression and confers resistance to apoptosis in human breast cancer cells. Clin Cancer Res **12,** 11–19.

Hung, W., and Elliott, B. (2001). Co-operative effect of c-Src tyrosine kinase and Stat3 in activation of hepatocyte growth factor expression in mammary carcinoma cells. J Biol Chem **276,** 12395–12403.

Ito, S., Ito, Y., Senga, T., Hattori, S., Matsuo, S., and Hamaguchi, M. (2006). v-Src requires Ras signaling for the suppression of gap junctional intercellular communication. Oncogene **25,** 2420–2424.

Khoo, N.K., Zhang, Y., Bechberger, J.F., Bond, S.L., Hum, K., and Lala, P.K. (1998). SV40 tag transformation of the normal invasive trophoblast results in a premalignant phenotype. II. Changes in gap junctional intercellular communication. Int J Cancer **77,** 440–448.

Lampe, P.D., and Lau, A.F. (2004). The effects of connexin phosphorylation on gap junctional communication. Int J Biochem Cell Biol **36,** 1171–1186.

Lampe, P.D., Tenbroek, E.M., Burt, J.M., Kurata, W.E., Johnson, R.G., and Lau, A.F. (2000). Phosphorylation of connexin43 on serine368 by protein kinase C regulates gap junctional communication. J Cell Biol **149,** 1503–1512.

Lin, R., Martyn, K.D., Guyette, C.V., Lau, A.F., and Warn-Cramer, B.J. (2006). v-Src tyrosine phosphorylation of connexin43: regulation of gap junction communication and effects on cell transformation. Cell Commun Adhes **13,** 199–216.

Littlefield, S.L., Baird, M.C., Anagnostopoulou, A., and Raptis, L. (2008). Synthesis, characterization and Stat3 inhibitory properties of the prototypical platinum(IV) anticancer drug, [PtCl3(NO2)(NH3)2] (CPA-7). Inorg Chem **47,** 2798–2804.

Pahujaa, M., Anikin, M., and Goldberg, G.S. (2007). Phosphorylation of connexin43 induced by Src: regulation of gap junctional communication between transformed cells. Exp Cell Res **313,** 4083–4090.

Raptis, L., Brownell, H.L., Firth, K.L., and Mackenzie, L.W. (1994). A novel technique for the study of intercellular, junctional communication; electroporation of adherent cells on a partly conductive slide. DNA Cell Biol **13,** 963–975.

Raptis, L., Brownell, H.L., Vultur, A.M., Ross, G., Tremblay, E., and Elliott, B.E. (2000). Specific inhibition of growth factor-stimulated ERK1/2 activation in intact cells by electroporation of a Grb2-SH2 binding peptide. Cell Growth Differ **11,** 293–303.

Raptis, L., Vultur, A., Brownell, H.L., and Firth, K.L. (2006). Dissecting pathways; *in situ* electroporation for the study of signal transduction and gap junctional communication. In *Cell Biology: A Laboratory Handbook*, Volume 2, Chapter 44. J.E. Celis, ed. (Elsevier Academic Press, Burlington, MA), pp. 341–354.

Raptis, L., Vultur, A., Brownell, H.L., Tomai, E., Anagnostopoulou, A., Arulanandam, R., Cao, J., and Firth, K.L. (2008). Electroporation of adherent cells *in situ* for the study of signal transduction and gap junctional communication. In *Electroporation Protocols*, Chapter 12. S. Li, ed. (The Humana Press Inc., Totowa, NJ), pp. 167–183.

Royal, I., Raptis, L., Druker, B.J., and Marceau, N. (1996). Downregulation of cytokeratin 14 gene expression by the polyoma virus middle T antigen is dependent on c-src association but independent of full transformation in rat liver nonparenchymal epithelial cells. Cell Growth Differ **7,** 737–743.

Shah, M.M., Martinez, A.M., and Fletcher, W.H. (2002). The connexin43 gap junction protein is phosphorylated by protein kinase A and protein kinase C: *in vivo* and *in vitro* studies. Mol Cell Biochem **238,** 57–68.

Theiss, C., Mazur, A., Meller, K., and Mannherz, H.G. (2007). Changes in gap junction organization and decreased coupling during induced apoptosis in lens epithelial and NIH-3T3 cells. Exp Cell Res **313,** 38–52.

Tomai, E., Brownell, H.L., Tufescu, T., Reid, K., Raptis, S., Campling, B.G., and Raptis, L. (1998). A functional assay for intercellular, junctional communication in cultured human lung carcinoma cells. Lab Invest **78,** 639–640.

Turkson, J., Bowman, T., Garcia, R., Caldenhoven, E., De Groot, R.P., and Jove, R. (1998). Stat3 activation by Src induces specific gene regulation and is required for cell transformation. Mol Cell Biol **18,** 2545–2552.

Turkson, J., Ryan, D., Kim, J.S., Zhang, Y., Chen, Z., Haura, E., Laudano, A., Sebti, S., Hamilton, A.D., and Jove, R. (2001). Phosphotyrosyl peptides block Stat3-mediated DNA binding activity, gene regulation, and cell transformation. J Biol Chem **276,** 45443–45455.

Turkson, J., Zhang, S., Palmer, J., Kay, H., Stanko, J., Mora, L.B., Sebti, S., Yu, H., and Jove, R. (2004). Inhibition of constitutive signal transducer and activator of transcription 3 activation by novel platinum complexes with potent antitumor activity. Mol Cancer Ther **3,** 1533–1542.

Vinken, M., Vanhaecke, T., Papeleu, P., Snykers, S., Henkens, T., and Rogiers, V. (2006). Connexins and their channels in cell growth and cell death. Cell Signal **18,** 592–600.

Vultur, A., Arulanandam, R., Turkson, J., Niu, G., Jove, R., and Raptis, L. (2005). Stat3 is required for full neoplastic transformation by the Simian Virus 40 Large Tumor antigen. Mol Biol Cell **16,** 3832–3846.

Vultur, A., Cao, J., Arulanandam, R., Turkson, J., Jove, R., Greer, P., Craig, A., Elliott, B.E., and Raptis, L. (2004). Cell to cell adhesion modulates Stat3 activity in normal and breast carcinoma cells. Oncogene **23,** 2600–2616.

Warn-Cramer, B.J., and Lau, A.F. (2004). Regulation of gap junctions by tyrosine protein kinases. Biochim Biophys Acta **1662,** 81–95.

Wei, C.J., Francis, R., Xu, X., and Lo, C.W. (2005). Connexin43 associated with an N-cadherin-containing multiprotein complex is required for gap junction formation in NIH3T3 cells. J Biol Chem **280,** 19925–19936.

Yu, H., and Jove, R. (2004). The STATs of cancer—new molecular targets come of age. Nat Rev Cancer **4,** 97–105.

Zhou, L., Kasperek, E.M., and Nicholson, B.J. (1999). Dissection of the molecular basis of pp60(v-src) induced gating of connexin 43 gap junction channels. J Cell Biol **144,** 1033–1045.

Address correspondence to:
Leda Raptis, Ph.D.
Departments of Microbiology and Immunology and Pathology
Queen's University
Botterell Hall, Stuart St. 18
K7L3N6 Kingston, Ontario
Canada

E-mail: raptisl@queensu.ca

Received for publication November 14, 2008; received in revised form January 26, 2009; accepted April 6, 2009.

This article has been cited by:

1. M. Geletu, R. Arulanandam, S. Chevalier, B. Saez, L. Larue, H. Feracci, L. Raptis. 2013. Classical cadherins control survival through the gp130/Stat3 axis. *Biochimica et Biophysica Acta (BBA) - Molecular Cell Research* . [CrossRef]
2. Mulu Geletu, Rozanne Arulanandam, Samantha Greer, Aaron Trotman-Grant, Evangelia Tomai, Leda Raptis. 2012. Stat3 is a positive regulator of gap junctional intercellular communication in cultured, human lung carcinoma cells. *BMC Cancer* **12**:1, 605. [CrossRef]
3. Samantha Greer, Rice Honeywell, Mulu Geletu, Rozanne Arulanandam, Leda Raptis. 2010. Housekeeping genes; expression levels may change with density of cultured cells. *Journal of Immunological Methods* **355**:1-2, 76-79. [CrossRef]
4. Rozanne Arulanandam, Mulu Geletu, Hélène Feracci, Leda Raptis. 2010. Activated Rac1 requires gp130 for Stat3 activation, cell proliferation and migration. *Experimental Cell Research* **316**:5, 875-886. [CrossRef]

Journal of Immunological Methods 355 (2010) 76–79

Contents lists available at ScienceDirect

Journal of Immunological Methods

journal homepage: www.elsevier.com/locate/jim

Technical note

Housekeeping genes; expression levels may change with density of cultured cells

Samantha Greer [1], Rice Honeywell [1], Mulu Geletu, Rozanne Arulanandam, Leda Raptis *

Department of Microbiology and Immunology, Queen's University, Kingston, Ontario, Canada K7L 3N6
Department of Pathology and Molecular Medicine, and Queen's University Cancer Institute, Queen's University, Kingston, Ontario, Canada K7L 3N6

ARTICLE INFO

Article history:
Received 9 September 2009
Received in revised form 5 February 2010
Accepted 10 February 2010
Available online 19 February 2010

Keywords:
α-tubulin
GAPDH
Hsp90
β-actin
Gel electrophoresis
Cell confluence

ABSTRACT

Western blotting is a powerful technique to characterize a multitude of cellular proteins. As an internal control, the blots are commonly probed for "housekeeping" gene products. In this communication, we show that cell confluence significantly affects the levels of two such widely used proteins, α-tubulin and Glyceraldehyde-3-Phosphate Dehydrogenase. On the other hand the levels of heat-shock protein-90 and β-actin remained unchanged at a wide range of cell densities, making these proteins into more reliable loading controls.

1. Introduction

Western immunoblotting is a powerful technique to detect and characterize a multitude of proteins. Since the first trials in 1979 (Towbin et al., 1979), Western blotting methods have been used extensively to examine protein levels in different cells or tissues (Kurien and Scofield, 2003). Proteins are usually resolved by sodium-dodecylsulphate-polyacrylamide gel electrophoresis (SDS-PAGE) at first, then transferred electrophoretically to a membrane. The subsequent detection of the membrane-bound proteins using specific antibodies has evolved into a powerful tool for cell biology. The experimental protocol invariably involves the comparison of levels of a given protein or its modifications under study between different cell preparations. For this reason, it is necessary to ensure that all lanes of the gel were loaded with equal amounts of total protein and this can be achieved by determining protein concentrations in the cell lysates. However, as an internal control, and to take protein degradation into account, it is also necessary to probe for a protein which is not expected to change with the different conditions ("housekeeping" gene product). In fact, antibodies to a number of such proteins have been commercially developed. Most are also very abundant proteins in the cell, such as β-actin, heat-shock protein-90 (Hsp90), Glyceraldehyde-3-Phosphate Dehydrogenase (GAPDH) and α-tubulin, to name a few.

Cells in normal tissues or in tumors have extensive opportunities for adhesion to their neighbors in a three-dimensional organization. This is reproduced *in vitro* by culturing cells in dishes to high densities; such dense cultures, albeit only two dimensional, may in part mimic some of the physiological signals that occur *in vivo*. In fact, cell to cell adhesion in cultured, normal epithelial cells and fibroblasts triggers an increase in activity of the Rac1 and Cdc42, Rho family GTPases (Etienne-Manneville and Hall, 2002), which plateaus at a confluence of ~90%. Rac1/Cdc42, in turn, were found to cause a dramatic increase in the phosphorylation of the Signal transducer and activator of transcription-3 at tyr705 (Stat3-ptyr705) (Arulanandam et al., 2009). The peak is usually at 1–

* Corresponding author. Department of Microbiology and Immunology, Queen's University Botterell Hall, Rm. 713 Kingston, Ontario Canada K7L3N6. Tel.: +1 613 533 2462; fax: +1 613 533 6796.
E-mail address: raptisl@queensu.ca (L. Raptis).
[1] The first two authors contributed equally to this work.

0022-1759/$ – see front matter © 2010 Elsevier B.V. All rights reserved.
doi:10.1016/j.jim.2010.02.006

2 days after confluence, depending upon the cells' growth rate (Vultur et al., 2004; Raptis et al., 2009). In such experiments, it is important to employ a gene product whose levels are not affected by cell density, as a control for protein loading.

In our search for a suitable marker, we examined the effect of cell density upon the levels of a number of commonly used housekeeping gene products. The results showed that the levels of GAPDH and α-tubulin increased gradually with cell density starting at 10% confluence and plateauing at ~90%. Hsp90 and β-actin levels on the other hand did not change with cell density, from 10% confluence up to 5 days after confluence, indicating that these proteins may be appropriate controls. This is the first report on the effect of density of cultured cells upon the levels of certain commonly used, housekeeping gene products.

2. Materials and methods

2.1. Cell growth, protein extraction, and Western blotting

Mouse NIH3T3 fibroblasts (subclone DL+10) were previously described (Vultur et al., 2004). They were grown to different densities in Dulbecco's modification of Eagle's medium supplemented with 5% calf serum. Cells were scraped with a rubber policeman into 1.8 mL microcentrifuge tubes, washed with cold phosphate-buffered saline (PBS) and the cell pellet resuspended in the different extraction buffers. Three buffers were used: NP-40 [50 mM Hepes pH 7.4, 150 mM NaCl, 10 mM EDTA, 10 mM $Na_4P_2O_7$, 1% NP-40, 100 mM NaF, 2 mM Na_3VO_4, 0.5 mM phenylmethylsulphonyl fluoride (PMSF), 10 μg/mL aprotinin, 10 μg/mL leupeptin], radioimmunoassay precipitation assay buffer [RIPA, 150 mM NaCl, 1% NP-40, 50 mM Tris, pH 8.0, 0.5% sodium deoxycholate, 0.1% sodium dodecyl sulphate (SDS), 5 mM NaF, 2 mM Na_3VO_4, 1.25 mM PMSF, 10 μg/mL aprotinin, 10 μg/mL leupeptin] and SDS buffer [1% SDS, 10 mM ethylene-diaminetetraacetic acid, 80 mM Tris, pH 8.1, 5 mM NaF, 2 mM Na_3VO_4, 1.25 mM PMSF, 10 μg/mL aprotinin, 10 μg/mL leupeptin]. To optimize protein quantitation, the amount of extraction buffer was proportional to cell numbers, 100 μL/10^6 cells. Following extraction, NP-40 and RIPA lysates were clarified by centrifugation. SDS extracts on the other hand were passed through a syringe to break up the DNA and liquefy the preparation. Protein determination followed on clarified

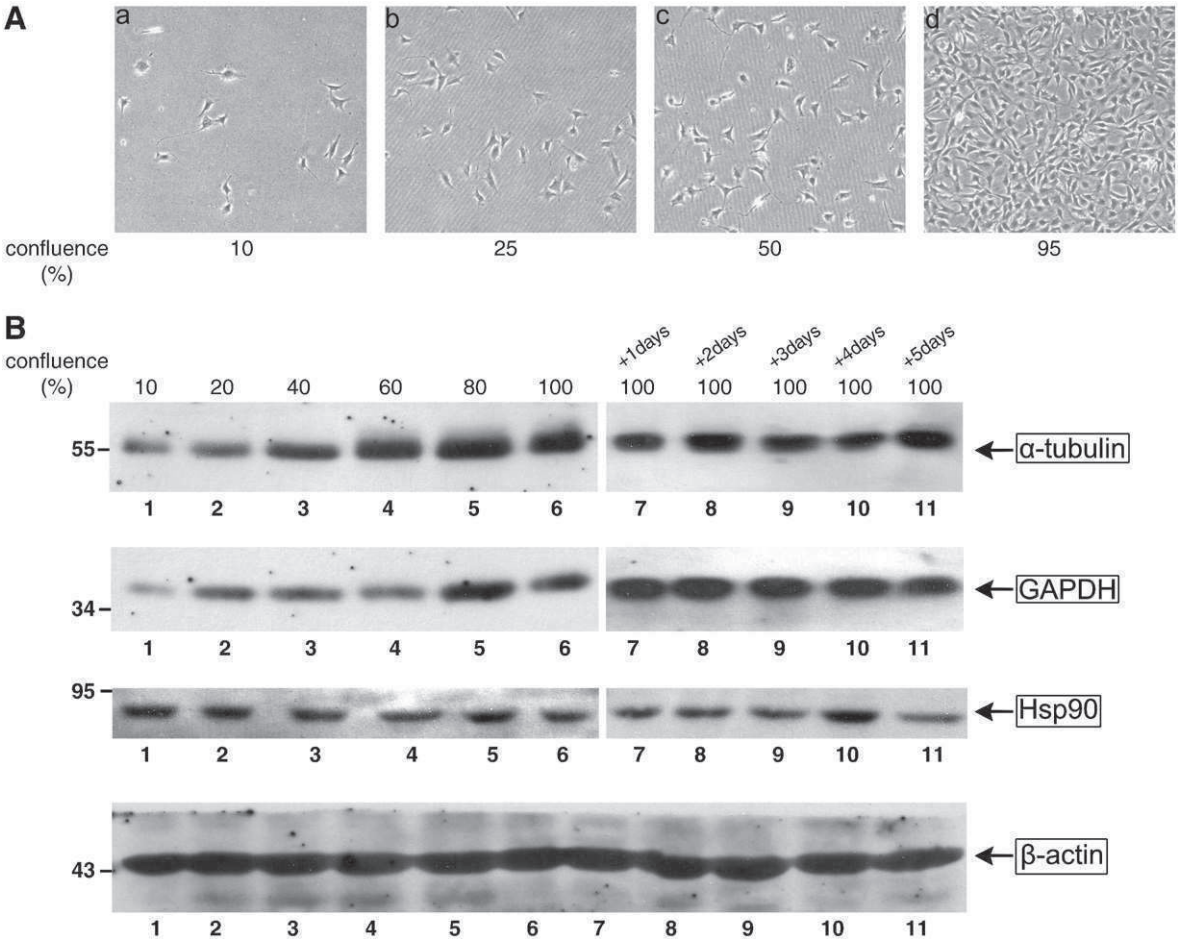

Fig. 1. α-tubulin and GAPDH levels increase with cell density, while Hsp90 and β-actin levels remain unaffected. A. NIH3T3 fibroblasts grown to the indicated confluences were photographed under phase-contrast illumination. Magnification: 140×. B. RIPA extracts from NIH3T3 cells grown to different densities were resolved by gel electrophoresis and blots probed for α-tubulin, GAPDH, Hsp90 or β-actin, as indicated. Numbers at the left refer to molecular weight markers. 30 μg total protein were loaded per lane.

extracts and 30 μg protein from each preparation were loaded onto SDS-PAGE gels. Lysates were clarified by centrifugation (10,000 *g*, 20 min) and protein determination conducted using the bicinchoninic acid kit (Sigma, Cat.# BCA1-1KT) for the NP-40 or RIPA extracts or the *DC* protein assay kit II (Bio-Rad, Cat.# 500-0112) for the SDS extracts. Proteins were resolved by SDS-PAGE and electrophoretically transferred to a nitrocellulose membrane (Bio-Rad). Blots were probed with antibodies to α-tubulin (Cell Signaling, Cat.# 2125), GAPDH (Cell Signaling, Cat.# 2118), Hsp90 (Stressgen, Cat.# SPA-830) and β-actin (Biovision, Cat.# 3598-199), followed by alkaline phosphatase-conjugated secondary antibodies and ECL reagents, according to the manufacturer's protocols (Biosource, Pierce). Bands were visualized using enhanced chemiluminescence (PerkinElmer Life Sciences, Cat.# NEL602), or SuperSignal West Femto Maximum Sensitivity Substrate (Pierce, Cat.# 34095). Quantitation was achieved by fluorimager analysis using the FluorChem program (AlphaInnotech Corp.).

3. Results and discussion

Mouse NIH3T3 fibroblasts were grown in tissue culture dishes at different densities, ranging from 10% confluence to 5 days after 100% confluence (Fig. 1A). To eliminate any effects of extraction efficiency differences, we used three commonly employed lysis buffers. In initial experiments, cells were lysed directly on the plate and protein determination conducted on extracts clarified by centrifugation. However, significant amounts of serum proteins (mainly bovine serum albumin) present in the growth medium were found to attach non-specifically to the plastic tissue culture dish and be eluted with the detergent-containing extraction buffer. The amounts were found to vary from 2.22 μg/cm^2 to 9.46 μg/cm^2 for cells grown in 5% calf serum, and they could disturb the determination of protein concentration in the lysate significantly, especially at lower cell densities. To avoid this problem, cells were scraped in ice-cold PBS, transferred into microcentrifuge tubes, washed once in PBS and the extraction

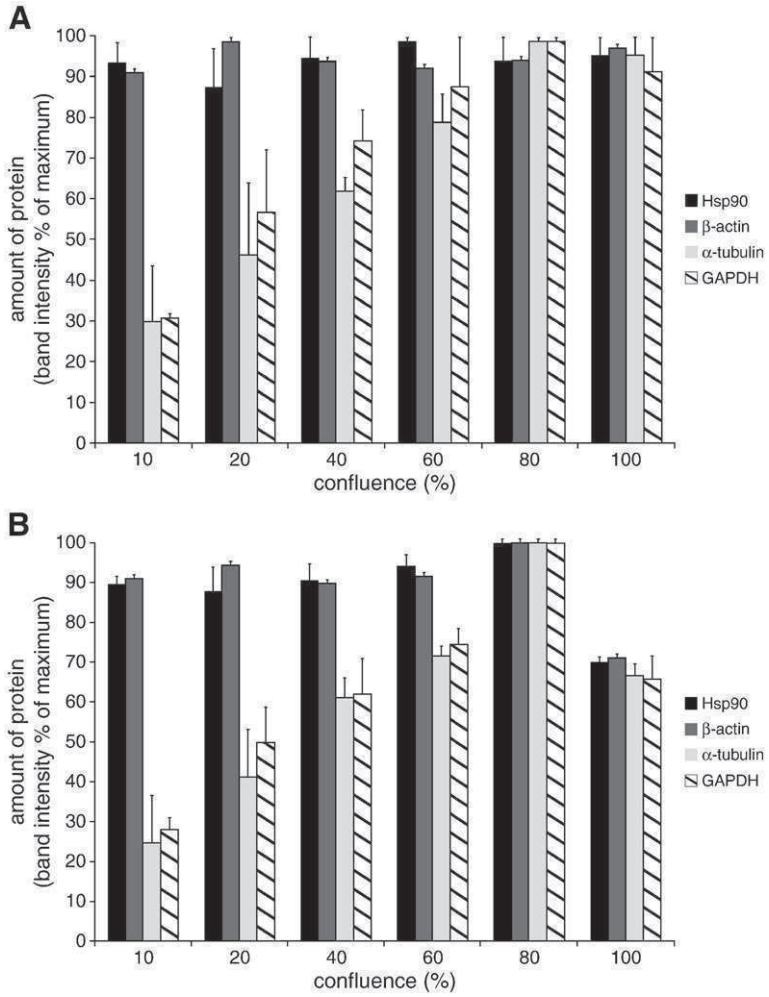

Fig. 2. Quantitation of protein levels at different densities. A. The results of quantitation of band intensity of the different proteins are presented, loading 30 μg total protein per lane. Values shown represent units expressed as a percentage of the highest value obtained for each protein, means ± s.e.m. of at least 3 experiments, each performed in triplicate, with each extraction buffer. B. The results of quantitation of band intensity of the different proteins are presented, loading the protein from 60,000 cells per lane. Values shown represent units expressed as a percentage of the highest value obtained for each protein, means ± s.e.m. of 3 experiments, each performed in triplicate, with each extraction buffer.

buffer added to cell pellets for 10 min with vigorous pipetting. Three different, commonly employed buffers were used, NP-40, RIPA and SDS (see Materials and methods) and 30 μg total protein loaded per lane. As shown in Fig. 1B and Fig. 2A, there was a ~3× increase in the amount of α-tubulin detected in cells grown to 100%, compared to 10% confluence. A similar increase was seen in the levels of GAPDH, and it was the same regardless of extraction method used. However, Hsp90 and β-actin levels remained essentially unchanged with cell density. Similar results were obtained with a number of other cell lines, such as the A549 and SK-Luci-6 lung carcinoma (Tomai et al., 1999), the MDA-MB-468, MDA-MB-231 and MDA-MB-453 breast carcinoma (Vultur et al., 2004), normal mouse breast epithelial HC11 (Arulanandam et al., 2009), rat liver epithelial T51B (Geletu et al., 2009), and mouse primary and spontaneously established fibroblasts, before and after transformation by the middle tumor antigen of polyoma virus (Raptis et al., 1985) or the large tumor antigen of Simian Virus 40 (Vultur et al., 2005).

Since the content per cell of many proteins may change with cell density, these experiments were repeated, loading the protein from an equal number of cells (60,000) per lane (Fig. 2B). This amounted to 30 μg protein for actively growing NIH3T3 cells, i.e. at confluences of up to 75%, while the same number of cells at 100% confluence had 23.3 μg as expected, due to the higher proportion of cells in Go/G1. The results showed that at densities of up to ~75% Hsp90 and β-actin levels were unchanged with density, while the levels of GAPDH and α-tubulin increased as above. However, at confluences equal to or greater than 100% the amounts of all housekeeping proteins examined were lower compared to cells grown to 75% confluence, indicating that their levels are proportional to the amount of cellular protein loaded, regardless of cell numbers.

To compare the efficiency of extraction with the different buffers, the levels of these proteins remaining in the pellets were assessed; following NP-40 or RIPA extraction, the pellets were solubilised by resuspending in SDS buffer and the amounts of residual α-tubulin and GAPDH quantitated by Western blotting. Pellets from cells extracted with NP-40 contained approximately equal amounts of α-tubulin as the supernatants, and twice the amounts present in the pellets from cells extracted with RIPA buffer, indicating that the RIPA buffer can extract ~2× higher amounts of α-tubulin than the NP-40. However, no GAPDH was detected in any of the pellets, indicating that both buffers can extract most of this cytosolic protein.

Conclusions

In this communication we examined the levels of four gene products which are commonly used as loading controls in Western blotting experiments. The results revealed that levels of α-tubulin and GAPDH increased significantly with cell confluence from 10% to 100%, which shows that these proteins may be unsuitable as loading controls for Western blotting experiments requiring growth of cells to subconfluence. On the other hand, our results demonstrate that Hsp90 and β-actin levels were essentially unaffected by cell confluence, making these proteins into reliable gel loading controls for a wide range of cell densities.

Acknowledgements

The financial assistance of the Canadian Institutes of Health Research (CIHR), the Canadian Breast Cancer Foundation (Ontario Chapter), the Natural Sciences and Engineering Research Council of Canada (NSERC), the Ontario Centres of Excellence, the Breast Cancer Action Kingston, the Clare Nelson bequest fund and the Canadian Breast Cancer Research Alliance through grants to LR is gratefully acknowledged. RA was supported by a Canada Graduate Scholarships Doctoral award from CIHR, the Ontario Women's Health Scholars Award from the Ontario Council on Graduate Studies and a Queen's University Graduate Award (QGA). SG was supported by an NSERC USRA award. MG was supported by a fellowship from the Ministry of Research and Innovation of the Province of Ontario and a postdoctoral fellowship from the US Army breast cancer program.

References

Arulanandam, R., Vultur, A., Cao, J., Carefoot, E., Truesdell, P., Elliott, B., Larue, L., Feracci, H., Raptis, L., 2009. Cadherin–cadherin engagement promotes survival via Rac/Cdc42 and Stat3. Mol. Cancer Res. 17, 1310.

Etienne-Manneville, S., Hall, A., 2002. Rho GTPases in cell biology. Nature 420, 629.

Geletu, M., Chaize, C., Arulanandam, R., Vultur, A., Kowolik, C., Anagnostopoulou, A., Jove, R., Raptis, L., 2009. Stat3 activity is required for gap junctional permeability in normal epithelial cells and fibroblasts. DNA Cell Biol. 28, 319.

Kurien, B.T., Scofield, R.H., 2003. Protein blotting: a review. J. Immunol. Methods 274, 1.

Raptis, L., Arulanandam, R., Vultur, A., Geletu, M., Chevalier, S., Feracci, H., 2009. Beyond structure, to survival: Stat3 activation by cadherin engagement. Biochem. Cell Biol. 87, 835.

Raptis, L., Lamfrom, H., Benjamin, T.L., 1985. Regulation of cellular phenotype and expression of polyomavirus middle T antigen in rat fibroblasts. Mol. Cell. Biol. 5, 2476.

Tomai, E., Brownell, H.L., Tufescu, T., Reid, K., Raptis, L., 1999. Gap junctional communication in lung carcinoma cells. Lung Cancer 23, 223.

Towbin, H., Staehelin, T., Gordon, J., 1979. Electrophoretic transfer of proteins from polyacrylamide gels to nitrocellulose sheets: procedure and some applications. Proc. Natl. Acad. Sci. U. S. A 76, 4350.

Vultur, A., Arulanandam, R., Turkson, J., Niu, G., Jove, R., Raptis, L., 2005. Stat3 is required for full neoplastic transformation by the Simian Virus 40 Large Tumor antigen. Mol. Biol. Cell 16, 3832.

Vultur, A., Cao, J., Arulanandam, R., Turkson, J., Jove, R., Greer, P., Craig, A., Elliott, B.E., Raptis, L., 2004. Cell to cell adhesion modulates Stat3 activity in normal and breast carcinoma cells. Oncogene 23, 2600.